ISSN 0725-2986

The Institution of Engineers, Australia

SPECIAL ISSUE: THE AUSTRALIA TELESCOPE

IREE

Five of the antennas of the Australia Telescope Compact Array, near Narrabri, NSW
Photo: J Masterson, CSIRO

JOURNAL OF ELECTRICAL AND ELECTRONICS ENGINEERING, AUSTRALIA

Published by
The IREE Australia
The IE Aust College of Electrical Engineers

Registered by Australia Post Publication No. NBP2876

Volume 12, No. 2
June 1992

EDITORIAL POLICY

The policy of the publishers of the Journal of Electrical and Electronics Engineering, Australia is to publish a variety of contributions to the science and practice of electrical engineering. Major fields of interest include electronics and communications engineering; electric energy; automation, control and instrumentation; computer and information technology. The Journal of Electrical and Electronics Engineering, Australia aims to publish reviewed technical papers in the major fields of interest, as well as in allied fields.

Papers should relate to the relevant field and will usually fall into one of the following categories:

a. Research paper. A paper making an original contribution to engineering knowledge.

b. Special interest paper. Report on significant aspects of a major or notable project.

c. Review paper for specialists. A critical survey of a relevant area, intended for specialists in the field covered.

d. Review paper for non-specialists. An overview of a relevant area, suitable for a reader with an electrical/electronics background.

e. Tutorial paper. A paper which explains an important subject or clarifies the approach to a matter of design or investigation.

f. Engineering Communication. A technical communication or a letter to the Editors not sufficiently developed or extensive in scope to constitute a full paper.

g. A contribution to discuss a published paper to which the original author's response will be sought.

From time to time invitations are presented to particular authors to write a paper for the Journal. This most usually occurs when it is decided to collect a number of papers relating to one subject into a given issue, often with a guest editor.

The expected length of acceptable contributions will vary considerably but 4 000 to 5 000 words or word equivalents for papers could be the norm. Engineering communications should not exceed 1 000 words and contributions to discuss published papers should not exceed 500 words.

JOURNAL OF ELECTRICAL AND ELECTRONICS ENGINEERING AUSTRALIA

Published by
The IREE Australia
The IE Aust College of Electrical Engineering

Volume 12, No. 2
June, 1992

contents

Published by: The Institution of Engineers, Australia, 11 National Circuit, Barton, A.C.T. 2600. Telephone: (06) 270 6555 and The Institution of Radio and Electronics Engineers Australia, Commercial Unit 3, 2 New McLean Street, Edgecliff, N.S.W. 2027. Telephone (02) 327 4822.

Printed by Ambassador Press Pty. Ltd., 51 Good Street, Granville 2142.

Journal of Electrical and Electronics Engineering, Australia is published quarterly by The Institution of Engineers, Australia and The Institution of Radio and Electronics Engineers, Australia. All correspondence, including manuscripts and advertising enquiries, should be addressed to the Secretary of either Institution. Abstracting is permitted with due credit to the Journal of Electrical and Electronics Engineering, Australia. Price: members; $10.00 per annum (included in annual subscription), $7.50 per single extra copy; non-members, $48.00 per annum, $15.00 per single copy. REPRINTS: Reprints of technical articles are available. Quantities of not less than 25 may be ordered.

FOREWORD

The Australia Telescope is an example of the best design and engineering skills of this country. We who have been associated with it take great pride in that it was built with an unprecedentedly high Australian content, that the Australian companies involved showed themselves to be internationally competitive in price and quality, that it was completed within the agreed budget and that it is now performing as a world-class astronomical instrument. This is no accident. Extensive planning went into the design, and into the considerable task involved in getting it funded. It was funded fully by the Australian Government. In this special issue, those responsible for key aspects of the design, construction and early stages of operation of the Australia Telescope describe the elements of this complex system.

The Australia Telescope owes its existence to the presence in Australia of a healthy and coherent astronomical community, involving many scientists and engineers in universities and other organisations around the country. The existence of a number of these internationally competitive groups is partly due to the decision, made back in the 1950s, to build the Parkes Telescope. The construction of the Parkes telescope was seen in the CSIRO Division of Radiophysics as the way forward at a time when several, now famous, Australian astronomers working in the Division had competing ideas for major new facilities.

Competing proposals came from J. P. (Paul) Wild, W.N. (Chris) Christiansen and B.Y. (Bernie) Mills. Paul's proposal to build a radioheliograph was supported by the Chief of the Division of Radiophysics at the time, E. G. (Taffy) Bowen. It is interesting that the Parkes Telescope and the Radioheliograph at Narrabri were built with substantial US money from the Rockefeller and Ford Foundations. With two major facilities in train, it was clear that the future for Bernie Mills and Chris Christiansen lay elsewhere. Bernie went to the School of Physics and Chris to the School of Electrical Engineering, both at the University of Sydney. Bernie obtained funding, primarily from the US National Science Foundation, for the Molonglo Mills Cross; Chris arranged to take over the historic Fleurs observatory from the CSIRO and set about converting the Chris-Cross solar radio telescope into a compound interferometer synthesis telescope. Funding for this came from the University and the embryonic Australian Research Grants Committee, as did the later funding for the Mills Cross.

The major proponent of the Parkes Telescope was Taffy Bowen. Assistant Chief at the time was J. L. (Joe) Pawsey. Long acknowledged as the 'father' of Australian radio astronomy, Joe accepted the position of Director of the National Radio Astronomy Observatory, Green Bank, USA in 1962, one year after the Parkes telescope was officially opened and its first Director, John Bolton, appointed. Joe Pawsey died in 1963 before he was able to take up his new duties.

By the 1970s, Australia had five world-ranking groups in radio astronomy: those at Molonglo, Fleurs, the University of Tasmania, led by Graham (Bill) Ellis, and the Radiophysics groups at Parkes and Narrabri. Each had expertise in key areas of radio-telescope instrumentation.

The possibility of building a large synthesis telescope in Australia became a topic of discussion among the world's astronomers in the early seventies. The Westerbork Telescope, for example, had been a highly successful venture in the Netherlands, and Dutch astronomers were considering ways of establishing a comparable instrument in the south – a 'southern Westerbork'. At this time, too, the Cambridge 5-km telescope was operating in the UK, and the VLA (very large array) was under construction in the US.

In 1975, a steering committee was established, under the chairmanship of Paul Wild, to build an Australian Synthesis Telescope. Dr Kelvin Wellington was chairman of the Technical Design group associated with

this proposal. By that time, the astronomical community had a well-identified need, and it was clear that, within the various Australian groups, we had the necessary scientific knowledge and engineering skills to conduct such a major project. The Steering Committee and an associated Design Study Group worked on various designs during the late 1970s. This led to a proposal being developed for the Australian Government to fund a new facility (the Australian Synthesis Telescope) on the Parkes Telescope site.

When RHF became Chief of the Division of Radiophysics in 1981, this first proposal was well on the way to being rejected. When this was formally known, he was faced with a dilemma. The project had been dangerously under-budgeted. Its scope was limited in terms of the ability of the proposed telescope to meet future needs, and we ran a high risk of getting devastating interference from proposed mining operations at Goonumbla, near Parkes. The proposal was not resubmitted the following year.

By this time, RHF, as Chief, had already decided to close down the Radioheliograph at Narrabri, giving us an available site. The original proposal had not provided for very-long-baseline-interferometry (VLBI) use but, by having the main array at Narrabri, we would have Narrabri, Parkes and the 70-m antenna of NASA's Canberra Deep Space Communications Centre at Tidbinbilla available for VLBI. A discussion with Dr Brian Robinson late one afternoon on the radio-interference problem at Parkes led to a discussion of alternatives. Restricting alternatives to serviced sites, we realised that a main array at Narrabri with a single antenna at Siding Spring mountain near Coonabarabran gave an almost perfect four-element array with Parkes and Tidbinbilla. The new proposal was conceived. Specifications for the system were reworked to be more competitive in every dimension of proposed operation, and we were ready to promote it.

The timing of the proposal was such that we were looking at the possibility of opening the telescope in the bicentennial year, 1988. We named it the Australia Telescope and promoted it as a Bicentennial Project. It was formally endorsed by the Bicentennial Committee and funded by Malcolm Fraser's Government in the 1982 budget. It was opened in September 1988, a month after the first pair of antennas had been operating successfully as an interferometer. During its construction, a close association developed between CSIRO and the engineering firm Macdonald Wagner (now Connell Wagner) which has continued into successful commercial ventures.

The completed instrument is the work of many people, some of whom appear as authors in this issue. We commend the skill and cooperation of the Laboratory's Engineering Services Group, including the workshop and drawing office. Thanks are due also to the administration and support groups, and to Mrs Eileen Barnett, personal assistant to RHF, for her diplomatic handling of issues concerning the Office of the Chief. Mr John Masterson, assisted by the staff of the photographic laboratory, was responsible for many fine photographs taken during the construction of the Australia Telescope and for many of those in this issue.

The expert advice and support given to the project by the late Alec Little was invaluable. Two other members of staff, now deceased, made substantial contributions to the project – Dr Max Komesaroff in the area of polarization, and Mr Paul Rayner in computing. We also owe thanks to Mr Arthur Watkinson who joined the project in 1986 as systems adviser, and to our friends at the US National Radio Astronomy Observatory for the support and advice they gave so freely.

The task of making the material for this issue presentable has been tirelessly and meticulously carried out by Dorothy Goddard, editor at the Radiophysics Laboratory. Brian Cooper (ex Radiophysics and engineer par excellence) undertook the colossal task of refereeing. Gwen-Anne Manefield's secretarial help is gratefully acknowledged.

What follows in this issue is the 'nuts and bolts' side of building a radio telescope. Some of the more colourful aspects will have to wait for another time.

R H Frater
J W Brooks
Guest Editors

Journal of Electrical and Electronics Engineering, Australia
Special Issue

THE AUSTRALIA TELESCOPE

Chapter 1

The Australia Telescope

The Australia Telescope Overview

R.H. Frater*, J.W. Brooks* and J.B. Whiteoak*

SUMMARY On the second day of September, 1988, at a windy ceremony held at CSIRO's Paul Wild Observatory near Narrabri, some 600 kilometres north-west of Sydney, Australia's then Prime Minister, the Hon. R.J.L. Hawke, declared the Australia Telescope officially open. This heralded a new exciting era in Australian scientific research, because the Australia Telescope is an advanced radio telescope network which will keep Australia at the forefront of radio astronomy for many years to come. Designed and built in Australia, and containing a high Australian content, this 50-million dollar national facility is a substantial monument to Australian manufacturing expertise and high-technology capability.

1 INTRODUCTION

In general terms, the Australia Telescope (AT) is a collection of eight antennas located at three different sites in New South Wales (see Fig. 1). Six new identical antennas, each with a parabolic reflecting surface 22 metres in diameter, are located at the Paul Wild Observatory near Narrabri. A seventh 22-m antenna (the Mopra antenna) has been constructed a few kilometres west of Coonabarabran. The 64-m diameter Parkes antenna completes the collection; after more than thirty years of operation it continues to yield high-quality radio astronomy results.

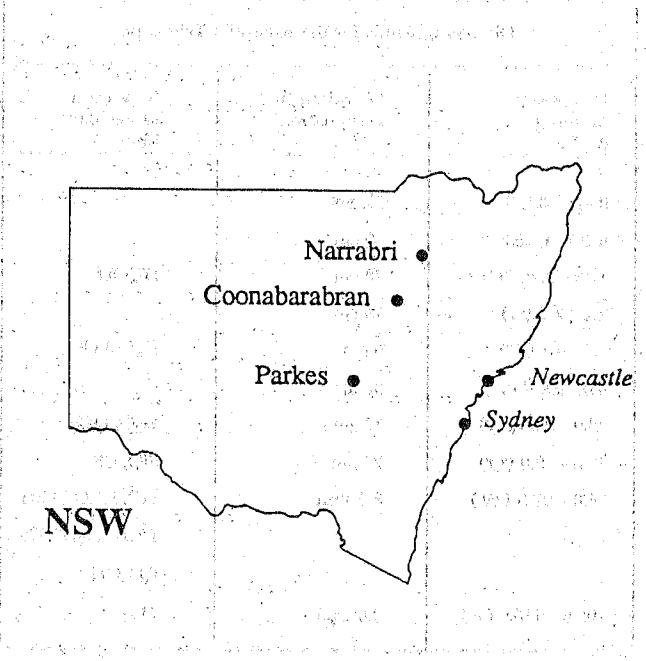

Figure 1 Sites of AT antennas and other antennas used in long baseline array networks.

1.1 Compact Array

The six antennas near Narrabri form the 6-km Australia Telescope **Compact Array** (Fig. 2). They operate together as a 'synthesis' telescope. All can be self-propelled along a railtrack; five are set on a 3-km east-west section, while the sixth is on a small 75-m track a further 3 km to the west. For operation, the antennas are installed with an accuracy of a few millimetres on stable concrete platforms ('stations'), 35 along the large track and two along the small track. The signals received by the individual antennas are transmitted to a central control building for processing using specially developed correlators.

The construction budget provided for Compact Array operation in wide bands centred at frequencies of 1.5, 2.3, 5.0 and 8.6 GHz. Dual-polarization systems are currently available for these frequencies. For the 6-km array operating at the highest frequency, the angular resolution is 0.8 arcsec, similar to that of conventional optical telescopes under stable atmospheric conditions. When fully developed, the Array will also operate at other frequencies between 0.3 and 116 GHz (see Table 1). Many of the bands were selected to include the

* Institute of Information Science & Engineering, CSIRO, PO Box 93, North Ryde NSW 2113, Australia.
** Australia Telescope National Facility, CSIRO, PO Box 76, Epping NSW 2121, Australia.
Submitted to The Institution of Radio and Electronics Engineers Australia in June 1992.

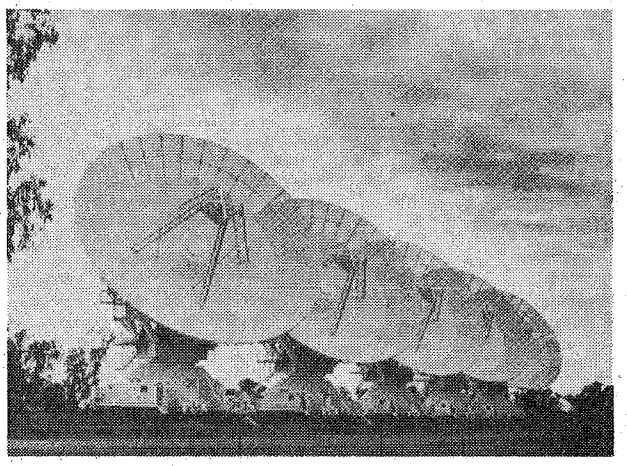

Figure 2 Five of the six antennas of the AT Compact Array.

TABLE 1

Observing Bands for the Australia Telescope

Frequency Coverage (GHz)	Wavelength Designation	Important Molecular Lines
0.322 - 0.329	90 cm	
0.582 - 0.603	50 cm	
1.25 - 1.78 ('L') *	20 cm	HI, OH
2.2 - 2.5 ('S') *	13 cm	
4.4 - 6.1 ('C') *	6 cm	H_2CO, OH
8.0 - 9.2 # ('X') *	3 cm	
20.0 - 25.5 ('K')	12 mm	H_2O, NH_3
42.0 - 50.0 ('Q')	7 mm	SiO, CS
84.0 - 98.5 ('W')	3.5 mm	SiO, HCO^+, C_2H, HCN, N_2H^+, CS, CH_3OH
105.0 - 116.0 ('F')	2.6 mm	CO

* bands available initially
\# later extension to 10.7 GHz

frequencies of astrophysically important spectral lines from interstellar atoms, ions, radicals and molecules. Other bands contain the frequencies commonly used by VLBI (very large baseline interferometry) networks. The frequency range coverage was extended up to 115 GHz to enable observations of a line of carbon monoxide, one of the most abundant interstellar molecules.

1.2 What is a 'Synthesis' Telescope?

A synthesis radio telescope is an array of separated antennas which, operating together, can synthesize an aperture much larger than those of the individual antennas. For a conventional reflector telescope the angular beamwidth varies as the inverse of the antenna aperture measured in wavelengths. To obtain a beamwidth of one second of arc, which is similar to that of conventional optical telescopes under average atmospheric conditions, an aperture of 200,000 wavelengths would be needed. This aperture would be 40 km for operation at a wavelength of 20 cm, i.e. at a frequency of 1.5 GHz! Clearly, such a single aperture is not possible. However, it is possible to synthesize the aperture using observations with a two-dimensional array of antennas arranged to cover all the spacings of the synthesized aperture. By correlating the signals from pairs of antennas, and two-dimensional Fourier transforming the product total, a radio source image is produced with angle resolution appropriate to the synthesized aperture.

However, the Compact Array is only one dimensional. Although it provides high angular resolution in the direction of the array extension, the angular resolution in the orthogonal direction is only that of a 22-m antenna. Fortunately, for radio astronomy observations, the rotation of the Earth enables high-resolution observations to be made in all directions. This technique, known as **Earth-rotation synthesis**, was first applied to cosmic radio sources in a survey of the north polar region published by Ryle and Neville [1] in 1962. As a radio source moves across the sky, it appears to rotate, and an array tracking the source for long periods of time can sample the different orientations. The degree of rotation depends on the location of the source. For southern sources, the Compact Array can sample all orientations. However, observations of more northern sources near the celestial equator yield images with high resolution only in an east-west direction; to provide high resolution at other orientations, antennas with north-south separations would also be required.

The number of spacings for n antennas is n(n-1)/2. Six antennas provide only 15 spacings, and the Compact Array cannot provide all the spacings to cover the synthesized aperture fully in a single observing period. However, additional spacings can be added by observing with the antennas set at different confiigurations of stations. Many configurations would be needed to provide a 'filled' array, but by using sophisticated image processing techniques it is possible to obtain high-quality images with as few as three.

1.3 Long Baseline Array

The Compact Array, Mopra antenna, and Parkes radio telescope can be linked together to form the Australia Telescope **Long Baseline Array**. The signals received at each site are recorded with tape recorders. At the moment, correlating the signals from all the sites is carried out at the US California Institute of Technology. Ultimately, correlation will be possible at Narrabri. AT

frequency bands between 1.5 and 23 GHz will be used for observations. The array extends more than 320 km in a north-south direction, providing an angular resolution fifty times higher than the Compact Array. Even higher resolution is required for some studies, and the Array will be incorporated into large VLBI networks containing other antennas in Australia, in other countries, and in orbit.

1.4 'Stand-alone' Operation

Apart from its use in the Long Baseline Array, the Parkes radio telescope will continue to be used for 'stand-alone' operation. In addition, it is planned to outfit the Mopra antenna for wide-band (700 MHz) operation at 115 GHz; at this frequency its only competitor in the Southern Hemisphere will be the 14-m Swedish-ESO Submillimetre Telescope (SEST) in Chile.

2 THE AUSTRALIA TELESCOPE CONSTRUCTION PROJECT

2.1 Background

The reference to astronomical and meteorological observations in Section 51 of the Constitution of the Commonwealth of Australia implies a responsibility to carry out such observations. Australian astronomers have accepted this challenge. Large optical telescopes have been built, starting with the Great Melbourne Telescope in 1858, and progressing to the present 4-m Anglo-Australian Telescope (AAT) near Coonabarabran in NSW.

Australians featured prominently in developing the younger science of radio astronomy. At the end of World War II, pioneering work was carried out by scientists formerly engaged in wartime radar research at CSIR (now CSIRO). Their achievements in radio astronomy, initially obtained using surplus radar equipment, brought great prestige to Australia. Australian research remained at the forefront for the next thirty years as CSIRO and university scientists constructed a succession of fine radio telescopes. The more recent additions include the Parkes 64-m antenna (completed in 1961 [2]), the 1.6-km Molonglo Cross array (completed in 1965 [3]), the Culgoora Radioheliograph (completed in 1967 [4]), and the Fleurs Synthesis Telescope, commissioned in 1973 [5]). Many important discoveries were made, particularly involving unique and important objects of the southern skies which cannot be viewed from northern observatories.

In subsequent years both the Parkes antenna and the Molonglo Cross were upgraded; even today they continue to support good research, and produce scientific breakthroughs from time to time. However, during the 1970s, it became apparent that the existing instruments could not operate at the high frequencies required for some astronomy research, nor could they image celestial objects with the fineness of detail available with optical and space telescopes. Moreover, other countries were constructing a new generation of telescopes that could give their astronomers the leading edge in research. It was obvious that a new radio telescope was needed to preserve the research vitality of Australian radio astronomers.

In 1975 a steering committee, chaired by Dr J.P Wild (then Chief of CSIRO Division of Radiophysics) and with members drawn from CSIRO and Australian universities, developed a proposal for a high-resolution radio telescope, the Australian Synthesis Telescope (AST). The proposal was supported by ASTEC (Australian Science and Technology Committee) in 1979, which recommended that "the Australian Synthesis Telescope be given first priority among telescope proposals...". The Executive of CSIRO included the request for funds in their 1980/81 list of high priority projects that was submitted to the Fraser Government. However, funding was not made available.

Dr R.H. Frater became Chief of Radiophysics in 1981, and immediately initiated a redeveloped proposal, the Australia Telescope. As a result of widespread consultation, the AT was more in tune with the astronomical objectives of Australian radio astronomers than the AST. In addition, it planned to use front-line technology that would result in an instrument capable of leading-edge research up to and beyond the turn of the century. Learning from their previous experience with the unsuccessful AST, radio astronomers lobbied politicians, and embarked on a major program to inform the public of their needs. Preliminary technical specifications were drawn up, based on the results of a symposium 'Astrophysical Objectives for the Australia Telescope' held at the Radiophysics Laboratory in February 1982. These defined the AT as a set of six 22-m antennas in a 6-km array at Narrabri, a seventh 22-m antenna on Siding Spring Mountain, near Coonabarabran, and the Parkes radio telescope. The high-frequency limit was set at 40 GHz.

In May 1982 ASTEC recommended in a report 'New Telescopes for Australian Astronomy in the 1990s' that the AT be accorded the highest level of priority, for reasons including:

(i) national prestige

(ii) responsibility to study the southern skies

(iii) impetus for technological innovation and manufacture of radio and other equipment

(iv) status as sole current source of observations of southern skies at radio wavelengths needed to complement those of other wavelengths made from ground and space instruments.'

In 1982/83 CSIRO's Executive gave the proposal top priority. The Minister for Science and Technology also included it as the top priority item in his submission of new policy proposals for 1982/83. In its 1982 August budget, the Fraser Government approved funding for the AT at the level of $25 million (January 1982 values) spread over six years. It also agreed that the project be endorsed as a Bicentennial Project, with an official opening as part of the 1988 celebrations. An AT Advisory Committee was set up; at its first meeting in October 1982 it enlarged its membership to include overseas scientists. An AT System Concept Workshop was held in December 1982 to establish a total concept and to identifiy key personnel requirements for the project.

The Hawke Government gained office early in 1983 and referred the project to a Parliamentary Standing Committee on Public Works. Following the Committee's inspection of the Radiophysics Laboratory and the proposed sites for the facility in August 1983, and a public enquiry in Canberra a month later, the Government finally approved the AT project in November 1983, at a level of $30.7 million (indexed to March 1983). As recommended by ASTEC, it was agreed that the AT "be built and operated by CSIRO...[and] that the telescope be regarded as a National Facility available for use by all Australian astronomers". Within CSIRO, responsibility for the design and construction was vested in the Chief of Radiophysics.

The major construction lasted five years, during which time inflation and currency indexation took the project cost to $50 million. After the first interferometer tests and during the 1988 Bicentennial celebrations, the AT was formally opened. It was then fitted out in time to begin operating as a National Facility in April 1990.

2.2 Management

A well-structured management group was set up to build the AT. After the system concepts had been defined, and core ideas established, teams were formed to explore and expand these concepts to gauge feasibility, and to estimate the financial and human resources required to implement them. Team leaders were selected who were technically strong, system orientated and stimulated by new challenges. They also had established track records. Other key positions developed during the course of the project.

The management of the construction project was carried out by the CSIRO Division of Radiophysics, and was divided into policy and planning groups, technical and construction groups, and advisory and working groups (Fig. 3). Dr R.H. Frater, Chief of Radiophysics at the beginning, and Director of the CSIRO Institute of Information Science and Engineering later, spearheaded the management as Project Director; directly responsible to him was the Project Manager, Mr J. W. Brooks.

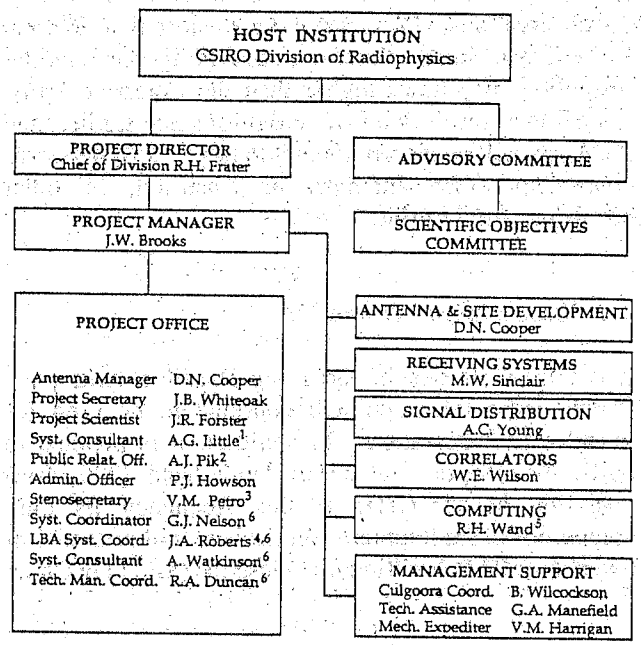

[1] until his untimely death in 1985
[2] until 1986
[3] replaced by L.F. Carrig in 1986
[4] later R.P. Norris
[5] later led by M.J. Kesteven and then R.P. Norris
[6] appointed in 1985 or later

Figure 3 Management structure for AT construction.

Progress monitoring

Progress monitoring was carried out at several different levels. At the top level, an Advisory Committee was established in the initial stages of the project to provide general policy guidance on construction, and to review critical areas. The Committee, chaired by Dr R.H. Frater, consisted of three scientists from the Division of Radiophysics, three non-CSIRO Australian astronomers, and three experts from overseas radio astronomy institutions. It met at intervals of approximately six months and produced an annual progress report for the Federal Minister for Science. It was advised on detailed scientific matters by a sub-committee, the AT Scientific Objectives Committee (ATSOC). Chaired by Dr R.N. Manchester, ATSOC's membership represented astronomers at Australian universities and other institutions.

The Project Office, the Director, and others when relevant, met regularly to review management and contractual issues. The Project Manager held monthly meetings with the technical groups, project office and site representatives, to monitor and coordinate progress. When required, other *ad-hoc* review or information meetings were organised to discuss key problem areas; the participants included both Radiophysics staff and relevant external experts.

Several documents were used in the monitoring process. At the start of the project, a system definition document was drawn up, providing the goals against which progress could be measured. In addition, the groups produced 'critical path charts' related to their operations. These brought into stark relief critical areas such as the development of the correlator. From a project management view, they showed clearly the scope of the project and the required sequencing of tasks. After extensive consultation with the groups, standards were set for various components of the construction. These were documented and followed by all groups. This undoubtedly facilitated the interfacing of hardware.

Finance and Personnel

Careful financial management was a key requisite of the project. The construction project was initially funded in March 1983 dollars (at $30.7 million). In agreement with the Federal Department of Finance, quarterly balances were calculated, indexed for variations in the CPI (Consumer Price Index), wage rates and foreign exchange. Due mainly to these factors, over the course of the construction the total amount expended on the project increased to $49.5 million (June 1987 dollars).

Some 40 extra staff were employed during construction. Many members of Radiophysics joined the project, some by secondment. In all, 73 positions were associated with it. Many of the new appointments were short-term. Although this practice affected the continuity of the project it was nevertheless consistent with a policy supporting the transfer of training and expertise from CSIRO to industry. Furthermore, in the final stages, it enabled a smooth conversion of construction positions into operations positions.

Public Relations

Publicity was an important facet of the project. Many technical presentations were made at engineering and astronomy meetings, and during visits to Australian and overseas scientific and engineering institutions.

In addition to the Annual Report prepared for the Minister, numerous pamphlets and brochures were produced before and during construction, illustrating both the technical extent of the project and the proposed use of the finished product for radio astronomy. A six-monthly series, *Countdown*, ran from January 1984 to December 1988. It followed the progress of the project, and highlighted new developments in astronomy that would be relevant to the Telescope's future operation. Another series, *AT Newsletter*, focused more on the actual progress of the project. It is now produced at four-monthly intervals and deals with operational aspects and scientific results.

In 1986, a contract was let to produce a video documentary of the construction history. This resulted in two VCR versions, a 65-minute, and a shorter, 17-minute version.

The construction project had a high profile, and there was a constant demand for speakers by astronomical societies and groups, service clubs and schools. Significant events were given a wide coverage by the news media.

Both the Parkes and Paul Wild Observatories now have extensive visitors centres. The Parkes Observatory Visitors Centre began operating about 20 years ago, and has been extremely successful. The Centre at Narrabri was completed in 1990.

3 SCIENTIFIC DESIGN GOALS

In planning the AT we recognized that the instrument would have to compete on equal or better terms with overseas radio telescopes already operating or being planned, such as the US Very Large Array (VLA), the UK Multiple Element Radio Linked Interferometer Network (MERLIN), high-frequency arrays in France, Japan and the USA, and the US Very Long Baseline Array (VLBA). In operation it would have considerable geographic advantage; the only large radio telescope in the Southern Hemisphere for the foreseeable future, it would have unrivalled access to many southern celestial objects denied to northern instruments.

It would complement the new generation of telescopes operating in Australia at other wavelengths. These include ground-based optical telescopes: the AAT, the Australian National University's 2.3-m Advanced Technology Telescope (ATT), the 1.3-m UK Schmidt Telescope, and the Sydney University Stellar Interferometer (SUSI). Also included are orbiting gamma-ray, X-ray, ultraviolet, optical and infrared telescopes that already exist or are being planned.

In the initial planning, several performance requirements were identified:

(i) an ability to map large fields of view with high sensitivity and a maximum detail that would far exceed that seen with conventional optical telescopes

(ii) a specially designed spectral-line capability for studying narrowband signals from the multitude of atoms and molecules in dense interstellar gas clouds and the outer envelopes of some stars

(iii) a capability for accurate measurement of polarization, by means of which magnetic fields, important constituents of galaxies, can be traced

(iv) the ability to observe at two widely spaced wavelengths simultaneously.

4 BUILDING THE AUSTRALIA TELESCOPE

4.1 Major tasks

The major tasks identified in the final specifications presented to the government in 1983 were to design and construct the following:

(i) seven 22-m diameter antennas, operating at frequencies of up to 115 GHz

(ii) precision servo-control tracking systems

(iii) high-precision surface panels for use at frequencies up to 115 GHz

(iv) antenna feed systems to operate in a wide frequency range, and with simultaneous reception at two frequencies

(v) low-noise receiving systems and frequency conversion units

(vi) fibre-optics signal network linking the Compact Array antennas

(vii) reference-frequency signals to transmit to Long Baseline Array sites via satellite

(vii) systems, requiring the development of a suitable VLSI chip, to correlate signals from pairs of antennas capable of handling up to 2×10^{12} products per second.

4.2 Choices and Decisions

Choice of sites

In the original AST design, the array would have been located at the Parkes Observatory, incorporating the 64-m radio telescope as one of the array elements. For the AT, although a similar location would have been an advantage in terms of array collecting area, there was some concern that electrical equipment (e.g. crushing machinery) for mining, planned for the vicinity of the Observatory, would produce harmful radio interference in the operating frequency bands of the array. Furthermore, it was desirable to have the array separated from the Parkes radio telescope to provide a reasonable baseline in a long-baseline configuration. On the basis of these considerations, we decided to construct the Compact Array on land already owned by CSIRO near Narrabri. However, because the CSIRO site was not large enough to contain the entire array we bought a small parcel of land for the 6-km antenna from a neighbouring landowner. A 10-m wide easement on the land between this site and the CSIRO site was established to provide an access road and accommodate buried cables between the two sections of the Array.

The 22-m antenna near Coonabarabran was originally planned for an elevated location on Siding Spring Mountain, on land owned by the Australian National University. However, the site was found to be unsatisfactory on several grounds: potential radio interference from line-of-sight microwave link transmitters, poor quality of foundation material, prevalence of high winds, inadequate protection from bushfires, and objections to the antenna's 'visibility' from the adjacent Warrumbungles National Park. During 1985, following radio interference measurements, an alternative site, protected from both interference and high winds, was selected on the property 'Mopra' near the base of Siding Spring Mountain. The location was approved by the NSW National Parks and Wildlife Service, the Federal Department of Arts, Heritage and the Environment, and local governing bodies.

Compact Array design

Like most large constructions, the final design of the Compact Array was driven by the amount of money available. The concept of a linear array was accepted early in the planning as the cheapest means of achieving the longest spacings (i.e. highest angular resolution). Aligning the array east-west rather than north-south facilitated some of the image formation and processing. The addition of a north-south arm was ruled out mainly because of the extra cost. We realised that images of objects located near the celestial equator would have poor north-south angular resolution, but reasoned that such objects would be easily accessible to the large arrays of the Northern Hemisphere. Nevertheless, early in 1984 the Advisory Committee supported the future provision of a north-south spur.

Aside from cost, the rationale behind the selection of a 6-km maximum spacing was that, for observations at the highest frequencies implemented on the Array (8.6 GHz), the angular resolution (0.8 arcsec) would be similar to that obtained with ground-based optical telescopes. From this evolved the plan to locate one antenna at the 6-km position, and the others on a 3-km–long railtrack at the other end of the array. Preliminary estimates indicated a high cost for providing connecting railtrack to enable the single

antenna to be moved to the 3-km railtrack (for the purpose of participating in configurations with maximum baselines of 3 km and less), and so, to save money, we decided to forgo the connection.

If we were designing the Compact Array today, we would probably give more consideration to providing a north-south extension, because the self-calibration routines used in processing observations to improve final images appear to be less effective for data obtained with linear arrays. More emphasis might be given to station settings yielding better configurations with small maximum baselines. Experience has shown that small configurations (e.g. 0.75-km and 1.5-km sets) are suitable for many spectral-line projects, and even smaller configurations will be desirable when high-frequency capabilities are implemented on the Array.

The required number of stations and their locations along the railtrack were investigated by an *ad-hoc* configuration-study group chaired by Dr R.N. Manchester. The aim was to provide for both minimum-redundancy grating arrays and grating arrays with sufficient redundancy to enable antenna phase errors to be calibrated. The final results [6] provided good baseline distributions with four or more different antenna settings, for 1.5-, 3- and 6-km array configurations. Thirty-seven stations, including two at the 6-km location, were required.

The new 22-m antennas

The antenna design began during the 1970s. In 1978 budget estimates were sought from several overseas manufacturers. These were considered quite high. Consequently, CSIRO commissioned Macdonald, Wagner and Priddle (now Connell Wagner) in association with Dutch antenna engineer Ir B.G. Hooghoudt, to design an antenna which could be built in Australia with high local content. This work was carried out between 1979 and 1982. Macdonald, Wagner and Priddle used the results, in conjunction with advice from CSIRO and overseas experts, for final design optimization studies. Because the base of the Coonabarabran antenna is fixed, a 'stiffer' wheel-on-track design was adopted in preference to the fork-and-yoke design of the Narrabri antennas. The former was expected to yield a better high-frequency performance, and lower pointing errors. The extra design costs were offset by cheaper construction costs. In July 1985, a $15 million contract was awarded to Evans-Deakin Industries, a former shipbuilding company based in Brisbane, to construct and erect the antennas. Each antenna contains six concentric rings of reflecting panels backed with circumferential ribs. Relatively low-cost techniques for panel construction were developed in the Radiophysics workshop, and these were taken over by the company manufacturing the antennas.

Feed systems

For the antenna feedhorns operating at frequencies above 1 GHz, Radiophysics produced an innovative wideband design enabling dual-polarization observations at two widely separated frequencies. Currently, dual-frequency 1.5 GHz/2.3 GHz and 5.0 GHz/8.6 GHz feedhorns are mounted within a rotatable turret offset from the centre of the reflecting surface, and an appropriate rotation sets the required feedhorn at the Cassegrain focus of the antenna. The 1.5 GHz/2.3 GHz feedhorn is quite large - over 2 m long and up to 1 m wide. If constructed conventionally from a cast aluminium billet (as for the smaller 5.0 GHz/8.6 GHz feedhorn), the weight would have been prohibitive. In 1985 a new construction technique was devised, in which a 'light-weight' corrugated conical horn was constructed from bands and rings of sheet aluminium.

Feed systems operating over the frequency range quoted above require band splitters which provide dual-polarization outputs in two frequency bands up to an octave apart. These were not available commercially in 1984, and development work was started at Radiophysics. After considerable discussion between astronomers and engineers [7,8] it was decided to use linearly, rather than circularly polarized, systems. Technically, the former provided a wider frequency coverage, less cross-polarization, lower insertion loss, and more engineering flexibility. Astronomers were undecided; some argued that a linearly polarized system could yield accurate measurements of low levels of circular polarization, while others were concerned about the use of such a system in calibrating system gains. In 1987, after testing several types of polarizer, a quad-ridged polarizer design was adopted. These units were constructed in the Radiophysics workshop.

Receiver systems

The signals collected by the feedhorns are fed to low-noise receiver systems for amplification and conversion to signals at lower, more manageable frequencies. Separate systems for the two frequency ranges of each feedhorn are housed in a common stainless steel Dewar directly below the feedhorn, and refrigerated down to -263° C with a closed-cycle helium gas system. The receivers initially contained low-noise field effect transistor (FET) amplifiers; in future upgrades, the high-frequency FETs will be replaced with high electron mobility transistors (HEMTs).

Data transmission

Each antenna provides four signal streams with bandwidths of up to 256 MHz for transmission to the Control Centre through optical fibres. These signals are digitised at 512 MBaud/s before transmission. One early difficulty in setting up this system was to obtain

an optical-fibre connector robust enough to withstand repeated disconnection and reconnection in the dusty environment of the Observatory. Because of potential reciprocity and phase problems with the fibres, the narrowband reference-frequency signals required by each antenna are transmitted from the Control Centre through conventional coaxial cables.

For the Long Baseline Array, it was originally proposed to interconnect the Parkes, Coonabarabran and Narrabri sites using microwave links. However, the available bandwidths would have been too small to provide good sensitivity and enable effective on-line correlation. In addition, the annual licence fees would have been substantial. Therefore, in 1984 we decided to store the antenna signals received at each site on magnetic tape, for subsequent correlation at Narrabri. The lack of suitable recording and playback systems has delayed this part of the project. Suitable recording units at a reasonable cost have now been developed in Canada and will be purchased. In 1987 we decided to use the communications satellite AUSSAT (now Optus) to beam to the sites the frequency reference signals transmitted from the Narrabri Control Centre.

Correlators

The signals reaching the Control Centre from the Compact Array antennas or on magnetic tape are processed in large correlator systems. (At full Compact Array operation using all 15 baselines, the correlator must carry out 2×10^{12} multiplications per second.) A correlator has been constructed to process Compact Array observations. Smaller correlators have also been constructed for the Parkes and Mopra antennas, to support 'stand-alone' operation at these sites. The Long Baseline Array correlator has still to be constructed; it will be separate from the Compact Array correlator.

Specifications for the correlator system were established at a Correlator Workshop held at Parkes Observatory in November 1983. The success of the AT design depended largely on the success of the correlator design, which in turn depended on developing a suitable very large scale integration (VLSI) chip. The chip was based on test structures developed by Dr J.G. Ables and Mr A.J. Hunt as part of the Australian Multi-Project Chip program of the CSIRO Division of Computing Research in Adelaide. Designed by Dr W.E. Wilson to operate at 14 MHz, the chips were found to operate successfully at higher frequencies. Therefore, in 1986 the operating frequency was increased to 16 MHz, thus increasing the Compact Array bandwidths from 160 to 256 MHz.

The largest computational load for the correlators is provided by spectral-line observations. The spectral-line emission and absorption associated with gas clouds in our and other galaxies have frequencies that are Doppler shifted according to the line-of-sight motions of the clouds. Therefore, to study these motions, images are required over the range of the shifted frequencies.

Computing

Software based on a sophisticated processing package AIPS (Astronomical Image Processing System), initially developed for the US Very Large Array, was adapted to enable final analysis and image processing of Compact Array data. This is generally carried out on an off-line computer network at the Radiophysics Laboratory, although computing facilities at Narrabri can also be used. In 1988 a CONVEX C1 supercomputer was added to the Radiophysics network, and has been progressively upgraded to a dual-process CONVEX C/220 configuration. Other computing facilities in the network include a MicroVAX 3400 processor, several SUN workstations, and an Intergraph IP-120 workstation.

5. CONCLUSION

5.1 From Construction to Operation

During the latter phases of construction, system testing became a major activity. It began in 1986, when a multi-frequency receiver system containing dual-polarization prototype models of all receivers currently on the Compact Array, was installed on the Parkes telescope for real-time testing. This system is still supporting front-line research at Parkes. At the end of 1987, a room was set up at Radiophysics for testing overall systems before installing them on the Compact Array. During the same year, tests of the Narrabri antennas operating as an interferometer array began; the first successful operation occurred in August 1988. The incorporation of an antenna into a VLBI network a few months later marked the first use of the Array for radio astronomy. During the following two years, additional antennas were brought into operation and periods of time were allocated for radio astronomy observations. In April 1990, with five operating antennas, one polarization, and two operating frequencies, the Compact Array began operating as a National Facility. By mid-1991 it was operating with all antennas, four frequencies, and two polarizations. In November 1991 the Mopra antenna was used for radio astronomical observations. In that month, the Steering Committee announced the formal completion of the construction project. The Australia Telecope had arrived!

5.2 General milestones in the AT Project

1975

Nationally representative Steering Committee proposes to ASTEC that a new high-resolution radio telescope be built in Australia.

1979
ASTEC recommended that the Australian Synthesis Telescope be given first priority among telescope proposals.

1981
Unsuccesssful request by CSIRO for Government funding of the AST. Redeveloped proposal (the Australia Telescope) becomes CSIRO top priority item.

August 1982
Approval of Australia Telescope Project by Australian (Fraser) Government.

November 1983
Final Government approval as a $30.7 million construction project (March 1983 values).

September 1984
Ceremony at Paul Wild Observatory Narrabri to mark official inauguration of construction.

July 1985
Government approval of project recosting to $43.094 million (March 1985 dollars).

December 1985
Completion of civil works.

May 1987
First completed 22-m antenna handed over to Minister for Science, Custom and Small Business (B.O. Jones) at a Narrabri ceremony.

July 1987
Parkes radio telescope officially incorporated into Australia Telescope Project.

December 1987
Construction of the seven 22-m antennas formally completed.

January 1988
Government approval for revised cost estimate of $49,457,700 (as on 30th June 1987).

February 1988
R.D. Ekers takes up appointment as Foundation Director of Australia Telescope.

August 1988
First correlated cosmic signal detected using two of the 22-m antennas.

September 1988
Prime Minister Hawke officially opens Australia Telescope at a Narrabri ceremony.

November 1988
Australia Telescope antenna at Narrabri included in Australian VLBI project.

December 1988
First radio astronomy results with two-antenna array — flare-star observations by O.B. Slee and colleagues.

January 1989
Australia Telescope National Facility becomes independent CSIRO unit with Divisional status.

April 1990
Compact Array begins operation as a National Facility.

April 1991
Sixth antenna at Narrabri incorporated into Compact Array.

November 1991
First observations made with the Mopra antenna. Formal completion of the Australia Telescope Construction Project.

6 ACKNOWLEDGMENTS

We thank the many people who contributed to the project either directly or by serving on our various committees and working groups. We are also very grateful to Mr Phil Howson, the Australia Telescope Project Administrative Officer, who was involved with the project from its inception. He not only provided invaluable help in the financial and control areas, but was responsible for administering the personnel side of AT management.

7 REFERENCES

1. Ryle, M. and Neville, A.C., "A Radio Survey of the North Polar Region with a 4.5 Minute of Arc Pencil-Beam System", Mon.Not.R.Astr.Soc., 125, 39-56, 1962.

2. Bowen, E.G. and Minnett, H.C., "The Australian 210-foot Radio Telescope", Proc.IREE Aust., 24, 98-105, 1963.

3. Mills, B.Y., "The Molonglo Observatory Synthesis Telescope", Proc.Astron.Soc.Aust, 4, 156-159, 1981.

4. "The Culgoora Radioheliograph", Proc.IREE Aust., Vol. 28, No. 9, September 1967 (Special Issue), by J.P. Wild *et al.*

5. "The Fleurs Synthesis Telescope", Proc.IREE Aust., Vol. 34, No. 8, September 1973 (Special Issue), by W.N. Christiansen *et al.*

6. Manchester, R.N. "A Configuration for the AT Compact Array", Australia Telescope Doc. AT/10.1/036, 1984.

7. Forster, J.R. "AT Feed Polarization", *Ad hoc* Meeting, Australia Telescope Doc. AT/21.3.5, 1984.

8. Komesaroff, M.M. "Feeds for the AT: Should They be Circularly or Linearly Polarized?" Australia Telescope Doc. AT/21.3.1/010, 23 January, 1984.

DR R.H. FRATER

Dr Bob Frater graduated BSc, BE and then PhD from the University of Sydney. He was later awarded the DScEng for his work on instrumentation in radio astronomy. After graduating in 1960, he spent two years in industry before joining the University of Sydney to work on the electronics systems for the Mills Cross radio telescope. He also worked on the development of the stellar interferometer and the Fleurs synthesis telescope. Dr Frater was appointed to the University's academic staff in the School of Electrical Engineering in 1968. At the time of his appointment as Chief of the Division of Radiophysics in 1980, he was Director of the Fleurs Observatory. Dr Frater was Project Director during the construction of the Australia Telescope and was appointed Director of the CSIRO Institute of Information Science and Engineering in 1988.

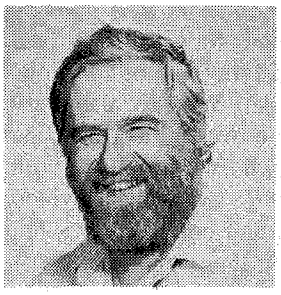

MR J.W. BROOKS

John Brooks obtained the BSc (Tech) degree from the University of New South Wales in 1964, and the ME degree in 1974 from the same University. In 1964-65 he was employed by the University of Manchester (UK) and worked at their radio astronomy facility at Jodrell Bank. Since 1965 he has worked for CSIRO, initially on low-noise receiving systems for the Parkes 64-m radio telescope. In 1977 he spent a year as visiting engineer at the National Radio Astronomy Observatory in Greenbank, USA. In 1983 he was appointed Project Manager of the Australia Telescope, and in 1988 was awarded a CSIRO medal for his work on the project. He is currently Assistant Director of the Australia Telescope National Facility and Assistant Chief of the Division of Radiophysics, CSIRO.

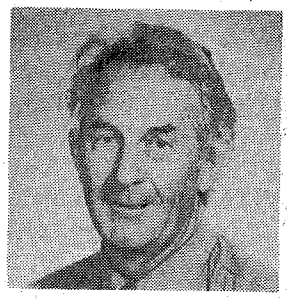

DR J.B. WHITEOAK

Dr John Whiteoak has a BSc degree from the University of Melbourne and a PhD in astronomy from the Australian National University (1962). He joined the CSIRO Division of Radiophysics in 1965, after a two-year Carnegie Fellowship at Mt Wilson and Palomar Observatories and a year at the California Institute of Technology. In 1971-1973 he spent two years on leave at the Max-Planck-Institut für Radioastronomie, Bonn. Dr Whiteoak was involved in the construction of the Australia Telescope as Project Secretary. Since 1989 he has been Deputy Director of the CSIRO Australia Telescope National Facility. His main research interest lies in the study of molecular clouds in our Galaxy and other galaxies.

The Australia Telescope System Description

G.J. Nelson*

SUMMARY The Australia Telescope Compact Array comprises six 22-m moveable antennas with a maximum east-west baseline of 6 km. Provision is made for operation in the frequency range 0.3 to 116 GHz. Flexible array configurations, wide, instantaneous bandwidths and tuning ranges, high polarization purity, aberration-free wide-field imaging, simultaneous operation at two frequencies, powerful spectral-line capabilities and high time-resolution operation are important features of the system.

1 INTRODUCTION

The design of the overall Australia Telescope (AT) Compact Array was a compromise between scientific objectives, costs and technical feasibility. For example, the number and size of the antennas was a trade-off between antenna, receiver and correlator costs. As a result, the decision was made to build six (quite a small number) antennas in an east-west array allowing wide-field, aberration-free imaging. This was judged to be the most scientifically rewarding configuration. The additional costs of providing a two-dimensional array may, for example, have resulted in one less antenna.

The design of the receiving system was partly driven by the availability of octave-bandwidth feeds and linear polarizers. This led to a receiving system which provided wide bandwidths and tuning ranges, and high polarization purity. The availability of fibre-optic and VLSI chip technologies enabled the wide bandwidths available at the receivers to be readily transmitted and correlated. The correlator technology also offered very powerful spectral-line capabilities and good time-resolution.

In the following discussion I will describe the AT system as originally conceived and will indicate which parts have been completed to date. It is unlikely that all of the remaining parts will be implemented exactly as envisaged but the provisions made to accommodate them have influenced the design in a number of ways.

* Australia Telescope National Facility, CSIRO, PO Box 94, Narrabri NSW 2390, Australia.
Submitted to The Institution of Radio and Electronics Engineers Australia in June 1992.

2 ANTENNAS

Five of the Compact Array antennas are transportable on a 3-km rail track with 35 stations on which antennas can be positioned. The sixth antenna is located a further 3 km to the west and is transportable to either of two stations separated by 75 m.

The antennas are each powered by a diesel generator when being moved between stations. When on station they are powered from a mains supply which is distributed underground to eliminate RF interference.

The antennas are steerable about azimuth and elevation axes; the azimuth bearing is a 4-m diameter slewing ring. Two servo-controlled d.c. motors power motion about each axis and the positions are measured by 23-bit encoders. The range of motion is from ~10 to ~ 95° in elevation and nearly 540° in azimuth.

The optics are Cassegrain with both the main and sub-reflectors 'shaped' (non-parabolic) to improve illumination efficiency and to reduce reception of ground radiation. Both reflectors are symmetrical and the feed is located on the optical axis at the Cassegrain focus. A rotating turret allows different feeds to be moved to the focal position with minimal loss of observing time. The main reflector is sufficiently accurate to operate at frequencies up to 50 GHz. The inner 15 metres is more accurate and is designed to operate to 116 GHz. The surface of these more accurate inner panels is solid, whereas the outer panels are perforated to reduce wind loading on the structure.

The total design of the antenna structure provides for a tracking accuracy of better than 10 arcsec in winds of up to eight metres per second. To avoid differential heating

by the Sun the whole of the structure below the elevation axis is shielded and is either air-conditioned or ventilated with ambient air. Tilt meters to be installed at the elevation axis will further reduce thermal effects on the pointing accuracy.

Focusing of the antenna is achieved by moving the sub-reflector. Initial transverse adjustments were carried out to produce a circularly symmetrical antenna pattern. Axial movement under computer control is then used in real time to compensate for changes in focus of the main reflector with elevation and for the variation with frequency of the focal point in the compact corrugated feeds.

3 ARRAY CONFIGURATIONS

The positions of stations along the 6-km east-west baseline were chosen to meet many criteria. The stations on the 3-km rail track are such that all baselines between 30 m and 3 km in 15-m increments are available. They can all be achieved with minimum redundancy using a set of 25 different antenna configurations. Whereas ten different baselines are obtained simultaneously with the 3-km array, only five are obtained in the range 3 to 6 km by adding the 6-km antenna. Baselines in that range are therefore less well distributed and only half as dense. Similarly a set of 12 configurations is available that gives complete coverage of baselines up to 1.5 km.

With several years of operational experience we have found that many observations require configurations considerably different from those originally envisaged. Fortunately the distribution of stations is such that a very rich variety of specialized configurations can be easily realised. At present 14 different configurations are used routinely. These include sets of four configurations with maximum baselines of 0.75, 1.5 and 3 km. Each member of a set gives a relatively uniform distribution of baselines while the combined set also gives a good but more dense distribution with no redundancy. The 6-km antenna can be used with any of these sets to give longer baselines but will be used, most commonly, with the 3-km set to add baseline coverage between 3 and 6 km.

Even shorter arrays with maximum baselines of 120 and 375 m are in frequent use where reduced resolution and increased brightness sensitivity are needed. These shorter arrays also highlight the inadequacies of having strictly 15- or 30-m baseline increments. These so-called 'grating' arrays produce strong artefacts in some images that will be removed only by adding new stations to provide different baseline increments.

One reason that sets of four configurations are adequate, even when imaging quite complex regions, is that all baselines can be effectively varied simply by changing the observing wavelength. The wide instantaneous and tuning bandwidths available with the Compact Array receivers means that frequencies (and effective baselines) can be changed cyclically during an observation, reducing the need to observe with additional physical baselines. This flexibility is, of course, not available when observing specific spectral lines or regions with complex spectral index in the continuum.

4 FREQUENCY COVERAGE

Figure 1 shows the AT frequency coverage as currently planned. The cross-hatched areas represent frequencies now in use. Originally, two bands sharing a common feed were planned in the range 20 to 50 GHz. These have now been replaced with the bands from 12 to 26, and 42 to 50 GHz. Two separate feeds will now be needed. Signals at frequencies above 1.25 GHz are accepted by wideband corrugated feed horns on a rotating turret. Feeds are rotated as required to the Cassegrain focus which is located on the axis of the main reflector. Signals at frequencies below 1.25 GHz will be accepted either by arrays of dipoles near the Cassegrain focus or by dipoles near the prime focus.

Any two frequencies within the bands covered by a given feed can be observed simultaneously. These two frequencies can be as close together as required or up to an octave apart. Frequencies can be changed with complete flexibility at the end of each array cycle (typically ten seconds) with no loss of observing time.

The change to a pair of frequencies covered by a different feed requires a rotation of the turret and takes about ten seconds. There are no serious operational limits to the number of such rotations. Thus a time-sharing observing sequence which includes all available bands is quite feasible.

5 THE CONVERSION SYSTEM

Figure 2 depicts the conversion system for the 8.6- and 5.0- GHz, and 2.3- and 1.5- GHz receivers. From the first conversion onwards only one of the four IF

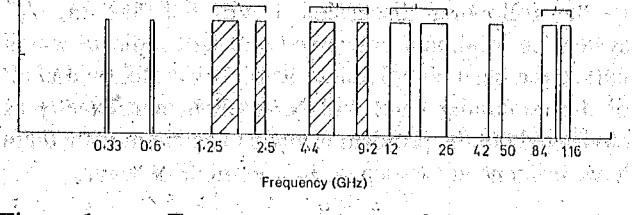

Figure 1 Frequency coverage of the Compact Array receivers. The bands shown cross-hatched are currently available. Bands shown bracketed share the same feed and are available simultaneously.

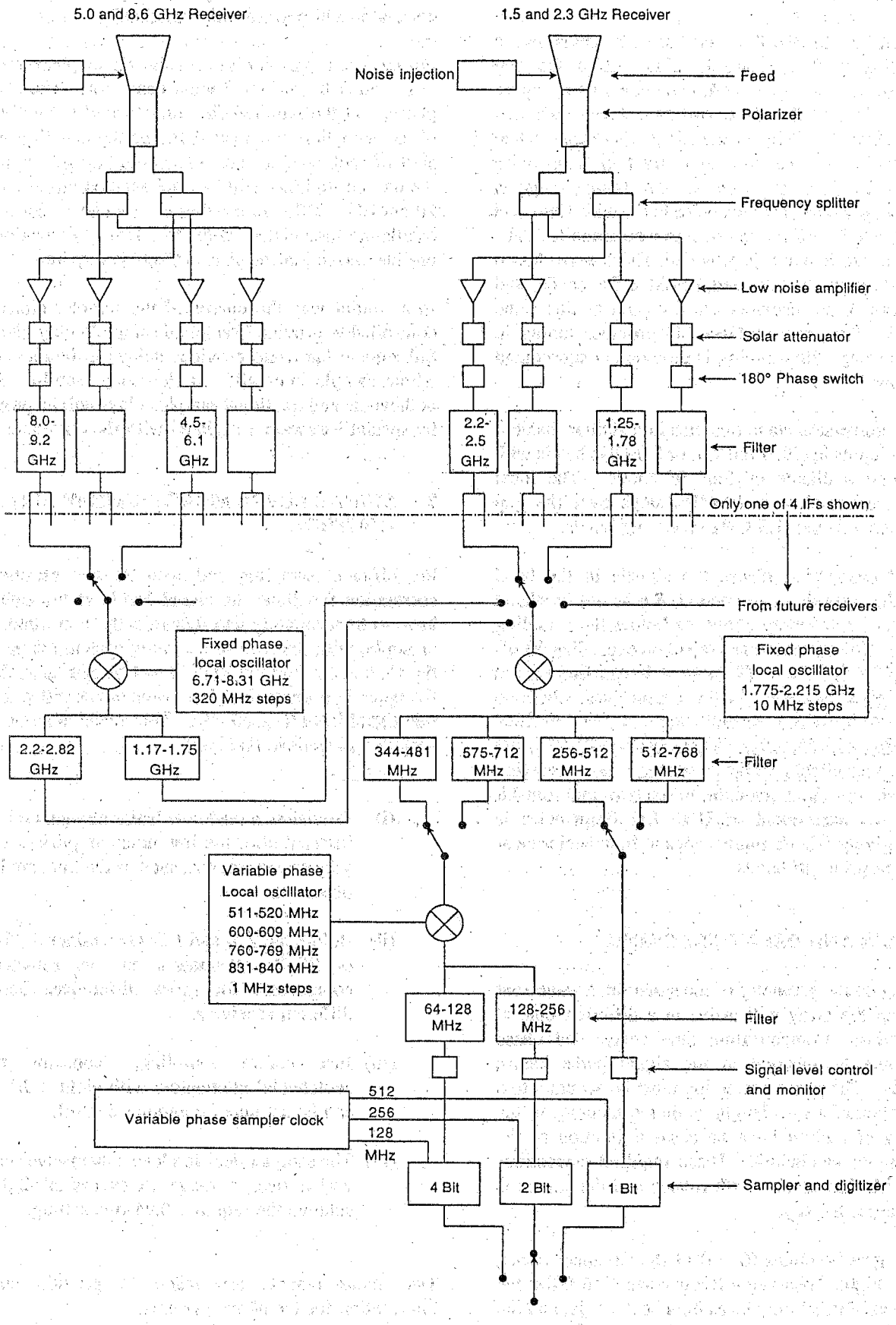

Figure 2 The Compact Array receiver system. The conversion system is designed so that local oscillator frequencies are in the gaps between the wide front-end bands. To achieve wide front-end tuning ranges with narrower LO tuning ranges, a choice of two IF channels is provided after each mixer.

channels (two frequencies, two polarizations) is shown. Provision is made at each stage to accept IF signals from future receivers.

The first mixer for the 8.6- and 5.0-GHz bands uses a local oscillator (LO) tuneable only within the gap between the bands. It therefore operates as an upper sideband mixer at 8.6 GHz, and as a lower sideband mixer at 5.0 GHz. This narrow LO range is imposed so that in dual-frequency operation any two frequencies within the bands may be used. The tuning range is insufficient to allow all frequencies in the wide front-end bandwidths to be converted down to a common IF. Thus a choice of two IF bands is provided. These were chosen to coincide with the 2.3- and 1.5-GHz RF bands, and inputs from these receivers are accepted at this same stage. The 8.6- and 5.0-GHz LO provides tuning in 320-MHz steps. Finer tuning is provided at subsequent conversions.

The next conversion stage operates in a similar fashion, accepting inputs in either the 2.3- or 5.0-GHz bands with outputs into a choice of four IF bands. The local oscillator is tuneable in 10-MHz steps over the gap between the 2.3- and 1.5-GHz observing bands.

The final conversion places the signals in the band required for sampling. In general, this is not baseband but a band immediately above or below the sampling frequency. This allows image rejection exceeding 40 dB to be readily achieved. (Signals at image frequencies produce 'ghost' features in the synthesized telescope image.) Three choices are available: one-, two- or four-bit digitizing with sampling frequencies of 512, 256, and 128 MHz respectively. In the one-bit case no conversion is required. For the conversion to the two- and four-bit samplers, an assortment of UHF LO frequencies is provided giving 1-MHz tuning steps at frequencies clear of the appropriate IF bands.

6 PHASE AND DELAY TRACKING

Depending on the geometry of the situation, a wavefront incident on the array will arrive at a different time at each antenna. Compensating time delays and phase offsets must be inserted in the signal paths before correlation. The phase correction must be accurate to a small fraction of a wavelength while the accuracy of the time-delay correction must be a small fraction of the inverse signal bandwidth. These required corrections change with time as the earth rotates and the source is tracked across the sky.

On the largest baselines (6 km) of the Compact Array, and at the highest observing frequencies (116 GHz) the rate of phase change may be as high as 2.5 kHz, and the corresponding rate of delay change is ~ 25 ns $^{s-1}$. Higher rates are required for the Long Baseline Array (i.e. the six 22-m antennas at Narrabri, a seventh 22-m antenna at Coonabarabran and the Parkes 64-m antenna).

In the Compact Array the phase corrections are provided by controlling the phases of various local oscillators. (In the Long Baseline Array, special hardware in the correlator will perform this function.)

For two- and four-bit digitized signals the phase rotation is provided by the UHF local oscillator. The starting phase, and the required first and second derivatives of phase with time are loaded for implementation at the start of each array cycle. Phase rotation for signals to the one-bit digitizer will be implemented at the 13- and 20-cm LO. Different starting phases can be set for the oscillators associated with the two polarizations if on-line correction for phase offsets is required.

In a similar way the phases of the sampler clocks are controlled to provide 'fractional sample' delay tracking. Subsequent hardware provides delays in increments of whole sample intervals. In the Long Baseline Array both whole and fractional sample delays will be provided by special hardware associated with the correlator.

7 SIGNAL-LEVEL MEASUREMENT AND CONTROL

For efficient sampling and accurate normalisation of correlation functions the signal levels at the samplers have to be accurately and dynamically controlled. For example, with the two-bit sampling system adopted for the Compact Array the signal level should be such that the upper and lower decision levels are at ± 0.94 of the rms signal level respectively. Four levels of control are provided to achieve this goal.

(i) Provision is made for 'solar attenuators' to be inserted after the low-noise amplifiers where very strong sources, such as the Sun, are being observed.

(ii) Before the 2.3- and 1.5- GHz mixer 0-, 6-, 12- or 25-dB attenuators can be selected to compensate for gross differences between different receivers.

(iii) Just before sampling, 'constant phase switchable' attenuators with eight 2-dB steps can be set under computer control.

(iv) The sampler decision levels themselves can be varied over a range in excess of 2 dB to achieve the required 0.94-rms setting.

Two measurements are made to provide control information for the above systems.

(i) A total power monitor directly determines the signal level at the input to the sampler and can be used to control the 2-dB attenuator steps.

(ii) The distribution of samples amongst the four possible states is measured. For white noise with a Gaussian amplitude distribution, 17.3% of samples should be in each of the extreme states if the decision levels are set at 0.94 rms.

The decision levels are automatically adjusted until the required result is achieved. Similarly, the zero (sign) decision level is adjusted so that 50% of samples are positive. Small errors in the reference levels can be corrected in the correlator by applying appropriate d.c. offsets or normalisation factors.

8 AMPLITUDE AND PHASE CALIBRATION

The digitized signals sent to the correlator from each antenna contain no information about signal power because the signal levels are adjusted to match the sampler decision levels precisely. The correlator measures the correlation between each pair of such signals. If two signals are identical the correlation is 100%. To determine the noise power of the correlated component requires separate knowledge of the noise power at each sampler. To achieve this, a small but stable noise step is periodically injected into each feed. Its amplitude is typically 5% of the total system noise. Phase-sensitive detectors measure the noise step for comparison with the total power at the input to the samplers. The noise steps themselves are calibrated against standard astronomical calibrators.

The added noise is also used to measure the phase difference between orthogonal polarization channels. The noise is injected at 45° to the polarization planes and a correlator between the two channels is controlled to accumulate positively while the noise is on, and negatively when it is off. The phase of the resulting cross power spectrum is the required phase difference. It is a crucial factor in accurately determining the polarization parameters of the incoming signals.

9 INTERFERENCE AND IMAGE SUPPRESSION

Correlated internal interference such as local oscillator leakage or d.c. offset errors in the samplers can be reduced by cyclically imposing 180° phase changes on incoming signal and then removing the effect by synchronously reversing the sign of the sampler outputs. The antenna signal is thus unaffected, but spurious signals injected between the two 180° reversals carry the cyclic phase reversal through to the correlator. Provided the switching waveforms used are orthogonal between all antennas then in principle the effect of the correlated interference integrates to zero in the correlator. In practice, depending on the precision of the 180° phase change, suppression of up to 30 dB can be achieved. Provision has been made to implement such a system on the Compact Array using square-wave switching functions with frequencies of 0.125, 0.25, 0.5, 1, 2 and 4 kHz. Provided the integration time is a multiple of 8 ms these waveforms are orthogonal for all lags in the correlation function.

Another system using similar waveforms to impose cyclic 90° LO phase shifts can be used to suppress signals at image frequencies. At various phases of the two waveforms the signals are in phase (50% of the time) + 90° out of phase (25%) and - 90° out of phase (25%). At the same times, signals at the image frequency are offset in phase by 0°, -90° and 90° respectively. In the correlator, correlation functions are separately accumulated for the 0, 90° and -90° phase-offset periods. The phase offsets are then corrected and the separate correlation functions are added. After this process, signals at the image frequency have zero phase offset for half the time, and 180° phase offset for the other half. In the final correlation function they therefore cancel. The degree of image suppression that can be achieved again depends on the precision of the 90° phase steps.

Locally generated interference that enters the receivers via the feeds is not removed by the 180° phase switching. To protect against this, provision has been made for RF shielding of the vertex rooms of the antennas. Most potential sources of interference such as the oscillators are located in these rooms. The feeds and low-noise amplifiers are in a separate room higher up in the antennas.

10 BANDWIDTH

The Compact Array has been designed to provide bandwidths ranging from 0.5 to 256 MHz, incrementing by factors of two.

The 128-MHz bandwidth, sampled and digitized to two bits, is the standard for continuum observations. (The 256-MHz, one-bit option offers the same continuum sensitivity, the loss in sample efficiency cancelling the improvement due to the wider bandwidth.) The other bandwidths are required for spectral-line observations where the bandwidth is matched to the Doppler spread of the source. The number of cross-spectrum channels available from the correlator increases inversely as the bandwidth decreases. The frequency resolution therefore increases as the inverse square of the bandwidth.

The 64-MHz bandwidth is digitized to four bits at the antennas. At the control centre these data can undergo digital-to-analog conversion, narrowband filtering and re-sampling to provide bandwidths below 64 MHz. It is planned that these filters will be located in a common thermal environment to improve bandpass tracking between antennas. There will be several conversion stages in the filtering process so that most filters will have ~ 50% bandpass. This system has not yet been implemented but in the interim a selection of filters can be connected in series with the 64-MHz filters at the

antennas. These filters have ~ 5 and 10% bandpasses respectively and are each in different thermal environments. The effect of the correspondingly poorer bandpass tracking on closure phase and dynamic range has not yet been evaluated.

11 FIBRE-OPTIC DATA TRANSMISSION

Whether or not the IF signal is digitized to one, two or four bits, the data rate is the same; 512 Mbits s^{-1} for each of the four IFs. These data are Manchester coded and used to amplitude modulate a 1300-nm fibre-optic laser driver. Four multi-mode fibres run from each antenna station to the correlator (one for each of the four IF channels). The coding ensures that a level transition occurs at every clock interval enabling the recovery of the clock at the correlator. Synchronizing code is added to the data stream at the start of each array cycle. This allows each bit to be correctly identified at the correlator irrespective of temporal changes in length of the fibres. The timing of the synchronizing code is determined by a special-purpose clock running on the LO reference signal at 128 MHz.

The data fibres are also used to transmit time-frame information from the central clock to the antennas and to provide communications between the central computer and the antenna computers. To achieve this, light at 850 nm is modulated with the required information and multiplexed onto the fibres with the 1300-nm data carrier.

12 LOCAL OSCILLATOR DISTRIBUTION

The local oscillator is distributed from the central building on a common coaxial cable to the 35 stations on the 3-km array and via mono-mode optical fibre to the isolated 6-km antenna. In each case, reference frequencies of 5 and 160 MHz are used. To compensate for temporal changes in travel times, the signals are returned to the central building and the 'round-trip' travel times monitored. Corrections for variations can be applied off-line to the data, or on-line by individually compensating the starting phases of the phase-tracking oscillators in each antenna. The outgoing and return reference signals are time-multiplexed onto the common coaxial cable for the five antennas of the 3-km array. Flywheel oscillators at each antenna are used to maintain phase stability while the coaxial cable is multiplexed amongst them. For the isolated 6-km antenna, separate fibres in the same bundle are used for the outgoing and returning signals, and no time multiplexing of the fibre is required.

The LO distribution system is designed to achieve relative timing between antennas of about 1 ps. This error is generally smaller than the relative delays imposed on the signals to the various antennas while traversing the Earth's atmosphere.

13 CORRELATION

In the control building the digitized IF data streams are individually delayed in the digital delay system before being transferred to the correlator. In this process the synchronizing code is identified and the data streams aligned so that all samples entering the correlator at a given time are from the same wavefront at the antennas.

The input to the correlator involves a serial-to-parallel conversion so that the correlator runs at a manageable 16 MHz rather than at the 512 MHz of the incoming data. Cross-correlation functions are then computed for all combinations of antennas. Both parallel and orthogonal polarization signals are correlated so that the full polarization state of incoming signals can be determined. The correlation functions are Fourier transformed to produce cross-power spectra.

At the end of each correlator cycle the output therefore consists of a matrix of correlation measurements of the incoming radio signal as a function of frequency, polarization, baseline and orientation of the array (determined by the rotation of the Earth). Each correlation is a measure of the one-dimensional spatial Fourier component of the brightness distribution across the sky corresponding to the frequency, baseline and orientation of the observation. If such Fourier components are measured for sufficient baselines and orientations, then a two-dimensional Fourier transform of the data will yield images of the brightness and polarization distribution as a function of frequency across the region of sky being observed. In practice, these data are accumulated for as wide a range of baselines and orientations as is demanded by sensitivity requirements or by the complexity of the region being imaged. The subsequent Fourier transformation and image enhancement is done off-line.

14 COMPUTER CONTROL

The various and quite intricate operations of the Compact Array system are coordinated by a network of computers. The functions of each computer were allocated mostly for ease of initial development. Thus the servo-control of the antennas, the control of other antenna systems, the operation of the correlator and the design of the main observing control system were developed independently, each with its own computer and each with simple and clearly defined network interaction.

This approach was successful in many ways but networking problems encountered in operation now make it worthwhile to amalgamate some of these distributed functions. At this stage the antenna servo-control and the general antenna control have been re-implemented in a single computer at each antenna. In future, the correlator control and the main observing control will almost certainly be combined in a single machine.

15 CONCLUSION

More detailed descriptions of the implementation and performance of each part of the system are given elsewhere in this issue.

The basic operation of the system was proved in Laboratory tests before the various components were installed at the Observatory. Final testing on a single pair of antennas was undertaken in mid-1988 before full-scale production was begun. Testing and refining the system, as new capabilities are added, is still continuing. To date, no insurmountable problems have been identified but many areas of potential improvement remain.

16 ACKNOWLEDGMENTS

The design of the Australia Telescope system involved many people, including many of the authors in this special issue of *JEEEA*. Others who contributed in important ways include the late Alec Little who laid the foundations of the system design, Rick Forster who, as project scientist, influenced most areas of the system, the late Max Komesaroff who strongly advocated the use of a wideband linearly polarized system, and Dick Manchester, Geoff Poulton and Don McLean who undertook a configuration design study and specified the distribution of stations along the array.

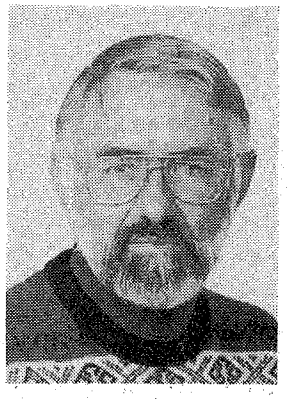

DR G.J. NELSON

Dr Graham Nelson is a graduate of the University of Sydney. He was awarded the degrees of BSc in 1962, BE in 1964, and PhD in 1968. During 1965 he worked as an electrical engineer in the NSW Electricity Commission. In 1968 he was a Nuffield Foundation Fellow working on the development of the Fleurs Synthesis Radiotelescope. During 1969 and 1970 he worked at the Arecibo Observatory in Puerto Rico. In 1971 he joined the CSIRO Division of Radiophysics' then solar observatory at Narrabri, NSW, using optical techniques to study magnetic fields and flares on the Sun, and later using the metre-wave radioheliograph and radiospectrograph to study the dynamics of the solar corona. During this time he was also the resident radio engineer for these instruments. In 1985, with the closing of the radioheliograph he moved to the Division's Epping Laboratory to work on the overall system design of the Australia Telescope and to do research into the coronae of active stars. In 1988 he returned to Narrabri as Officer-in-Charge of the Paul Wild Observatory and maintains his interest in the physics of the atmospheres of the Earth, Sun and stars and in the development of radio-telescope systems.

Journal of Electrical and Electronics Engineering, Australia
Special Issue

THE AUSTRALIA TELESCOPE

Chapter 2

Signal Path

The Antennas

D.N. Cooper*, G.L. James*, B.F. Parsons* and D.E. Yabsley*

SUMMARY As part of the Australia Telescope construction project CSIRO, in conjunction with Macdonald Wagner & Priddle (now Connell Wagner), produced two new designs for 22-m diameter antennas (one mounted on bogies, the other fixed), to operate at frequencies up to 116 GHz. In the evolution from currently operating antennas, special attention was given to transportability, azimuth transfer, control systems, thermal performance, wind loading, and surface panel manufacture. Seven antennas were constructed, six movable instruments in an array near Narrabri, and a single, fixed ('wheel-on-track') antenna near Coonabarabran.

1 INTRODUCTION

The Australia Telescope project included the design and construction of seven 22-m diameter antennas, six (the Compact Array) located at the Paul Wild Observatory near Narrabri, and the seventh (the 'Mopra' antenna) near Coonabarabran. These antennas had their origins in the design study undertaken for an earlier unsuccessful proposal, the Australian Synthesis Telescope (AST). The AST antenna design provided a good benchmark for an updated version. The original intent was to produce a design capable of manufacture in Australia with a very high Australian content. This became even more of an imperative for the Australia Telescope and a target of at least 80% was set. The specifications for the new antennas were considerably tightened, to enable operation at frequencies up to 50 GHz using the full reflecting surface (compared with a maximum frequency of 22 GHz for the AST), and up to 116 GHz using a significant part of the surface. Another major change in design was the need for the Compact Array antennas to be movable, so that a full coverage of baselines to the maximum of 6 km could be attained for radio-source imaging with high dynamic range. A third change was the inclusion of a long baseline array (LBA) configuration in the Australia Telescope. This consisted of the Narrabri Compact Array operating in conjunction with the fixed Mopra antenna and the Parkes 64-m radio telescope.

The Division of Radiophysics maintained overall responsibility for the design and construction of the new antennas, subcontracting many aspects of the work. In not using a more traditional design-and-construction contract, CSIRO was prepared to trade the performance risks for additional flexibility and reduced cost during the design and construction stages.

The Division's considerable experience gained from designing, and continually upgrading, the Parkes radio telescope provided a confident base from which to embark on the new project. As well, the Division had, over the years, developed new techniques for high-quality-surface panel fabrication suitable for local manufacture through both the surface upgrades of the Parkes antenna and the Interscan landing system project.

The metamorphosis of the AST antenna design into the Australia Telescope antennas has been fully described by Cooper and Guoth [1].

2 THE AUSTRALIA TELESCOPE 22-m ANTENNAS

2.1 Design Development

In planning the AST, the design by 1979 called for a number of antennas with diameters in the 18 to 24-m range, operating at frequencies from 1.4 to 22 GHz. Budgetary estimates for the antenna elements were requested from a number of overseas antenna manufacturers. After reviewing these estimates the AST Steering Committee, given that the CSIRO Division of Radiophysics had considerable experience in all facets of antenna design and construction, assessed the possibility of having the antennas designed and manufactured in Australia. As a result, CSIRO engaged an experienced European antenna consultant, Ir.B.G. Hooghoudt, to advise a design team consisting of CSIRO staff and private consultants. This team undertook a design study

* Division of Radiophysics, CSIRO, PO Box 76, Epping NSW 2121, Australia.
Submitted to The Institution of Radio and Electronics Engineers Australia in June 1992.

for antennas suitable for Australian manufacture, with the express purposes of educating an Australian company in the field of precision antenna structures, and obtaining cost estimates for an antenna with a very high Australian content.

The AST failed to gain Federal Government funding. However, the AST antenna design work provided an excellent springboard for another proposal. This new proposal considerably modified the AST design and was renamed the Australia Telescope (AT). The AT received Australian Government funding in the August 1982 budget and was endorsed as a Bicentennial Project in 1983. The responsibility for its design and construction remained with the CSIRO Division of Radiophysics. The Division established a design team comprising groups within CSIRO for the radio-frequency 'optics', feed and panel aspects, the consulting engineers Connell Wagner (then Macdonald Wagner & Priddle) Pty Ltd for the civil, structural, mechanical and electrical work, and the University of Newcastle for the control system design. Towards the end of 1982 a detailed design began. The consultants worked closely with CSIRO under the direction of the AT antenna manager in establishing specifications and details for seven new 22-m diameter antennas.

The first phase of the AT project required a critical review of the antenna design with particular regard to the size/cost trade-off [2]. During this period several overseas radio astronomy institutions and antenna manufacturers were visited to obtain up-to-date comment on the AST design and on recent developments in antenna structures. As a result of this study tour some specific observations were made.

(i) The dish back-up structure required deepening to improve stiffness.

(ii) The plated fork-and-yoke approach to elevation axis support could result in serious thermal distortion effects under solar loading.

(iii) Fixed wheel-on-track antennas using a ground-level azimuth transfer cost less and are superior in performance.

Also, studies in Australia concluded that careful design of the quadrupod system would obviate the need for mechanised lateral subreflector movement, saving the cost and weight of complex equipment at the prime focus position. An assessment of panel manufacturing techniques, particularly the low-capital equipment approaches developed at the Division of Radiophysics, led to adopting a 2 x 2-m maximum panel size.

As a consequence, the dish back-up structure and its support were re-designed. A preliminary cost study evaluated 18-, 20-, 22- and 24-m diameter dish designs and concluded that seven 24-m or eight 22-m diameter antennas were possible within the original budget. Subsequent detailed costing of the overall project established the final choice of seven 22-m diameter antennas. The upper frequency range was extended to 50 GHz over the complete aperture, with operation to 116 GHz over the half-diameter central region.

In early 1983, a preliminary wheel-on-track approach was evaluated, incorporating a re-designed, deeper back-up and quadrupod structure. Although the ultimate decision was to retain movable elements for the AT, examination of the wheel-on-track antenna approach suggested incorporating its best features into a movable antenna array. The solution finally adopted, as recommended by the mechanical engineers, was to use a large slewing ring, trading off the costs of what was becoming a complex bogie system.

The effect of bearing compliance on antenna performance reduces as the cube of the diameter. Consequently, the largest possible slewing ring will allow less stringent specifications for bearing manufacture, enable the widest possible separation of the elevation bearings and provide good pointing performance. The best trade-off was found to be in the 5-m diameter range. Finally, a diameter of 4 m was selected to accommodate the machining capabilities of Australian industry. The final antenna design is illustrated in Fig. 1.

The stiffness of the basic back-up structure was assured by a relatively deep radial truss system supported on a stiff central ring truss. The transfer of dish loads

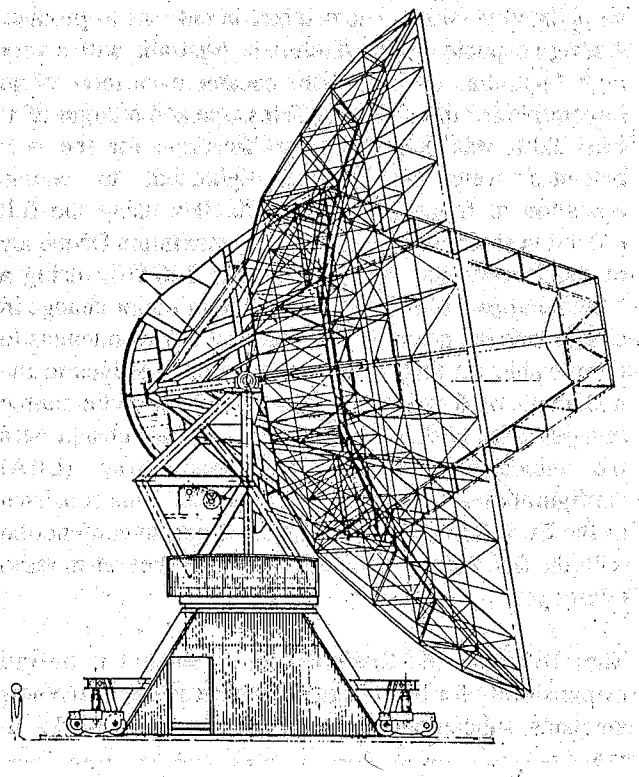

Figure 1 Final design for the AT slewing-ring, open-alidade, movable 22-m diameter antenna.

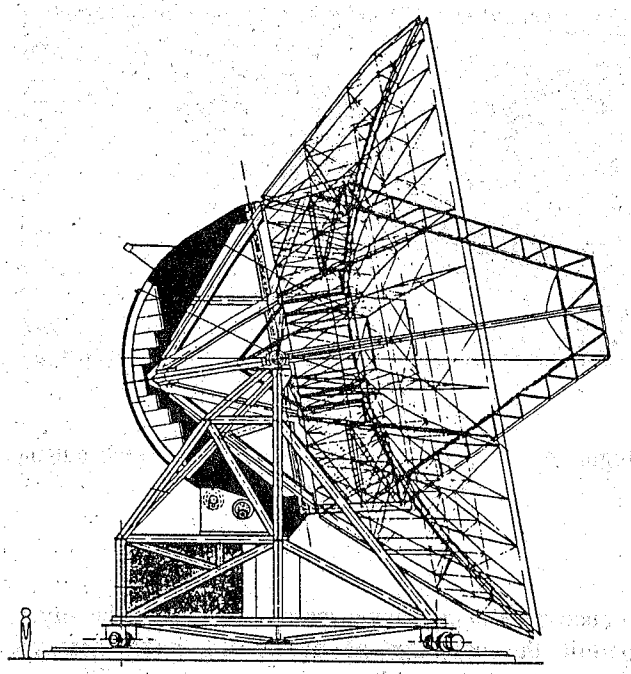

Figure 2 Final design for the AT wheel-on-track, fixed 22-m diameter antenna.

through to the elevation bearings is accomplished by a cone-pyramid member system. The ring truss is attached at eight points to a 'cone' of heavy members. The apex of this cone is coincident with a pyramid of members formed by the elevation-gear rack structure and connections to the elevation bearings. At the zenith positions, loads are transferred through this apex. The near-uniform loading condition on the reflector maintains symmetry in surface deflections.

The quadrupod is supported directly from the pyramid, totally decoupling it from the back-up structure. This results in little movement in the focus position. The net lateral distance between the subreflector focus and the best-fit paraboloid focus is constrained within the design criterion of ± 4 mm. The axial movement of the focus is designed to be within the specified ± 2 mm.

The design for the fixed Mopra antenna (Fig. 2) was developed from the earlier conceptual wheel-on-track layout. The possibility of stand-alone usage at high frequencies made the improved performance over the movable antennas attractive. The additional design costs were balanced by expected savings in construction. The pointing errors for this antenna were expected to be only 70% of those for the movable antennas. In a wheel-on-track design, to rotate a very heavy structure on a circular rail to high accuracy presents considerable difficulties. Typically, the task of transmitting large loads through wheels can be simplified by limiting individual wheel loads by an equalising bogie system. If variation in frictional torque is to be minimised however, it is essential that the wheels rotate without skew, requiring the wheel axis to align to the centre of rotation — in this case, the intersection of the top-of-rail

Table 1

Australia Telescope
Antenna Element Design Parameters

Diameter	22 m	
Focal ratio	0.32	
Elevation range	10° to 90°	
Azimuth range	± 285°	
Cone of avoidance	1°	
Optics	shaped dual reflector; on-axis feeds	
Surface accuracy	0.43 mm rms (D = 22 m) 0.24 mm rms (D = 15 m)	
Operating frequencies	1.25 - 116 GHz in rotating turret 330, 600 MHz (nominal) 2.3/8.4 GHz simultaneous (VLBI)	
Pointing accuracy	11-arcsec rms, precision operation	
Wind restrictions	8 m s^{-1} precision operation 20 m s^{-1} mechanical limit ('autostow') 45 m s^{-1} survival	
Axis rates:	Azimuth	Elevation
maximum tracking	0.3° s^{-1}	0.15° s^{-1}
minimum tracking	0	0
slewing	0.8° s^{-1}	0.4° s^{-1}
slew acceleration	0.3° s^{-2}	0.15° s^{-2}

plane and azimuth axis. The alignment of two wheel axes in a single bogie frame is therefore a relatively complex, costly fabrication and machining exercise, and is avoided where cheaper solutions are possible. The design selected for the Australia Telescope used a traditional wheel support in conjunction with a crowned rail tread.

Table 1 gives a summary of the AT antenna element design parameters [3]. We stress here that these were the design goals. The performance actually achieved for parameters such as surface accuracy are given later.

2.2 Mechanical Features of the AT 22-m Antennas

The seven new AT antennas are of dual-reflector design with axisymmetric Cassegrain optics. Figs 3 and 4 show the Compact Array and Mopra antennas.

Movable Compact Array Antennas

Each of the antennas at Narrabri is composed of three main parts.

(i) The **reflector** consists of the reflecting panels, their back-up structure, and a pyramidal support frame which rotates to form the elevation axis in a vertical plane about a horizontal axis. It also includes the quadrupod which supports the subreflector.

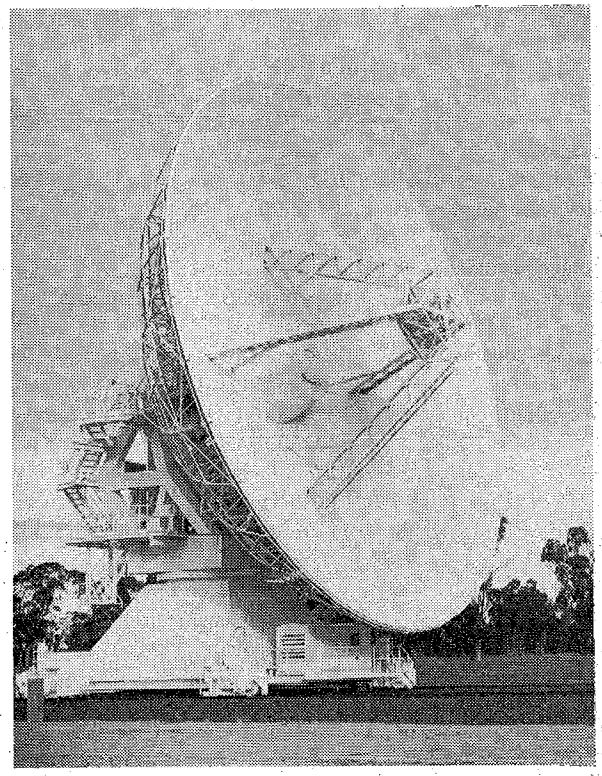

Figure 3 One of the six movable 22-m antennas of the AT Compact Array near Narrabri.

(ii) The **alidade** supports the reflector structure and rotates in plane to form the azimuthal axis about a vertical axis on a 4-m diameter slewing bearing.

(iii) The **pedestal** supports the slewing bearing and is normally fixed in position on reinforced concrete footings. For relocation, the pedestal is jacked up from its footings and driven along the rail track to reconfigure the array.

Electric systems provide the facilities for changing the position of the antenna in azimuth and elevation, rotating the feed-cone turret, focusing the subreflector, and moving it along the railtrack. Safety interlocks and emergency trip devices are major features of the systems. The power supply for each antenna is provided either from the mains, via a flexible 'umbilical' cable, or from an on-board diesel generator set.

The major mechanical items are the main axes bearings, main axes drives, feed-horn turret, subreflector support, and antenna relocation mechanism.

The **elevation axis bearings** are self-aligning, spherical roller bearings, both mounted as fixed bearings to distribute axial loads evenly to the alidade. Extra-high-precision bearings were selected and mounted with zero internal clearance and mutually aligned points of maximum inner-ring run-out for the two bearings to

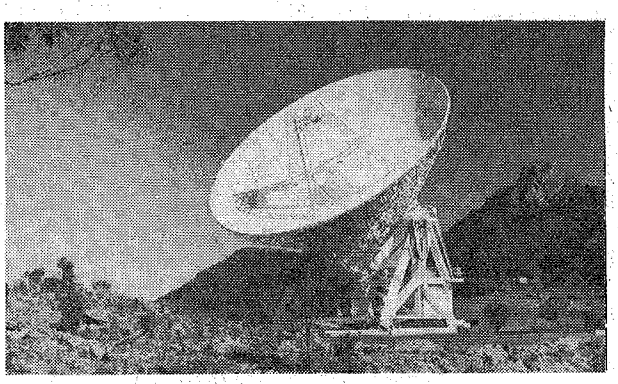

Figure 4 The Mopra 22-m wheel-on-track antenna near Coonabarabran.

reduce random pointing error and, more significantly, to permit the coupling of the 23-bit inductosyn-type position encoder with a minimum of misalignment-induced errors.

The **azimuth axis bearing** is a three-row roller-caged slewing ring, mounted between companion structures on the pedestal and alidade. The selected bearing represented the best compromise against the competing requirements of low capital cost, maximum internal stiffness, maximum accuracy with respect to pointing error, encoder coupling, and optimum frictional characteristics (minimum variation in frictional torque). The last characteristic in particular proved to be difficult to overcome, given both an accuracy-dictated zero-clearance roller configuration, and undetermined roller, cage and lubricant behaviour at the exceptionally low rotational speeds. Frictional testing carried out by the bearing manufacturer, however, helped to establish an upper bound to possible frictional torque variation which, when applied step-wise to the drive control system, gave an acceptable predicted pointing-error component. Differential deflections around the 4-m bearing are approximately 0.25 mm in 20 m s^{-1} winds. The run-out for the bearing is specified as 0.075 mm both radially and axially, and the compliance as 10^{-8} mm N^{-1}.

Direct-current motors driving through multistage planetary gearboxes and pinions were selected for both **axis drives**, using a large-diameter bullgear for elevation, and an internal gear integral with the bearing for azimuth. Two torque-bias drives on each axis resulted in zero backlash operation. Output gearing accuracy was determined on the basis of the predicted pointing-error component from a gearing transmission error applied through the drive control system. Gearbox selection proved to be dictated by stiffness requirements, whereby the lowest natural frequencies of the antenna were refined to be appreciably above the closed-loop bandwidth of the drive control system for stability. To maximise stiffness, all output pinions were supported on outrigger bearings.

The rotation about the two antenna axes is controlled by a **servo control system**. It ensures that the antenna dish follows the desired trajectory at the desired rate while maintaining pointing accuracy, despite the effects of external disturbances such as wind. The system consists of two identical d.c. drive motors for each axis, servo control, instrumentation (azimuth and elevation shaft encoders and tachometers), and a position-control computer. During tracking, a differential speed or torque bias is applied between the two motors on a given axis. This bias depends on the speed of the axis rotation, and is used to overcome gearbox backlash, and to improve the antenna pointing accuracy.

A **turret**, eccentrically mounted in the focal plane of the antenna dish, houses four separate feed horns and associated cryogenic receiving systems for operating over a range of radio frequencies. A drive system can rotate the turret so that any of the feed horns can be positioned in the focal plane. The system consists of a two-speed, pole-changing, reversing electric motor fitted with an electrically operated brake, an index pin thruster, and a rotary limit switch. The automatically operated indexing pin aligns the feed horn to an accuracy of better than 1 mm. The system is discussed more fully in [4].

The electromagnetic design incorporates the use of a **subreflector** and signal collection at the Cassegrain focus. To achieve remote axial focusing of the 2.75-m diameter subreflector, a novel support system using 16 pre-tensioned, stainless-steel wire ropes was developed. Axial movement is provided by an electric actuator, with positional adjustment to a fraction of a millimetre over a 50-mm travel range. Control is by a microprocessor, which communicates via a serial data link with a position-control computer in the pedestal room.

Observing programs with the Compact Array require frequent changes in the array configuration, effected by **relocating** the antennas. Accordingly, a self-propelled, long travel system was provided for each antenna. Bogies are located at the four corners of each antenna pedestal; a hydraulic jacking system is incorporated into each bogie. Under operating conditions the antenna pedestal rests on concrete piers for maximum stability. Extending the four rams results in raising the 230-tonne antenna off the piers, and support being transferred to the bogies. With a nominal 100-mm ground clearance, the antenna can then be driven to a new location. The drive system is a diesel-electric, two-speed a.c. drive system with a variable-frequency speed control for 'inching' at low speeds. The maximum travel speed is 1 m s^{-1} in winds up to 18 m s^{-1}. At the new location, the antenna is inched into position to within 5 mm; the error is subsequently calibrated out via optical measurement. The antenna is then lowered onto the new piers to resume operating the new array. During long travel, two of the hydraulic rams are interconnected to provide a statically determinate support for the antenna under varying conditions of vertical rail alignment.

Mopra Antenna

In contrast to the Narrabri antennas, this antenna is not transportable. The supporting structure consists of an alidade with a square base, the four corners of which have wheels running on a circular track. This configuration was chosen in preference to the Narrabri design, to provide a stiffer structure, more suitable for high-frequency observations. The extra design costs were offset by lower production costs.

In the main, mechanical components for the antenna were designed to be identical to those on the Narrabri antennas. The obvious exception to this is the azimuth support and drive whereby wheels on a circular track take the place of the azimuth slewing ring as used at Narrabri.

As already stated, a **wheel-on-track** design, rotating a very heavy structure on a circular rail to high accuracy presents difficulties. The selected design uses a traditional wheel support in conjunction with a crowned rail tread, giving an elongated ellipse contact area. Allowable stresses were evaluated on the basis of comparable mechanical components such as roller bearings, noting however that dissimilar parameters (such as steel quality and lubrication) required careful evaluation. The final design was a compromise between steel hardness, rail width and structural stiffness, ensuring that the contact ellipse remained on the rail surface under all conditions of loading and installation tolerance.

The **azimuth drive** consists of two torque-biased-driven wheels, with the gearbox spline-mounted onto the wheel shaft for maximum stiffness. This arrangement, in turn, requires accurate alignment of the wheel-bearing housing to ensure minimum additional loads into wheel and gearbox bearings. There is a centre pintle bearing consisting of a four-point-contact ball-bearing, sized to permit the transfer of electrical cables through its centre.

2.3 Electromagnetic Design Features [5]

Fig. 5 shows a cross-sectional diagram of the reflector area. Given the diameters of 22 and 2.75 m for the main reflector and subreflector respectively, it was necessary to optimise the reflector optics from an electromagnetic point of view.

In dual-reflector antenna design, it is standard practice to shape the reflector profiles in such a way that, for a given feed-horn radiation pattern, any desired aperture distribution can be produced. For maximum gain, a uniform aperture distribution is required. While this has been widely used in the past, it is not necessarily the optimum solution, since high levels of energy at the reflector edge give rise to correspondingly high far-out sidelobe levels, and thereby a higher antenna temperature, T_A. A better measure for antenna

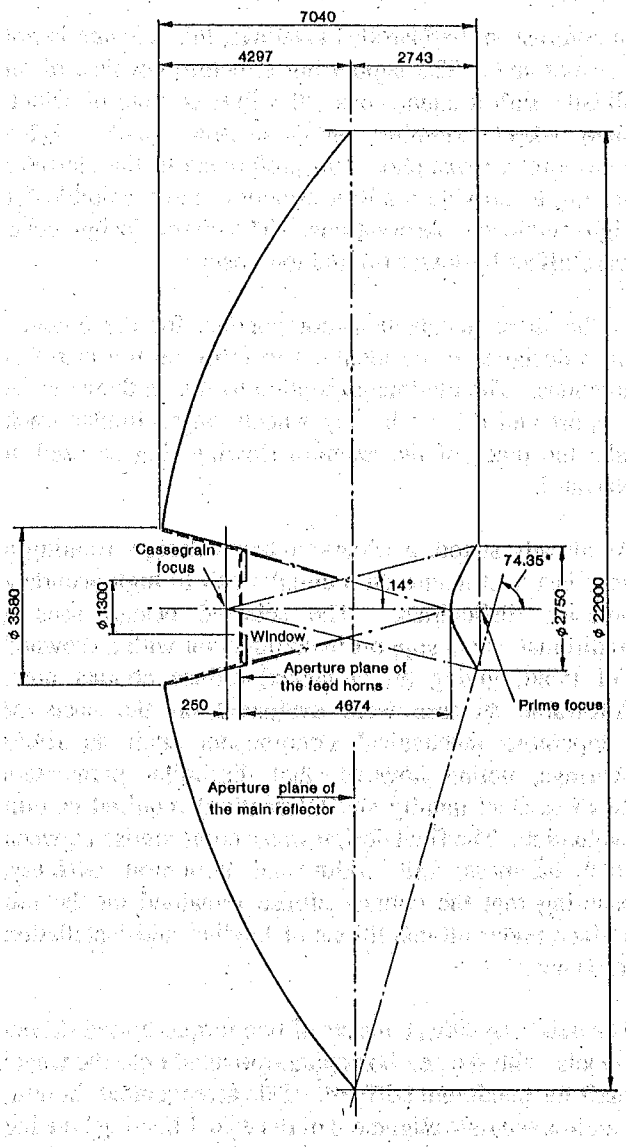

Figure 5 Cross-sectional diagram of the reflector area of the AT antennas.

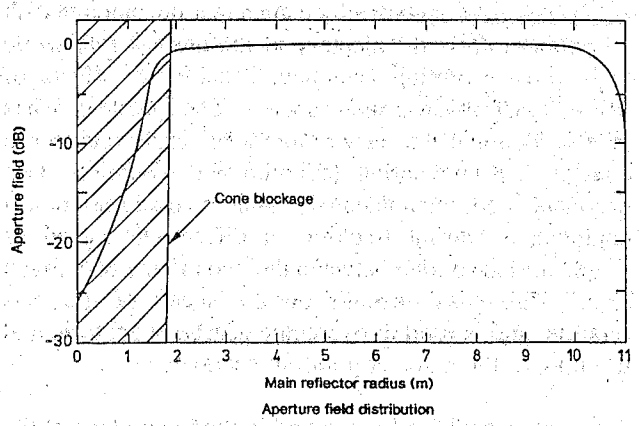

Figure 6 Aperture distribution used for design of reflector optics.

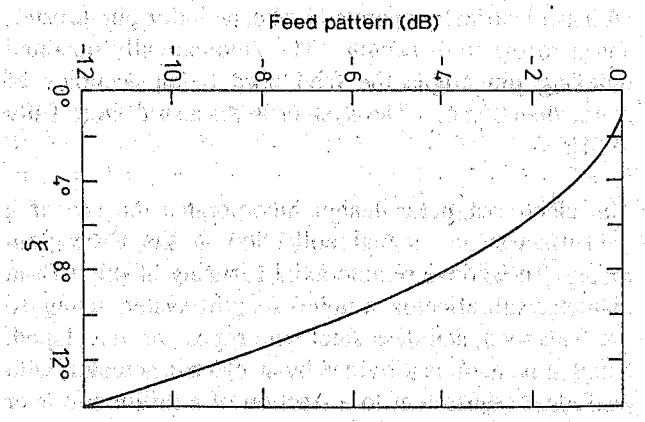

Figure 7 Feed radiation pattern used for designing reflector optics.

performance is the ratio of gain G to antenna temperature, G/T_A. Using this criterion, an aperture distribution with a taper towards the outer edge of the main reflector is found desirable in order to minimise T_A. In maximising G/T_A, the aperture distribution shown in Fig. 6 was finally chosen as the basis for designing the reflector optics. Note that as well as tapering the field towards the outer edge, the centre of the reflector, which is taken up by the base of the feed-cone housing, is under-illuminated.

Given the set dimensions of the main reflector and subreflector diameter, a variable to be chosen was the semi-angle from the Cassegrain or secondary focus to the subreflector edge. The choice of this value is a compromise between the space within the feed cone required, size of the feed horns, and the accessibility of the associated electronics. As shown in Fig. 5, a value of 14° was finally chosen.

For maximum efficiency, the feed radiation pattern taper to the subreflector edge should be in the vicinity of -18 dB (with respect to the on-axis intensity). However, several feed horns will be required to support operation in bands within the frequency range 1.25 - 116 GHz. To be able to accommodate all feed horns within the cone without the latter getting too large, the size of the feed horns, especially the large 1.25 - 2.5 GHz band horn, had to be minimised as much as possible. This led to a compromise in the feed-pattern taper; the taper to the subreflector edge was reduced to -12 dB. This compromise in edge illumination, causing an increased subreflector spillover, together with the use of compact corrugated horns, resulted in a reduction in overall efficiency.

While the various feed horns do not have identical radiation amplitude patterns, the optics design is not especially critical for small deviations in amplitude distribution between horns. In designing the optics, the typical feed radiation pattern of the 1.25 - 2.5 GHz horn at around 1.4 GHz was used, as shown in Fig. 7. This,

together with the aperture distribution given in Fig. 6, determined the reflector profiles. The resultant subreflector is somewhat conical in shape. The profile for the main reflector shows deviations from the best-fit parabola (Fig. 8). This means that if the main reflector is considered for use in prime focus mode, it no longer has a point focus. For the AT design, the reflector has a point of 'least confusion', denoted as the 'prime focus' position in Fig. 5. Compared with the best-fit parabola focus, this position is 46 mm towards the main reflector vertex.

In an axisymmetric dual reflector it is usual for the base of the cone housing to be within the shadow cast by the subreflector. However, although the development of wide bandwidth feed horns reduced the number of feeds required to cover the desired radio astronomy bands to four, it was nevertheless necessary to enlarge the feed-cone base to a diameter larger than that of the subreflector, to have all the feeds available within the cone housing. Thus, it is seen from Fig. 5 that the feed-cone base diameter of nearly 3.6 m is somewhat larger than the shadow cast by the subreflector.

Given the extremely wide frequency-range requirement for the AT antennas, the reflector profiles were designed on purely geometrical optics principles. However, in calculating the overall electromagnetic performance of the antenna, a full diffraction analysis was undertaken. Table 2 is a summary of the overall predicted performance of the antenna at a number of selected frequencies.

To verify the theoretical design, the far-field radiation pattern of a completed antenna was measured at the AUSSAT (now Optus) satellite beacon frequency of 12.25 GHz. The results are shown in Fig. 9, and the close agreement between theory and experiment is clear, providing a considerable measure of confidence in the overall performance.

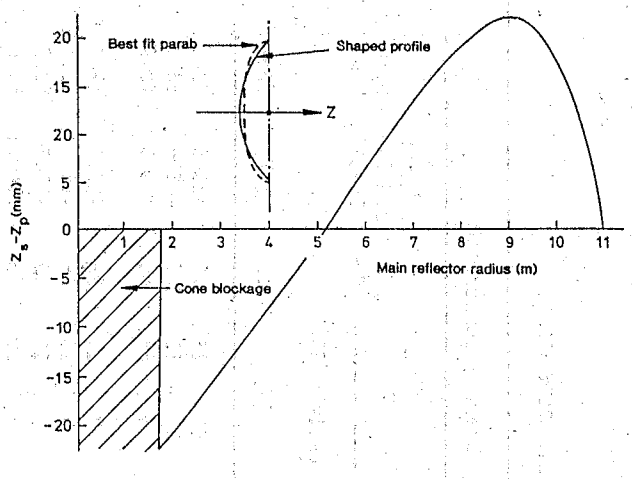

Figure 8 Deviations from the best-fit parabola for chosen main-reflector profile.

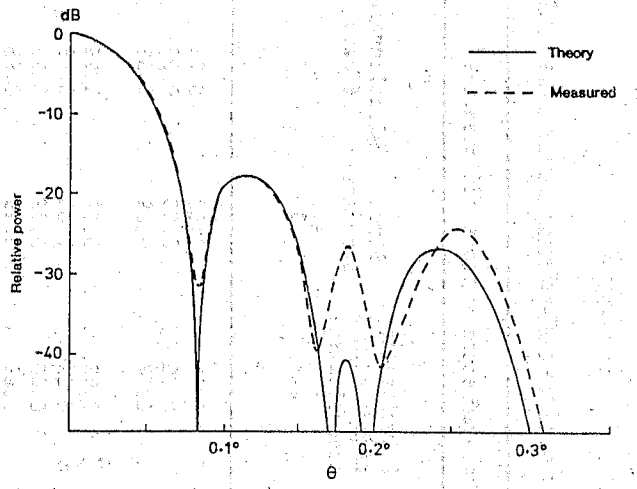

Figure 9 Comparison of measured far-field radiation pattern of 22-m antenna with theoretical pattern.

2.3 Structural and Servo Mechanism Design Features [3,6,7]

The structural and mechanical designs of large radio telescopes are dominated by the overall surface and pointing accuracy requirements. In both respects, antennas for radio astronomy differ significantly from their communication counterparts. Access to all the sky is usually required. Continuous tracking at a sidereal rate must be possible, and the pointing accuracy must be high in all directions. On the other hand, continuity of service is less important, and lower maximum wind speeds are accepted for precision operation.

The design centres on achieving the required specifications under normal operating conditions. In practical terms, the object is to support the collecting surfaces of the antenna in a way which permits the antenna to be pointed anywhere in the sky above a defined lower limit near the horizon, with the required degree of accuracy. The tolerances involved are such that survival conditions tend to be automatically satisfied; deflections and dynamics control the design. For the most part, wind is the important design parameter.

For the AT, there were some other special considerations. Of necessity, mechanical simplicity and ease of maintenance became important criteria in the design.

Surface Accuracy

The surface error is defined as the rms deviation between the real distorted surface and the so-called 'best-fit paraboloid'. The latter is an ideal surface which best fits the distorted shape with the least rms of residual errors. Table 3 gives the actual data, as manufactured, for panel and subreflector surface errors, for both the full 22-m antenna and the smaller central region.

Table 2

Predicted performance at selected frequencies of the dual-reflector antenna to be used in the Australia Telescope array

	Frequency (GHz)	Feed details: Spillover efficiency η_s	Feed details: Taper at 14° (dB)	Feed details: Loss due to pattern taper & phase errors, & to defocusing (dB)	Dual-reflector antenna efficiencies[4]: Surface errors η_1	Illumination, diffraction & cone blockage η_2	Strut blockage η_3	Miscellaneous effects η_4	Overall performance: Overall efficiency η_0	T_A Zenith (K)	T_A 80° (K)	T_S[5] (K)	First sidelobe level[6] (dB)	Gain (dB)
I[1]	0.327	0.58	-4.0	-2.4	1.0	0.82	0.89	0.95	0.40	51	85	40	-15.0	33.6
	0.408	0.70	-6.5	-1.6	1.0	0.83	0.89	0.95	0.49	31	85	40	-15.3	36.4
	0.650	0.85	-24.0	-0.8	1.0	0.77	0.89	0.95	0.55	13	58	40	-16.3	40.9
II[2]	1.25	0.85	-8.5	-0.4	1.0	0.93	0.89	0.95	0.66	7	19	25	-15.6	47.4
	1.5	0.92	-11.0	-0.2	1.0	0.89	0.89	0.95	0.69	7	19	25	-15.4	49.1
	1.8	0.92	-11.0	-0.7	1.0	0.80	0.89	0.95	0.62	7	19	25	-15.5	50.3
	2.1	0.90	-9.5	-1.2	1.0	0.69	0.89	0.95	0.52	7	19	25	-14.9	50.9
	2.3	0.90	-10.0	-1.5	1.0	0.67	0.89	0.95	0.51	7	19	30	-14.3	51.6
	2.5	0.92	-11.0	-1.4	1.0	0.68	0.89	0.95	0.53	7	19	30	-13.2	52.5
III[3]	4.4	0.85	-8.5	-0.14	0.99	0.92	0.89	0.95	0.65	7	18	35	-15.4	58.3
	5.9	0.92	-13.5	-0.05	0.99	0.93	0.89	0.95	0.72	7	19	35	-16.0	61.2
	7.4	0.92	-13.0	-0.42	0.98	0.87	0.89	0.95	0.65	7	20	40	-16.7	62.8
	8.8	0.96	-15.0	-0.45	0.97	0.83	0.89	0.95	0.64	7	29	50	-16.1	64.3
	10.6	0.97	-18.0	-0.4	0.97	0.82	0.89	0.95	0.65	7	30	50	-15.0	65.9

[1] Group I results have assumed a feed array mounted on top of the feed cone. The 2.2 m diameter effective aperture of the array is assumed here to be ideal in having uniform illumination with zero phase deviation across the aperture.

[2] Group II results have assumed a profiled corrugated feed horn using, at each frequency, the measured amplitude and phase patterns (from a scale model feed) taken at the phase centre and at a distance from the horn corresponding to the subreflector position. Using these realistic values for the feed pattern the subsequent loss in gain is indicated in the Table.

[3] Group III results also assume a profiled corrugated feed and treated in the same manner as for Group II.

[4] Dual-reflector efficiencies: η_1 assumes an RSS error of 0.43 mm for the reflector surfaces; η_2 results from a theoretical evaluation of the radiation pattern performance of the antenna system; η_3 is the strut blockage assuming struts of rectangular cross-section 0.23 m x 0.18 m with the base of the strut at a radius of 5 m; η_4 is to allow for miscellaneous effects such as feed and window losses, misalignments, etc.

[5] Assumed system temperature up to the feed aperture. Cooled receivers assumed for frequencies above 1 GHz.

[6] The first sidelobe level given here is in the plane between the struts. For radiation plane close or in the plane of the struts, the first sidelobe level can be expected to increase by around 3 dB to the value given here.

Table 3

Actual Surface errors for the AT antennas

	50 GHz rms (mm)	115 GHz rms (mm)
Panel manufacture	0.18	0.10
Panel measurement	0.05	0.05
Panel deflection	0.12	0.08
Panel adjustment	0.12	
Antenna holography		0.05
Structural deflection	0.13	0.03
Subreflector	0.15	0.10
rss	**0.32**	**0.18**

Table 4

Pointing errors budgets (arcsec)

	Mean peak		Remarks
	Narrabri	Coonabarabran	
Reflector	10.5	5.0	
Alidade	3.0	3.0)	
Companion		.)	
structure	2.0	-.-)	not
Pedestal	2.0	-.-)	independent
Foundations	2.0	1.0)	
Mechanical	2.0	2.0	
Servo			
Mechanism	2.0	2.0	

The surface accuracy is limited by the economical panel manufacturing methods available. The AT budget was deliberately chosen to ensure that the panel fabrication technology developed by the Division of Radiophysics could be used (see later). The most significant back-up structure deflections are due to gravity loads as the shape changes during elevational rotation. There is a technique of design, known as homology, which produces relatively 'soft' structures. These always deform into near-perfect paraboloids under changing gravity loads. However, this flexibility causes large changes in focal position, and a mechanised subreflector is normally required to follow the changes to prevent degradation in electromagnetic performance. These soft structures also deform more under wind loading. Wind can degrade both surface accuracy and pointing. For the 22-m AT antennas, it was feasible to use both a design that controls its shape by minimising deflections, and to incorporate some features of the homologous geometry.

Apart from the weight of the back-up structure, two other important elements control the distortions of the reflector. The quadrupod, which supports the subreflector system, can have a major influence on surface accuracy if supported directly from the back-up structure. On the AT the quadrupod legs are supported independently from the reflector. The dish support system has been designed to apply uniform loading to the back-up structure and yet transfer the load through to the two 'hard' points at the elevation bearings.

Pointing Accuracy

The pointing specification is 11-arcsec rms error in winds less than 8 m s^{-1}. In practice, the errors depend on site wind characteristics, the definition of rms, and the precision operating wind speed. Long-term statistics on pointing errors do not necessarily provide the correct information for an astronomer observing under particular weather conditions. Pointing errors are often based on empirical combinations of calculated sub-components, known to provide a good working value. For the AT, site wind statistics were combined with wind-tunnel data to provide a comprehensive assessment of pointing errors.

The maximum thermal and wind-pointing errors are mutually exclusive. The greatest thermally induced errors occur in very still conditions when large temperature differentials may exist across a structure. Quite low wind speeds of 1 to 2 m s^{-1} allow convective heat transfer from the structure and reduce the thermal gradients. Thermal pointing errors are contained by careful design of open structures. These allow good ambient air circulation; the differences between shaded and sunlit parts of structures are minimised.

Structural stiffness is most important in reducing the influence of wind on pointing errors. Stiff structures minimise changes in the shape of the reflector, due to wind for example. There is another, more subtle, gain from stiff structures, in that they considerably improve the dynamic performance of the structure and servo mechanism. Increasing stiffness raises the natural resonant frequencies of the structure, allowing wider bandwidth servo loops with a 'tight' response and good disturbance rejection. Disturbance rejection completely controls the servo design rather than the acceleration rates, which are very low for astronomy antennas. Although increased stiffness, more than any other factor, can improve pointing, it must be balanced against overall weight and hence cost.

The AT pointing-error specifications were calculated for all precision operating conditions. For much of the time the errors will be considerably less than the 11 arcsec specified. The wind-induced errors vary proportionally as the square of velocity. The upper precision operating wind speed was defined to include observing time when the fifth highest gust in any one hour is not greater than 8 m s^{-1}. This somewhat arbitrary approach was taken after examining continuous wind data records taken at the Narrabri site. It was assumed that at least five 30-s data blocks could be rejected each hour. Under the above definition, precision operating conditions occur 93% of the time.

The assigned pointing-error budgets for the movable and fixed antennas are given in Table 4. The entries in this table were allocated for the independent design of the

listed components. They were chosen to give an acceptable overall peak value. They are the means, calculated from all the peak values which occur at 8 m s^{-1} winds. The corresponding rms wind speed for pointing-error calculations is about 3.5 m s^{-1}. This reduces the errors to some 20% of the peak values.

The surface errors contributed to the overall antenna by the structure itself are totally dependent on the dish-alidade and dish-quadrupod connection systems. The stiffness and relative deflections of these systems influence the pointing performance under wind loading. Repeatable variations due to gravity loading are calibrated by radio astronomy pointing checks. Evaluating both surface accuracy and pointing requires that the properties of the best-fit paraboloidal surface [2] and quadrupod deflections be examined for a number of different loading conditions. Assessing gravity loading is relatively straightforward. However, wind-loading calculations are complex and the exact loading conditions uncertain. To aid in this latter assessment, wind-tunnel experiments were undertaken at Monash University.

Wind Loading

To model the porosity of the proposed AT antennas accurately, CSIRO was advised to carry out wind-tunnel tests on a model of the antenna before the design was finalised. Monash University was engaged to carry out the wind study with two main aims:

(i) to predict the distribution of normal pressures over the reflector surface of the antennas. This was used to determine the change of shape of the reflector structure due to wind load which produces both pointing error and a degradation in surface accuracy.

(ii) to predict the forces and moments on the supporting structure, alidade and pedestal and the foundations as well as the mechanical parts of the antenna — the azimuth bearing, elevation bearings and the gear boxes and drive motors.

An appraisal of the results was made, and design curves developed for the forces and moments. In these tests it was shown that porosity of about 40% for the outer panels reduced the wind loading on these panels by 25% compared with the solid counterparts. In addition to the direct reduction in wind-distributed amplitude, a secondary damping of edge vortices is achieved by the porous outer panels.

Based on overseas experience, the design was developed with the intent that the antennas should operate with full precision with a wind velocity up to 8 m s^{-1}. The mechanical equipment was designed for automatic stowing of the antennas when the velocity reaches 20 m s^{-1}. The antennas were designed for stresses which may occur when the antenna is in any observing position, for wind velocities of up to 28 m s^{-1} (to give a margin of safety).

When the antennas are stowed in the zenith position, the area of the panels projected to the wind is an optimal minimum. The antennas have been designed therefore for a survival-condition wind velocity of 45 m s^{-1} with the dish at zenith. This velocity has not been corrected for terrain and height. Rather, the provisions of the wind-tunnel testing as regards modelling of the terrain and variation of velocity with height have been adopted and the wind loads calculated from these data.

Tables 5 and 6 [8] summarise the calculated survival wind velocities for the transportable Compact Array antennas and the fixed wheel-on-track Mopra antenna. These values show that the antennas are well within the specifications and provide a wide margin of safety.

Thermal Design

The thermal control for the reflecting surface and back-up structure is the painting system, based on titanium dioxide filler. This material provides good reflectance of solar-heat radiation and yet re-radiates, efficiently, the longer wavelengths from the structure. The expected gradients of 3 to 4°C have no significant effect on the pointing distortions of the dish but may degrade the surface accuracy by 30 to 40μ rms.

Overseas experience has shown that the most serious pointing errors are caused by thermal-length variations of members on the pedestal and alidade structures. A number of features have been included in the AT antenna designs to overcome this problem. On the movable antennas, the entire pedestal structure is within the insulated and air-conditioned pedestal room, which houses computing equipment.

The alidade systems for both antennas are open-truss structures. The vertical members which could affect the pointing significantly are shrouded with insulating material. Ambient air is blown through the gap between the insulation and the member. The outer faces of the quadrupod legs are also covered with insulation.

Wherever possible, open-truss systems and open-rolled sections have been used in the structure instead of enclosed plated members and pipe sections. This avoids thermal lag by trapped air.

Servo Mechanism Design

The AT servo systems are based on four-quadrant SCR controlled linear d.c. drives. This technology was chosen for its robustness and maturity.

Table 5

Survival Wind Velocities
Transportable (Narrabri)

Item	Mode	Wind Velocity (m/s)		Comment
		Any Angle	Zenith	
Panels	Bolts Fail	55	68	
	Rib Yield	80	100	
Back-up Structure	Buckling of a Member	41	60	Not failure
Quadrupod	Buckling of a Member	63	63	Not failure
El. Bearings	Overload	N/C	*	See footnote
Bullgear, El. Drive	Brake Slip	54	*	
Alidade	Overstress	>100	>100	Fail >150
Azimuth Bearing	Overload	38	61	
Azimuth Drive	Brake Slip	37	*	(Lowest Value)
Pedestal	Overstress	>100	>100	Fail >150
Footing Pads	Lift Off	51	63	
	Slip	36	52	
	Damage	39	57	
Piers	Damage	45	55	Not failure of Antenna

NOTE:

Design Wind Velocities:

Operation	8 m/s	
Stowing	20 m/s	
Emergency	28 m/s	
Stowed	45 m/s (zenith)	

N/C : Not critical at feasible wind velocities

* : Preliminary calculation indicates adequate safety factor

Table 6

Survival Wind Velocities
Wheel-on-Track (Mopra)

Item	Mode	Wind Velocity (m/s)		Comment
		Any Angle	Zenith	
Panels	Bolts Fail	55	68	(as Narrabri)
	Rib Yield	80	100	"
Back-up Structure	Buckling of a Member	41	60	"
Quadrupod	Buckling of a Member	63	63	"
El. Bearings	Overload	N/C	*	See footnote
Bullgear, El. Drive	Brake Slip	>37	*	
Alidade	Overstress	74	93	Fail >100
Azimuth Wheels	Wheel Slip	44	>100	
	Lift Off	64	69	
Azimuth Drive	Brake Slip	37	*	
Pintel Bearing	Overload	60	80	
Rail	Overload	51	65	
Foundations	Centre Pier	48	60	
	Ring Beam	56	70	

NOTE:

Design Wind Velocities:

Operation	8 m/s	
Stowing	20 m/s	
Emergency	28 m/s	
Stowed	45 m/s (zenith)	

N/C : Not critical at feasible wind velocities

* : Preliminary calculation indicates adequate safety factor

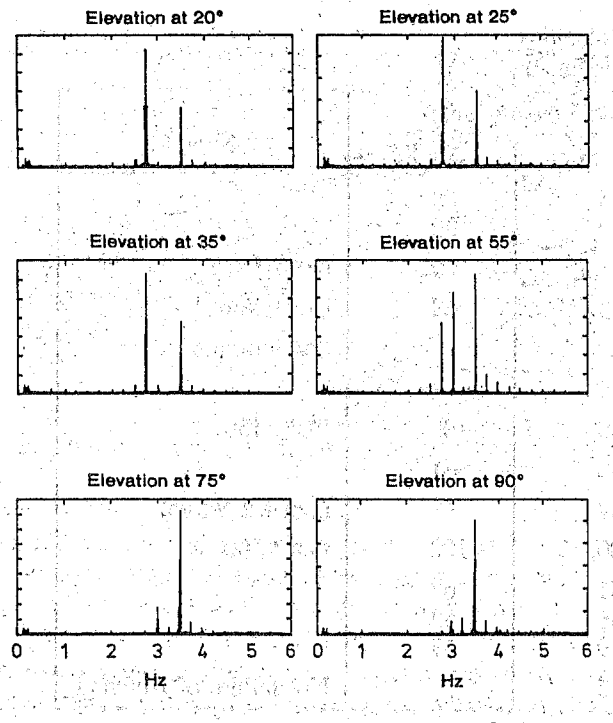

Figure 10 Movable antenna resonant frequencies from FFT analysis of antenna speed with step inputs over a range of elevation angles.

The drive for each axis has dual motors operating in a torque-bias, anti-backlash mode at low-demanded torques, and in a torque-share mode at high torques. The controllers use conventional current and tachometer-controlled rate loops. The wide dynamic range of speeds required for tracking astronomical objects is achieved under position control. A discrete position controller was implemented in a microprocessor. This allows flexibility in modifying the algorithm during commissioning. If measuring further antenna states with inclinometers or accelerometers is required later, expansion is easily accommodated. The position will be updated 15 times per second.

As wind-disturbance rejection is the prime design criterion for the servo mechanism system, bandwidths must be as large as possible. The lowest natural frequency for both AT designs is in the vicinity of 3 Hz for locked motor armature (Fig. 10), allowing a maximum position-loop bandwidth of 0.7 to 0.8 Hz. The rate-loop bandwidth must be much greater and approach that of the free rotor resonance, about 15 Hz. Provided the current loop appears as a pure torque source, which implies a bandwidth of 50 Hz or so, the rate loop has good disturbance cancellation and eases demands on the position loop.

Extensive simulation of the antenna and servo-control system was undertaken during the design phase to evaluate the effects of structural resonances, compliances and wind disturbance on the antenna pointing. For wind components based on Narrabri data, the overall rms errors for the design of the movable antennas were 1.7 and 1.4 arcsec in azimuth and elevation. The errors for the Mopra antenna were about 7% lower. For a wind-burst of 8 m s^{-1}, the errors increased to about 4.5 arcsec.

2.4 Development of High-Accuracy Low-Cost Surface Panels [9]

To operate the 22-m diameter antennas of the AT efficiently, the whole reflecting surface had to conform to the theoretical shape within a small fraction of the shortest wavelength of operation. For research instruments it is common to take as the operational limit the wavelength at which the surface efficiency falls to 50%. This occurs when the effective overall rms surface error (strictly the residual rms half-path deviation from the best-fit theoretical shape) is 1/15 of the wavelength. The reflecting surface of each AT antenna contains six concentric rings of panels — a total of about one thousand panels for the seven antennas. Efficient use of the whole surface is required at frequencies up to 50 GHz (6-mm wavelength), and of the central 15.2-m diameter region (i.e. the four inner rings of panels) for higher frequencies up to 116 GHz (2.6-mm wavelength).

When considering the accuracy of a reflecting surface, not only must the surface panels be taken into account but also the panel alignment, subreflector accuracy, effects of wind loading, and gravitational distortion of the back-up structure. In considering the square root of the sum of the squares (rss) of these errors, a maximum permissible value of 0.42 mm was set. Within this budget, the largest item was an allowance of 0.25 mm for the manufacture of panels that would be efficient at frequencies up to 50 GHz.

An overall rss value of 0.172 mm would be required to achieve a surface efficiency of 50% at 116 GHz. This was judged to be not attainable within the financial constraints of the project. Instead, a goal of 0.24 mm was set for the overall accuracy, with a value of 0.15 mm set for the inner surface panels. This would yield an efficiency of nearly 50% at 85 GHz but only 27% at 116 GHz.

In practice, the panels as manufactured far exceeded the design specifications, with an overall rms error for all perforated panels of 0.180 mm and, for the solid surface panels, an rms error of 0.100 mm.

Development Program

The manufacture of panels to this high standard of accuracy had not been attempted previously in Australia. However, over the last 20 years, the Division of Radiophysics has built up considerable experience in the design and manufacture of accurate doubly-curved

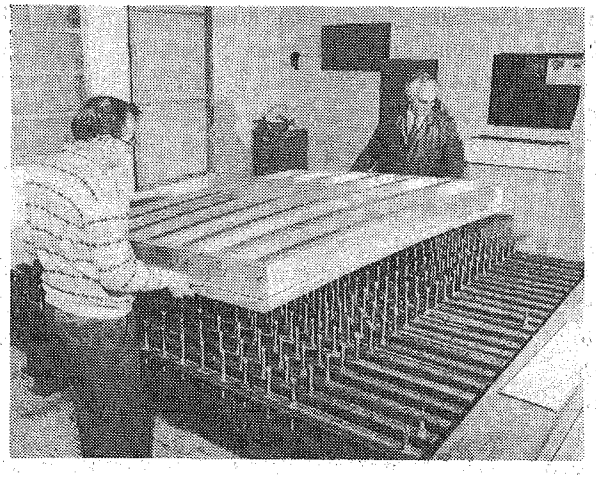

Figure 11 Finished panel being lifted from the adjustable assembly from 'bed of bolts'.

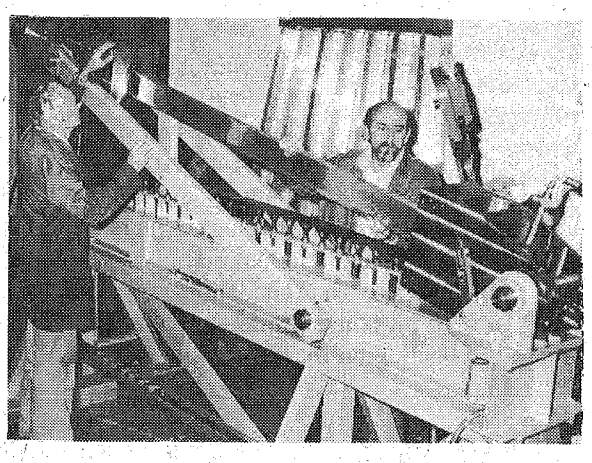

Figure 12 The stretch-forming machine for shaping the ribs of the panel frames.

surface panels. These panels were formed using perforated aluminium sheets riveted to extruded aluminium frames. The frames were constructed from preshaped members. These surface panels were satisfactory for frequencies up to about 25 GHz but, without further development, they would have been unsuitable for the AT project. Therefore, to meet the tight specifications on the panels while containing the cost, this technique was extended to enable low-volume manufacture without the need for expensive machined moulds.

The key element in the project was the construction of a 'bed of bolts', an assembly mould which could be adjusted to the contours of any of the six different panels. This adjustable form consisted of spherical-headed bolts on a 100-mm-square grid covering an area of 2.1 x 2.3 m^2 (Fig. 11). A self-aligning head with a flat surface 20 mm in diameter capped each bolt.

The procedure was simple; the main requirement was a beam fitted with 24 dial gauges at 100-mm spacing. The beam was initially set up over a calibrated straight edge. Each dial gauge was located in a slot which allowed its position to be adjusted vertically as part of the setting-up procedure. Then, with the aid of blocks of known thickness, the position of each dial gauge in its slot was adjusted so that all dials gave equal readings when the gauge tips lay on a curve identical with the specified profile.

For the backing frame, stretch-formed ribs were preferred to slotted frame members because of their greater strength/weight ratio. Figure 12 shows the stretch-forming machine which was developed and which can stretch-bend up to 2-m lengths of 'I' section aluminium to any of the required profiles. Extreme frame accuracy is not necessary, since the sheets making up the panel surface are held by pressure against the form with a layer of epoxy resin applied between frame members and the sheet. The epoxy plays a dual role, acting as both a bonding agent and a gap filler, thus removing the need for extreme accuracy in frame shape or assembly.

Solid aluminium sheets were used for the four inner rings of antenna panels. However, to decrease the wind loading, perforated sheets were used for the outer two rings. To enable efficient operation at 50 GHz, 2.84-mm diameter holes were spaced 4.22 mm apart, giving 40% open area.

3 CIVIL WORKS

3.1 Narrabri

The 3-km railtrack was designed, surveyed and built to be a straight line in space rather than a horizontal track. It could be considered a tangent to the Earth's curvature rather than a great circle as a 'horizontal' track would be. The foundation was made of lime-stabilised, natural site-material with a capping layer of crushed quarry material.

The antennas travel on a wide-gauge, 9.6-m railtrack. The rails are continuously welded, 68-kg/m head-hardened rails, connected to sleepers and rail ties with Pandrol clips. Each rail is supported on prestressed concrete sleepers set in ballast. Approximately every 10 m, rails are tied together with a steel beam supported and shaded by ballast. This configuration results in the distinctive grid pattern of the rail system.

The track crosses a very wide and shallow depression which is subject to flooding. It was not considered possible to bridge this area and low-level banks were built to channel the flow around the western end of the

track. Here a causeway was constructed which will flood but should still allow vehicular access except in the worst cases.

The 37 observing stations near Narrabri each consists of four concrete bored piers, one at each corner of the pedestal, connected below the ballast level of the rail track by a system of reinforced concrete beams. The surface sandy clay is underlain by a weakly cemented sandstone, and the 900-mm diameter piers were taken approximately 3 m into this material giving a total pier length of about 8 m. The foundations were designed to be very stiff to introduce a minimum of pointing error due to wind loading on the antenna.

The location of the observing stations was a very demanding surveying task. The specification required ± 5 mm in absolute positioning at the centre of the 3-km track, with ± 7 mm at the east and ± 12 mm at the west end. To achieve these high tolerances, an extensive network of surveying benchmarks, using geodesic techniques, had to be established on the site.

3.2 Coonabarabran Site

The civil engineering works included a sealed access road, bulk rock excavation, water supply, reinforced-concrete foundations and drainage works. A building was constructed to house computer and control equipment and some workshop facilities. The civil engineering and building work were carried out by Coonabarabran Shire Council and N. & J. Webber of Coonabarabran respectively, under the supervision of Macdonald Wagner & Priddle.

The Mopra antenna is supported on a reinforced-concrete ring beam excavated into rock with a central pier footing which restrains the antenna against lateral loads.

4 THE AT ANTENNAS IN RETROSPECT

To a large extent, the jury is still out on the performance of the AT antennas. The telescope has, so far, been commissioned to an upper frequency of 12 GHz only, far below the maximum design frequencies. However, observations often involve wide-field mapping of regions of the sky at lower frequencies. So far, the results (discussed in [10]) show that the specified dynamic range for observations is being met, which suggests that pointing errors are not significant at the field edges. Other conventional pointing-error checks at 12 GHz confirm that the antenna pointing is meeting the design criteria under most operating conditions. The actual surface errors will not be easily confirmed until the higher frequency systems are installed, but preliminary indications from the sidelobe performance and antenna-pattern null depths at 12 GHz show the expected performance.

One operating condition that has plagued, and continues to plague, telescope designers and users alike, is the so-called 'day-night' effect. At sunrise in particular, the change in solar loading on an antenna structure can cause uneven thermal distortions, often resulting in large unpredicted pointing errors until a new equilibrium is reached. The Australia Telescope has proved no exception. Although the design incorporated special features to ensure near-uniform temperature distribution across the structure, particularly the alidade, as yet unexplained errors still happen. Fortunately, an heuristic correction based on simple temperature measurements on site have enabled the high peak errors (up to the order of 30 arcsec) to be substantially corrected and the overall pointing held within the specified 11-arcsec rms.

CSIRO's decision to take a local approach for the design and construction of the AT antennas produced a very positive outcome. It gave Australian industry the opportunity to develop the ability to design and build large earth-station antennas indigenously. This is clearly demonstrated by the number of large antennas constructed for OTC Ltd (now AOTC) and the Department of Defence; the dish diameters range from 7.5 to 26 m. So far, about 18 of the larger dishes have been installed in Australia and Asia with considerable economic benefit to Australia (according to a Bureau of Industry Economics study).

5 ACKNOWLEDGMENTS

Overall, the AT antenna design effort would not have been possible without the contributions of many people, both within and without CSIRO. In particular, Mr N. Guoth of Connell Wagner, and Professor R. J. Evans of the University of Newcastle, made major contributions. The various contractors all treated the construction task as a 'flagship' project and produced an excellent product.

6 REFERENCES

1. Cooper, D.N. and Guoth, N., "The Australia Telescope Antennas: An All-Australian Approach", IREECON '85 International Digest, 709, 1985.

2. Guoth, N., "Australia Telescope: Review of the Antenna Element Design and Performance", Macdonald Wagner & Priddle Pty. Ltd. Report, August, 1983.

3. Cooper, D.N., Guoth, N. and Evans, R.J., "The Australia Telescope Antennas: Structural, Mechanical and Servo Mechanism Features", IREECON '85 International Digest, 705, 1985.

4. James, G.L., "The Feed System", JEEEA, 1992, this issue.

5. James, G.L., "The Australia Telescope Antennas: Reflector Optics and the Feed System'. IREECON '85 International Digest, 713, 1985.

6. Schafer, J.T., "The Australia Telescope - Aspects of the Structural Design", Proc. 1st National Structural Engineering Conference, Melbourne, 68, 1987.

7. Evans, R.J., Cooper, D.N., and Kennedy, R.A., "Servo System Design for the Australia Telescope", Proc. 3rd Conf. on Control Engineering, Sydney, 122, 1986.

8. Schafer, J.T., "The Australia Telescope – Survival Wind Velocities", AT Doc. AT/21.1.7/030, 28 April, 1987.

9. Parsons, B.F. and Yabsley, D.E., "The Australia Telescope Antennas: Development of High-Accuracy Low-Cost Surface Panels", IREECON '85 International Digest, 716, 1985.

10. Whiteoak, J.B. and Ekers, R.D., "The Australia Telescope: the First Radio Astronomy Results and Future Development", JEEEA, 1992, this issue.

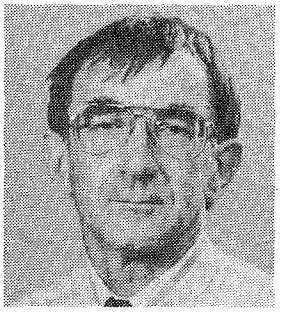

DR D.N. COOPER

Dr Dennis Cooper graduated from the University of Adelaide with a BE degree in 1963, and a PhD in Electrical Engineering in 1969. He joined the CSIRO Division of Radiophysics in November 1968. As a member of the Antenna Group, his initial research was on the design of mode converters for hybrid-mode feed horns. In 1972 he was transferred to a group working on INTERSCAN (a microwave landing system designed in the Division for civil aviation). Since 1972 he has been primarily involved in technology transfer from the research environment to industry. In 1983 he was appointed antenna manager for the Australia Telescope project. From 1981 to 1988 he was assistant Chief of the Division of Radiophysics. He was appointed Chief in August 1988.

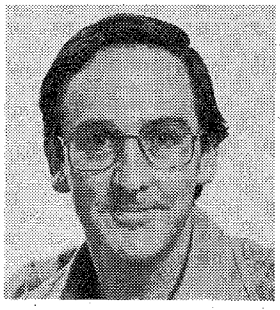

DR G.L. JAMES

Dr Graeme L. James received the BE and PhD degrees in Electrical Engineering from the University of Canterbury, New Zealand in 1970 and 1973 respectively. In 1964 he was awarded the DSc degree from the same university. Between 1973 and 1976 he was a post-doctoral fellow with the Department of Electrical and Electronic Engineering, Queen Mary and Westfield College, London, and since 1976 he has been a research scientist with the CSIRO Division of Radiophysics, Sydney. His main research interests are in the area of electromagnetic scattering and diffraction. In particular, he has been involved in a number of projects concerned with high-performance microwave antenna systems for both radio astronomy and satellite communication.

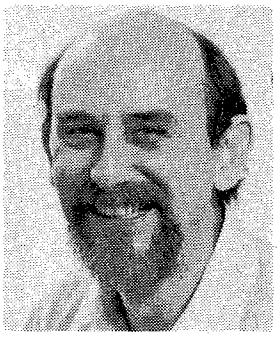

MR B.F. PARSONS

Barry Parsons has a Certificate in Engineering Surveying and obtained a degree in Mechanical Engineering from the New South Wales Institute of Technology (now the University of Technology, Sydney) in 1973. He has worked for Victa Lawnmowers as their development engineer, and for the State Rail Authority where he was responsible for motor-vehicle purchase and maintenance. As an employee of the CSIRO Division of Radiophysics since 1980, he has been responsible for general mechanical design work, both in day-to-day operations and in specific projects. These projects include Interscan, resurfacing the Parkes telescope, upgrading the OTC Moree earth station and, more recently, he was one of the engineers responsible for developing a method to produce high-accuracy antenna surface panels in low volumes and at low cost. He was also responsible for the accurate placement of these panels on both the OTC and the Australia Telescope 22-m antennas.

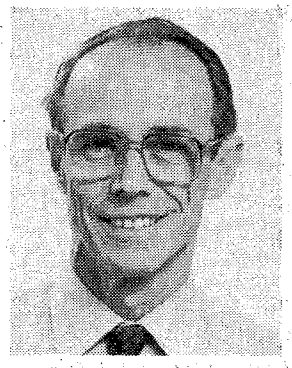

MR D.E. YABSLEY

Don Yabsley received the BSc and BE degrees from the University of Sydney in 1943 and 1944 respectively. In 1944 he joined the Division of Radiophysics, CSIR (now CSIRO). In 1963, after taking three years' leave as an exchange visitor at Cornell University in the USA, he joined with H.C. Minnett in studies which led to progressive upgrading of the reflector surface of the 64-m Parkes radio telescope, extending its operating range to millimetre wavelengths by the mid 1970s. More recently, he worked with B.F. Parsons and consulting engineers Macdonald Wagner (now Connell Wagner), to develop a manufacturing technique used to produce affordable high-performance surface panels for the antennas of the Australia Telescope. Since then he has developed a computer program and a technical manual to assist OTC in using these same techniques to manufacture surface panels for earth-station antennas for satellite communication services.

The Feed System

G.L. James*

SUMMARY This paper describes the wideband feed system of the elemental Cassegrain antenna used to form the Australia Telescope array. The development of the feed horn and orthomode transducer is put in an historical perspective and how the system evolved is discussed. Results are given showing the performance of the various components as well as the overall behaviour of the antenna.

1 INTRODUCTION

In any reflector antenna system, the feed-horn performance is one of the crucial factors in the overall operation of the antenna. It not only determines the reflector optics (see [1]) but also strongly influences the means of implementing the various frequency bands required for a given reflector antenna design. This is especially the case with the Australia Telescope (AT) antennas, which aim to provide for a large number of frequency bands (see Table 1). From past experience, this list is not immutable, as scientific objectives change with time. Some frequency bands not shown in Table 1 may well be required in the future, while some of the bands shown may decrease in priority. What is clear is that, for radio-astronomy purposes, numerous frequency bands within the range 327 MHz (the deuterium line) to the carbon monoxide molecular line at 115 GHz will be required. If solar observations are included, then frequencies below 327 MHz could well be desired. At the other end of the spectrum, operating at frequencies much above 115 GHz is impeded by atmospheric water absorption which begins to limit seriously reception for antennas on low-elevation sites, as in the case for the various AT locations.

Developing the feed system (which includes the feed horn and all passive microwave components before the LNAs), where the aim was to cover an extremely wide frequency range, proved to be a compromise between scientific objectives and engineering feasibility. I will begin by tracing this historical development, then give details of the feed system's components currently installed on the antennas, and end with a section on possible extensions.

* Division of Radiophysics, CSIRO, PO Box 76, Epping NSW 2121, Australia.
Submitted to The Institution of Radio and Electronics Engineers Australia in June 1992.

Table 1

Frequency Bands

	Band	Freq.Range(GHz)
(i) Initial Requirements		
21 cm	(L)	1.25-1.75
13 cm	(S)	2.20-2.50
6 cm	(C)	4.40-6.10
3 cm	(X)	8.00-9.20
(ii) Possible Extensions		
15 mm	(K)	20.00-25.50
7 mm	(Q)	42.00-50.00
3 mm	(W/F)	~85 and ~115.00
Below 1 GHz:-		
		~327 MHz
		~630 MHz
		~843 MHz

2 DEVELOPMENT OF THE FEED SYSTEM

2.1 The feed horns

When we began the electromagnetic design of the AT antennas in the early 1980s, the nearest comparable synthesis telescope design using Cassegrainian reflectors was the Very Large Array (VLA) in New Mexico [2]. The VLA achieved multifrequency operation by providing a narrowband feed for each frequency band complete with its cryogenically cooled LNA. The feeds are fixed and situated off axis while the subreflector is tilted at the appropriate azimuthal position corresponding to the feed horn (and hence frequency band) required for a particular observation. Thus, to cover, say, the four

initial bands given in (i) of Table 1, would require four feeds and associated cryogenics. A similar scheme was suggested for the proposed Canadian long baseline array [3] and the very long baseline array (VLBA) now being constructed across the USA uses this basic concept. Aside from the mechanical problems of ensuring trouble-free tilting of the subreflector, such a design, as a result of the offset feeds, seriously compromises the polarization purity of the antenna. This has been demonstrated in practice by the relatively poor performance of the VLA in this regard. While this problem was given some attention [4] with respect to the AT design, the strong desire to have good dual polarization characteristics, together with a wide field of view (out to the 3-dB point on the main beam) made any off-axis design look unattractive. It was decided, therefore, early in the design of the AT, that it should operate with both the feed horn and subreflector placed (symmetrically) on axis.

The initial set of frequency bands required was 1.25-1.75 GHz, 2.2-2.5 GHz, 4.4-6.1 GHz and 8.0-9.2 GHz, as shown in Table 1. Using narrowband designs, this would require four separate feed horns. Numerous alternative schemes were investigated at the time, including using the prime focus mode for the lower frequencies [5]. A more attractive alternative was to use a wideband feed design that would halve the number of feed horns required. This was a possibility as a result of the then newly developed corrugated conical horns, capable of high-performance operation over bandwidth ratios up to 2.2:1. (The development of these horns largely arose from work undertaken to upgrade the Moree I OTC earth station [6]. The final outcome is summarized in [7].) The problem still remained of course as to how to place the desired horn on axis in its operational position.

Wideband corrugated conical horns are characterized by a large aperture to produce the 'gain saturated' condition [8] and have a phase centre in the throat region of the horn. Given the reflector optics design discussed in [1], a wideband horn to operate over the frequency range 1.25 - 2.5 GHz would require an aperture of about 1.6 m in diameter and an overall length of over 3 m with most of the length protruding above the focus (since the horn phase centre is in the throat of the horn). The size, weight, cost of manufacture and blockage created by such a horn made it an unattractive proposition. Furthermore, given the size of the feed-cone housing on the reflector (see [1]) it would be difficult to fit into the space available, let alone attempt to provide some means of accommodating other feeds for higher frequency bands. Clearly, an alternative solution was called for. A number of possibilities were considered, including using prime focus operation for the 1.25-1.75 GHz band [5]. The solution finally chosen for the lower frequencies - ignoring for the moment the provision of operation at higher frequencies - was to develop the compact corrugated horn illustrated in Fig. 1. The main advantage of this horn is its relatively compact size with

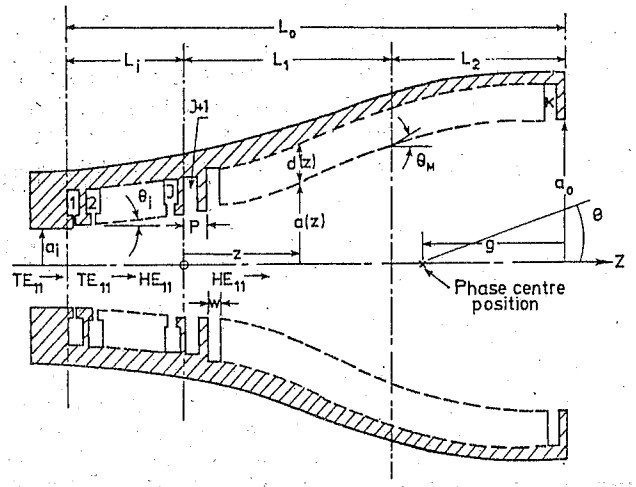

Figure 1 Cross-section view of a compact horn with a TE_{11} to HE_{11} mode converter using ring-loaded slots.

the phase near the horn aperture, so that the bulk of the horn can be housed inside the cone. This eliminates blockage problems that can arise with physically large wideband horns where most of the horn is situated above the top of the cone housing.

Initially, the compact corrugated horn was thought to be narrowband, thus requiring a separate horn for the 2.2-2.5 GHz band. However, subsequent analysis of this horn using both the accurate mode-matching method (previously developed in the laboratory for analysing wideband conical corrugated horns) and ring-loaded slots in the throat region of the horn (Fig. 1), showed that effective wideband operation was possible. For example, in feeding the AT Cassegrain antenna, the loss in overall gain was maintained within 0.5 dB over a bandwidth ratio of 2.4:1 with the focus at the average phase centre position [9]. It must be pointed out, however, that the compact corrugated horn does not have true wideband behaviour in that, while the match and cross-polarization characteristics are maintained at a low level across the band, the phase centre and beamwidth vary with frequency. This means that at the upper band edge, feed phase errors cause most of the loss, while at the lower band edge, the loss is mainly due to reduced beam efficiency with the increasing beamwidth of the feed. Nevertheless, the compact corrugated horn, when used as a feed in a Cassegrain antenna system, can give an overall performance close to that where a true wideband horn is used.

This (effective) wideband behaviour of the compact horn had a major impact on the AT design. It was now possible to consider secondary focus operation seriously for all frequencies above 1 GHz. Using corrugated horns with effective bandwidths in excess of an octave in range, meant that only four horns were required to cover the frequency bands above 1 GHz, as given in Table 1: a 1.25-2.5 GHz and a 4.4-9.2 GHz band horn where the compact horn design is used, and a

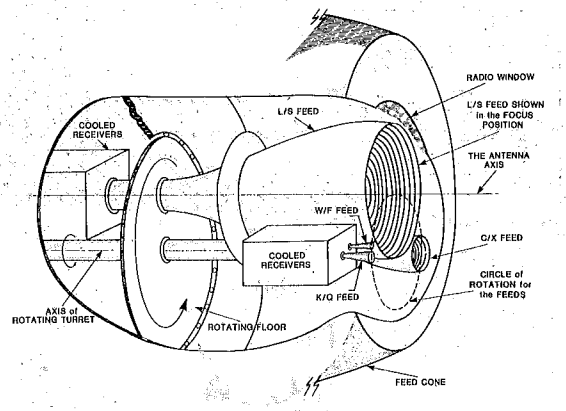

Figure 2 The rotating turret system.

20-50 GHz and a 85-115 GHz band horn where, given the smaller physical dimensions of these higher frequency horns, a conventional conical corrugated wideband horn design is feasible.

As stated earlier, on-axis operation of the feed was considered essential to maintain the dual polarization and wide field-of-view performance required of the AT. To this end, a rotating turret system was provided as the means to allow each feed horn to be brought on axis as required [5][10]. The mount arrangement for the four feeds is shown in Fig. 2. Even so, to fit all of these horns into the space available, we had to compromise further with regard to the larger 1.25-2.5 GHz compact horn. While the best average phase centre for this horn was at a position of ~870 mm inside the aperture, if placed in this position, it would still protrude too far in front of the focus, thus blocking the other horns. Given that the phase centre of the horn at 1.4 GHz is ~250 mm inside the aperture, then with the horn in this position, the antenna performance is optimized around this frequency and enough room is provided for the other three horns. However, as a result, the phase centre of the horn in the upper 2.2-2.5 GHz band is well removed from the focus, thereby reducing the overall efficiency of the antenna in this band. To correct for some of this gain loss, we provided for a small axial movement of the subreflector so as to improve the efficiency in this band by up to 10%.

Figure 2 shows the 1.25-2.5 GHz band feed to be in the on-axis operational position. Also note that all the feed apertures lie in the same plane. This was done deliberately to minimise blockage and interference effects between horns. It turned out to be fortuitous that the 250-mm phase centre position used for the 1.25-2.5 GHz horn was very close to the value of the best average phase centre position of the 4.4-9.2 GHz compact horn. The other two higher frequency horns, which are to be wideband conical corrugated horns as described in [7], are somewhat overdesigned. They are larger than necessary so that their apertures lie in the plane of the compact horns. In practice, this matters little as the overall performance is generally improved as the horn (electrical) length increases.

2.2 Orthomode transducer (OMT) design

With the adoption of wideband feeds capable of receiving a pair of bands, came the almost immediate demand for simultaneous dual-band operation. This not only increases the speed of the instrument, but also provides scientific advantages such as, for example, in monitoring the atmosphere in certain VLBI (very long baseline interferometry) experiments. The emphasis was therefore placed on developing other wideband components, such as polarizers and OMTs, to be used in conjunction with the horn. Since it was doubtful that a waveguide polarizer could be developed to match the bandwidth performance of the horns, it was agreed that linear polarization be the mode of reception with circular polarization, if required, reconstituted further down the line at the RF or IF stage. While this went against conventional wisdom at the time, it was argued that, from the scientific point of view [11], this was also the best choice of operation. Consequently, dual linear polarization was adopted and we devoted our attention to developing a wideband OMT to match the capabilities of the horn.

One problem in designing wideband waveguide components in general is the need to avoid exciting unwanted higher order modes. If propagated, they can have deleterious effects on the radiation pattern of the feed connected to the device. In particular, cross-polarization performance can be severely affected by the excitation of unwanted modes. Therefore, in investigating a wideband OMT design, it seemed appropriate to transform the circular waveguide output from the horn into a waveguide configuration that is inherently wideband, such as double or quad-ridged waveguide. (By wideband in this instance, we mean where the cutoff frequencies between the fundamental mode and the first unwanted higher order mode are widely separated. The fundamental mode can then be excited in the waveguide over a wide bandwidth without the unwanted higher order mode being excited and subsequently propagated.)

Some earlier work on quad-ridged OMT design was not particularly encouraging, obtaining a useable bandwidth ratio of up to 1.7:1 only [12]. A more promising approach appeared to be the finline OMT developed many years ago [13]. In essence, this OMT operates by having a pair of diametrically opposite tapered metallic fins fitted inside the waveguide to transform gradually the dominant propagating waveguide mode polarized parallel to the fins into a finline mode. The energy in the finline mode is essentially confined to the small gap between the fins in the centre of the waveguide. This energy can then be removed from the waveguide by simply curving the fins around a 90° bend and out

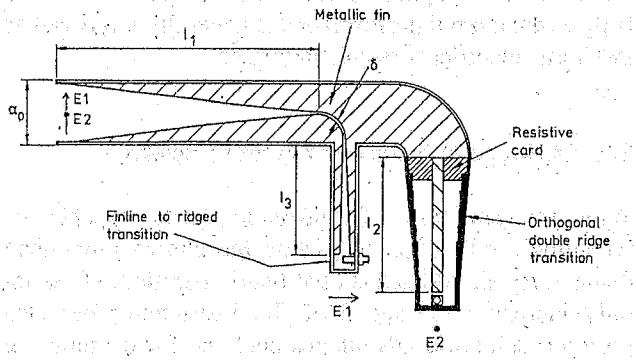

Figure 3(a) Cross-sectional view of the finline OMT.

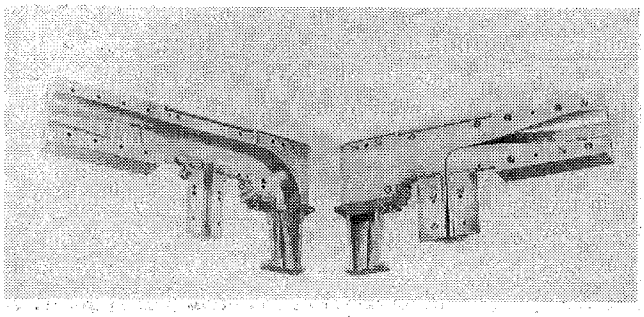

Figure 3(b) Exploded view of the prototype finline OMT.

through a small hole in the side of the waveguide. It is then possible to launch this energy into another waveguide as desired. The other dominant propagating mode polarized orthogonal to the fins continues to travel along the waveguide unperturbed, provided that the fins are sufficiently thin.

We spent some time investigating this type of OMT. Our implementation of a wideband finline OMT is illustrated in Fig. 3. Two orthogonal polarizations, E1 and E2, are assumed to be excited in square waveguide of width a_0. Polarization E1 is gradually transformed over a length l_1 to a finline mode within the small gap, d. This mode is then taken through a 90° bend and out through a hole in the waveguide wall to permit removal of E1 from the waveguide. A further transition from the finline to conventional, wideband, double-ridged waveguide over a length l_3 enables the signal to be extracted from the waveguide system by a conventional wideband coaxial-to-double-ridged waveguide adapter. The orthogonal polarization E2 is in turn transformed into double-ridged waveguide (to permit wideband operation) via a square-to-double-ridged waveguide transition of a length l_2, as shown in Fig. 3. The resistive card is necessary, as in [13], to suppress the excitation of unwanted modes at the termination of the fin. The only purpose of the 90° bend in the square waveguide is to permit the coaxial outputs containing E1 and E2 to be located physically close together.

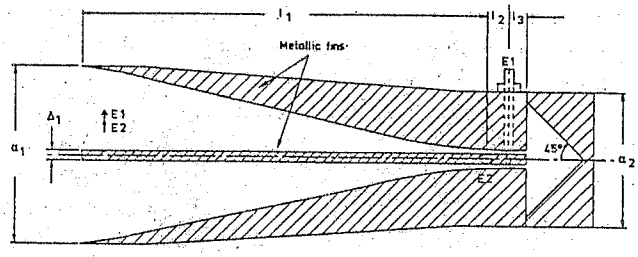

(a)

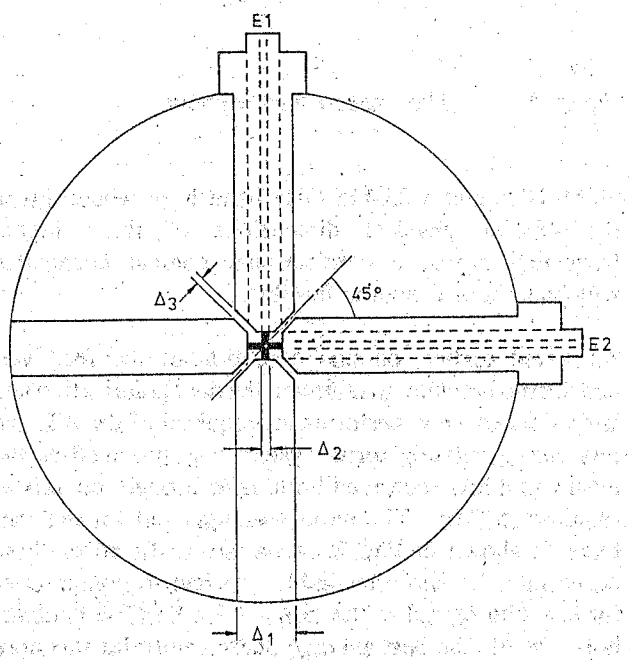

(b)

Figure 4 The quad-ridged OMT:
(a) cross-sectional view;
(b) end view with shorting cap removed.

For acceptable performance, the various dimensions of the OMT shown in Fig. 3 must be appropriately chosen. Suitable dimensions, together with a more detailed description of this device, are to be found in [14]. The major disadvantage of the finline OMT is the relatively high levels of higher order modes generated by the 90° bend which give rise to cross-polar peaks that are unacceptably high for the present application.

To get a better solution, we turned our attention to the quad-ridged OMT. This design is similar to the finline case in that tapered fins, or ridges, are used inside the waveguide, where, in this case, two orthogonal pairs of ridges concentrate the field into a small gap in the centre of the guide. The energy is extracted from the waveguide via coaxial lines passing through the centre of the ridges with orthogonal probes extending across the small gap between the ridges. An outline of the OMT is shown in Fig. 4.

With limited time available, we used the same sine-squared-type taper for the ridges that were the most successful shape for the finline OMT developed previously. Design details are presented in [14], but to achieve wideband performance to match that of the horn, it had to be sufficiently long - at least four wavelengths at the lowest operating frequency. This was about twice the length of the OMT developed in [12] and largely explains the latter's limited bandwidth performance.

The ridge profiles in [12] were designed on the basis of maintaining a constant cutoff frequency through the OMT. In waveguide transition design, this is a desirable approach for reducing the effects of changing cross-section. However, in any given design, it may not always be convenient to maintain the waveguide dimensions for constant cutoff. As an alternative, and for comparison with the previous results, we designed ridge profiles giving, with the aid of a computer program to analyse waveguides of arbitrary cross-section [15], the least change in cutoff frequency. Qualitatively, the results were similar to the earlier examples, and we concluded that, for adequate wideband performance, the length of the OMT is more important than the particular design of the ridge profiles, provided the latter are smoothly varying and the variation in cutoff frequency is not too large.

3 FEED COMPONENT PERFORMANCE

3.1 The compact horn

The same wideband compact horn design was used to cover the 1.25-2.5 GHz and the 4.4-9.2 GHz bands with the difference between the horns being only a matter of scale. Figs 6-9 show the results of the horn, normalised to the design frequency f_i where, for the 1.25-2.5 GHz horn f_i = 1.56 GHz, and for the 4.4-9.2 GHz horn f_i = 5.50 GHz. In Fig. 5 a selection of measured co-polar and cross-polar radiation patterns are shown across the band, where the narrowing of the beam is with increase in frequency. Also evident is the increase in aperture phase errors with increasing frequency as the first sidelobe is gradually absorbed within the main beam.

Figure 6 gives a summary of the beamwidth and cross-polar performance of the horn across the band. Also shown are the predicted values which generally are in close agreement with the measured data. Figure 7 plots the predicted beam efficiency which rapidly falls off with frequency. The variation in phase centre position is shown in Fig. 8. For the best average position for wide-bandwidth operation the value of g/l_i is set at around a value of 4.5 which is the setting of the 4.4-9.2 GHz horn with the nominal phase centre at 250 mm inside the horn aperture. With this setting, the g/l_i value for the 1.25-2.5 GHz horn is 1.3, which clearly favours the bottom end of the band as discussed earlier.

Figure 9 plots the return-loss performance of the horn where it is seen to be at high levels over the operating bandwidth.

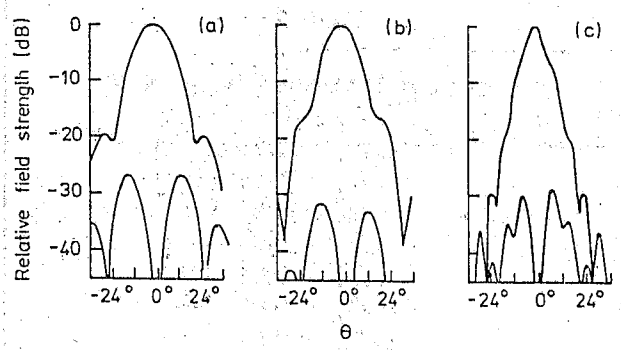

Figure 5 Measured co-polar and cross-polar radiation patterns in the ± 45° planes for the compact horn where θ_M = 15°, at the following frequencies:
(a) f/f_i = 0.83;
(b) f/f_1 = 1.0;
(c) f/f_i = 2.0.

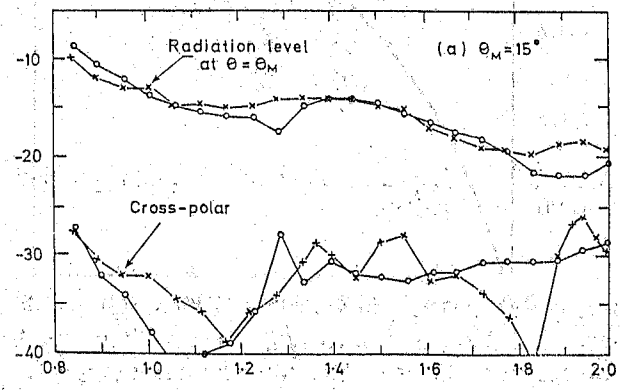

Figure 6 Co-polar and cross-polar radiation patterns of the compact horn
—o—o— theory;
—x—x— measured.

3.2 The quad-ridged OMT

The same basic OMT design is used for both the 1.25-2.5 GHz and 4.4-9.2 GHz bands. The OMT is illustrated in Fig. 4. Table 2 gives the parameters where for the lower band, l_i = 24 cm and for the upper band, l_i = 6.8 cm. For this latter case, the gap between the fins, Δ_3, is already very small at a value of 0.34 mm. For this reason, it is difficult to see this type of OMT being used for higher frequency bands, and alternative solutions will need to be found.

When connected to the associated wideband compact corrugated horn, the return loss and cross-polar performance are shown in Figs. 10 and 11 for the 4.4-9.2 GHz and 1.25-2.5 GHz OMTs respectively. These results are generally adequate for the AT needs, especially bearing in mind the wide bandwidth involved.

Table 2

Parameters for Quad-Ridged OMT

$\alpha_1/\lambda_L \approx 0.75$
$\alpha_2/\lambda_L = 0.44$
$\ell_1/\lambda_L > 4.0$
$\ell_2/\lambda_L = 0.015$
$\ell_3/\lambda_L = 0.04$
$\Delta_1/\lambda_L = 0.05$
$\Delta_2/\lambda_L = 0.01$
$\Delta_3/\lambda_L = 0.005$

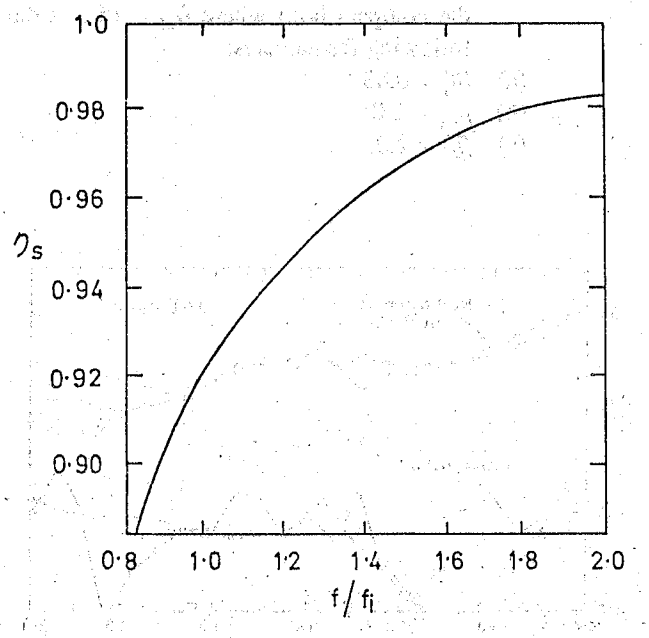

Figure 7 Beam efficiency η_s (fractional value of energy contained within the angle $\theta = \theta_M$ from boresight) as a function of normalized frequency f/f_i.

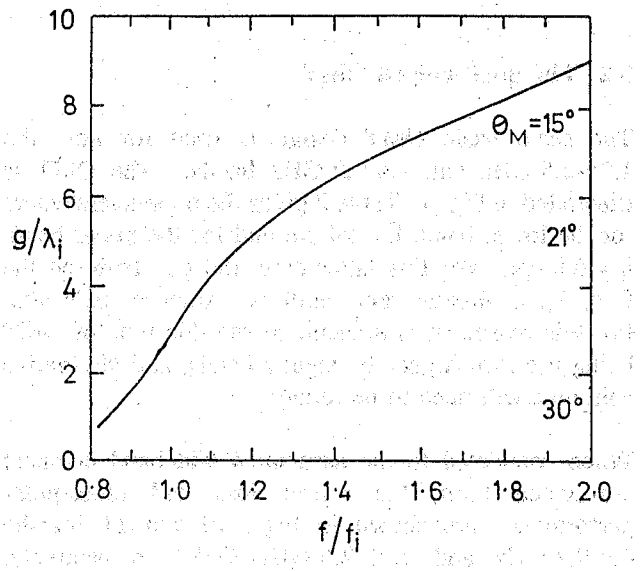

Figure 8 Variation in phase centre position from the aperture as a function of frequency.

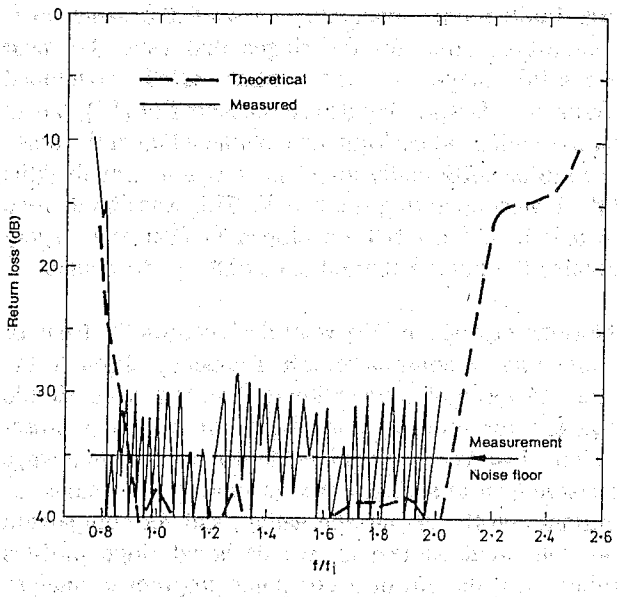

Figure 9 Return loss of the compact horn.

The two OMTs are not identical. One difference is in the coaxial connector. For the larger OMT the coaxial line through the ridge could be made the same dimensions as that of a Type-N connector, thus avoiding any mismatch problems. Practically, however, for the smaller ridges of the 4.4-9.2 GHz OMT, it was not possible to have the radius of the 50 Ω of the connector to be the same as the 50 Ω coaxial line through the ridge. Hence, an abrupt junction between these two lines occurs, and the characteristic shape on the return-loss curves in Fig. 10 compared to the 'flatter' response of the return-loss response in Fig. 11, is consistent with a (small) mismatch at the junction between these two lines.

Another difference between the two OMTs is in the shape of the ridge profiles. The 4.4-9.2 GHz OMT, which was developed first, uses a sine-squared-type taper for the ridge profiles developed for the earlier fin-line OMT. Further development continued with the 1.25-2.5 GHz OMT with a fin profile based on a minimal change in cut-off frequency. These two different profiles are shown in Fig. 12, and while in some ways quite different, we believe, based on comparison with other work such as in [12], that what is more important for adequate performance, provided the ridges are smoothly varying, is that the OMT be made sufficiently long.

Finally, Fig. 13 demonstrates the effects of higher order modes generated in the OMT on the fields in the main beam region of the AT Cassegrain antenna when illuminated by a feed system consisting of a quad-ridged OMT/wideband compact corrugated horn combination. Fig. 13(a) shows the co-polar and cross-polar response in the vicinity of the main beam with the feed system operating at a low frequency so that no higher order modes are excited. The response, as expected, is

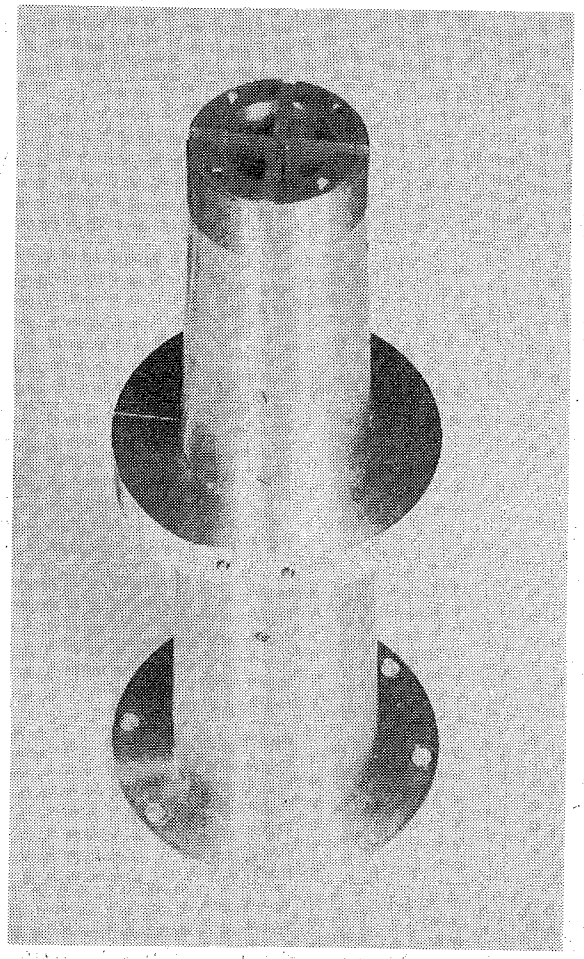

(a)

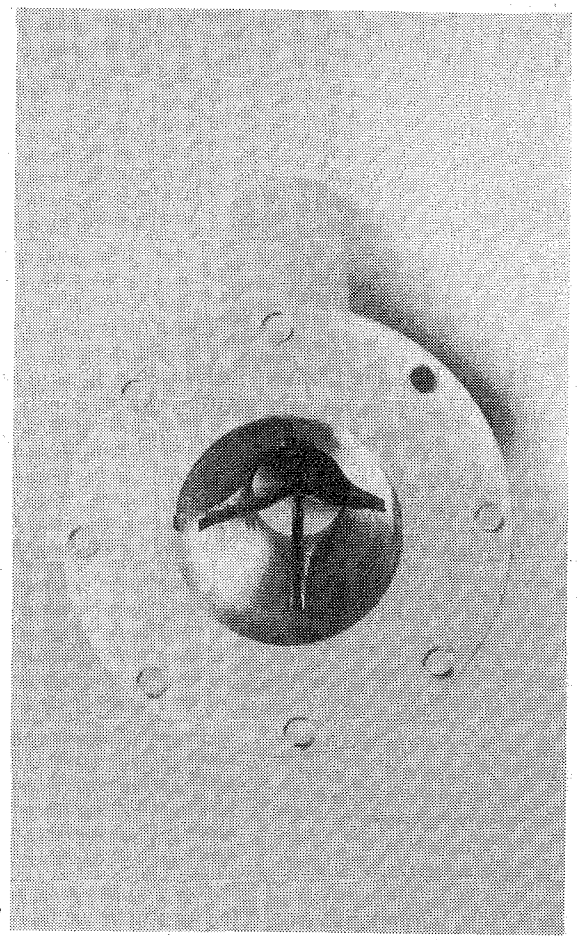

(b)

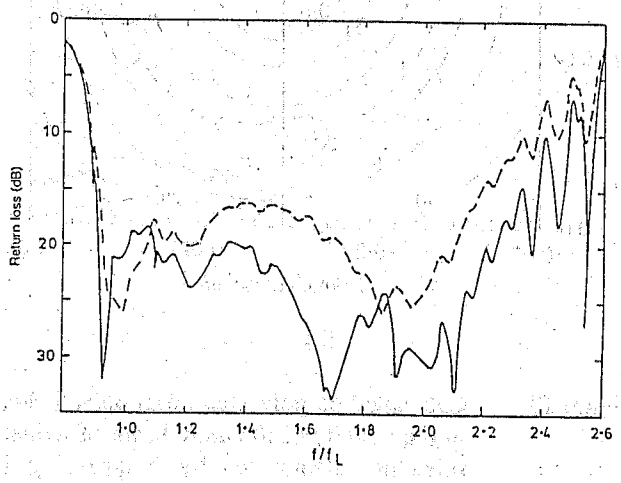

(c)

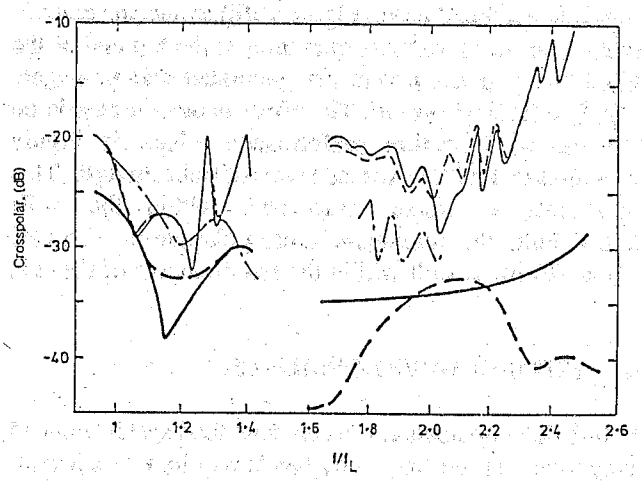

(d)

Figure 10 Photograph of a prototype quad-ridge OMT designed for C/X-band operation.
(a) General view with the shorting cap removed.
(b) View looking into the OMT.
(c) Measured return loss of the quad-ridged OMT connected to a wideband corrugated horn (f_L = 4.4 GHz): ———— E1 polarization; -------- E2 polarization.
(d) Measured cross-polar levels of the quad-ridged OMT/ corrugated horn combination (f_L = 4.4 GHz):
———— E1)
---------- E2) maximum cross-polar levels
— - — Horn alone)
———— E1)
— — — — — E2) on-axis cross-polar levels.

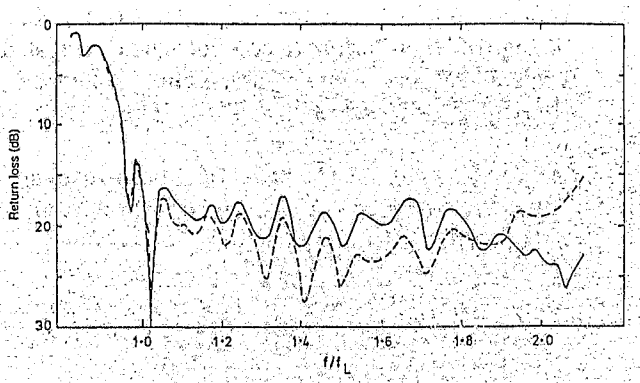

Figure 11 Measured return loss of the quad-ridged OMT where the profiles are designed for minimal change in cut-off frequency (f_L = 1.25 GHz);
——— E1 polarization;
-------- E2 polarization.

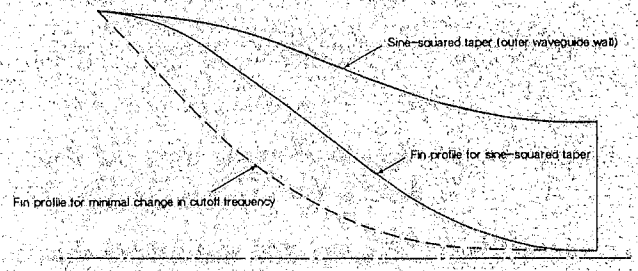

Figure 12 Comparison of ridge profiles used is the quad-ridged OMT design.

symmetrical with very low cross-polarization levels. This represents a 'best' case. Figure 13(b) shows the equivalent result for an antenna operating at the top end of the band when higher orders are generated and propagate through the feed system. The effect is most dramatic on the cross-polarization performance which is highly asymmetrical with increased levels of field strength. This represents a 'worse' case and, within the 3-dB beamwidth, the maximum cross-polarization level of about -26 dB is well within the requirements of the AT.

4 FUTURE DEVELOPMENTS

Future developments for the antenna feed system depend very much on the frequency bands required. As has already been mentioned, the quad-ridged OMT design will be unsuitable for higher frequencies above those currently operating. However, the smaller wavelength makes other options such as beam-waveguides, beam splitters, and other quasi-optical techniques, attractive. Up to 115 GHz, the corrugated horn remains a suitable choice.

For frequencies below 1 GHz, lightweight portable arrays which can be fitted on top of the cone housing may be suitable with prime-focus operating only a possibility at frequencies of ~327 MHz and below.

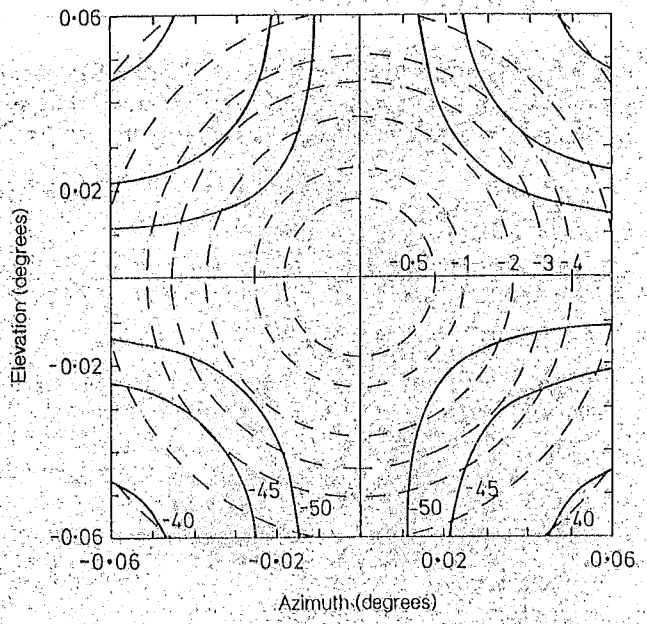

(a)

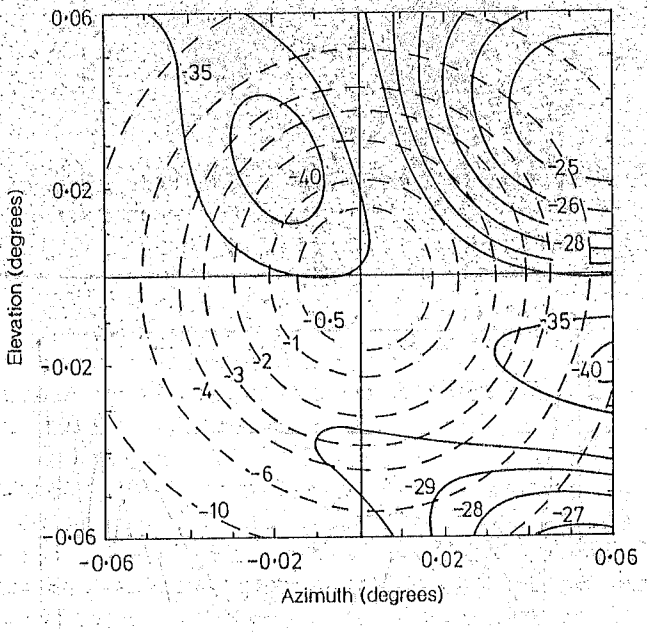

(b)

Figure 13 Calculated co-polar and cross-polar fields in the vicinity of the main beam of a dual reflector antenna fed by a quad-ridged OMT/wideband corrugated horn combination operating at a high frequency to show the effects of high-order mode excitation within the OMT.
(a) low-frequency response
(b) high-frequency response.

These and other methods will need to be developed as the usage of the AT evolves.

5 ACKNOWLEDGMENTS

The author is indebted to Dr B. MacA. Thomas for many useful discussions regarding the feed system, and to S. Skinner for his assistance in developing the OMT.

6 REFERENCES

1. Cooper, D.N., James, G.L., Parsons, B.F. & Yabsley, D.E., "The Antennas", JEEEA, this issue

2. Napier, P.J., Thompson, A.R. & Ekers, R.D., "The Very Large Array: Design and Performance of a Modern Synthesis Radio Telescope", Proc.IEEE, 71, 1295-1320, 1983.

3. "Antenna Design Study for a Long-Baseline Radio Telescope Array", SPAR Aerospace Ltd, Report No. RML-009-82-22, March 1982.

4. Thomas, B.MacA., "Some Thoughts on the Problem of Feeding and Band-Changing on the AT Antennas", AT Memoranda Series, AT/10.2/024, January 1983.

5. James, G.L., "A Dual-Reflector Antenna System for the Australia Telescope", ATDOC112, October 1982.

6. Thomas, B.MacA., Greene, K.J., James, G.L. & Parsons, B.F., "Upgrade of the Antenna for the OTC Moree 1 Satellite Earth Station", CSIRO Report No. RPP 2688, June 1983. Also, see Thomas *et al.*, "Upgrade of the OTC(A) Moree 1 Earth Station Antenna", JEEEA, 5, 180-188, 1985.

7. Thomas, B.MacA., James, G.L., & Greene, K.J., "Design of High-Performance Wideband Corrugated Conical Horns for Cassegrain Antennas", Trans.IEEE, Vol. AP-34, 750-757, 1986.

8. Chang, K. (ed). "Handbook of Microwave and Optical Components", Vol. 1, Section 11.3.4. New York, Wiley, 1989.

9. James, G.L., "Design of Wideband Compact Corrugated Horns", Trans.IEEE, Vol. AP-32, 1134-1138, 1984.

10. James, G.L., "An Improved Design for the Australia Telescope Elemental Antenna", ATDOC113, November 1982.

11. Frater, R.H., Brooks, J.W. & Whiteoak, J.B., "The Australia Telescope: Overview", JEEEA, this issue.

12. Davis, I. & Chignell, R.J., "Wideband Orthomode Transducers for Low Noise Applications", ERA Technology Ltd, UK, Report No.82-124, October 1982.

13. Robertson, S.D., "Recent Advances in Finline Circuits", Trans.IRE, Vol. MTT-4, 263-267, 1956.

14. Skinner, S.J., & James, G.L., "Wideband orthomode Transducers", *ibid*, Vol. MTT-39, 294-300, 1991.

15. Bird, T.S., "Microwave and Optical Guiding Structures: A Field Analysis by Hybrid-Finite Element Methods", PhD. Thesis, University of Melbourne, 1976.

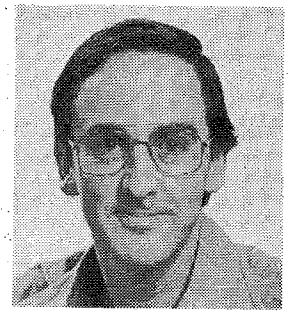

DR G.L. JAMES

Dr Graeme L James received the BE and PhD degrees in Electrical Engineering from the University of Canterbury, New Zealand in 1970 and 1973 respectively. In 1964 he was awarded the DSc degree from the same university. Between 1973 and 1976 he was a post-doctoral fellow with the Department of Electrical and Electronic Engineering, Queen Mary and Westfield College, London, and since 1976 he has been a research scientist with the CSIRO Division of Radiophysics, Sydney. His main research interests are in the area of electromagnetic scattering and diffraction. In particular, he has been involved in a number of projects concerned with high-performance microwave antenna systems for both radio astronomy and satellite communication.

The Receiver System

M.W. Sinclair*, G.R. Graves*, R.G. Gough** and G.G. Moorey*

SUMMARY The seven 22-metre antennas of the Australia Telescope (six at Narrabri and one at Coonabarabran, NSW) have been equipped with a range of low-noise microwave receivers. The system requirements, design concepts and construction techniques of the overall receiver system are discussed and some early performance date indicated.

1 INTRODUCTION

Constructing the new 22-m antennas for the Australia Telescope (AT) has offered many new challenges for modern receiver design engineers. Each of these antennas, equipped with low-noise receiver systems designed to amplify and down-convert incoming cosmic radio signals, must satisfy many new requirements demanded by modern synthesis radio telescopes.

To provide such a receiver system to match these requirements, many factors had to be taken into consideration. To begin with, the designated observing bands, 1.2 → 1.8 GHz, 2.2 → 2.5 GHz, 4.5 → 6.1 GHz and 8.0 → 9.2 GHz, selected either because of allocations to the radio astronomy service, or because of the presence of astronomically important atomic and molecular spectral lines, cover an extremely wide frequency range which cannot be covered effectively by one feed horn and one receiver. The polarization specifications called for an instrument that could perform high-precision polarization measurements over the entire half-power beamwidth of the antenna element. This feature required on-axis feeding of the antenna reflector and, because several horns and receivers were needed to achieve the wide frequency coverage of the instrument, these horn-receiver combinations were mounted on a rotating turret to enable rapid on-axis switching to the desired observing band.

* Australia Telescope National Facility, CSIRO, PO Box 76, Epping NSW 2121, Australia.
** Australia Telescope National Facility, CSIRO, PO Box 94, Narrabri NSW 2390, Australia.
Submitted to The Institution of Radio and Electronics Engineers Australia in June 1992.

Other receiver design features arising out of the special requirements for the Australia Telescope are:

(i) The receiver front ends must have the lowest noise temperature achievable, consistent with high reliability and wide percentage bandwidths of up to 30%.

(ii) Astronomers must be able to observe, simultaneously, widely different spectral-line features within a receiver passband, or from two different receivers with passbands separated by almost an octave in frequency.

(iii) They must have a high degree of gain, phase and frequency stability relative to a variety of external influences, the main one being temperature.

(iv) They must have a wide range of output bandwidths ranging from 0.5 to 256 MHz in octave increments. This allows for good velocity coverage at high resolution for a wide range of molecular spectral lines in the centimetre and millimetre wave bands.

(v) Wherever possible, no signals generated within the receiver system itself should fall into any of the signal or intermediate frequency bands.

(vi) The reliability and maintainability of the receiver system as a whole must be high. Because of the small number of antennas in the array, time lost due to equipment failure seriously limits the efficiency of the telescope. Consequently, a comprehensive monitoring system is required which can pinpoint problem areas quickly and facilitate maintenance when faults occur.

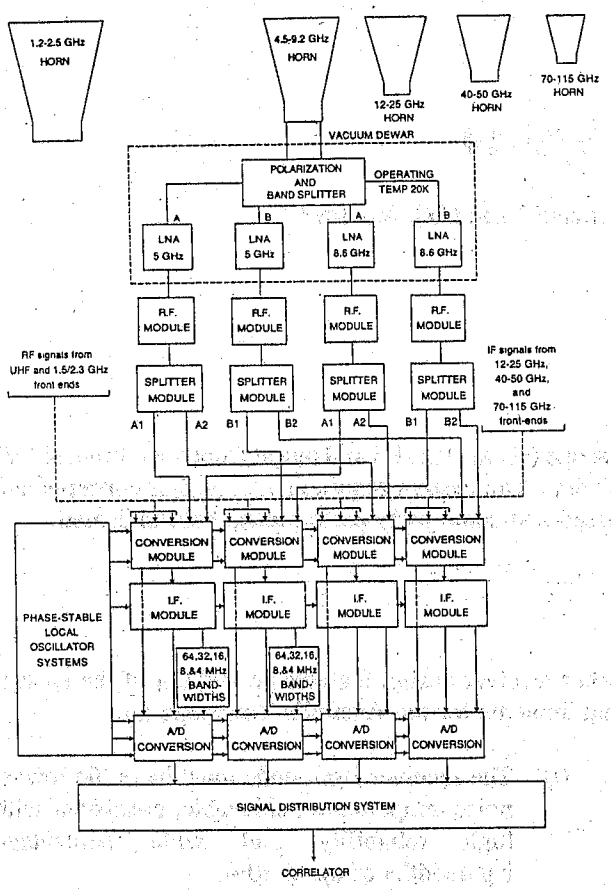

Figure 1 Overall Receiver system block diagram.

2 SYSTEM DESIGN

The system arrangement shown in Fig. 1 is that which was finally developed to meet the requirements indicated above.

The development of compact and conical corrugated feed horns providing high performance over a 2:1 bandwidth ratio [1] has enabled two AT observing bands to be received by one primary feed horn. This has resulted in a front-end design which uses a wideband orthomode transition (OMT) [2] to cover both AT bands provided by the feed horn, a band separation diplexer to select each AT band from the orthomode transition output, and a set of low-noise GaAs FET amplifiers all cooled to cryogenic temperatures.

The amplified radio frequency (RF) signals from the front ends (covering the designated AT bands) are then passed to a tuneable multi-frequency conversion system where, by appropriate filter selection and local oscillator (LO) settings, the final intermediate frequency (IF) output bands can be tuned to any part of an observing band with a resolution of 1 MHz. Four IF output channels are provided - two polarizations in each band from a dual-band front end, or two polarizations each in separated bands within a single front-end band.

One pair of IF channels has six output bandwidths available for narrowband spectral-line observations, all selectable remotely; the remaining pair of IFs has only two wide bandwidths (128 and 64 MHz) available which, in conjunction with the wide bandwidths of the first pair of IFs, gives four wideband IF channels for continuum observations. A future extension which will provide for a 256-MHz-wide IF band for millimetre-wave spectroscopy, is planned.

It is at this point that each IF output band, amplified to the correct level, is passed on to a high-speed sampling system [3], where the IF signals are digitised and then transmitted back to the central control site for correlation.

As well as the IF outputs, each channel provides a square-law detector output that enables the total power level in each band to be monitored. This system, in conjunction with a small modulated noise source signal injected into the input of the receiver and a synchronous demodulator, can be used to monitor continuously, the gain and system temperature of the receiver.

3 DETAILED SYSTEM DESCRIPTION

3.1 Front ends

The noise performance of a receiver system in a radio telescope will depend, critically, on the gain and noise performance of the input low-noise amplifier, and the loss in the transmission system connecting this amplifier to the receiving feed horn. This can be seen in the simple expression

$$T_A' = LT_A + (L-1)\,T_L = T_A + (T_A + T_L)(L-1) \qquad (1)$$

where T_A' is the noise temperature at the input to the feed horn, T_A is the amplifier noise temperature, and T_L is the physical temperature of the input transmission system with loss L.

Equation 1 shows that excess system noise due to input loss, depends not only on the physical temperature of the loss, but also on the following amplifier noise temperature. Clearly the system noise can be greatly reduced by cooling both the low-noise amplifiers and the input loss to cryogenic temperatures.

The octave-band feed horns, developed for the initial observing bands, require that the dual-band front ends simultaneously accept the frequency ranges $1.2 \rightarrow 1.8$ GHz and $2.2 \rightarrow 2.5$ GHz (the 1.5/2.3-GHz front end) with the 5.0/8.6-GHz front end accepting the $4.5 \rightarrow 6.1$ and $8.0 \rightarrow 9.2$-GHz bands.

To achieve this, each front end has been equipped with

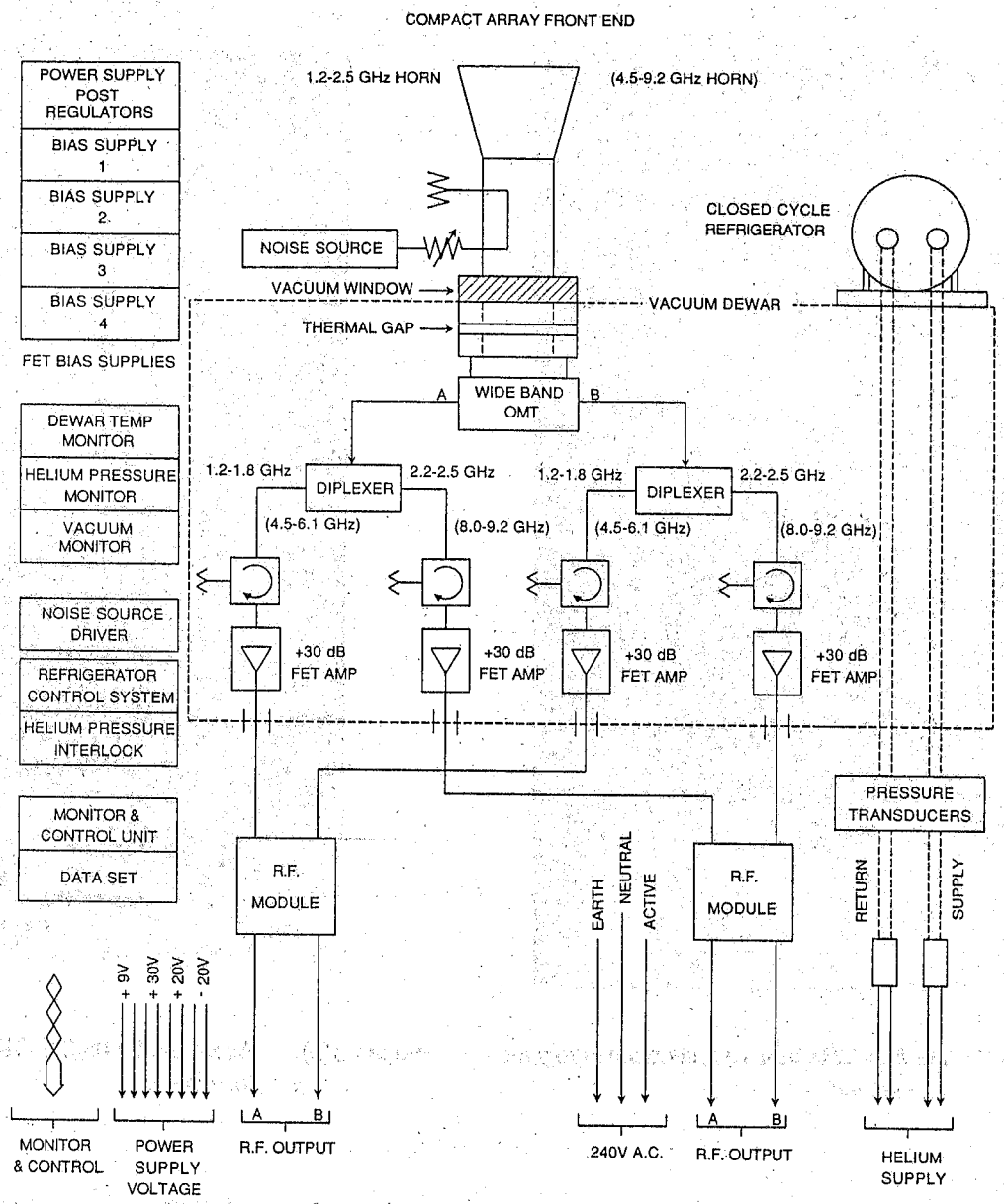

Figure 2 Front-end block diagram.

(i) an octave-band, thermally isolating, Dewar input waveguide system

(ii) an octave-band linear orthomode polarization transducer (OMT)

(iii) a band-separation diplexer for each polarization

(iv) a pair of low-noise GaAs FET amplifiers for each observing band

(v) a post-LNA ambient temperature amplifier and filter system to provide image rejection and extra RF amplification

(vi) a closed-cycle (helium) cryogenic refrigeration system capable of cooling a 10-watt thermal load to ~ 20 K.

The OMTs, the band-separation diplexers and the FET low-noise amplifiers, are all housed in a stainless steel vacuum Dewar to enable cryogenic cooling of all these components.

In the 5.0/8.6-GHz front end, diplexers and FET amplifiers are all cooled to less than 20 K. However, in the 1.5/2.3-GHz front end, the diplexers and FET amplifiers only are cooled to less than 20 K, whilst the OMT, because of its greater mass and size, is cooled to 75 K.

A block diagram of the front-end systems is shown in Fig. 2, Fig. 3(a) shows the cryogenic components of a 5.0/8.6-GHz front end, and Fig. 3(b) a fully assembled front end complete with feed horn.

Figures 4(a) and (b) are completed 5.0/8.6-GHz and 1.5/2.3-GHz front ends, mounted on the AT 22-m antennas.

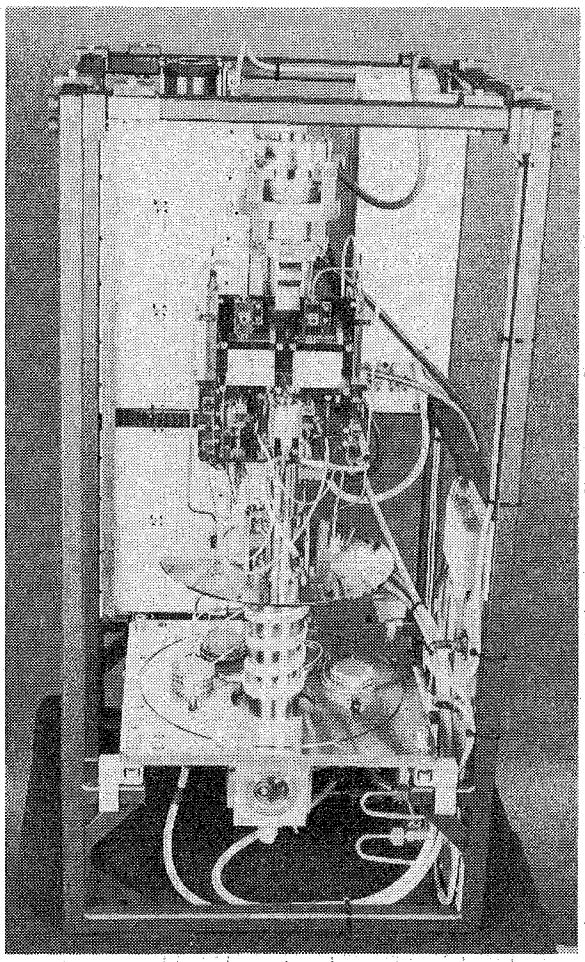

Figure 3(a) 5.08/8.6-GHz front end, showing cryogenic components.

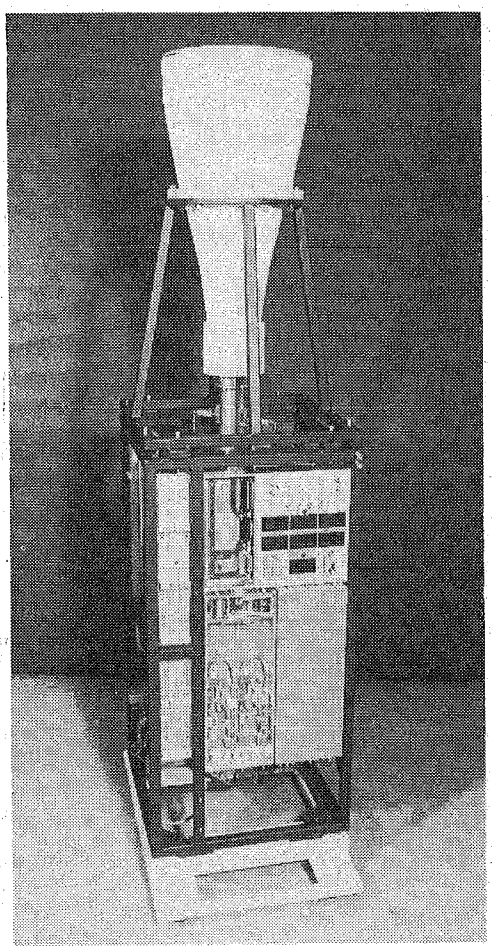

Figure 3(b) Assembled 5.08/8.6-GHz front end, with feed horn.

Dewar Input Waveguides and the Orthomode Polarization Transducers

The wide bandwidth nature of the front-end systems required that the input waveguide thermal isolation gap and vacuum window seal should be non-resonant. This requirement precludes the use of choke grooves in the waveguide gap and iris-type vacuum windows, because these are resonant devices. Instead, a very small gap dimension was adopted, with particular attention paid to gap compensation during the cooling process, by choosing appropriate materials and dimensions.

A broadband vacuum seal was achieved by using closed-cell expanded polystyrene foam (Ecco foam 1.04) plugs of appropriate length. This gives an extremely low-loss window with adequate vacuum sealing properties for the small diameter plugs used in the 5.0/8.6-GHz front end. The foam plug used on the 1.5/2.3-GHz front end, however, had to be sealed with a thin polyimide membrane (0.12-mm Kapton), because air diffusion through the closed-cell foam gave an unacceptably high leak rate through the much larger area of the window plug.

The wideband OMT [2] is required to have low-voltage standing wave ratio (VSWR) and high isolation properties across an octave bandwidth. These devices are based on a quad-ridged circular waveguide structure and have typical VSWRs at each orthogonal output of less than 1.5:1 for the band 4.5 to 10 GHz, and less than 1.3:1 for the band 1.2 to 2.4 GHz. Isolation between the orthogonal outputs for both bands is typically 35-40 dB. The insertion losses were measured at room temperature to be $\leq$ 0.3 dB for the 4.5 to 10-GHz unit, and $\leq$ 0.2 dB for the 1.2 to 2.5-GHz unit.

Band-Separation Diplexers

As this device is situated between the input waveguide and the first LNA, it is important that the insertion loss between the input and the band-selecting ports be kept to a minimum. For this reason the 5.0/8.6-GHz diplexer was realised in a suspended stripline format and consists of a low-pass/bandpass filter combination similar to that described by Dean and Rhodes [4], and was analysed and optimized using the microwave CAD program

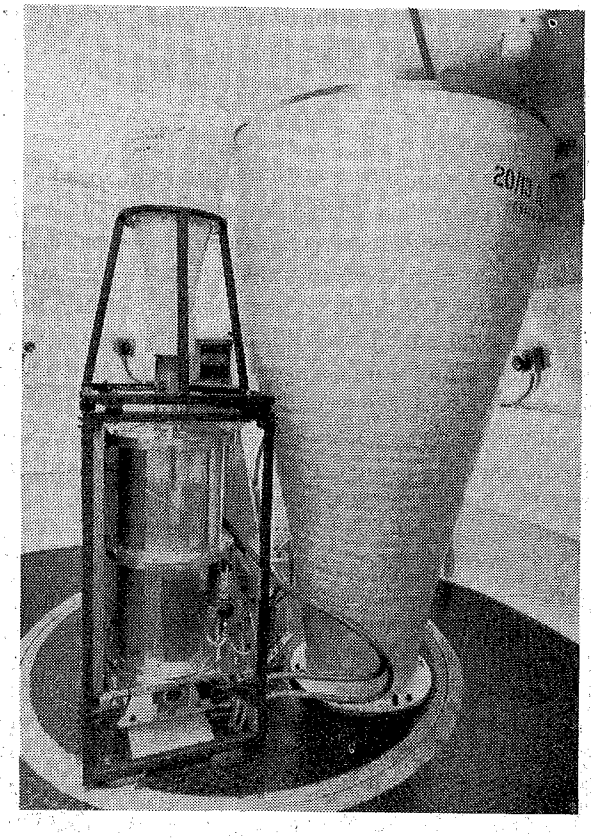

Figure 4(a) 1.5/2.3-GHz horn and 5.08/8.6-GHz front end, mounted on an AT 22-m antenna.

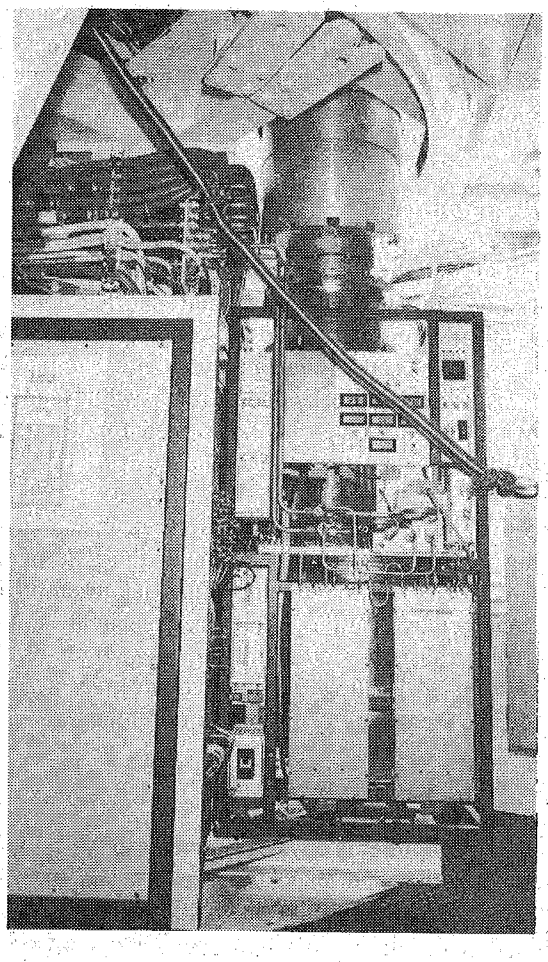

Figure 4(b) 1.5/2.3-GHz front end, mounted on an AT antenna.

'Touchstone' [5]. The 1.5/2.3-GHz device was realised in a microstrip format to minimise its physical size, but used the same design features as the 5.0/8.6-GHz unit.

Because these devices are cooled cryogenically (to 20 K) it was important to make sure that the device would operate reliably over a wide temperature range. In the microstrip structure, care was taken with all the soldered joints to prevent cracking at low temperatures, whilst the 0.12-mm Cuflon (Polyflon Corp.) [6] substrate used in the suspended substrate format was supported by Eccofoam 1.04 between the substrate and each ground plane. This is done to prevent the Cuflon substrate from wrinkling after thermal cycling of the device.

Typical insertion losses were 0.15 and 0.2 dB at 1.5 and 2.3 GHz in the microstrip device, whilst the 5.0- and 8.6-GHz losses were 0.2 and 0.5 dB at midband.

Low-Noise GaAs Mesfet Amplifiers

A detailed description of the four FET LNA designs used in the AT front ends has been given by Gough & Rasmussen [7]. However, a general outline of the design criteria and a brief description of each amplifier will be given here.

To ensure that the AT has good polarization performance, it is essential that the high isolation between the orthogonal outputs of the OMT be preserved by being well terminated in low VSWR loads. This requires that the band diplexers and cooled LNAs have low-input VSWRs. This was achieved in the LNAs by using source inductance feedback in the 1.5- and 2.3-GHz designs, and cooled isolators on the inputs of the 5.0- and 8.6-GHz amplifiers.

At the same time, to achieve optimum low-noise performance, a microwave FET needs to be driven by an optimum generator impedance, Z_{opt}, where $Z_{opt} = R_{opt} + jX_{opt}$. As both the R_{opt} and X_{opt} required by the FET change as the device is cooled cryogenically, designing and tuning the amplifiers was optimized for cryogenic operation.

The amplifier input-matching network is designed to transform the 50Ω system impedance to Z_{opt}. For a

narrow observing band, for example the 2.3-GHz band, a quarter-wave transformer can be used to transform the 50Ω system impedance to R_{opt}, and a series inductance will provide jX_{opt}. For bandwidths of about 30% (e.g. the 5.0-GHz band), we need an input-matching network which will approximate Z_{opt} over the required bandwidth.

1.5-GHz amplifier

The 1.5-GHz amplifier is based on that designed by Weinreb *et al.* [8]. This amplifier has a microstrip quarter-wave input transformer and shorted stub to broadband the input match and noise performance. The source inductance can be changed by moving small gold-plated brass-shorting blocks under fingers which support the FETs. These blocks are positioned for minimum source inductance for the second and third FETs.

The noise minimum of the amplifier can be tuned by adjusting the inductance in series with the gate of the first transistor. The input impedance of the amplifier can be matched by trimming the inductance in the source of the first transistor and adjusting the length of the shorted stub. Adjusting the input match has a small effect on the frequency of the noise minimum.

2.3-GHz amplifier

The 2.3-GHz amplifier is physically similar to the 1.5-GHz amplifier, but the input-matching network and the gain stages have been redesigned. As the required bandwidth is only about 13%, a narrowband input-matching network is used, consisting of a quarter-wave transformer and inductance in series with the gate of the first transistor. The amplifier tuning is similar to that of the 1.5-GHz amplifier, except that there is no shorted stub.

5.0-GHz amplifier

The 4.5 → 6.1-GHz observing band has a 32% bandwidth. Low-noise operation over this wide bandwidth is achieved using an input-matching network consisting of two, cascaded, microstrip, quarter-wave transformers and an inductance in series with the gate of the first transistor. The series inductance is formed by the gate lead of the first transistor. The noise minimum of the amplifier can be tuned by adjusting the length of this gate lead. Figure 5 shows the RF circuit in the upper cavity and the bias protection circuit in the lower cavity.

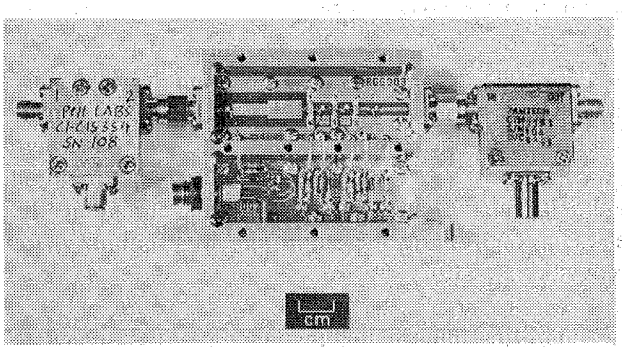

Figure 5 5.0-GHz low-noise amplifier.

The amplifier was built in a dual-cavity housing because a single one, large enough for the whole circuit, would have in-band cavity resonance modes.

Gain is achieved over the broad bandwidth by placing the three transistors close together, consistent with providing the second- and third-stage transistors with a gate-driving impedance approximating Z_{opt}.

8.6-GHz amplifier

The amplifiers for the 8.0 → 9.2-GHz observing band are based on the three-stage design described by Tomassetti *et al.* [9]. That design used square-section, coaxial lines with moveable, quarter-wave transformers at the input and output of each of the three gain stages. To meet the 30-dB gain requirement over this relatively wide band, the amplifiers are of a four-stage design. The matching networks between stages were designed to maximize the gain bandwidth. The capacitive coupling from the input line to the gate of the first transistor was maximised to increase the low-noise bandwidth of the amplifier.

Amplifier performance

The noise and gain performance of the best selected FET amplifiers, at both ambient and cryogenic temperatures, are listed in Table 1. The amplifier noise temperature given in the Table includes the noise contribution from the approximately 0.3-dB loss in the input isolators on the 5.0- and 8.6-GHz amplifiers. This loss increases the amplifier noise temperature by about 3 K at cryogenic temperatures, and about 30 K at room temperature. The noise and gain given at 290 K are for the amplifiers tuned for optimum cryogenic operation, but operating at room temperature.

Currently, the AT array front ends are equipped with amplifiers using FET devices, the best of these giving the performances outlined above.

Recent experiments with the 5.0- and 8.6-GHz amplifiers, whereby the input FET is directly replaced by a high electron mobility transistor (HEMT) has

Table 1

Amplifier noise temperature and gain

Observing Band (GHz)	Amplifier Ambient Temperature			
	290K		15K	
	Min. Noise (K)	Min. Gain (dB)	Min. Noise (K)	Min. Gain (dB)
1.5	50	29	8	36
2.3	55	31	10	37
5.0	150	26	22	28
8.6	220	20	29	29

resulted in the minimum noise temperature of the amplifier being reduced by about a factor of two. Thus, the minimum is ~ 10 K at 5.0 GHz and ~ 15 K at 8.6 GHz. A program to retrofit the array with these improved amplifiers will begin soon.

Post-LNA Amplifier Module

This module performs several functions, the first of which is to provide an extra 25-dB RF gain at the observing frequency before the first conversion stage. The input noise temperature of the commercial RF amplifiers used in these modules ranges from ~ 100 K at 1.5 GHz up to ~ 400 K at 8.6 GHz, and so with LNA gains of 30 dB or more, the contribution of these amplifiers to system noise is < 0.5 K.

Rejection of the image band of the first conversion stage is also achieved in this module. The microstrip filters are especially designed to cover the AT observing bands adequately, whilst providing at least 30-dB image rejection for the first converter. This, coupled with the FET amplifier gain roll-off and diplexer attenuation, provides more than the required 40 dB-image rejection.

The third function incorporates remotely controlled attenuators in each polarization channel which reduces the RF gain by 20 dB when observing strong solar radiation.

Finally, the module is designed to incorporate a pair of 180° phase modulators in each polarization channel, both switched at different rates. The function of these devices is to phase modulate the incoming RF signals at a point in the signal path which is as close to the LNA system as possible. Consequently, the effects of any unwanted RF interference entering the signal path after this point will be substantially reduced when a phase demodulation process is carried out in the digital correlator.

Cryogenics System

The microwave input components and FET amplifiers are all cooled by a closed-cycle helium refrigerator which has a second-stage thermal capacity of 10 watts at a nominal temperature of 20 K, and a first-stage capacity of 30 watts at 70 K.

This machine (manufactured by CTI of Waltham Mass.) uses the second stage to cool all the input components and FET amplifiers of the 5.0/8.6-GHz front end to approximately 15 K. The first stage is used to cool a nickel-plated copper radiation shield which encloses all the cooler 15-K components. The total cooled mass attached to the second stage is 7 kg of copper and aluminium which requires some 7-8 hours to cool to an operating temperature of 15 K.

The 1.5/2.3-GHz front end uses a different arrangement whereby the diplexers and FET amplifiers are cooled to 15 K, whilst the orthomode polarization transition is cooled to 75 K using the higher cooling capacity (30 watts) of the first stage.

The 1.5/2.3-GHz OMT is massive and weighs some 11 kg. In addition, its surface area is large, so that radiative loading on this device becomes a significant factor in the total thermal load on the refrigerator.

Nonetheless, the diplexer and FET amplifier load of some 4.5 kg is cooled to 13 K in five hours, but the OMT requires another 20 hours to reach the operating temperature of 75 K. Thermal insulation is obtained using stainless steel vacuum Dewars of cylindrical form which are carefully cleaned and electropolished. This is an important step to maintaining an inner Dewar surface emissivity of less than 0.1 which will minimise radiative loading, particularly in the 1.5/2.3-GHz front end.

The Dewar leak rates are estimated to be less than 1.5×10^{-4} mbar $\ell\ s^{-1}$ for the 1.5/2.3-GHz front end, and less than 3.0×10^{-5} mbar $\ell\ s^{-1}$ for the 5.0/8.6-GHz system.

Internal charcoal and zeolite (molecular sieve) getters attached to the second-stage cold plate, ensure an ultimately good cooled vacuum and a good recovery performance after power interruptions. The foam plug window on the 1.5/2.3-GHz front end gave some initial problems with air diffusion through the large projected area. However, this was largely eliminated by sealing the plug with a polyimide membrane of 0.12-mm Kapton.

The compressed helium for the refrigerator units is obtained from three compressor units mounted on the telescope alidade and piped to the antenna vertex room via well-cleaned stainless-steel piping. A distribution manifold board in the vertex room enables any one of these three compressors to supply helium to any one of three front ends by appropriate valving. It is also possible for front ends to share a common compressor for short periods during times of compressor breakdown. Table 2 gives a summary of the cryogenic system performance.

3.2 Conversion system

The conversion system accepts two orthogonally linear polarization channels from each front-end band simultaneously. Each of the two selected frequency bands are then down-converted to intermediate frequencies suitable for sampling. The system is quite flexible, allowing the received signals to be within the same band (e.g. both in the frequency range 4.5 to 6.1 GHz) or from each of the two bands received simultaneously by the wideband horns (e.g. one within the frequency range 4.5 to 6.1, the other in the band 8.0 to 9.2 GHz). As well as providing inputs for the receivers currently installed on the antennas, it also provides inputs for future development. Four IF

Table 2

Compact Array Cryogenic Performance

1.	Refrigerator type	CTI 1020 CP closed cycle Helium refrigerator	
2.	Compressor type	CTI 1020R (Air Cooled)	
3.	Front Ends		
		5.0/8.6 GHz	1.5/2.3 GHz
	2nd-stage operating temp.	10-15 K	12-15 K
	1st-stage operating temp.	40 K	75 K
	Cool-down times:		
	Load on 2nd stage	8 hr (13K)	5 hr (13K)
	Load on 1st stage	6 hr (40K)	25 hr (75K)
	Mass cooled by 2nd stage	7 kg	4.5 kg
	Mass cooled by 1st stage	2 kg	13 kg
	Survival time *	2 hr	2 hr
	Interval between maintenance	18,000 hr (2 yr)	18,000 hr (2 yr)

* Survival time is defined as the period during which the cooling process can be stopped and then restarted without re-evacuation of the Dewar.

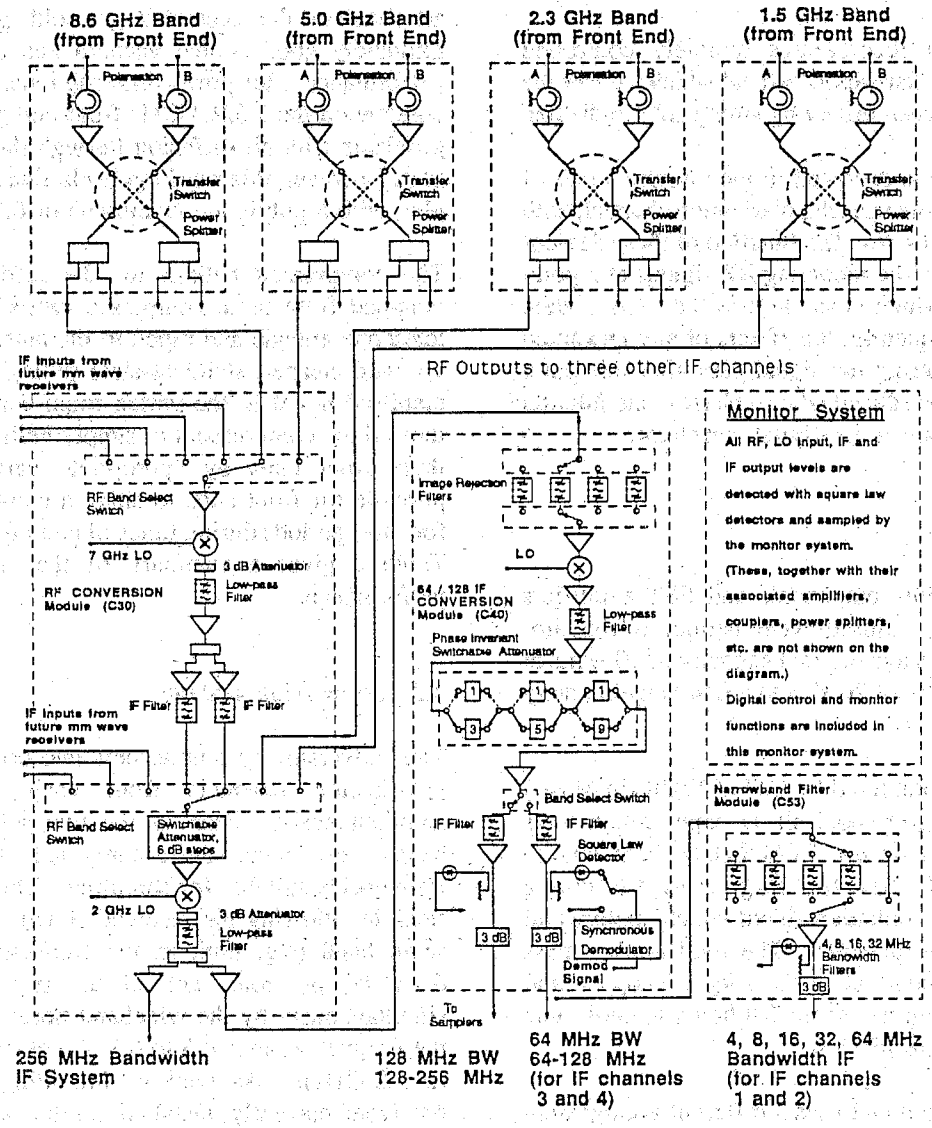

Figure 6(a) Conversion system block diagram.

channels are available. Two channels provide 128- and 64-MHz bandwidths for continuum observations (the first centred on 192 MHz and the second on 96 MHz), whilst the other two channels provide bandwidths of 128, 64, 32, 16, 8 and 4 MHz for both continuum and spectral-line work. These bandwidths are all selectable remotely. A 256-MHz bandwidth will be available when mm-wave observing bands are instrumented.

The system uses three conversions. The three LO signals, generated by the antenna LO system [10] have relatively narrow tuning ranges, lying in the region between the RF bands. (By keeping these LO signals out of the RF bands, we reduce the problems of self-generated interference that would restrict the reception of various portions of the bands.) In addition, by having a choice of several IF bands, the RF-band coverage can be maintained with an even smaller LO tuning range. For example, the lower portion of the 4.5 → 6.1-GHz band is converted to an IF range of 2.2 → 2.8 GHz, whereas the middle and higher portions of this band are converted to a band in the range 1.2 → 1.8 GHz. One or other of these two IF bands is then converted to frequencies in the ultra-high frequency (UHF) range by using the second mixer in the system. This mixer also converts the 1.5/2.3-GHz front-end RF output to the UHF range. The same design philosophy of multiple band inputs is used in the final IF mixing stage which sets the output bandwidth and centre frequency of the conversion system. This technique again extends the RF tuning range of the overall conversion system, whilst keeping the LO tuning range restricted. Another important feature of the system design was an analysis of the complex multiple mixing process to determine if higher order mixing products could produce spurious IF responses. This was done using a computer program developed at the Australia Telescope National Facility (ATNF) [11] based on expressions in a report on mixer intermodulation products [12]. The results of this analysis showed that the system was clear of any detectable spurious mixing responses. Figure 6(a) shows a block diagram of the full system, whilst Fig. 6(b) shows the relationships between the various RF, LO and IF filter bands.

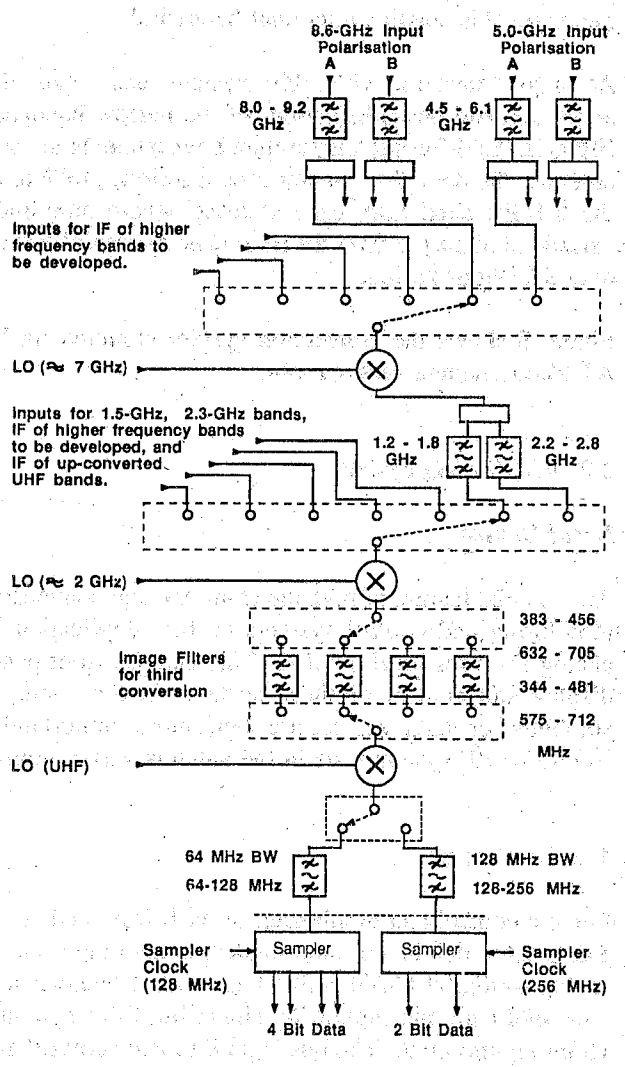

Figure 6(b) Conversion system, showing the relationship between the various RF, LO and IF filter bands.

To integrate this complex system into a reasonable space with a high degree of modularity, planar microstrip circuitry was adopted as the construction medium for all the sub-assemblies used in the conversion system. A synthesis telescope relies on a high degree of gain and phase stability to produce maps of good dynamic range and polarization purity. As indicated above, the down-conversion system is very flexible and covers a wide range of frequencies; the signal path is quite complex and passes through many sub-assemblies. Therefore, each of these sub-assemblies, and particularly the filters contained within them, needs to have very good stability in both amplitude and phase. By using high dielectric substrates, RT/Duroid (RT/6002, RT/6006 and RT/6010.5), manufactured by the Rogers Corp., the phase/temperature characteristics of the filters developed for this system were superior to most of the standard commercial filters tested.

For the same reasons, much effort was involved in measuring the room-temperature S-parameters of individual components and the variation of gain and phase of these components as a function of temperature. For several mixers used in the system, the change in IF phase as a function of local oscillator power was also measured. By adopting these lengthy testing procedures, the most suitable components were selected for use in the system, and a good estimate of the overall phase behaviour of the signal path could be obtained. Figure 7 shows a view of some of the microstrip components and sub-assemblies used in the main microwave conversion module.

Again, the design of all the microstrip components was realised using 'Touchstone'. All the photographic masks were then produced using an associated CAD program 'Micad' [13]. Initially, the masks were cut,

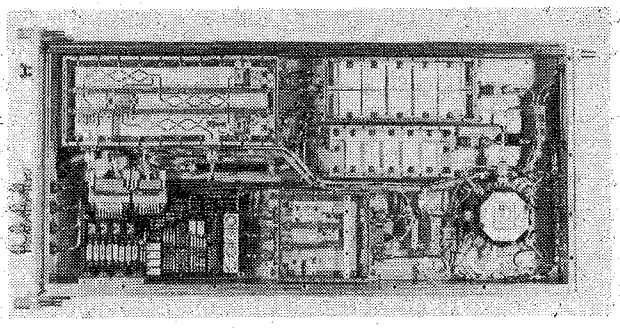

Figure 7 Conversion module (5.0/8.6-GHz side) with covers removed.

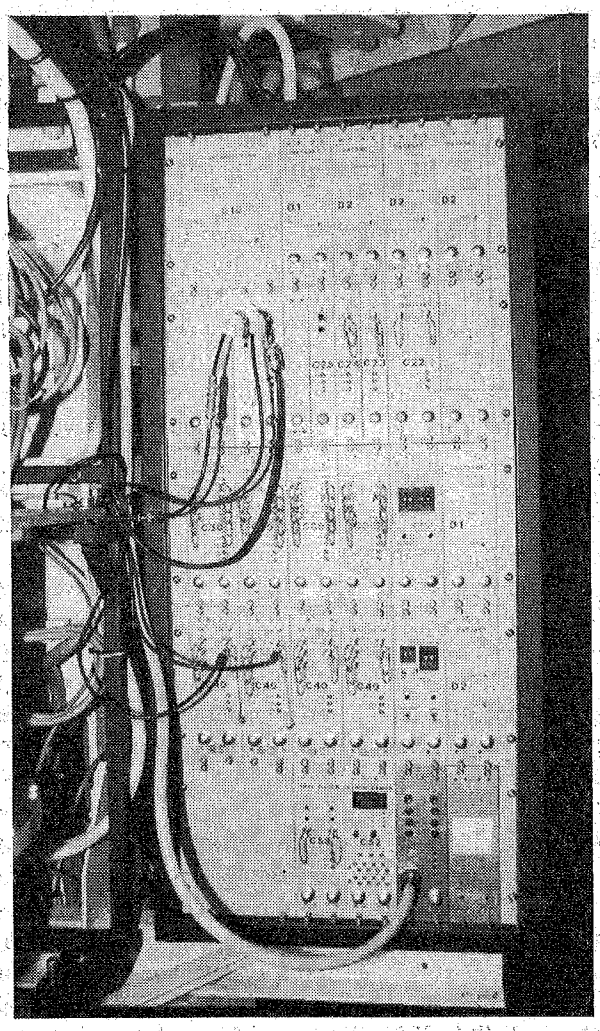

Figure 8 Conversion system, mounted in an AT 22–m antenna vertex room.

two or four times full size, onto a product equivalent to Rubylith. These were then photographically reduced to the correct size.

Generally, the (measured) VSWR for the filters was better than 1.2:1 with an insertion loss of about 0.3 dB. The higher order filters (sixth order) had a slightly worse VSWR (about 1.35:1) and the insertion loss was higher (approximately 0.5 dB). All the sub-assemblies have good input and output matches (VSWR < 1.5:1) and have very flat conversion gains, contributing to the excellent stability of the overall system.

The antenna-based narrowband filter system currently in use for spectral-line work, whilst simple in concept, presents some special problems due to location, and the frequency at which it is operating. In practice, the system consists of four selectable narrow bandpass filters placed at the 64-MHz bandwidth output of the main IF system. The final IF bandwidths available from the system are: 64 MHz (a through path), 32, 16, 8 and 4 MHz.

Because of their larger fractional bandwidths, the 32- and 16-MHz filters have been constructed with toroidal inductors and surface-mounted capacitors with high Q. The 8-MHz filter (7% BW) however, used a commercial type (K & L 6B111-92/R6.22, [14]) which is constructed using a tubular, lumped transmission-line technique, whereas the 4-MHz filter (5% BW) used a surface acoustic wave (SAW) device to obtain a good shape factor for this smaller fractional bandwidth.

A major concern with this system has been the amplitude and phase behaviour of the narrow bandpass filters in the differing temperature environments in each antenna. To date, this has not been a serious problem in the 8-MHz bandwidth case at least, where amplitude variations of only ± 0.05 dB (± 1%) have been observed over a 24-hour period.

Figure 8 shows the conversion system mounted in the AT 22-m antenna vertex room.

3.3 Monitoring system

Local Control

An essential feature of both the front-end and conversion monitoring and control systems is their duplication in analog form for local control. This enables front panel display and control of these systems in the event of computer or data set failure but, more importantly, simplifies RF system tests in the antenna vertex rooms.

Remote Control

Remote control and monitoring of each front end is via a data set which is a pseudo-modem containing a 12-bit analog-to-digital (A/D) converter, a data formatter, and a parallel data bus supporting single-bit, 8-bit byte and 16-bit input/output. The bus is used to latch control and monitor registers and to multiplex the 64 analog voltages representing the Dewar vacuum and temperature environment, FET bias supplies, helium pressures for the cryogenics and all front-end voltage supplies and post-

regulated outputs. The data sets are 'daisy-chained' to the antenna control computer by balanced RS422 transmission lines. Individual antenna control computers are connected to the central site computer via optical fibres.

A similar scheme is used to monitor and control the variable parameters of the conversion system remotely. Here, control words latched from the data set into interface modules are decoded and used to set microwave attenuators, switch in band-select filters and set the RF signal path through the conversion chain via multiple RF switches. RF and LO power levels are detected and their equivalent voltages multiplexed into the data set A/D converter.

4 CALIBRATION SYSTEM

When in operation, a synthesis telescope determines the degree of correlation of noisy signals arriving at each interferometer pair when the separated antenna elements in the array are all pointed at the same radio source.

To measure this correlation, the signals are first digitised in a high-speed 2-bit sampling system located in the antenna, conveyed back to the central control site with appropriate delay compensation, and then correlated.

Crucial to the sampling process however, is the need to keep the signal input power levels to the samplers constant. Analog methods to do this (automatic level controls) can produce system phase variations as the total power levels vary with consequent loss of dynamic range in the resultant map. An alternative method involves maintaining constant sampling statistics within the sampler system regardless of the total power input levels. This is the system that was adopted in the AT, but with the total power input variation limited to a range of 3 dB. This means, of course, that the effective 'gain' of the overall system (i.e. the degree of correlation for a given radio source flux) will change as the total power input levels to the samplers change. This is largely due to changes in system noise temperature, provided that the overall RF and IF system gain can be kept constant by good design and temperature control. To obtain the true radio source flux S, we need to scale the correlation C by some factor related to the system noise temperatures of the receivers in each antenna. Thus

$$S = K.C.\ \sqrt{T_{SYS_m} \cdot T_{SYS_n}} \qquad (2)$$

where T_{SYS_m} and T_{SYS_n} are the system temperatures of antennas m and n respectively, and K depends on a number of factors including antenna efficiency.

Synthesis observations are made by tracking a radio source for up to 12 hours, during which time the elevation angle of the antenna may change substantially. Contributions to system temperature from both ground radiation and attenuation through the atmosphere are elevation-angle dependent, and will change over the course of an observation, whilst rain clouds and water vapour also increase the system temperature. Consequently, it is important that the system temperatures be monitored accurately so as to correct the system 'gain' function as indicated above.

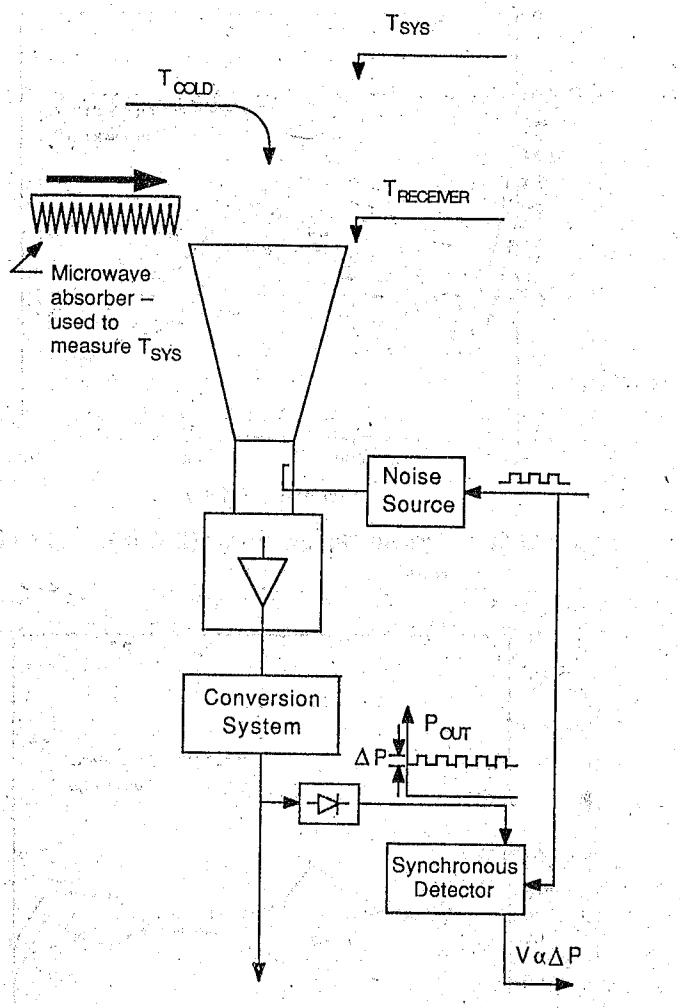

Figure 9 Gain and system temperature measuring system, showing T_{sys}, $T_{receiver}$ and T_{cold}.

Figure 9 shows a block diagram of how the gain and system temperature monitoring is performed. The system temperature is measured by continuously comparing the receiver output power, P_{OUT}, with the change in the output power, ΔP, which occurs when a calibration noise diode in the receiver input is switched on and off. Thus

$$T_{SYS} = T_{CAL}\ \frac{P_{OUT}}{\Delta P} \qquad (3)$$

where T_{CAL} is the size of the calibration noise source; ΔP is also a measure of receiver gain, from the noise source coupler to the power detector in the output.

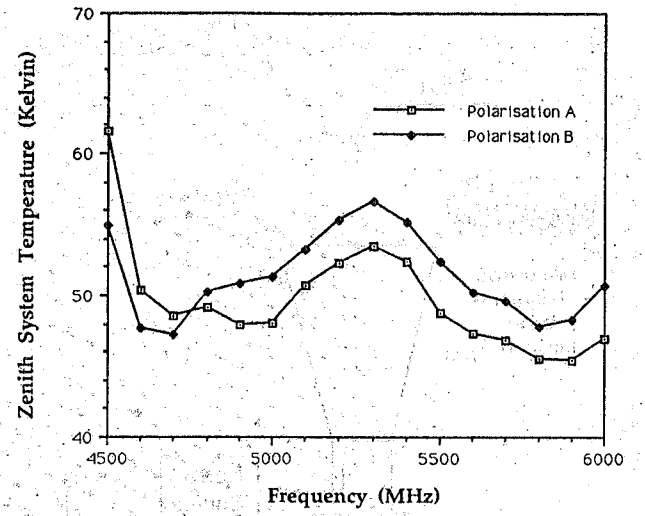

Figure 10(a) System temperature (Kelvin), 5.0-GHz band.

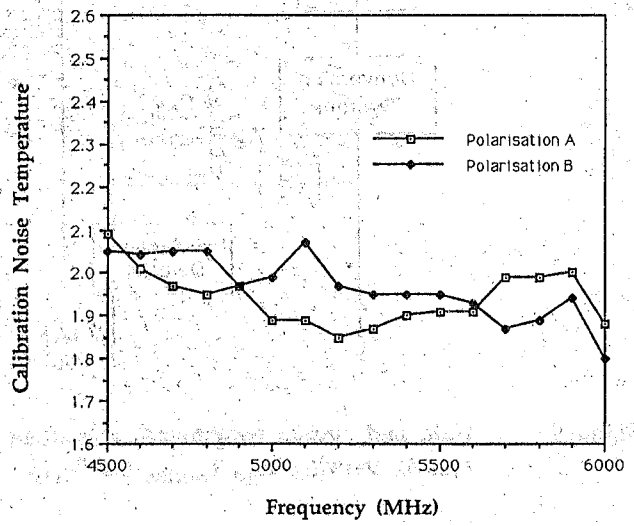

Figure 10(b) Calibration noise temperature, 5.0-GHz band.

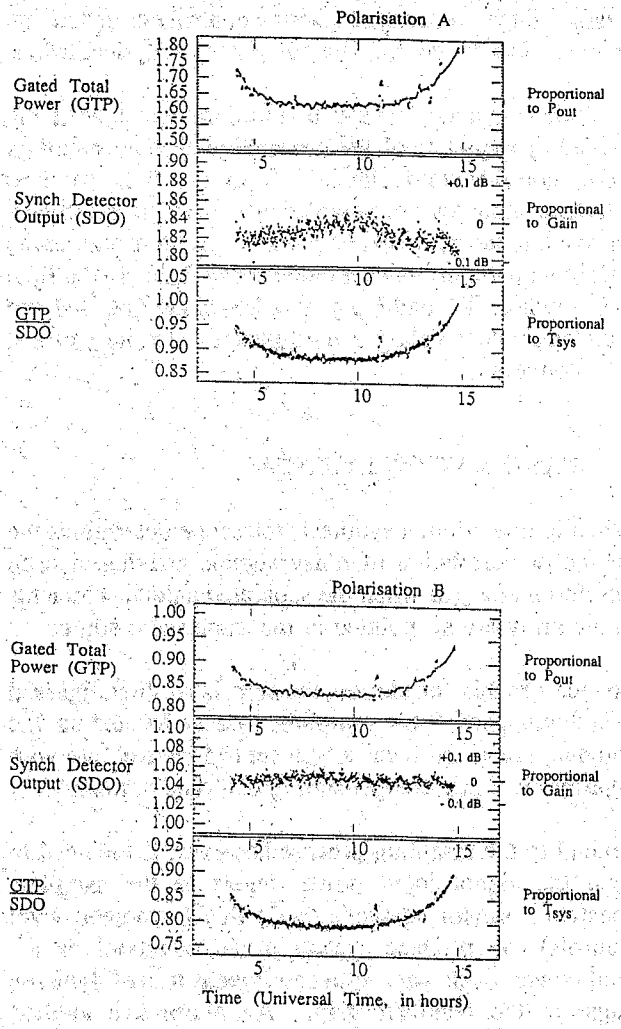

Figure 11 System performance and gain stability.

Table 3

C.A. Zenith System Temperature

	1.47 GHz (1472 MHz)	2.38 GHz (2380 MHz)	4.79 GHz (4790 MHz)	8.63 GHz (8630 MHz)
Background	2.8	2.8	2.8	2.8
Antenna	6.0	6.0	6.5	7.0
Atmosphere	2.2	2.4	2.75	4.0
Horn + Coupler	3.0	3.0	3.0	3.0
Polarizer	3.0	3.0	3.3	3.5
Band splitter	1.0	1.0	1.6	4.0
Cables :	3.5	3.5	1.0	2.8
FET Amp. *	10.0	13.0	28.0	30.0
2nd stage	<1.0	<1.0	<1.0	<1.0
Table	32K	35K	49K	57K
Measured average	33K	36K	50K	65K

* These are mean noise temperatures averaged over 12 channels.

P_{OUT}, ΔP, T_{SYS} and other array parameters are monitored continuously and are used in the gain correction process.

System temperature, T_{SYS} and T_{CAL} are initially measured using a conventional hot/cold load technique as described by Sinclair & Gough [15].

5 PERFORMANCE

The performance of the Compact Array receivers can best be described by Table 2 and Figs. 10 and 11.

Table 3 indicates the mean zenith T_{SYS} for the main observing frequencies in each of the 1.5-, 2.3-, 5.0- and 8.6-GHz bands, averaged over the whole array. In addition, the contribution of each component to T_{SYS} is identified.

Figure 10 gives some indication of a typical front-end system temperature performance across an AT band, in this case the 5.0-GHz band, and a measurement of the injected calibration noise temperature as a function of frequency. This was measured using a conventional hot/cold load technique.

Figure 11 shows gain stability and system performance plots. The total power and synchronously detected calibration outputs, from a 5.0-GHz receiver over a 10-hour observing period, are indicated. These show the inherent RF/IF gain stability of the system with an averaged gain variation of ± 0.05 dB over the 10-hour period.

The T_{SYS} plots show the variation of system temperature as a function of observing time as the antenna tracks from horizon to horizon during the course of the observation. The indicated T_{SYS} variation is used to correct the system 'gain' function which will be modified by the action of the sampler ALC system in response to higher T_{SYS} at low elevation angles.

6 CONCLUSION

To date, the overall performance of the receiver system has been very satisfactory. No major shortcomings have been found in the basic design of the system, and whilst there have been some cases of early component failures due to minor design or material problems, these have been corrected.

Reliability in general has been excellent. Some front-end and conversion systems have been operating on the array continuously for almost four years and have given few problems. Downtime for the front-end, conversion and cryogenics systems as a whole, is an extremely small percentage of the total overall operating time, and is currently estimated as being less than 2% of scheduled Telescope time.

The modular approach adopted in the design and construction of the conversion and LO systems has not only produced a system with excellent gain and phase stability and high reliability, but has also confirmed the operational maintenance benefits of the modular system.

7 ACKNOWLEDGMENTS

We thank our colleagues in the ATNF Receiver Group — Russell Bolton, Henry Kanoniuk, Grahame Gay, Peter Seckold, Patrick Sykes, Simon Hoyle and Graeme Carrad. Their skill, dedication and attention to detail has brought the initial receiver system development and construction to a successful conclusion.

We also thank former members of the Group — John Murray, Gerry Gerrard, Mark Leach, Hans Rasmussen and Malcolm Smith — for their valuable contributions during the development years.

We are also indebted to the Radiophysics Drawing Office staff for their assistance with design and drafting, and to the Radiophysics Workshop staff, whose skill and craftsmanship made the whole project possible.

8 REFERENCES

1. James, G.L., "The Australia Telescope Antennas: Reflector Optics and the Feed System", IREECON '85 Convention Digest, Melbourne, 713-715, 1985.

2. James, G.L. and Skinner, S.J., "The Wideband Feed System on the Australia Telescope", 6th International Conf. on Antennas and Propagation (ICAP 89), Part 1, 163-167, 1989.

3. Wilson, W.E. and Willing, M.W., "The Sampling and Data Synchronization Systems", JEEEA, this issue.

4. Dean, J.E. and Rhodes, J.D., "Design of MIC Broadband Contiguous Multiplexers", IEEE MTT-S Int. Microwave Symp. Digest, 147-149, 1980.

5. Touchstone CAD package produced by EEsof Inc., 31194 La Baya Drive, Westlake Village, CA 91362 USA.

6. Cuflon-Substrate material manufactured by the Polyflon Corporation, 35 River Street, New Rochell, NY 10801 USA.

7. Gough, R.G. and Rasmussen, H.K., "Low-Noise FET Amplifiers for the Australia Telescope", IREECON '89 International Proceedings, 345-348, 1989.

8. Weinreb, S., Fenstermacher, D. and Harris, R., "Ultra Low-Noise 1.25 - 1.7 GHz Cooled GaAs FET Amplifiers". Trans.IEEE Vol. MTT-30, 849-853, 1982.

9. Tomassetti, G., Weinreb, S. and Wellington, K., "Low-Noise 10.7 GHz Cooled GaAs FET Amplifiers". Electron.Lett. 17, 949-951, 1981.

10. Young, A.C., McCulloch, M.G., Ables, S.T., Anderson, M.J. and Percival, T.M., "The Local Oscillator System", JEEEA, this issue.

11. Graves, G.R. and Gough, R.G. "Spurious Mixer Products", Australia Telescope National Facility, CSIRO Internal Memo 22.1.1/036.

12. Henderson, B.C. "Reliably Predict Mixer IM Suppression", Microwaves & RF, November 1983, 63, 1983.

13. Micad-CAD Package produced by EEsof Inc.

14. K & L Filters - Manufactured by K & L Microwave.

15. Sinclair, M.W. and Gough, R.G., "System Temperature Calibration of the Australia Telescope Receiver Systems". IREECON'91 International Proceedings, 381-384, 1991.

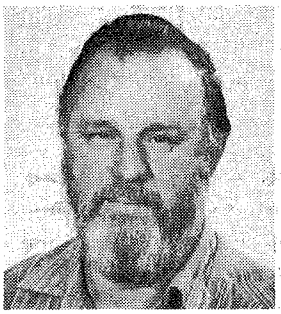

MR M.W. SINCLAIR

Malcolm Sinclair joined the Division of Radiophysics in 1954 as an apprentice electrical fitter. After completing the trades training, he attended the University of NSW and completed a Radio Engineering Diploma (ASTC) in 1964. Since then he became a member of the CSIRO Division of Radiophysics Receiver Group, developing low-noise microwave receiver systems for the Parkes 64-metre radio telescope. Between 1977 and 1979 he worked in the USA where he was responsible for the installation of cooled microwave receivers on the 27 antennas of the Very Large Array, built by the National Radio Astronomy Observatory in New Mexico. He rejoined the Division of Radiophysics in early 1980, and in 1983 he was appointed head of the Australia Telescope Receiver Development Group.

MR G.R. GRAVES

George Graves received the BSc degree, and the DipEd from the University of Sydney in 1967 and 1968 respectively. He was awarded a Dip. Electronics from Macquarie University in 1973 and an MEngSc from the University of Sydney in 1983. He was a High School teacher from 1968 to 1973 and a research assistant at the University of Sydney's Fleurs Radio Telescope from 1974 to 1982. He has been with the CSIRO Division of Radiophysics since 1983, and the Australia Telescope National Facility since January 1989 as a member of the Receiver Group for the Australia Telescope project. At present he is a senior experimental scientist with the Australia Telescope National Facility and is primarily engaged in the design and construction of the down-conversion and IF system electronics for the Australia Telescope.

MR R.G. GOUGH

Russell Gough received his BSc, BE and MEngSc degrees from the University of Sydney. He worked at the University's Fleurs synthesis telescope until 1981, when he moved to West Germany to work at the Max-Planck-Institut für Radioastronomie. In 1983 he returned to Sydney to work on the development of low-noise FET amplifiers for the Australia Telescope project at the CSIRO Division of Radiophysics. In 1989 he moved to the CSIRO Australia Telescope National Facility's Paul Wild Observatory, Narrabri, where he has been working on the monitoring and maintenance of the receiver systems for the Australia Telescope.

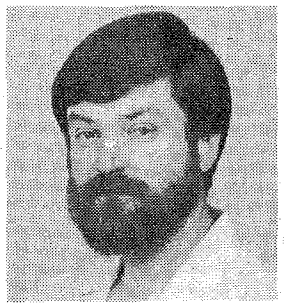

MR G.G. MOOREY

Graham Moorey joined the Receiver Group of the Division of Radiophysics, CSIRO in 1968 after working for four years with STC as a technician. He was awarded a BA from Macquarie University in 1976. In 1982 he went to the USA for two years to the National Radio Astronomy Observatory in Tucson, Arizona, where he worked on millimete-wave receiving systems. On his return to CSIRO in 1984, he rejoined the Receiver Development Group as deputy leader, working mainly on the front-end electronics system for the Australia Telescope project.

The Local Oscillator System

A.C. Young*, M.G. McCulloch**, S.T. Ables*, M.J. Anderson* and T.M. Percival***

SUMMARY The Australia Telescope receivers require a complex, highly stable local oscillator system for signal tuning and for conversion to lower frequencies. All twelve oscillators within each antenna must be precisely phaselocked to a central frequency reference oscillator up to 5 km away. One oscillator in each antenna must also be phase rotated at many thousands of degrees per second whilst maintaining a phase accuracy of 1°. This paper outlines the combination of techniques used to meet these requirements.

1 INTRODUCTION

The Australia Telescope (AT) has six 22-m diameter antennas at Narrabri, each containing four receivers. These receivers have a frequency range which extends from about 1 GHz and, ultimately, will exceed 100 GHz. Such high frequencies must first be down-converted to a lower value before being sampled and then vector multiplied and integrated in a digital correlator (see [1]). To reduce the incoming signal frequency to a more manageable value, a stable local oscillator (LO) frequency is subtracted from the signal frequency, as in any conventional radio receiver. Several LO signals are needed for the multiple-frequency conversion stages within each antenna, as outlined in the paper on the receiver system [2]. To set the receiver tuning, the local oscillators which produce these signals are variable in frequency. The requirements placed on the oscillators within a synthesis radio telescope are far in excess of those normally associated with conventional local oscillators.

2 REQUIREMENTS

Since the entire radio telescope is a phased array, the phase of each LO signal must be precisely controlled to preserve the phase through each receiver channel. Any phase variation during each signal integration period will reduce the coherence of the signals and result in a reduced correlator output and thus a loss of sensitivity. Of even greater importance is the random phase error from one integration period to the next, since this will seriously reduce the quality of the final image. For high-dynamic-range imaging, a maximum phase variation of 1° rms is required between the elements of the array. At higher frequencies, however, the ultimate limiting factor is the path-length fluctuations within the atmosphere. Although these vary from day to day, a value of 0.5 mm rms, for periods up to 30 minutes, is typical during good conditions. This corresponds to about 6° rms at 10 GHz, and the aim is to keep all LO variations less than this to avoid degrading the receiver output information, even when the antennas are spaced over a distance of up to 6 km.

This is most demanding and means that each antenna oscillator must be accurately locked in a specific phase relationship with the other antennas. This is achieved by sending to all antennas a reference oscillator signal to which all antenna LOs are phaselocked. A round-trip 'phase-transfer' system constantly measures the phase changes (inevitable due to cable movement and temperature variations) within the distribution cables and permits appropriate corrections to be applied.

Another requirement is that the relative phase between the LOs in different antennas must be incremented to remove the relative phase rotation (due to the rotation of the earth) in the signals received by different antennas. The phase-rotation rates required vary with antenna separation, frequency and pointing angles. For a 6-km array, the rate is typically 1 Hz for each 1 GHz of receive frequency, but extends to many kHz for the long baseline array (LBA) which uses antennas up to 3000 km away. The phase information is, typically, loaded only once every 10 seconds and the phase rotators must 'free wheel' over this period to a precision of 1° even when rotating at many thousands of degrees a second.

* Australia Telescope National Facility, CSIRO, PO Box 76, Epping NSW 2121, Australia.
** Present address, Nobeyama Radio Observatory, Minamisaku, Nagono 384-13, Japan.
*** Division of Radiophysics, CSIRO, PO Box 76, Epping NSW 2121, Australia.
Submitted to The Institution of Radio and Electronics Engineers Australia in June 1992.

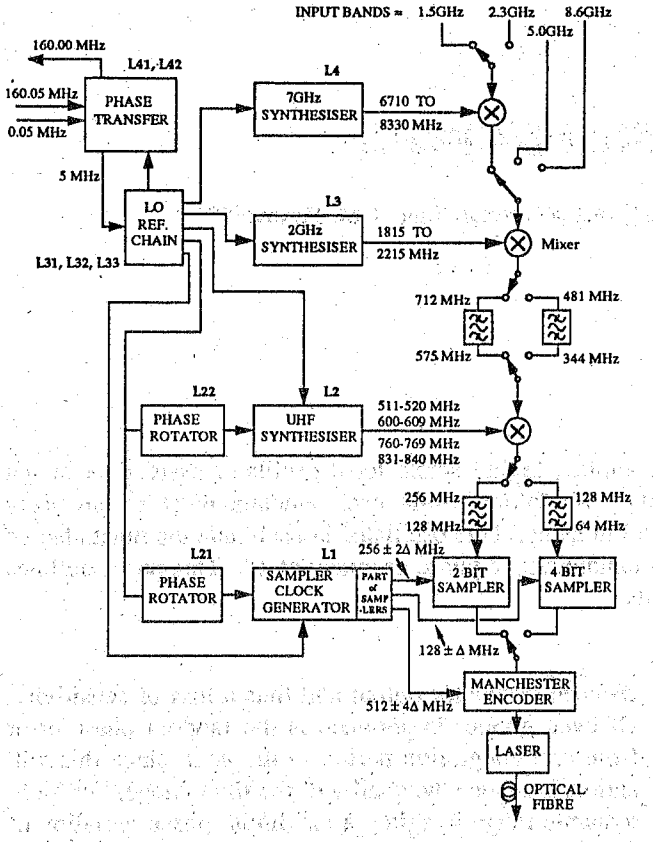

Figure 1 The antenna LO system showing its relationship to the Conversion system. The LO and Conversion systems are shown in a very basic form and only one of the four channels is shown.

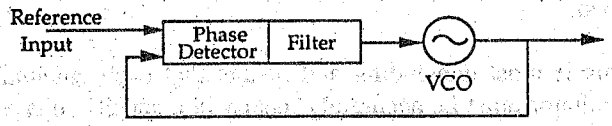

Figure 2 A basic phaselock loop.

A further requirement was that unwanted leakage and spurious signal levels must be extremely low. With highly sensitive, cryogenically cooled receivers and long integration times, a very small, interfering, leakage signal can swamp the received spectrum, with disastrous effects. Heavy screening was therefore imposed on the design of the modules and machined boxes which contain the LO signals.

Small spurious signals produced within the LO phase-lock loop (PLL) circuits can also travel along the LO cables and enter the conversion mixers along with the wanted LO signal. To avoid interference, these spurious signals must be, typically, more than 120 dB below the wanted LO signal level rather than the 60 dB normally specified for commercial synthesisers.

The frequency of each oscillator must be adjustable in precisely defined steps to tune the receiver centre frequency. This tuning must be achieved within 20 ms to permit rapid receiver switching with the added constraint that, after switching, the phase must be predictable. This prevents the use of many commonly used PLL architectures.

Each of the six Narrabri antennas contains four separate receiver channels with three conversion stages in each channel. The first two LO signals are shared between two channels but the final LO and sampler oscillators are independent. This results in a total of 12 independent oscillators within each antenna. Figure 1 shows the various sub-units, for one receive channel, within the LO system. This system is for the first stage of operation with receiver frequencies to 10 GHz. With so many systems needed for full operation, a high degree of reliability and maintainability is essential.

3 SYSTEM COMPONENTS

The method used to set and control the phase of all the local oscillators precisely, is based around the PLL. This uses feedback techniques to ensure that the phase, and hence frequency, of an oscillator is tightly slaved to a reference frequency, F_r. A basic PLL is shown in Fig. 2. The essential components for a PLL are an electronically tunable oscillator, a reference source, a phase detector and a filtered feedback path.

The receiver LO chain uses three different types of oscillators, depending on the application. YIG tuned oscillators use Yttrium Iron Garnet crystal spheres whose resonant frequency is controlled by a variable magnetic field. They are confined to the microwave part of the spectrum. Hybrid varactor-tuned oscillators are used in many places, with different oscillators used between 40 and 800 MHz. Voltage-controlled crystal oscillators, which have a very narrow tuning range, are used in a few specialised applications, usually below 10 MHz.

A phase detector (PD) is a device whose output voltage is a function of the phase difference between the two input signals. A d.c.-coupled, double-balanced mixer is often used as a phase detector, since the output signal is a simple cosine function of the phase difference between the signals at the RF and LO input ports. This type of detector has a useful input phase range of less than ± 90°, with the result that a PLL using it, loses lock or slips cycles easily when triggered by noise transients. This approach was not used.

Another very common type of PD which, in its simplest form, uses two flip-flops and an AND gate, is shown in Fig. 3. Versions of this type of detector are available in the CMOS, TTL and ECL logic families. In operation, one of the outputs always has a very narrow output pulse, and the other output has a pulse width proportional to the input phase difference [3]. A differential

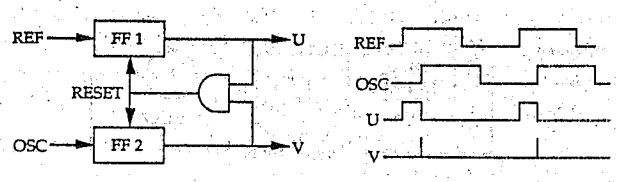

Figure 3 A basic phase/frequency detector.

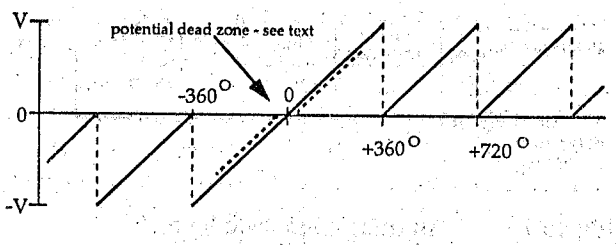

Figure 4 Phase/frequency detector output characteristic.

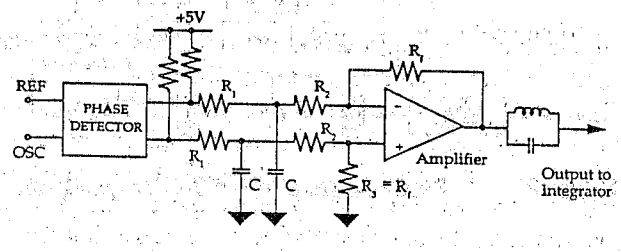

Figure 5 Phase detector circuit arrangement.

amplifier is used to produce an output voltage proportional to the difference in pulse width between the two outputs. The resultant performance is shown in Fig. 4.

For our application, this type of PD has several major advantages. The phase characteristic is very linear, and extends a full ± 360°. This reduces the chances of noise-induced cycle slipping, since minor disturbances are less likely to take the PD outside the ± 360° range. Also, for a frequency difference between the two inputs, which is equivalent to an increasing phase difference beyond ± 360°, the output never goes through zero but has an average d.c. value which tends to drive the oscillator in the correct direction to acquire lock. Therefore, the PD is able to indicate, unambiguously, frequency offset as well as phase differences. This frequency discrimination characteristic is vital for fast phaselocking and also removes the need for a separate sweep circuit.

For our purposes, the ECL version of this type of PD had the best temperature stability above a few MHz input frequency, while the TTL version was better at lower frequency. The CMOS version had a 'dead zone' of a degree or two about zero phase, resulting in uncertainty in the phase of the locked oscillator. This type of PD was, therefore, not used in the AT local-oscillator system.

The output of the oscillator is a sine-wave signal and the phase detector requires a digital (either TTL or ECL) square-wave signal. To turn the sine wave into a square wave, a comparator is used, but care is essential in this area. Any noise, or ringing due to reflections, or a tendency of the comparator to oscillate will give multiple output edges for each input transition. This will then appear to the PD as a signal at twice the frequency (or more) and was the most common reason for failure to lock during development. Hysteresis intentionally introduced on the comparator will prevent this problem but the phase will then be dependant on any changes of the input signal level. This can be avoided by noting that the PD only responds to one (usually the rising) edge and by ensuring that hysteresis changes only the non-critical edge.

The PD is followed by a loop integrator or filter which is used to control the loop stability and response time. The design of this filter follows the standard PLL procedure [4]. To obtain low phase noise, the loop bandwidth must be high (typically 100 kHz) and this requires that all loop components are flat to about 5 MHz. Special coil drivers and 50-MHz bandwidth loop-amplifiers are widely used in the YIG-based oscillators.

In all the loops used in the AT's local oscillator system, the PD digital outputs are connected to a differential amplifier via low-pass RC filters to average the d.c. output and remove most of the output pulses. This is usually followed by a notch filter, resonant at the PD operating frequency. These measures greatly reduce the presence of small amounts of the PD operating frequency on the output of the phase detector thus avoiding frequency modulating the oscillator. Any small remnant is usually removed by adding a small amount of bias to balance the PD and amplifier combination. In this way the PD pulse width is minimised. The general arrangement is shown in Fig. 5. The overall sensitivity of the phase detector and amplifier combination is about 0.3 volts per radian.

Often the output frequency of a phaselocked loop needs to be much higher than the reference frequency. However, both inputs to the PD must be at the same frequency. The output of the oscillator must therefore be converted down, in some way, to the same frequency as the reference; this can be done in two ways. A digital divider may be used to divide the output down to the same frequency as the reference frequency or, alternatively, a converter, using a mixer and another oscillator, can translate the output signal down to the lower frequency. Variations of both schemes are used within the AT local oscillator system.

For a PLL with a digital divider (Fig. 6), the output frequency is given by $F_o = N * F_r$, where N is the divider ratio. As N is changed, the output frequency changes in increments of F_r. This provides a convenient way of tuning the output of the PLL. A divider can also

be included in series with the reference line to give smaller increments with $F_o = N * F_r / M$. However, phase continuance will be lost if the loop is taken from one frequency to another and then back to the first frequency again, unless M is not varied. Such a frequency change would require a recalibration sequence to re-establish phase each time frequency was changed, thus preventing fast frequency switching. A divider within the loop does not have this problem.

The AT uses, mostly, PLLs with mixers to down-convert the oscillator output frequency (Fig. 7). A sample of the oscillator output is applied to the mixer, and the conversion signal is typically a 'comb' of frequencies over the range of the main oscillator. The output of the mixer, at the same frequency as the reference frequency, is amplified and filtered before being applied to the phase detector. In this case, the output frequency is $F_o = F_r + N * F_c$ where $N * F_c$ is the 'nth' comb line. The comb of signals is generated by a harmonic generator with a very similar output level at all harmonics. These signals must have very low phase noise, so that the resulting mixer IF signal is a faithful representation of the oscillator's output, with minimum contamination added by the comb. For this reason, the comb signal is generated from a highly stable reference chain and harmonic generator combined with a very low phase-noise reference source.

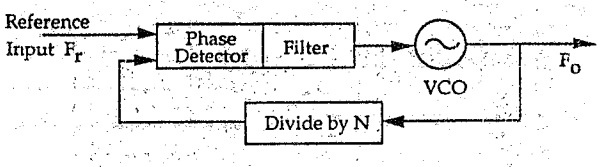

Figure 6 A phaselock loop with divider.

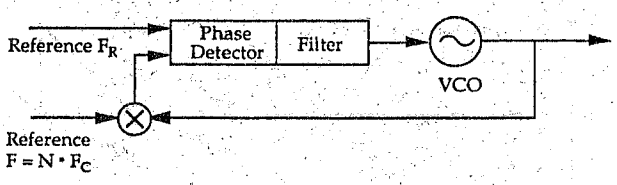

Figure 7 An offset phaselock loop.

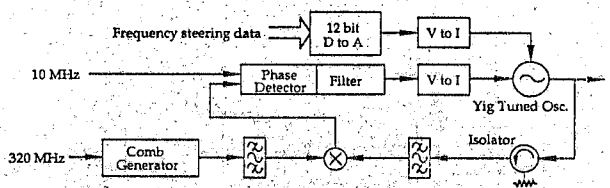

Figure 8 Block diagram of the 7-GHz oscillator.

4 MICROWAVE OSCILLATORS

Two different microwave oscillator modules, with different YIG oscillators, are used within the present receivers. One covers 1800 to 2215 MHz in 10-MHz steps, and the other covers 6.4 to 8.3 GHz in 320-MHz steps. These two modules are very similar, both use mixer conversion, and will be described together.

Typically, YIG-tuned oscillators have a wide-range main tuning coil and a much less sensitive but higher speed 'FM' tuning coil, both requiring current drives. For the oscillators used, the main tuning coil has a sensitivity of 20 MHz per mA and is linear to better than 0.1% over the range of interest. This coil is driven by a high-precision voltage-to-current converter, utilising a high stability resistor and a four-terminal measurement technique to preserve this linearity. Frequency control of a module is by a 16-bit word from the antenna control computer. Each module has a digital interface, which stores data for two frequencies, for use after the start of the next integration period. A 12-bit DAC (digital-to-analog converter) is used to give a voltage which is directly proportional to the desired operating frequency. This voltage drives the precision current driver for the main tuning coil.

Each time the module is retuned, the oscillator is taken first to the top of its frequency range, and then brought down to the final frequency. This ensures that it always approaches the final frequency from the same direction, minimising any magnetic hysteresis effects in the tuning characteristic. Two adjustments on the interface board enable variations in individual oscillators and other components to be accommodated. The FM coil, with a sensitivity of 310 kHz per mA, is used for the PLL feedback drive and uses a simpler voltage-to-current converter, since accuracy is not important within the feedback loop.

A block diagram is shown in Fig. 8. Figure 9(a) is a photograph of the main RF side of a completed module, while Fig. 9(b) shows the remainder of the RF components, the two current-to-voltage converters and, outside the partition, the interface board. When designing and constructing these modules, reliability, high phase-stability and low spurious outputs were major considerations. When RF seals are placed in the edges of the module, and the side covers are in place, a sealed compartment is created and signal leakage is reduced to a very low level. All d.c. voltages into or out of this compartment are via RF filter networks.

The YIG-tuned oscillator is followed by a low-pass filter to remove the output frequency harmonics. The filtered output is then split three ways: two outputs for the dual-polarization receiver conversion system, and one to give a sample for the phaselocked loop. This sample of the output is the 'local oscillator' for the internal microwave mixer, and the 'signal' is a comb of frequencies generated in a harmonic generator. These signals are the harmonics $N * F_c$ of the comb-driving frequency F_c, and

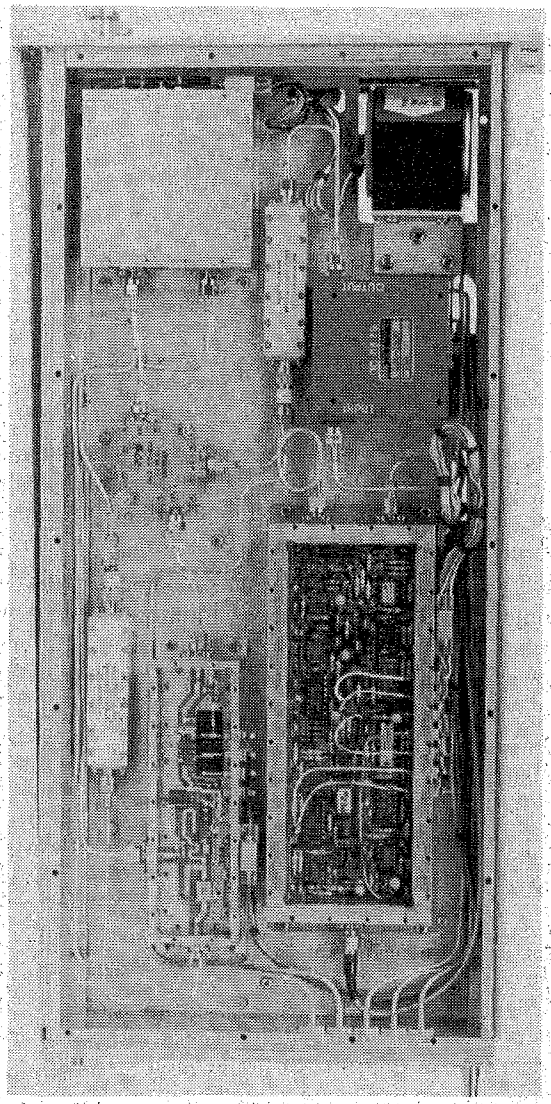

Figure 9 (a) The 7-GHz oscillator.

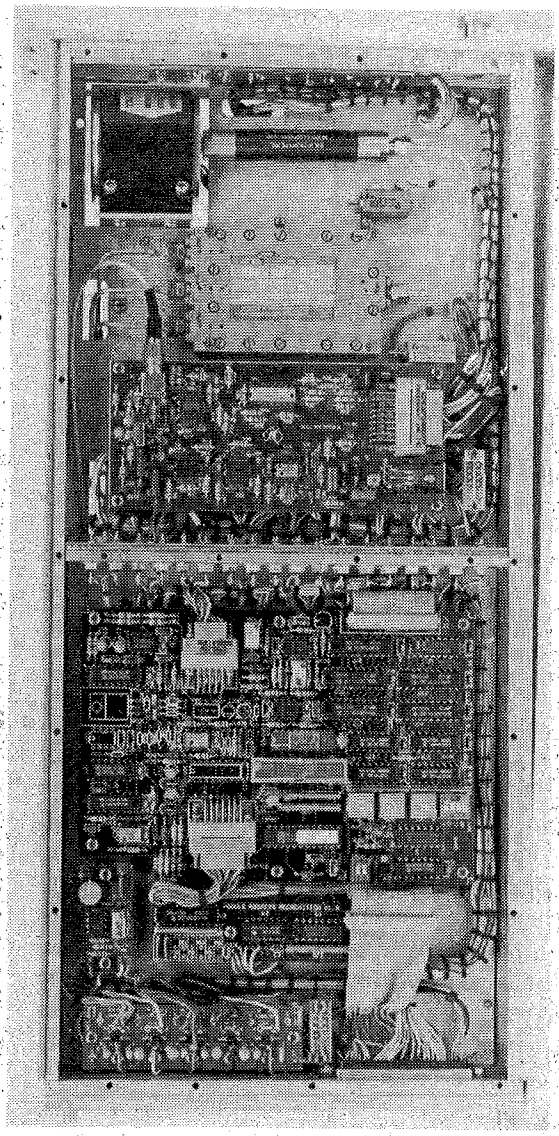

Figure 9(b) The 7-GHz oscillator.

extend well beyond the oscillators' highest operating frequency.

The harmonic or 'comb' generator for the 7-GHz module consists of a step recovery diode (SRD), a power amplifier and matching circuits, as shown in Fig. 10. The input signal of F_c = 320 MHz is amplified to +24 dBm in a power amplifier. The impedance of the diode is matched to the output of the amplifier at 320 MHz. The diode is situated in a circuit which is resonant at 10 GHz. A 40-dB attenuator on the output provides a well-defined match for the comb generator. It also attenuates the comb generator output to the lowest possible useable level to minimise the presence of spurious signals in the output spectrum. The comb generator for the 2-GHz module is a similar design with a 3-GHz resonant frequency and an input drive at 20 MHz.

The output of the microwave oscillators is tightly phaselocked to the output of the comb generators. The comb lines must therefore have high phase stability and

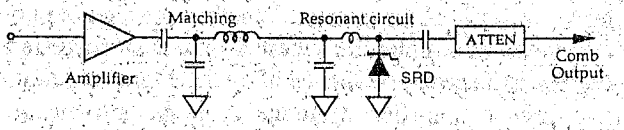

Figure 10 The SRD comb generator.

extremely narrow spectral width to satisfy the demanding phase requirements. Extensive tests showed that the operating point of the 2-GHz SRD could be varied in a closed-loop system to lock the phase of the sixteenth comb line to a 320-MHz reference. In this way the highest component of temperature drift can be removed. This technique proved to be unnecessary within the '7-GHz' module due to the smaller SRD multiplication ratio. Narrow spectral width is achieved by careful design and by the use of an ultra-low-phase-noise crystal oscillator driving the comb generators via the reference chain. Any phase noise on this oscillator

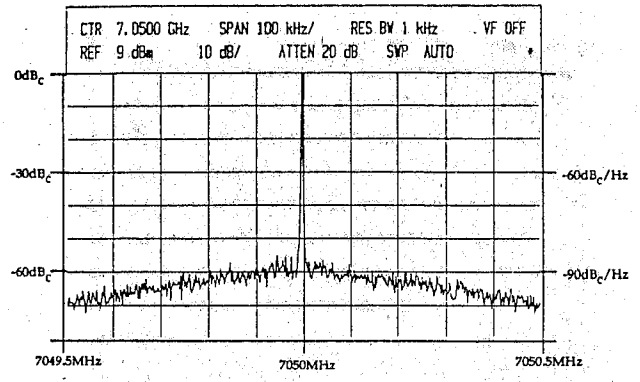

Figure 11 Output spectrum of the locked 7-GHz oscillator.

will be multiplied by a factor of order 1000 (60 dB) to appear on the microwave LO outputs.

To reduce further the leakage of spurious signals from the comb generator, a double isolator was placed in the feedback path before the mixer. This proved to be very effective within its specified band of operation but, outside this band, the isolation was insufficient. To overcome this, a bandpass filter was added to attenuate any comb products outside the isolator's operating band. To reduce the temperature effects on the output phase caused by this filter, an identical filter was included in the comb generator output line, so that the two paths would track with temperature. This also further reduced the level of spurious feed-through at the most critical frequencies at bands centred around $F = F_{LO} \pm F_{IF}$.

When the loop is closed, the final frequency is $F_o = N * F_c \pm F_r$, where F_r is 10 MHz and F_c is 320 MHz for the 7-GHz module. For the 2-GHz module the values are 5 and 20 MHz. The precision of the steering DAC and coil driver is such that, before locking, the oscillator is tuned to within 0.1% (i.e. 7 MHz) of its final frequency. Whether the sign is plus or minus is determined by whether or not an inverting amplifier is inserted, by means of a CMOS switch, after the difference amplifier. Care had to be taken to ensure that the range of the FM tuning coil would not allow the oscillator to lock to the incorrect comb signal. This is more difficult for the 2-GHz module since the comb lines are separated by only 20 MHz. For this reason, the FM tuning range is limited to about ± 10 MHz.

As mentioned earlier, when modules undergo a frequency change, they are first taken to their highest, and then brought down to their final frequency. During this time, the loop is disabled by means of a CMOS switch across the integrator. The loop is not re-enabled until the oscillator has stopped adjacent to the correct comb signal, so ensuring that lock occurs at the correct frequency. This process takes approximately 10 ms. Fig. 11 shows the output spectrum of a locked 7-GHz oscillator.

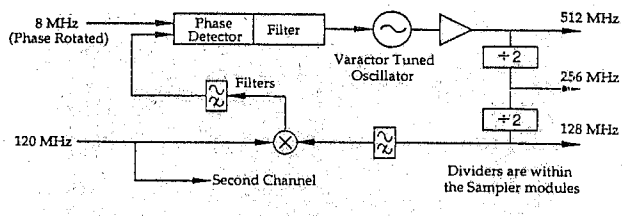

Figure 12 Block diagram of the sampler clock.

5 OTHER OSCILLATOR MODULES

There are two different types of modules with phase-locked outputs in the UHF range and both modules have phase rotation, as described later. One module, the 'sampler clock-generator', has an output of 512 MHz which is used for the digital samplers. The other module, the UHF oscillator module, provides local oscillators for the final conversion stage. It has an output which is tuneable in 1-MHz steps over four bands: 511 to 520, 600 to 609, 760 to 769 and 831 to 840 MHz. Both modules used hybrid, varactor-tuned oscillators.

The sampler clock-generator module has two identical loops in one module. Both a digital divider and mixer are used to convert the oscillator output down to 8 MHz for the phase detector. Depending on the operating mode of the samplers (1, 2 or 4 bit), they require 512, 256 or 128 MHz. This was obtained by sending 512 MHz to the sampler, where it is divided by four, with 128 MHz returned to the generator module. This arrangement ensured that no phase ambiguity was introduced by using dividers. The returned 128-MHz signal is mixed with 120 MHz, to give 8 MHz to the PD. The reference input for the PD is the 8-MHz output of a phase rotator (see later). The 120-MHz mixer signal is generated in a reference chain (also see later), and divided two ways by a splitter for the dual PLL units within each module. A diagram of one half of the module is shown in Fig. 12.

During development, it was found necessary to partition off the 512-MHz oscillator and buffer amplifier in a separate RF-tight compartment to keep the 120-MHz signal completely free of any 512-MHz signal. Although the two loops in the module have the same nominal frequencies, these could be slightly different in practice, due to different phase rotator rates. Even if a small amount of 512 MHz from one half of the module finds its way into the mixer of the other half, for example via the common 120-MHz signal, it will cause a spurious IF signal (only slightly different from 8 MHz in frequency) to be generated and applied to the phase detector, along with the required 8 MHz. This results in a strong component of up to a few kHz appearing on the output of the integrator which, in turn, produces unacceptable phase wobble and spurious sidebands on

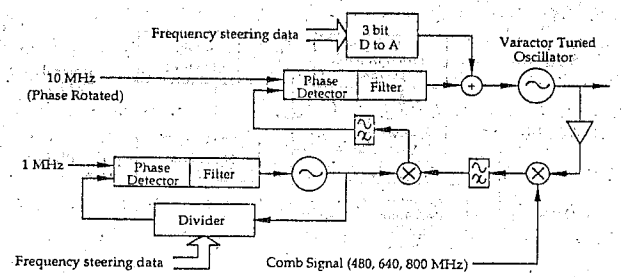

Figure 13 Block diagram of the UHF oscillator.

the spectrum. A 21-MHz low-pass filter is included in the IF to remove higher order spurious products on the mixer IF output since this also produced spurious sidebands on the final spectrum. Note that, within the sampler, the clock signals at 256 and 512 MHz have, respectively, twice and four times the phase-rotation rate, due to the divider action of the sampler module.

The UHF oscillator module contains two loops, as shown in Fig. 13. Although the main oscillator tunes from 500 to 850 MHz with only one voltage-tuning input, a special network allows it to have, effectively, a coarse and a fine tuning input. Because there is considerable curvature and variation in the voltage-tuning characteristic between oscillators, coarse tuning has been customised for each oscillator by using an 8-bit DAC and a small ROM. These allow data stored into four locations in the ROM to steer the oscillator to the centre of the chosen 10-MHz band. The PD drives the fine-tuning input to close this loop.

A sample of the main oscillator output is applied to the local oscillator input of a mixer. This first mixer uses a special comb signal which has only three components, at 480, 640 and 800 MHz, generated in the reference chain by mixing 640 and 160 MHz. The resulting IF, always between 31 and 40 MHz, is filtered by a low-pass filter, and then applied to a second mixer. The LO for this mixer is the output of a subsidiary 41 to 50-MHz loop. The 10-MHz IF output, after further filtering and amplification, is sent to the phase detector. The PD reference input is the output of a phase rotator at 10 MHz (described later). To enable the output to be set in 1-MHz steps, the subsidiary loop generates an output between 41 and 50 MHz, with 1-MHz steps. It uses a programmable divider, to give a 1-MHz output which is applied to the TTL phase detector. The digital divider does not introduce phase ambiguity because it is within the loop feedback path.

Maintaining an acceptably low level of spurious outputs proved to be particularly difficult with this module. To reduce the level of comb-signal breakthrough onto the output, an extra amplifier was inserted to give higher reverse isolation in the feedback path to the first mixer. Also, again to minimise breakthrough, the lowest possible level of comb signal was used, and arranged to act as the low-level RF input to the mixer. Some of the higher order mixer products were found to be leaking across the printed board and bypassing the low-pass filter. To obtain sufficient suppression, the IF filter was broken into two sections, each part in separate RF boxes. The filter on the 10-MHz IF also proved to be critical to maintaining low levels of spurious outputs. This filter required a rapid roll-off with a notch at 25 MHz to remove a troublesome mixer product.

6 PHASE ROTATION

In synthesis radio telescopes based on interferometer pairs of antennas, each antenna must remain pointed at the astronomical source for considerable periods of time so that very low level signals can be enhanced by integration. As the direction of signal arrival varies, due to the rotation of the earth, the relative path lengths to each antenna change. This results in the signals to each antenna going rapidly in and out of phase. If nothing is done to remove this, it would be necessary for the correlator to use very short integration times. To maintain maximum sensitivity, this modulation must be removed and this is achieved by adding an extra, time-varying delay to the signal from the antennas closest to the source. The time delays are then equalized and the source remains on a peak of the interferometer gain pattern during the entire observation. This process is referred to as 'delay tracking' (see [5]).

It is easiest to insert this time delay either at baseband, or at the final intermediate frequency since this is constant for all observing frequencies. Also, at this low frequency, delay is relatively easy to implement with digital circuits. However the phase difference that this time delay produces at IF is different from the phase difference it would produce at the observing frequency; this leaves a residual, time-varying phase error to be corrected by 'phase rotating' the local oscillator signal in the receiver. The phase-rotation rates are typically 50° for every millisecond at the highest frequencies. Also, to obtain sufficiently small steps of delay tracking, the sampling clock is phase rotated. In the AT, these rotations are achieved by varying the phase of the reference frequencies applied to the UHF local oscillator and the sampler clock.

The phase rotator consists of a digital section producing a phase-rotated 10-kHz output and a PLL upconverter which translates the phase-rotated signal to 10 MHz (8 MHz for the sampler clock). The digital section has two basic components, the first of which is a variable ratio divider circuit producing small phase increments or decrements in a 10-kHz output signal. A second circuit determines when these increments (or decrements) should occur. The phase rotator is programmed with 11 bits of 'start phase' P, which is the initial value of phase loaded into the phase rotator at the start of each 5- or 10-s timing period. Also loaded are 24 bits of 'start rate' S, the initial value of the rate, and 18 bits of 'second derivative' X, the speed at which the rate is

increased (i.e. acceleration). After 10 seconds of rotation at rates of up to 10^5 degrees per second the phase accuracy is maintained at better than 1°.

The phase-changer circuit shown in Fig. 14, is a special, synchronous divide-by-2000 counter which divides 20 MHz down to 10 kHz. The counter/divider is split into two sections, each of which counts down and can be preloaded to start from a partially full state. This sets the starting phase, since the first output transition will then occur earlier than would be the case if the counters began from a full state. To allow for phase changes after counting has started, the first counter of the chain can be set to divide by either 3, 4 or 5. It is normally programmed to allow for dividing by 4, by counting down from an initial value of 4 and, when zero is reached, by sending a pulse to the next counter. To retard the phase, the INCREMENT line is activated by an 'increment generator' and division by 5 is programmed for one cycle of the first counter. An extra 20-MHz cycle must then be counted before completing a 10-kHz cycle so that the 10-kHz output is retarded by 360°/2000 = 0.18°. To advance the phase, the RATE SIGN is changed to allow division by 3 and this results in the 10-kHz cycle being completed one 20-MHz cycle early. In this way, if the INCREMENT line is pulsed, then the phase is advanced (or retarded depending on the 'rate sign' bit) to give a single 0.18° phase change. If this line is pulsed repetitively, then the phase will be continually slipping or 'rotating', and this results in an increased (or decreased) output frequency. The output frequency can be varied in this manner over the 8 to 13.33-kHz range.

The INCREMENT line is driven by the increment generator, shown in Fig. 15. The heart of the increment generator is an accumulator which has the 24-bit 'rate' value, R added to its contents for each cycle of F_u (nominally 5 MHz). The accumulator produces an output signal each time its contents become full and this 'carry' signal is the desired increment signal. The accumulator counts up in steps equal to the contents of the rate buffer and produces an increment signal each time the accumulator 'overflows' and starts accumulating again. A large value of R will make the accumulator overflow quickly and the rate at which it overflows is therefore proportional to the rate R.

The 18-bit 'second derivative' X, determines the value of the clock frequency F_x by means of a standard 'rate multiplier' device. The 'start rate' S, is loaded into the rate buffer/counter which acts initially as a data latch at the start of the timing period. The transitions of the clock signal F_x, increment (or decrement) the contents of the rate buffer/counter so that, at time t, it has a value S +(or-) $F_x * t$ in its latches. After each cycle of F_u the contents of the rate buffer/counter are added to the accumulator contents. Thus the number in the accumulator is increasing at an accelerating rate, where the acceleration is determined by F_x which is determined by X. The ability to set a second derivative of phase

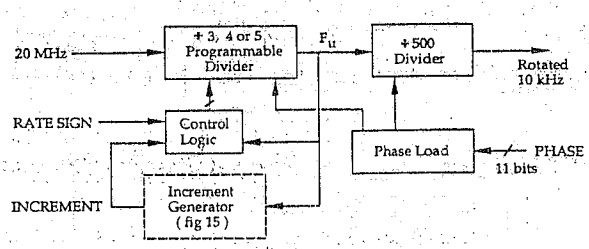

Figure 14 The phase-changer circuit.

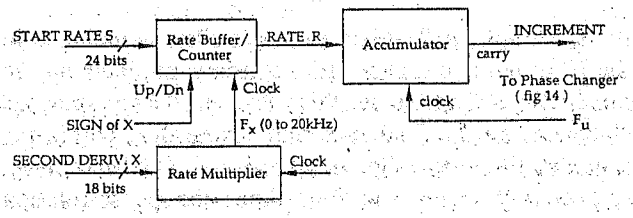

Figure 15 The increment generator.

allows for longer periods between updates, especially for very long baselines.

The digital phase rotator is followed by an upconverter circuit using an offset PLL. The UHF phase rotator upconverts from 10 kHz to 10 MHz using a voltage-controlled crystal oscillator (VCXO). The feedback loop uses a mixer with a 9.99-MHz reference, the IF is at 10 kHz and the 10 kHz from the digital phase rotator provides the phase detector reference. The sampler clock rotator is identical except for a 7.99-MHz reference and an 8-MHz output. A more detailed discussion of the digital phase-rotator design, is given in [6].

7 REFERENCE GENERATOR

To achieve the required high phase stability, all LO output signals within an antenna must be phaselocked to stable reference signals. These signals are supplied by the reference generator and must in turn be phaselocked to a master reference signal which is common to all antennas. The central master reference for the AT is a 5-MHz signal supplied by either a rubidium or maser frequency standard. A 5-MHz low-phase-noise, oven-controlled, crystal oscillator at each antenna is phaselocked to this master reference by a 'phase transfer' system (described later). From this 5-MHz source, reference frequencies ranging from 1 to 800 MHz are generated. Most frequencies are generated through a chain of doublers which produce 5, 10, 20, 40, 80, 160, 320 and 640 MHz. Combinations of some of these frequencies are mixed to generate other references such as 120, 480 and 800 MHz. To produce the 9.99- and 7.99-MHz references required by the phase rotators, offset phaselocked loops are used in combination with digital dividers which have special protection from phase jumps.

The chain of doubling stages is the heart of the reference generator. Each doubling stage consists of a passive doubler placed between two RF amplifier modules followed by a specially designed doubler filter. The doubler is essentially a wideband, transformer-coupled, full-wave rectifier. Each stage is connected to the next through a directional coupler.

The purpose of the amplifiers is two-fold. Firstly, loss through each doubler is about 12 dB (when supplied with 6-mW drive) which, in combination with coupling losses, adds up to a total of approximately 170 dB (through the six doubler stages) which must be made up by amplification. Secondly, each doubler should be driven from a stable 50 Ω source impedance to minimise spurious frequency generation and ensure stable phase characteristics. The doubler filter was designed to reduce further the spurious products produced by the doubling process.

Typically, a doubler produces the most troublesome spurious signals at the third and fourth harmonics of the input frequency. The fourth harmonic can be as high as -15 dBc relative to the desired second harmonic. The third harmonic is lower, at about -30 dBc. Instead of a filter with a narrow bandpass to reduce these spurious signals, we used an elliptic bandpass filter with a 'Q' of approximately 2, with rejection notches tuned to the spurious frequencies at the input and fourth-harmonic frequencies. The advantage of this technique is that, because of the lower Q, it has much better phase-versus-temperature stability. The drive level into the doubler is critical and tests showed that a drive level of 6 mW provided the least phase-sensitivity to variations in drive level.

Between each doubling stage is a directional coupler with the coupled port driving the next stage. This increased isolation between stages was necessary to reduce the effect of doubler impedance changes on the filter and hence on the temperature coefficient of phase. The 'through' port is passed through another amplification stage to provide buffering and to generate sufficient drive levels, after splitting, for the final LOs. Doubler chain frequencies of 5 and 20 MHz are used directly as references for the 2-GHz local oscillator, and the 10- and 320-MHz references for the 7-GHz local oscillator.

Further reference signals are generated by mixing pairs of signals generated in the doubler chain. A typical mixing stage consists of a passive double-balanced mixer with buffer amplifiers on the LO, RF and IF ports followed by a clean-up filter. Combinations of frequencies were chosen to give a desired reference without producing close-in spurious signals which are difficult to filter. In typical mixers, undesired products, such as three times the LO frequency minus the RF frequency, can be as high as -10 dBc relative to the desired sum or difference frequency. The reference frequencies produced via mixing are 8 MHz (10 - 2 MHz), 120 MHz (40 + 80 MHz), 480 MHz and 800 MHz (640 ± 160 MHz). The 8- and 120-MHz references are for the sampler clock. The 480- and 800-MHz references are combined with 640 MHz to give a 'comb' which is used by the UHF local oscillator.

A divider chain divides down from the 20-MHz signal to produce the 1-MHz reference required by the UHF local oscillator and the 2-MHz and 10-kHz signals used within the reference chain. To avoid phase changes caused by noise or power transients, the power supply and shielding required special treatment and each output was individually buffered. The power supply uses a combination of diodes, large reservoir capacitors and dedicated regulators operating with a large voltage drop.

An offset phaselock loop produces the 9.99-MHz reference needed by the phase rotators, using a 10-MHz mixer reference and 10-kHz phase-detector reference. To ensure sufficiently low phase noise and reliable lock acquisition, this loop uses a voltage-controlled crystal oscillator. A simple mixing stage uses 9.99 and 2 MHz to produce the 7.99 MHz needed by the sampler phase rotator.

8 PHASE TRANSFER

The phase transfer system ensures that the antenna 5-MHz reference oscillator is phaselocked in a known phase relationship with the central master reference, independently of cable-length changes. The phase stability that is required of this system is dependent on many factors, including the frequency at which astronomical observations are made. As indicated earlier, the rms phase variation of any LO measured at 1 GHz must be less than 1° over time intervals up to 30 minutes. This corresponds to 0.005° at the 5-MHz reference frequency.

Each of the six antennas which make up the Australia Telescope array at Narrabri, has a highly stable 5-MHz voltage-controlled crystal oscillator (VCXO) with extremely low levels of phase noise. These oscillators provide the base reference for the LO systems within each antenna. Each oscillator is phaselocked to the master reference, also at 5 MHz, at the central building on the site. This is either a rubidium or hydrogen maser frequency standard to achieve the long-term stability required for the very-long-baseline interferometry (VLBI) techniques used in astronomy. To achieve the phaselocking, the master reference is distributed to the five antennas in the 3-km section of the Array through large diameter, pressurised, coaxial cable. For the sixth antenna, which is located 4.5 km from the central site, this signal is transferred over optical-fibre cable because it has a lower signal loss and is less expensive. These lines, whether coaxial or fibre, undergo changes in length due to thermal effects and cable movement. The resulting phase changes must be measured and accounted for to achieve the required phase stability.

Each of the five antennas in the 3-km section of the array can be located at any of 35 station posts (connection points) along the rail. Two lengths of coaxial cable (eastern and western arms), with couplers at each station post, distribute the central standard. This standard is multiplied to a frequency of 160 MHz for transmission down the cable. Since each coupler or connector has a less-than-ideal match to the cable, reflections occur which ultimately cause phase errors. The couplers are pressurised to reduce moisture degradation and increased reflection. Losses in the line can actually help by reducing the multiple reflections which are the major problem. The cable has an attenuation of 0.017 dB/m at 160 MHz and the through-loss of each coupler is approximately 0.6 dB, giving a maximum loss down each arm, including the coupling factor and antenna cables, of almost 60 dB.

A simplified diagram of the system is shown in Fig. 16. The method of phaselocking the antenna VCXOs to the central standard is as follows. In the central building, the master 5 MHz is multiplied by 32 (5 doublers) and translated to 160.05 MHz by a PLL with an offset frequency of 50 kHz. This signal is sent along the coaxial cable to all antennas. Inside each antenna, the 5-MHz output of the VCXOs is multiplied to 160 MHz and mixed with the incoming 160.05-MHz signal. The difference product is then compared in a phase detector with a 50-kHz reference which has been independently sent along the cable. The error voltage obtained is then used to control the VCXO, thus completing the PLL. The loop bandwidth is designed to be about 1 Hz. This ensures that high-frequency noise introduced through cable loss and amplifiers does not degrade the short-term phase stability of the VCXO.

A round-trip phase-measurement scheme is used to measure changes in cable length. The 160-MHz signal generated in each antenna is sent back along the cable to the central building and the phase difference between this return signal and the reference standard at 160 MHz is measured. Changes in cable-length L cause corresponding phase changes of magnitude

$$\Delta\Phi = \frac{720.\Delta L}{\lambda} \text{ [degrees]} \qquad (1)$$

where λ is the wavelength $\in$ the cable.

To allow five antennas to share the same cable, time multiplexing is used. Each antenna in turn sends a return signal for a duration long enough for the phase measurement to be made in the central building. The minimum measurement time is 20 μs since the actual measurement is made at 50 kHz (by first mixing the 160 MHz with 160.05 MHz). The time between measurements is 0.1 s and, to ensure settling before measurement, a delay period of 2 ms is allocated. While a return signal is being sent, the 160.05-MHz out-going reference signal is removed, so that all antenna VCXOs

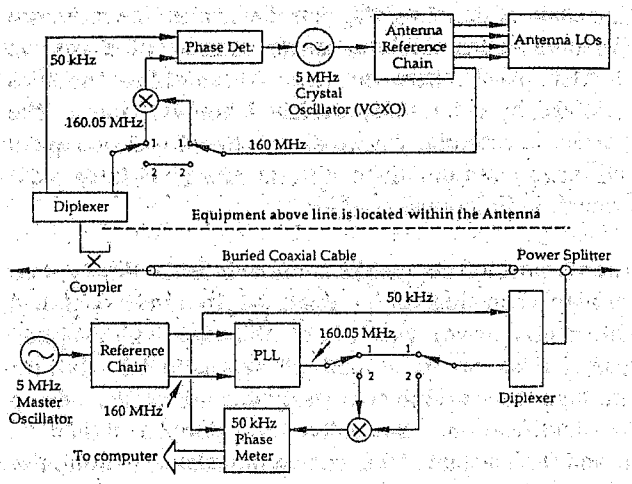

Figure 16 Simplified phase-transfer system.

must 'free wheel' with a constant control voltage during the delay and measurement periods. To ensure stable phase during these periods, the control voltage is held by a 'sample-and-hold' circuit with a very low drift-rate. The VCXO is also selected for extremely low drift-rate with constant control voltage. Experiments show that the combined sample-and-hold plus VCXO drift, over a period of 300 ms, results in less than 0.005° drift at a frequency of 5 MHz. Since the phase drift with time approximately follows the law $\Delta\Phi = kt^2$, the drift can be extremely small over a period of a few milliseconds.

The changes in cable length that are expected to occur can be separated into slow and fast components. The short 20-m exposed portions of cable around the antenna elevation 'cable-wrap' will be affected directly by short-term changes in ambient temperature caused by shading and wind (< 20° C over 5 min.), while the buried 2-km lengths will be affected only by the daily cycling of the ground temperature (< 0.2° C per hr). Estimating the cable temperature coefficient as 40 ppm/°C, we calculate the worst cases to be

$$\left|\frac{dL}{dt}\right|_{diurnal} < 5\times10^{-6}\, ms^{-1} \qquad \left|\frac{dL}{dt}\right|_{fast} < 5\times10^{-5}\, ms^{-1} \qquad (2)$$

Since the worst case translates to 15 mm over 5 minutes, and since 1 mm is approximately equal to 1° at 1 GHz, we require that the phase-transfer control loop provides more than a 10-fold improvement to meet AT specifications. Other effects such as mechanical changes in connectors can result in even larger phase shifts and must also be corrected. Bench tests showed that these performance targets could be met but, since the full system is only now being installed, long-term test results are not yet available.

If cable-length changes exceed 0.94 m (half wavelength at 160 MHz) then the measured phase change becomes

greater than 360° and this can result in misinterpretation. To resolve this and other ambiguities in the multipliers, 5 MHz is also sent down the cable so that a simple 5-MHz phase measurement can be made at each antenna. At 5 MHz, a 0.94 -m length change corresponds to 5.6° so that a resolution of a few degrees is quite adequate.

Once cable-length changes are known, compensation can be made. There are several methods of achieving this. In the AT, real-time corrections can be made by using the previously described LO phase rotator circuits. Alternatively, since cable variations are slow, phase corrections can be made to the final correlator output data.

The AT uses optical fibres to transfer the IF from each antenna to the central building where correlation is performed. (For details, see [7].) Major improvements in the technology of optical fibre makes it also a consideration for LO distribution where advantage can be taken of its low signal-loss, wide bandwidth and low cost. As with coaxial cable, length changes must be measured and accounted for. Experiments performed on fibres supplied by the Pirelli company showed that the temperature coefficient of length is about 10 to 25 ppm/°C (twice as good as coaxial cable). Good phase stability combined with the close temperature tracking of fibres within the same cable meant that time multiplexing could be avoided by using two separate fibres within the same sheath for the forward and return signals. This avoids the complexity of time and frequency multiplexing onto a single fibre and gives similar performance. Phase transfer over optical fibre is implemented using essentially the same techniques as with coaxial cable but with the 160.05-MHz outward signal modulating the diode lasers for transfer. A separate laser, fibre and receiver is used for the 160-MHz return signal.

For the remote Long-Baseline Array antennas near Coonabarabran, Parkes and at other future sites, it is not practical to use land-lines to carry the LO reference signal. Instead, a system using the domestic satellite 'AUSSAT' (now Optus) can be used to distribute reference signals to any site within Australia. Atmospheric path variations are removed by a round-trip system similar to that already described for the cable phase-transfer system. Optus uses different up and return frequencies and this leads to incomplete removal of variations in the ionospheric delay; the residual error, however, is sufficiently small.

The satellite is not stationary but moves over a small range with a maximum velocity of almost 1 m s^{-1}. Due to this large rate of change, the task of removing the effects of such path changes is considerably more challenging than with the cable phase-transfer system. To limit the cost of satellite usage, the transmitted power is kept to a minimum and great care is then required to extract the signal from the receiver noise. This requires a PLL with only 1-Hz bandwidth and an ultra-stable crystal oscillator. The reference signal is sent as a 192q-MHz difference between two carriers and the system uses a dedicated 4.6-m antenna with about 0.1 W per carrier. System performance has been verified at the prototype stage and installation at the first sites is under way. Details of the system and the performance achieved will be given in a future paper.

9 CONTROL AND MONITORING

The entire LO system is computer controlled with no manual controls. This avoids the problems caused by leaving a critical switch in the wrong position. There is also an absolute minimum number of preset controls — typically, just one to set the centre frequency of each oscillator. This greatly simplifies maintenance and calibration. Each module also has typically 10 analog monitor points which can be accessed remotely via the data sets, antenna computers and the central control computer. These are allocated to allow monitoring of phase-detector outputs, signal levels and temperature and are used to locate faults, warn of degraded performance and drifts and to correct for temperature effects. The entire LO system has 250 monitor points in each antenna with 1500 such points in the full array - excluding those in the power supplies and those monitoring the LO drive within the conversion system. Although the LO system is extremely complex, the above precautions have led to exceptional reliability with any faulty modules being quickly identified and replaced.

10 ACKNOWLEDGMENTS

The authors thank all those who contributed to the LO system, including M. Hayes for his excellent work on SRD design, P. Hrebenuik for his early work on phase rotators, R. Gardyne, G. Lee and J. Bolton for their valuable assistance in translating the designs into reality, and all those who contributed to the first-rate mechanical and assembly work. We give a special acknowledgment to the late Alec Little for the early system-design work.

11 REFERENCES

1. Wilson, W.E, Davis, E.R., Loone, D.G. and Brown, D.R., "The Correlator", JEEEA, 1992. this issue.

2. Sinclair, M.W., Moorey, G.G., Gough, R.G. and Graves, G.R., "The Receiver System", JEEEA, 1992, this issue.

3. *MECL Device Data Handbook*, Motorola Inc.,1989.

4. Gardner, F.M., "Phaselock Techniques", Wiley, 1979.

5. Wilson, W.E. and Carter, C.N., "The Delay System", JEEEA, 1992, this issue.

6. Percival, T.M.P. and Young, A.C. "Accurate Digital Control and Rotation of the Phase of Microwave Signals.", Trans.IEEE, Vol. IM-37, 1988, p. 626.

7. Young, A.C., Anderson, M.J., Hayes, M.J.W. and Ticehurst, R.C., "The Optical Fibre System", JEEEA, 1992, this issue.

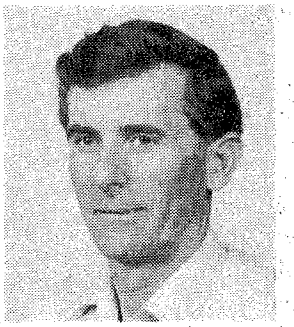

DR A.C. YOUNG

Dr Alan Young received the BSc degree from the University of New South Wales in 1971 and the PhD degree from the University of Sydney in 1982. Until 1982 he was a member of the Air Navigation Group at the University of Sydney, primarily involved in the analysis and scale modelling of the Instrument Landing System. From 1982 to 1984 he was part of the group at the California Institute of Technology responsible for developing the instrumentation for the new millimetre-wave radio astronomy array at Owens Valley, California. He joined the CSIRO Division of Radiophysics in 1984 where he became leader of the Local Oscillator and Signal Distribution Group for the Australia Telescope project.

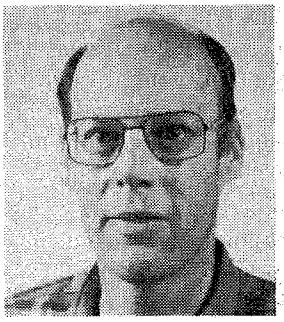

MR M.G. McCULLOCH

Gerry McCulloch holds the degree of BE from the NSW Institute of Technology (now the University of Technology). He joined the CSIRO Division of Radiophysics in 1970 as a technician. Initially, he worked on receiver systems for the Parkes 64-metre telescope, then with millimetre-wave receivers for use on both the Parkes and the 4-metre telescope at Marsfield. In 1982, he went to the National Radio Astronomy Observatory in Greenbank, USA, to work on a 43-GHz maser amplifier which was subsequently used at Parkes. In 1984, he joined the Local Oscillator and Signal Distribution Group of the Australia Telescope project, where he was involved with all phases of the design, construction and installation of the local oscillator system. Since September 1991, he has been at Nobeyama Radio Observatory, Nobeyama, Japan, where he is working on SIS millimetre-wave receivers.

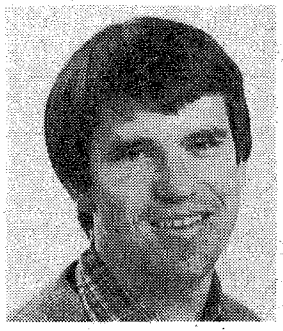

MR S.T. ABLES

Sean Ables received the BSc degree in physics from the University of Tasmania in 1985. In 1986 he joined the CSIRO Division of Radiophysics then the Australia Telescope project as a member of the Local Oscillator and Signal Distribution Group.

MR M.J. ANDERSON

Michael Anderson received the BE and MEngSc degrees from the University of Sydney in 1967 and 1974 respectively. He joined the Department of Civil Aviation (DCA) as a Cadet Engineer in 1966 and during two years' national service in the Australian Army, spent 18 months as an instructor in basic electronics at the RAEME Training Centre, Bandiana. On his return to DCA he worked on the installation and maintenance of communication systems, aircraft navigational aids and radar. In 1986 he joined the Local Oscillator and Signal Distribution Group within the CSIRO Australian Telescope project. His main activities are in fibre optics, satellite links and equipment production and installation.

DR T.M. PERCIVAL

Dr Terry Percival obtained a BE and a PhD from Sydney University in 1977 and 1985 respectively. He was a postgraduate student and later a research assistant at the Fleurs Radio Observatory from 1977 to 1983. In 1983 he joined the Division of Radiophysics to work on the design of the local oscillator and signal distribution systems for the Australia Telescope. In 1985 he joined the CSIRO Division of Applied Physics where he worked on time and frequency standards, satellite time transfer systems and microwave superconductivity. In late 1987 he joined the R & D department of OTC Australia. He was head of the optical fibre transmission and technology section, and later the satellite communications and IC design research sections. His work there included the system design for the new INTELSAT digital VISTA service and he was the co-inventor of a new multiple-access scheme for VSAT systems. In 1992 he joined the Program for LANs and Network Services at the Division of Radiophysics, CSIRO. His current research interests are microwave system design and modulation and coding techniques for high-speed wireless local area networks.

The Sampling and Data Synchronization Systems

W.E. Wilson* and M.W. Willing*

SUMMARY The sampler, digitiser and data synchronization systems of the six antennas which make up the Australia Telescope Compact Array are described. The sampler/digitiser units, which are located at the antennas, convert the analog outputs of the receivers to digital form and encode the resulting data streams into a form suitable for transmission via fibre-optic links to the central control building. The method by which the various data streams are synchronized is explained.

1 INTRODUCTION

This paper describes the devices whose main function is to convert the IF signal outputs of the receivers to digital form. It also describes the techniques used to transmit and synchronize the resulting digital data. In the analog-to-digital conversion, a sample of the input signal is taken at a particular instant and the resultant analog voltage is quantised into a fixed-length binary word. Ideally, the conversion should not give rise to any significant loss of information from the original signal. Factors affecting the degree of information loss are the frequency with which the samples are taken, the 'sampling rate', and the length of the binary word, N bits or 2^N levels, used to represent the sampled voltage.

2 SPECIFICATIONS

The samplers are specified to operate in one of the three modes shown in Table 1.

Table 1

Mode	Nominal input Frequency range	Sample rate (mega-samples /s)	Number of bits	Number of levels
1	256 to 512 MHz or 512 to 768 MHz	512	1	2
2	128 to 256 MHz	256	2	4
3	64 to 128 MHz	128	4	16

3 SAMPLING RATE

The samplers operate at the minimum sampling rate which satisfies the Nyquist sampling criterion, i.e. at twice the nominal input bandwidth. A somewhat unusual feature of the sampling process is that the input signal is not at baseband, but rather occupies a frequency range either immediately below or above the sampling frequency. These two cases are referred to as lower sideband sampling and upper sideband sampling. As long as the total bandwidth is limited to less than half the sampling frequency, then this arrangement also satisfies the requirement that information loss through aliasing should not occur. As is the case with lower sideband mixing, lower sideband sampling also leads to an inversion of the final frequency scale.

4 QUANTISATION

The very coarse quantisation employed is acceptable only because of the nature of the signals and the way in which these signals are processed. The signals received at each antenna can be considered to be random Gaussian noise voltages. The required processing forms the cross-correlation functions of pairs of these signals. It has been shown (e.g. [1,2]), that the cross-correlation coefficient of coarsely quantised random noise signals is a monotonic function of the correlation coefficient of the original analog signals. Some uncertainty is added to the digital measurement in the form of quantisation noise but this is the price that is paid for the relative simplicity of the digital signal processing. As is to be

* Australia Telescope National Facility, CSIRO, PO Box 76, Epping NSW 2121, Australia.
Submitted to The Institution of Radio and Electronics Engineers Australia in June 1992.

expected, the amount of added noise is greatest in the 1-bit case where the signal-to-noise ratio, or sensitivity, is 64% of the figure that would be obtained with a perfect analog correlator.

The 1-bit digitiser places the result in one of two possible levels. Therefore it takes account only of the sign of the input signal, determining whether the nominally zero mean Gaussian noise input voltage is positive or negative at each sampling instant. In this case there is a simple sine relationship between the measured digital correlation coefficient, p_d, and the actual value, p, such that,

$$p = \sin(P * p_d / 2)$$

where both p_d and p have been normalised to 1.0 at 100% correlation.

The 2-bit digitiser has four possible levels and so has both a 'sign' bit and a 'magnitude' bit, as shown in Fig. 1(a). The sensitivity of a 2-bit correlator is a function of both the magnitude decision level, V_m, measured relative to the rms input voltage, V_{rms}, and w, the relative weight given within the correlator to samples with large and small absolute magnitudes. The sensitivity has a broad maximum at w = 3.3 and $V_m = 0.98V_{rms}$, where it is 88.3% of that of an analog correlator. In practice, the digital multiplier within the correlator is more easily implemented with a value of w = 4, in which case the optimum sensitivity is degraded only slightly to 88.0% at $V_m = 0.94V_{rms}$. The 2-bit digitiser is maintained at optimum sensitivity by counting the number of samples occurring in each of the four levels and adjusting the decision levels accordingly. As the input noise voltage is assumed to follow Gaussian statistics, the level control system seeks to maintain 17.3% of the samples in each of the outer levels and 50% of the samples in the positive levels. In the case of a 2-bit correlator, there is no simple analytical relationship between p_d and p. It is very closely linear at low p_d (< 0.1) where a linear approximation can be used to recover p. At larger values of p_d a polynomial must be used to approximate a curve which becomes highly non-linear as p_d approaches 1.0. As the relationship between p_d and p is also a complex function of V_m, the fact that V_m is held constant greatly facilitates the recovery of p.

The 4-bit digitiser provides a sampled data stream which is sufficiently accurately quantised to enable reconstitution of the analog signal at the central site and digital 'tying' of the array. The array is 'tied' by adding the signals from all antennas in such a way as to produce a composite response from the entire array. Once again the placement of the decision levels [Fig. 1(b)] is determined by a feedback control system acting on measurements of the number of samples below $-V_4$, above V_0 and above $+V_4$. The AT correlator operates

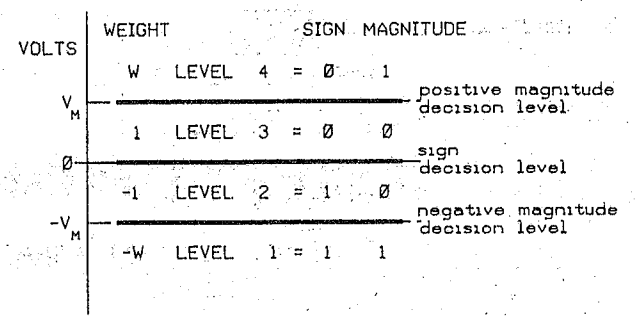

(a)

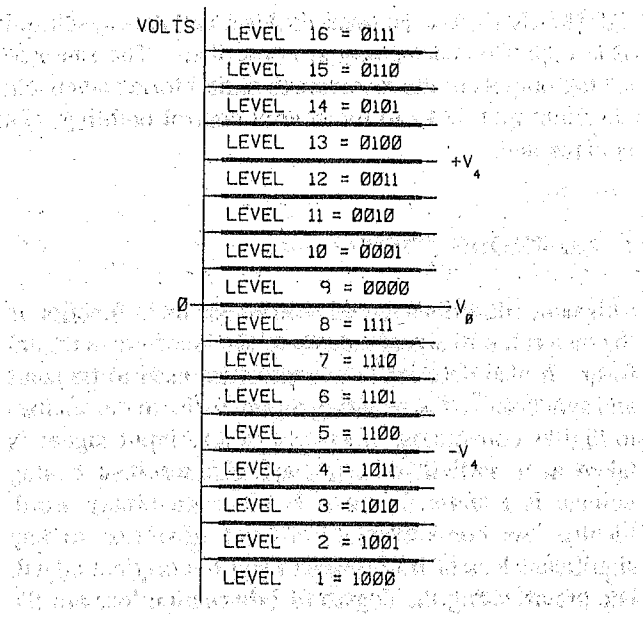

(b)

Figure 1 Sampler decision levels and coding scheme.
(a) 2-bit sampler.
(b) 4-bit sampler.

either in 1-bit or 2-bit correlation mode, and so the 4-bit data cannot be fed directly to the correlator. If required, it must first be converted to 2-bit data, a function which is achieved in the delay system [3].

5 DATA CODING AND SYNCHRONIZATION

A combined switching, time-division multiplexing circuit (Fig. 2) is employed to select one of the three digitisers and convert its output to a single-bit stream at 512 Mbits/s. This data stream then passes through the synchronization circuit, which inserts the synchronization bit sequence (Fig. 3), in the data at the start of each integration period. This process is controlled by a signal called BLANK, which is produced in a special-purpose pulse generator known as the integration clock (see below). During the BLANK time, typically 16 ms, the

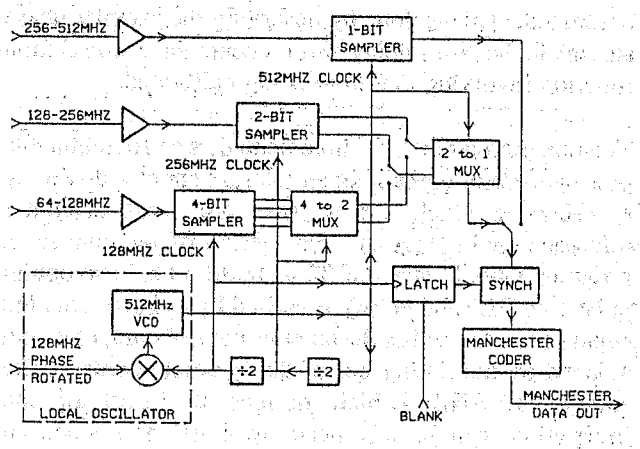

Figure 2 Sampler module block diagram.

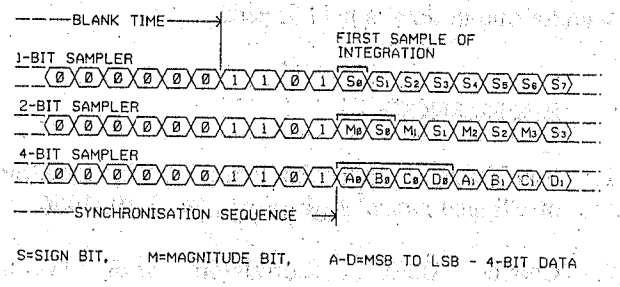

Figure 3 Serial data bit sequences at the start of an integration.

synchronization circuit closes off the data path and, instead, sends a steady stream of zeros. The BLANK signal passes through a latch circuit which ensures that the next 128-MHz sampler clock pulse following the end of the BLANK pulse marks the beginning of the final four bits of the synchronization sequence. At the central site, detection of the synchronization sequence allows the first sample of each integration period to be identified. It also provides a reference point from which the 2-bit and 4-bit data can be correctly demultiplexed, as shown in Fig. 3.

The data then pass through a Manchester coding circuit which performs an exclusive OR function and a suitably phased 512-MHz clock signal. The data finally emerge from the sampler in a form suitable for insertion into the fibre-optic transmission system.

6 IMPLEMENTATION

The samplers are situated in the vertex cabin of each antenna. There are four sampler modules, one for each IF channel. Each IF channel is split into three signals, each at a different bandwidth, corresponding to the three modes shown in Table 1. A sampler module has three inputs and three distinct sampling units, only one of which is operational at any one time.

The 1-bit sampler uses a GaAs D-type flip-flop with comparator input as its sampling device. The 2-bit sampler uses a high-speed silicon bipolar quad-latched comparator, with three of the comparators employed to define the three decision levels. The 4-bit sampler uses a commercial high-speed 4-bit analog-to-digital-converter. The high-speed digital circuits are implemented with commercial ECL devices.

7 SAMPLER CLOCK PHASE ROTATION

Adjusting delays in the various signal paths in the Compact Array, to compensate for path length differences, is done in two stages. The sampled data streams are delayed in the digital delay system (see [3]) where the smallest possible delay step is one sample period. Finer delay adjustment is achieved by varying the phase of the sampler clock signal. The local oscillator system produces a phase-rotated 128-MHz reference signal to which all sampler clocks are locked, as shown in Fig. 2.

It is a consequence of the latching of the BLANK signal by the 128-MHz sampler clock that only those samples which are coincident with the 128-MHz sampler clock can be selected as the first sample in an integration, i.e. every second sample in 2-bit mode and every fourth sample in 1-bit mode. This means that the sampler phase has an adjustment range of 8 ns (= 1/128-MHz), regardless of which sampler is in use. This converts to a range of phase adjustment in the clocks at the samplers of one sampler period in 4-bit mode, two sampler periods in 2-bit mode and four sampler periods in 1-bit mode. Hence, the delay system operating on the sampled data at the central site need only have a minimum 8-ns delay step.

8 THE INTEGRATION CLOCK

The purpose of the Integration Clock is to produce a signal which defines the start of each integration to an accuracy of a fraction of a sample period. This enables the array control computer to specify precisely the first sample in each integration. The major difficulty with this process arises from the fact that the phase of the sampler clock is continually being rotated. It follows that, with any fixed integration period, inevitably the situation will occur where the start time is close to a 128-MHz sample time. Then the finite delays in the synchronization latching circuit will give rise to an uncertainty in the choice of the first sample of the integration. The circuit may choose the correct sample, as specified by the array control computer, or it may choose a sample 8 ns earlier or later. If it makes an error, an 8-ns delay error would be present in any correlation function involving this input.

As the array control computer can calculate the time difference between the nominal start time and the first

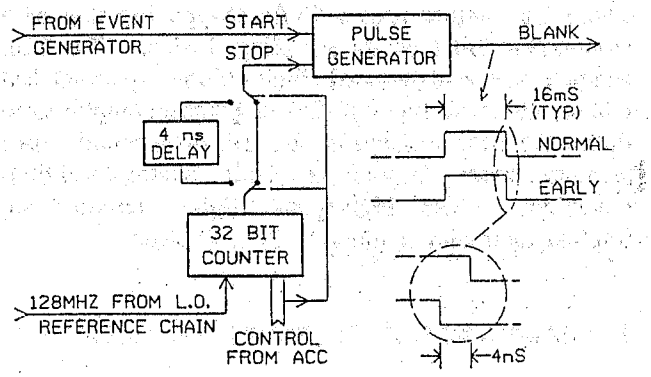

Figure 4 Integration clock block diagram.

sample time in each integration, it can also predict when an error of the type described above is likely to occur. When this is the case, the array control computer sends a request to the integration clock to produce a start signal which is 4 ns earlier than the nominal start time, hence avoiding the region of uncertainty. The chances of error are further reduced by using this 'EARLY' start signal whenever the first sample time is within 2 ns of the nominal start time and the 'NORMAL' start signal at other times.

In practice, the NORMAL start signal will not coincide with the nominal start time, but will be offset by some initially unknown value. If the array control computer is to choose correctly between the EARLY and the NORMAL start signals, any such offset must first be calibrated. This is done by observing the sampler phase at which the 8-ns delay error occurs in a correlation function involving the input being calibrated.

The integration clock is implemented as a programmable pulse generator containing an internal counter driven by a 128-MHz clock signal from the local oscillator reference chain (Fig. 4). The period of the counter is programmable in steps of 32 ns up to 33 s. The output pulse (the BLANK pulse), is started by a signal from the event generator within the antenna control computer, and stopped by the timing out of the internal counter. The end of BLANK, which defines the start of the integration, can be advanced by 4 ns to produce an EARLY start time. As the timing of the end of BLANK is controlled by the local oscillator reference chain, it is stable to within a fraction of a sample period. The BLANK pulse is typically 16 ms long. During this time the system is set up for the next integration and the sampler output data is held at zero.

9 REFERENCES

1. Van Vleck, J.H. and Middleton, D., "The Spectrum of Clipped Noise' IEEE.Proc., 54, 2-19, 1966.

2. Cooper, B.F.C., "Correlators with Two-bit Quantisation", Aust.J.Phys, 23, 512-527, 1970.

3. Wilson, W.E. and Carter, C.N., "The Delay System," JEEEA, 1992, this issue.

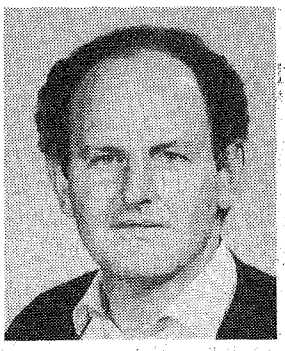

DR W.E. WILSON

Dr Warwick Wilson obtained his BSc in 1967, his BE in 1969 and his PhD in 1975 from the University of Sydney. From 1971 to 1979 he worked at the Max Planck Institute für Radioastronomie in Bonn, initially as a research fellow and later as a research engineer, working on receiver and systems development for the Effelsberg 100-m radio telescope. From 1977 to 1979 he was leader of the electronics group at the Effelsberg Observatory. In 1979 he returned to Australia to work on the Interscan project with AWA. In 1980 he joined the CSIRO Division of Radiophysics and was seconded to Interscan Australia Pty Ltd, working in the USA until 1983 on the design of the microwave landing system. In 1983 he was appointed leader of the Correlator Group in the Australia Telescope project.

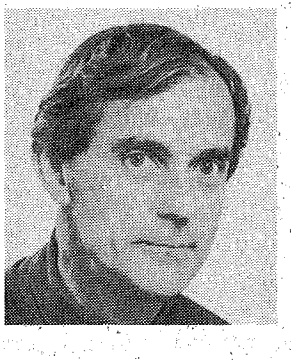

MR M.W. WILLING

Michael Willing obtained the Diploma of Communication Engineering in 1956 from the Royal Melbourne Technical College. His first position was at the Commonwealth Ammunition Factory during 1955, where he was involved in the design and construction of specialised test equipment. In 1956, he joined the CSIRO Division of Industrial Chemistry, producing equipment for spectroscopic research. He transferred to the Division of Radiophysics in 1958 as an Experimental Officer, and was initially involved in observational astronomy at the Fleurs Radio Observatory (now operated by the University of Western Sydney). He then turned to digital design and produced data processing equipment for the Division of Radiophysics' observatories at Parkes and Narrabri, NSW. From 1983 he has participated in the construction of the Australia Telescope and, as a member of the Correlator Group, is now with the CSIRO Australia Telescope National Facility.

The Optical Fibre System

A.C. Young*, M.J. Anderson*, M.J.W. Hayes** and R.C. Ticehurst***

SUMMARY The Australia Telescope has made extensive use of optical fibres for the return of high-speed signals from the receivers. This unusual application of fibres required many short links operating at 1-Gigabit speeds in combination with the need for easy disconnection in a dusty or wet environment. The system also uses fibres to carry a local-oscillator reference over a 5-km distance and to carry communication links to all antennas. This paper outlines the techniques used to meet these requirements.

1 INTRODUCTION

The Australia Telescope (AT) is the first radio telescope to make extensive use of optical fibre technology. This means that many difficult choices had to made during the design process. Our success and that of others after us, should, however, ensure its future use in most radio telescopes. The AT array at Narrabri has six antennas, and optical fibres are used to transfer the output signals from each antenna receiver to a central correlator. They are also used to carry a phase reference signal to which antenna local oscillators (LOs) are locked. Present radio telescopes use coaxial cable for these purposes but this becomes quite costly for systems requiring either a large bandwidth or distance. The US Very Large Array (VLA) radio telescope uses very costly circular waveguide which is now no longer available. Before discussing the design of the AT optical-fibre system, a summary of the relevant aspects of fibre technology is worthwhile.

2 OPTICAL FIBRE

Optical fibres are made from high-purity glass, have a typical outer diameter of 0.125 mm and are usually contained within a thin plastic jacket. Cables are made by enclosing many such fibres within a thick protective sheath. The simplest type of fibre has a radial step change in refractive index such that light travelling through the fibre is confined, by internal reflection, to the inner core of higher refractive index. However, step-index fibre supports a large number of waveguide modes with a wide variation in propagation velocities. This modal dispersion causes pulse smearing, and results in a low bandwidth which decreases with fibre length. Graded-index fibre was developed to increase fibre bandwidth by reducing modal dispersion. A radial gradient of refractive index is used to equalize the propagation velocity of the various modes in the fibre core and can result in a bandwidth-distance product of more than 1 GHz km. Single-mode fibre is a step-index fibre with a central core of less than 10 microns to allow the propagation of the HE11 mode only. With narrow spectral-width lasers to minimise spectral dispersion, a system bandwidth well in excess of 10 GHz over more than 10 km can be achieved. Operating wavelength is in the infrared range 0.85 to 1.55 μm. A wavelength of 1.3 μm is often chosen since, at this wavelength, silica-glass fibre has a low attenuation and the material chromatic dispersion cancels with waveguide dispersion to give very low spectral dispersion.

Optical fibre has several advantages for the system designer and cost is a major one. Fibre cable capable of carrying 500 MBaud over 2 km is about one fifth of the cost of coaxial cable of comparable capacity. At typically 0.5 dB per km, fibre loss is also very much lower than coaxial-cable loss and it does not have to be equalized in the way that coaxial cable, because of its severe frequency dependence, does. Fibre-system bandwidth in excess of 1 GHz is readily achievable and systems in excess of 10 GHz are planned. Radio-astronomy applications also benefit because optical fibres produce no electrical interference.

Most fibre systems use simple digital modulation which is normally achieved by directly turning a diode laser on and off. LED devices are used in low-speed systems but

* Australia Telescope National Facility, CSIRO, PO Box 76, Epping NSW 2121, Australia.
** Australia Telescope National Facility, CSIRO, PO Box 94, Narrabri NSW 2390, Australia.
*** OTC, 231 Elizabeth Street, Sydney NSW 2000, Australia.
Submitted to The Institution of Radio and Electronics Engineers Australia in June 1992.

they do not have the power or speed for high-capacity systems. Optical receivers usually rely on direct detection using photo-diodes followed by low-noise amplifiers. Coherent detection is still not economical and analog transmission is not widely used due to poor noise and linearity performance. A frequency-modulated (FM) sub-carrier is used for cable TV transmission to overcome such analog transmission limitations, but at the expense of a much reduced bandwidth. Digital transmission is usually the most cost-effective option. Several different optical carriers at different wavelengths can use the same fibre to obtain increased bandwidth, but this requires optical multiplexers, and the increased cost often makes using extra fibres a more attractive solution.

3 APPLICATIONS AT THE AT

The most obvious use of fibres is to transfer the signals from the antenna receivers to the correlator in the central building. (For details about the correlator see [1].) The choice of fibre and connectors was crucial and determined much of the system design. A robust connector is needed to connect the antenna optical fibre to the cable returning to the central site. The most common butt-joint style of connector is totally unsuited to making frequent connections in a harsh external environment. Alternative proposals which either protect or remove the connector altogether were cumbersome or produced other problems. Many connectors were evaluated but the only sufficiently robust connector was a military-style, four-fibre lensed one. Unfortunately, all such lensed or 'expanded-beam' connectors available at that time used multi-mode graded-index fibre which would not normally have been the fibre of choice for such a high bandwidth application.

As mentioned earlier, multi-mode fibre does not have the generous bandwidth of single-mode fibre and is also subject to modal noise. Modal noise occurs when there is some misalignment, and hence loss, at the junction of two fibres such as at a splice or connector. In the plane of the junction, the multiple modes form an interference pattern which can vary with any change in the fibre's conditions, such as temperature, wavelength or movement. This variation in the interference pattern causes the power transferred across the junction to vary, and this appears as both wideband noise and amplitude drift at the receivers. This effect can be minimised by having a wide-range, fast-response automatic gain control (AGC) in the receiver, by selecting a low-coherence laser-transmitter and by ensuring minimum loss in all connectors, splices and optical components. Modal noise occurs due to the combination of multi-mode fibre and the high coherence of lasers but alternatives, such as LED sources, do not have sufficient bandwidth. Sufficient system bandwidth can be obtained by using lasers and by specifying an optical fibre with the very high bandwidth-distance product of 2 GHz km. After tests confirmed that the desired performance could be obtained, a system was designed using multi-mode fibre, lasers and expanded beam connectors.

4 IF DATA TRANSFER

To carry the IF signal from the output of the antenna receivers to the correlator, analog transmission was rejected due to poor noise performance and because reflections produce ripples on the passband amplitude. The very low loss of fibre accentuates this problem and the time variability of fibre delay (due to temperature changes) prevents the removal of these ripples during calibration. Since the IF signal must be sampled and digitised before it is sent to the digital correlator, the logical solution is to sample at the antenna and transfer a digital stream over the fibres. Sampling and digitisation at the antennas also permits easy removal of cable delays by inserting synchronization pulses every few seconds. Within each antenna, the samplers produce a digital stream at 512 Mbits per second for each of the four receiver channels. Several channels could be time multiplexed onto a single fibre but, due to the large bandwidth requirement, multi-mode fibre would then be inadequate. Instead, four separate fibres run from each antenna with each fibre carrying 512 Mbits per second.

Before transmission, the signal is XORed with a 512-MHz clock to produce a Manchester coded signal. This permits the easy extraction of the clock at the receive end and also reduces the low-frequency components of the signal, simplifying system design. However, it results in a transmitted data rate of 1024 Mbits per second which requires a system bandwidth of about 1 GHz. More efficient codes are quite difficult to implement and, for our needs, do not give any significant advantage. The lowest system bandwidth achieved was 980 MHz on the longest fibre length of 2.2 km. No attempt was made to reduce inter-symbol interference by providing optimum bandpass roll-off shape, since this would be very difficult to maintain with connector and cable-length variation as antennas were moved. Instead, a generous bandwidth with slow roll-off is provided to ensure adequate performance.

The 1-GHz bandwidth requirement meant that a low-power laser diode was needed for the transmitting light source. Lasers produce about 1 mW optical power and give a generous signal-to-noise margin. The wavelength chosen was 1.3 μm, which is the optimum for minimum spectral dispersion in graded-index fibre. The lasers are of the Fabri-Perot type and contain inbuilt Peltier cooling, and temperature and power output sensors. External feedback loops are included to control these parameters to ensure a stable output power and extended laser-diode life.

The optical receiving devices are avalanche photo-diodes (APDs) followed by six low-noise, 50 Ω linear amplifier stages with a total gain of 60 dB. APDs provide greater sensitivity than the alternative PIN-photo-diodes but

require a high voltage bias. The final stages contain an AGC system to reduce output-level changes caused by component variation and modal noise. The output level is sufficient to drive the ECL logic directly within the delay units. Clock recovery and data synchronization is provided within the delay units, as described in [2].

5 WAVELENGTH-DIVISION MULTIPLEXING

Wavelength-division multiplexing is used to allow the four fibres carrying the IF data to carry lower speed signals also. Multi-mode fibre permits transmission at a wavelength of 0.85 μm where bandwidth is much lower but components are cheaper. Wavelength-division-multiplexers based on concave mirrors and dichroic filters are used to separate the two wavelengths and, on one fibre, a fibre directional-coupler is used to enable 0.85-μm signals to be sent in both directions. These additional low-speed channels are used to transmit the time-frame signal for time synchronization, up-link and down-link channels for computer communications, and a safety tone which turns off the lasers if a break in the fibre is detected. Although the optical power is very small and the risk of eye damage is low, precautions are necessary to ensure a low risk of injury. The collimated expanded beams from the lens connectors pose the greatest risk. An electronic detection circuit is used to switch off a laser whenever its signal fails to appear in the remote receiver — for example, when a connector is undone. Warnings are also displayed on equipment, and safety shutters cover the output connectors of the laser modules.

To minimise the number of different system types, the modules used for all 0.85-μm links were designed to be universal, with any differences handled by jumpers. To allow for future expansion of the link speed above 80 kbits per second, the links were designed to permit operation at up to 10 Mbits per second. Fibres are also used within the antennas to carry some of the receiver control and data signals from the antenna control computer in the base of the antennas to the vertex room just below the surface of the dish. Advantage is taken of the radio-frequency interference immunity of fibres to transfer these signals. Miniature commercial 'RS422' to optical modems are used to send these signals over multi-mode 'cord' cables.

6 CABLES AND PATCH PANELS

The five antennas of the 3-km sub-array travel on a rail line and are able to operate at any of the 35 stations along the line. At each of these stations the telescopes are plugged in to power, communications and fibre cables. The fibre cables from the stations to the central building are run as separate four-fibre cables from each station. Since the antennas are only ever at five stations at a time, only a small subset of the fibres are used at any one time. A study of link loss and cost ruled out the alternatives which used trunk cables with many more connectors or couplers. At the central equipment room, only five of the 35 four-fibre cables contain signals coming from an antenna. A method of selecting these signals and directing them to the appropriate inputs of the correlator delay units was necessary. Various switching matrix arrangements were considered, but rejected due to complexity and expense. A manual patch-panel using simpler lens connectors was chosen with a separate panel for each IF. All 35 fibres come into each panel and five patch cords pick up the IF from the five antennas and direct the optical signal into the receivers.

A gel-filled, slotted-core, Telecom-style cable containing four 50/125 graded-index fibres is used for the buried cable from the antenna-station posts back to the central building. This was chosen largely because it was the most widely used type for underground installation at that time. In contrast, a 'loose-tube', gel-filled cable was chosen for the 4.5-km run to the isolated sixth antenna, since this cable is also used to carry the local oscillator (LO) reference signal (see below). Tests showed good phase tracking between fibre pairs in this cable and there was a concern that friction between the fibre and a slotted core could lead to sudden jumps in the phase delay of the fibre. The 35 cables between the station posts and the central building were manually installed in underground PVC ducts. The cables were pulled into the ducts from 'figure-of-eight' coils laid out on the ground beside the cable pits. The cable to the sixth antenna site was buried directly by Telecom Australia, using specialised cable-laying tractors. Within the antennas, the fibre cables have to hang in long, unsupported drops, and for this application tight-buffer cord cables were chosen. Without a tight-buffer coating around them, the fibres would be under tension from their own weight and this could affect stability and long-term reliability. A simplified block diagram of the fibre system for the 3-km sub-array is shown in Fig. 1.

7 PHASE TRANSFER

Optical fibre can also be used to transfer LO phase-reference signals to each antenna. Early experiments showed that the required phase stability would be difficult to achieve due to the large reflections associated with many components, especially optical connectors. Because of these limitations, coaxial cable was chosen to send the LO reference signal to the five antennas of the 3-km sub-array (see [3] for a description of this system). The sixth antenna is, however, a special case because connectors are not essential, and so single-mode fibre was chosen to carry LO reference signals over the 4.5-km run to this site. Compared with coaxial cable, this was both less costly and less complex. Once the decision to use single-mode fibre to the sixth antenna was made, it was then logical to use the same type of single-mode fibre for the IF return, giving both complete freedom from modal noise and generous

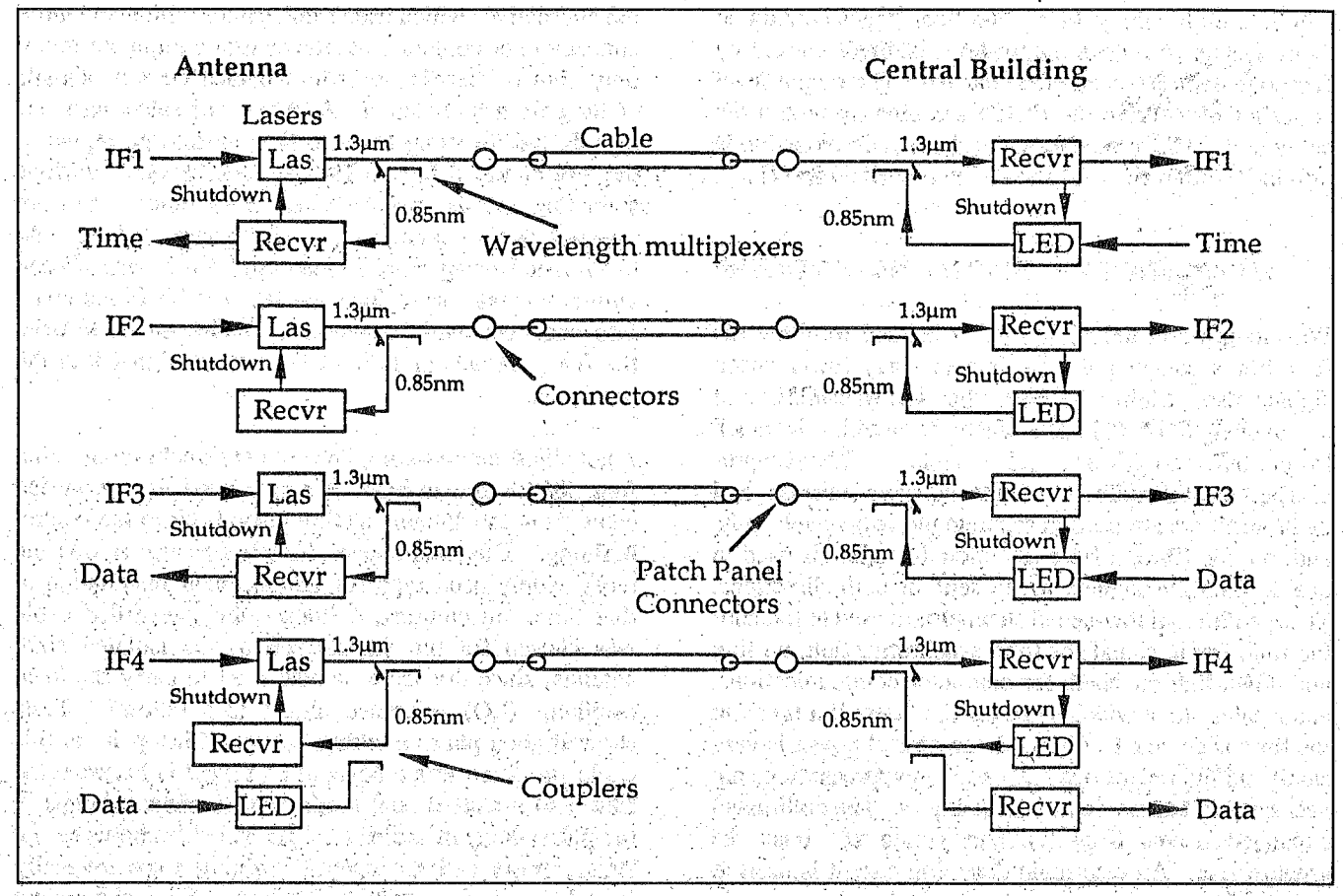

Figure 1 Functional block diagram for each 3-km array antenna.

bandwidth. Sufficient bandwidth would have been difficult to achieve with multi-mode fibre over this distance. This meant, however, that wavelength-division multiplexing of 0.85-μm signals was not possible, and so separate multi-mode fibres are used for these lower speed links.

8 OPERATING EXPERIENCE

For the AT, using optical fibre instead of coaxial cable for a wide variety of applications has resulted in a simpler, less costly system with better noise immunity. It has met all expectations and has proved to be very reliable, with very few failures and no drift in any important parameter.

9 ACKNOWLEDGMENTS

The authors thank all those who contributed to the fibre system: P. Miller for his painstaking early measurements, N.V.G. Sarma for his study of the use of fibres for LO phase transfer, T. Percival for his early work and W. Chandler and his associates for the excellent cabling, splicing and construction work. For his contributions, we give special acknowledgment to the late Alec Little.

10 REFERENCES

1. Wilson, W.E. and Davis, E., "The Australia Telescope Correlator System", JEEEA, 1992, this issue.

2. Wilson, W.E. and Carter, C.N., "The Delay System", JEEEA, 1992, this issue

3. Young, A.C., McCulloch, M.G., Ables, S.T., Anderson, M.J. and Percival, T.M., "The L o c a l Oscillator System", JEEEA, 1992, this issue.

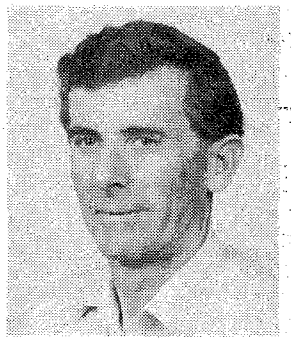

DR A.C. YOUNG

Dr Alan Young received the BSc degree from the University of New South Wales in 1971 and the PhD degree from the University of Sydney in 1982. Until 1982 he was a member of the Air Navigation Group at the University of Sydney, primarily involved in the analysis and scale modelling of the Instrument Landing System. From 1982 to 1984 he was part of the group at the California Institute of Technology responsible for developing the instrumentation for the new millimetre-wave radio astronomy array at Owens Valley, California. He joined the CSIRO Division of Radiophysics in 1984 where he became leader of the Local Oscillator and Signal Distribution Group for the Australia Telescope project.

MR M.J. ANDERSON

Michael Anderson received the BE and MEngSc degrees from the University of Sydney in 1967 and 1974 respectively. He joined the Department of Civil Aviation (DCA) as a Cadet Engineer in 1966 and during two years' national service in the Australian Army, spent 18 months as an instructor in basic electronics at the RAEME Training Centre, Bandiana. On his return to DCA he worked on the installation and maintenance of communication systems, aircraft navigational aids and radar. In 1986 he joined the Local Oscillator and Signal Distribution Group within the CSIRO Australian Telescope project. His main activities are in fibre optics, satellite links and equipment production and installation.

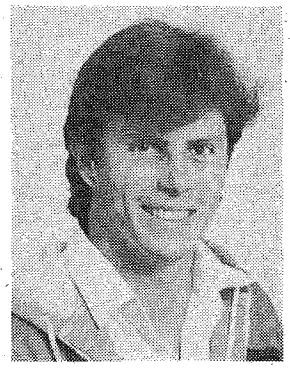

MR M.J.W. HAYES

Michael Hayes graduated in 1986 with the BE degree from the James Cook University of North Queensland. He joined the CSIRO Division of Radiophysics in 1987 as a member of the Australia Telescope's Local Oscillator and Signal Distribution Group. He is presently the local oscillator and signal transmission engineer at the CSIRO Australia Telescope National Facility's Paul Wild Observatory, Narrabri and is completing a PhD (Physics) in radar oceanography at the James Cook University of North Queensland.

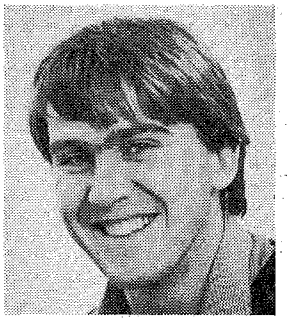

MR R.C. TICEHURST

Robert Ticehurst received his BE and MEngSc degrees from the University of New South Wales in 1984 and 1988 respectively. From 1985 to 1988 he was with the CSIRO Division of Radiophysics as a member of the Local Oscillator and Signal Distribution Group for the Australia Telescope project. He was primarily involved with the development and installation of the high-speed, fibre-optic system. Since 1988, he has been with the Satellite and IC section of OTC Australia Transmission R & D. His major work has been in the development of MMIC-based microwave systems for satellite communications.

The Delay System

W.E. Wilson* and C.N. Carter**

SUMMARY We describe the delay system for the six antennas which make up the Australia Telescope Compact Array. The digital data from the antennas arriving at the central site first pass through the delay system. The amount by which each data stream is delayed differs from antenna to antenna, and changes over the course of an observation. The delay system performs this function and converts the data into a format suitable for subsequent processing.

1 INTRODUCTION

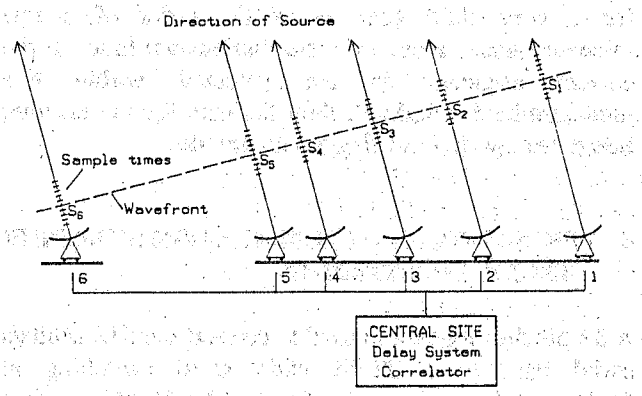

Figure 1 The wavefront concept.

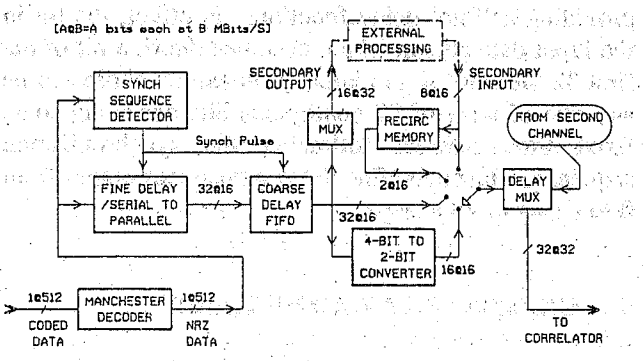

Figure 2 Delay System block diagram.

* Australia Telescope National Facility, CSIRO, PO Box 76, Epping NSW 2121, Australia.
** Alcatel-TCC, 1 Moorebank Avenue, Liverpool NSW 2170, Australia
Submitted to The Institution of Radio and Electronics Engineers Australia in June 1992.

The delay system for the Australia Telescope provides the interface between the incoming digital data from the antennas and the correlator. Its main function is to delay the various data streams in such a way that, when presented to the correlator, they are 'wave-front' aligned; that is, samples taken at each antenna which originate from a particular wavefront (the S_i shown in Fig. 1) arrive simultaneously at the correlator. The wavefront in question is perpendicular to the direction in the sky at which the array is pointed. The signals from a radio source in this direction received by the antennas in the array will then travel the same distance from the source to the correlator. This ensures that the components of the signals at all frequencies within the observing band arrive in phase at the correlator and allows the instrument to operate over a wide instantaneous bandwidth.

As the delay system operates on sampled digital data, the minimum delay increment is one sample time. Finer delay adjustment is made at the antennas by varying the relative phases of the various sampler clocks. The maximum delay required from the system is approximately 30μs and is determined by the maximum source-to-antenna path-length difference (6km = 20μs) plus the maximum central site-to-antenna pathlength difference (3km = 10μs).

The digital data emerge from the fibre-optic transmission system at the central site and are fed to the delay system. As shown in Fig. 2, the delay system comprises a number of functional blocks, each of which is described below.

2 MANCHESTER DECODER

The coded input data are restored to non-return-to-zero (NRZ) format in the Manchester decoder. The clock is extracted from the data in a phaselock loop circuit which

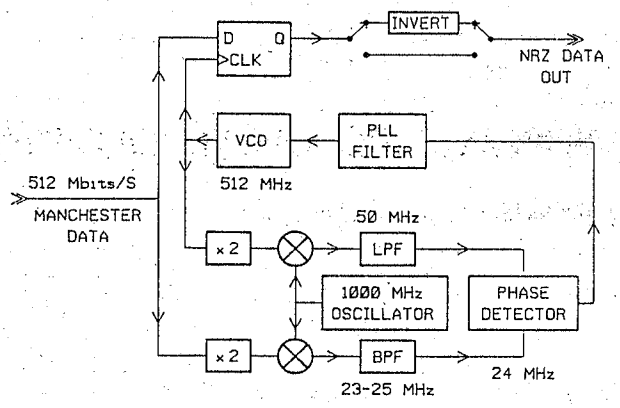

Figure 3 Manchester decoder.

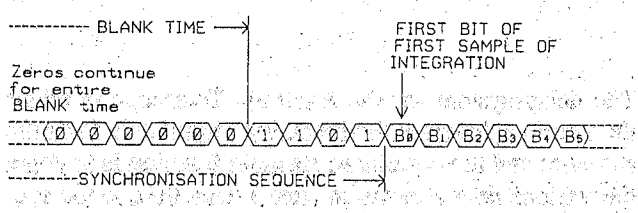

Figure 4 Synchronization Bit sequence.

makes use of the fact that Manchester coded data are differential 180° phase-shift keying. If the data are passed through a frequency doubler, the modulation on the 512-MHz carrier is removed, leaving a fixed-phase 1024-MHz signal. This signal is used as the reference frequency to which a voltage controlled oscillator (VCO) is phaselocked, as shown in Fig. 3. The VCO provides the clock to the decoder which is a high-speed D flip-flop. As is always the case with Manchester coding, the recovered clock has a phase ambiguity of 180° compared to the original clock at the encoder. This can lead to an overall inversion of the decoded data. This ambiguity is resolved by fixing the transmitted data in the zero state during a short time (the 'BLANK' time) each integration period. The NRZ data received during the BLANK time is examined in the decoder and, if necessary, an inversion is applied to the data during the ensuing integration period.

3 SYNCHRONIZATION SEQUENCE DETECTOR

To identify the first sample in each integration and to provide a time reference point, the sampler places a synchronization bit sequence in the digital data stream at the start of each integration (see [1]). The delays inserted by the delay system are measured relative to this reference time. During the BLANK time immediately preceding the start of each integration period, the data are held in the zero state. As the integration starts, the synchronization sequence shown in Fig. 4 is inserted, followed by the first sample of the new integration. The synchronization sequence detector searches for a sequence of 15 zeros followed by X1101, where X can be either 0 or 1. Nominally X should also be zero, but to facilitate implementing the detector, this bit is ignored. To minimise the possibility of detecting a false synchronization sequence, the detector is enabled only for a very short time — of the order of a few microseconds — around the nominal arrival time. If the correct sequence is not detected within this predetermined 'window', then the data for the ensuing integration period are flagged as invalid.

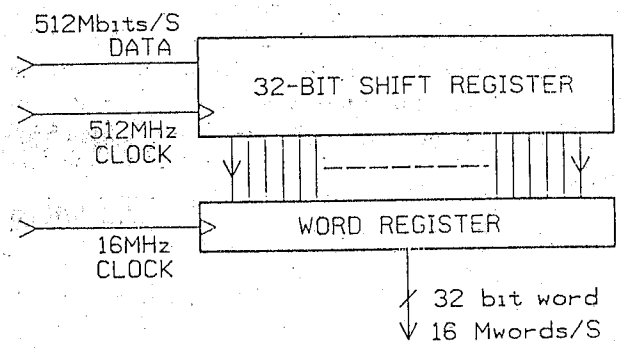

Figure 5 Serial-to-parallel converter.

4 SERIAL-TO-PARALLEL CONVERSION/FINE DELAY ADJUSTMENT

A 32-bit shift register is used to convert the 512 Mbits/s serial data to a 32-bit wide word switching at 16 Mwords/s, as shown in Fig. 5. The 16-MHz output clock is stopped during the BLANK time. It is restarted after a programmable time interval following the arrival of the synchronization sequence. This time interval can be varied over a range of 64 ns in 2-ns steps, thus providing a 'fine' delay function. In effect, the bit in the input data stream which becomes the first bit of the first 32-bit word in the integration can be chosen to be any one of a set of 32 contiguous bits occurring some fixed time interval following the synchronization sequence. Hence the fine delay adjustment ranges from 0 to 64 ns in 2-ns steps.

5 COARSE DELAY ADJUSTMENT

This circuit contains a large 32-bit wide first-in-first-out (FIFO) register. The FIFO is necessary to resynchronize the data, but also provides the means by which a 'coarse' delay is introduced. Due to the continuous phase rotation applied to the sampler clocks in each antenna, the input data rate to the delay unit differs from the nominal 512 Mbits/s by a small amount and is different for each antenna. Hence the 32-bit parallel data entering the FIFOs have a slightly different word

rate from each antenna. The data are 'realigned' by using a common fixed output clock rate for all FIFOs. The delay function is implemented by first clearing the FIFO during the BLANK time and then delaying the loading of the FIFO by a programmable number of word clocks following the first word of the integration period. In effect, a predetermined number of words are discarded at the start of each integration. The unloading of all FIFOs in the system begins simultaneously, some short time after all have begun loading. The result is that the data are delayed by the time that each word spends in the FIFO. The smallest increment of delay is one word-time, i.e. 64 ns, whereas the maximum delay of 64 μs is determined by the length of the FIFO. Care must be taken to ensure that the FIFO does not fill or become empty during the integration cycle. For a particular integration time, this places limits on the amount by which the input and output clock rates can differ, and on the timing of the loading and unloading.

6 4-BIT DATA PROCESSING

In the case of 4-bit sampling at the antennas, the data must pass through an intermediate processing stage before being sent on to the correlator. This is because the correlator cannot process 4-bit data directly (see [2]). The required processing is performed either within the delay system, or external to it. The internal function performed is a direct conversion of the 4-bit data to 2-bit data. In this conversion, the 4-bit sign bit becomes the 2-bit sign bit, while the third or fourth decision levels (see [1]) either side of zero in the 4-bit (16 level) data can be chosen as the 2-bit magnitude decision levels. External processing is provided for by the secondary output and secondary input, as shown in Fig. 2. Original plans for the Australia Telescope Compact Array included the construction of a unit containing a digital-to-analog converter, narrowband filters and a 2-bit sampler which would make use of the secondary output and input and provide narrowband operation. This unit is not yet implemented. All external data paths are in the form of balanced ECL signals on twist-and-flat cable.

7 RECIRCULATION MEMORY

At signal bandwidths less than 8 MHz (1-bit) or 4 MHz (2-bit) the input data rate is less than the clock rate of the correlator and the recirculation memory comes into operation. (For an explanation of the function of recirculating memory, see [2].) This unit contains a large dual memory, one half of which is loaded with data at the input data rate (8, 4, 2,... etc. Mbits/s), while the other half is unloaded into the correlator at its standard 16-Mbits/s rate. Hence the unloading operation can be repeated a number of times during the time it takes to complete the loading operation. In effect, the data are 'recycled' through the correlator. In the unloading process, two reads of the memory occur simultaneously, providing two output data streams. During any one unloading operation, a fixed offset is maintained between the addresses of the two reads, resulting in a fixed, but programmable, delay between the two data streams. This offset is changed for each recycling step.

8 OUTPUT SWITCHING

The output from a delay channel can come from one of four sources. These are:

(i) directly from the FIFOs
1, 2-bit mode 512 Mbits/s max.
(ii) from the 4-bit to 2-bit converter
4-bit mode 256 Mbits/s max.
(iii) from the secondary input
4-bit mode 128 Mbits/s max.
(iv) from the recirculation memory
4-bit mode 32 Mbits/s max.

The output to the delay multiplexer is selected from these four in an output switching matrix.

9 DATA MULTIPLEXER

To minimise the number of physical connections at the delay system output, two channels of data are time-division multiplexed before being sent to the correlator. Here a 'channel' is defined as one input Manchester data stream. The multiplexed output data are transmitted on two 20-pair twist-and-flat cables, using balanced ECL drivers and receivers. The data occupy 32 pairs with each twisted pair operating at 32 Mbits/s. This accommodates the maximum data rate from two 512 Mbits/s channels. Some of the spare cable pairs are employed to send a 500 kHz clock signal which is used by the correlator as a reference to which the correlator clock is locked.

10 PACKAGING AND CONTROL

The Manchester decoder, the synchronization sequence detector and the fine delay circuitry for one channel are all contained on one four-layer printed circuit board (PCB). The coarse delay unit, 4-bit to 2-bit converter, secondary output/input circuitry and output switch for one channel occupy one four-layer PCB, as does the data multiplexer for two channels. Two channels of recirculation memory are contained on one PCB.

The delay system is packaged in 6U Eurocard format, with the boards for four channels contained in a 19-inch rack-mounted bin. With six antennas and four channels per antenna, six bins are required for the complete system. The backplane of each bin is a custom four-layer PCB. Each bin has a controller board which provides a connection to a delay-unit control computer (DUCC) and event generator. The DUCC is a

PDP11/21++ CPU with a 20 MByte hard disk. A special-purpose interface board is connected to the Q-bus of the DUCC. It provides a 16-bit data bus to which all bins in the system are connected. The delay system is controlled via a serial interface between the DUCC and the correlator control computer (CCC). A description of the software running in the CCC is contained in [3].

11 ACKNOWLEDGMENT

Richard Lacasse performed some early investigations into the high-speed circuitry used in the synchronization sequence detector and the fine delay unit. His work contributed significantly to the present designs.

12 REFERENCES

1. Wilson, W.E. and Willing, M.W., "The Sampling and Data Synchronization Systems", JEEEA, 1992, this issue.

2. Wilson,W.E, Davis, E.R., Loone, D.G. and Brown, D.R., "The Correlator", JEEEA, 1992, this issue.

3. Kesteven, M.J., McConnell, D. and Deane, J.F., "On-line Computing for the Compact Array", JEEEA, 1992, this issue.

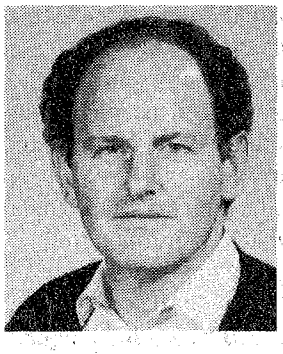

DR W.E. WILSON

Dr Warwick Wilson obtained his BSc in 1967, his BE in 1969 and his PhD in 1975 from the University of Sydney. From 1971 to 1979 he worked at the Max Planck Institute für Radioastronomie in Bonn, initially as a research fellow and later as a research engineer, working on receiver and systems development for the Effelsberg 100-m radio telescope. From 1977 to 1979 he was leader of the electronics group at the Effelsberg Observatory. In 1979 he returned to Australia to work on the Interscan project with AWA. In 1980 he joined the CSIRO Division of Radiophysics and was seconded to Interscan Australia Pty Ltd, working in the USA until 1983 on the design of the microwave landing system. In 1983 he was appointed leader of the Correlator Group in the Australia Telescope project.

MR N.C. CARTER

Craig Carter received the BE degree in Electrical Engineering from James Cook University in 1985 and the MEngSc degree from the University of Sydney in 1988. He worked at CSIRO Radiophysics from 1985 to 1988 on the design and implementation of the delay units for the Australia Telescope project. His work at Radiophysics enabled him to complete his Masters' thesis. At present he is manager of R & D and Repeater Development at Alcatel-TCC. His interests include optical amplification and very high speed digital design.

Journal of Electrical and Electronics Engineering, Australia
Special Issue

THE AUSTRALIA TELESCOPE

Chapter 3

Signal Processing

The Correlator

W.E. Wilson*, E.R. Davis*, D.G. Loone** and D.R. Brown***

SUMMARY This paper describes the correlator system of the Australia Telescope Compact Array. The Compact Array is located at Narrabri, NSW and comprises six of the Australia Telescope's eight antennas. The correlator is a special-purpose real-time digital processor which performs the first stage of data reduction for the Compact Array. It operates at the maximum data rate of 12 Gbits/s at the input, reducing this by a factor of order 5000 at the output.

1 INTRODUCTION

The basic function of the correlator is to form the cross-power spectra of pairs of sampled data input streams (see [1]). It does this by measuring the digital cross-correlation functions of the input pairs which are then Fourier transformed to produce the cross-power spectra. The cross-correlation function of two signals is a measure of the correlation of the signals as a function of the time delay between them. The digital cross-correlation function is computed at discrete delay intervals and is formed from measurements of the correlation of two sampled and digitised data streams. The process of sampling and digitising the data and the reasons for using very coarse digitisation of the data entering the correlator (1 bit or 2 bits) is discussed in [2].

The traditional method of building a digital correlator is shown in Fig. 1. [3]. In this case the delay is provided by a shift register so that the basic unit of delay is one sample interval, usually the Nyquist sampling interval. A number of processing elements are then used to produce the correlation measurements simultaneously at a series of discrete delays. The range of delay over which the correlation function is measured determines the spectral resolution. To obtain N independent channels in the frequency domain over a bandwidth B requires 2N delay measurements in the delay, or lag domain. This is illustrated in Fig. 2. For each pair of samples presented to its input, the processing element multiplies the samples and accumulates the result over a specified integration period. This implies that at least parts of the correlator, including the multiplication circuit, must operate at the input sample rate.

If it were constructed using the structure shown in Fig. 1, the complete Australia Telescope Compact Array (ATCA) correlator system, operating at maximum bandwidth (where N is specified to be 16), and correlating signals from 15 baselines, at two frequencies and four polarizations, would require almost 4000 processing elements, each operating at 512 Msamples/s. This was considered to be impractical. The architecture for the ATCA correlator is based on a concept developed by Dr. J.G. Ables and uses an array of correlators, fed by a 32-sample-wide parallel data stream [4]. It uses the

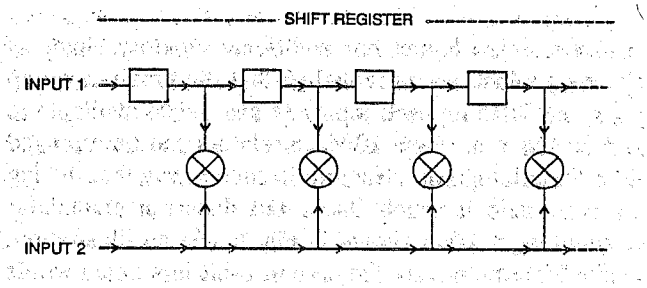

Figure 1 The traditional digital correlator structure.

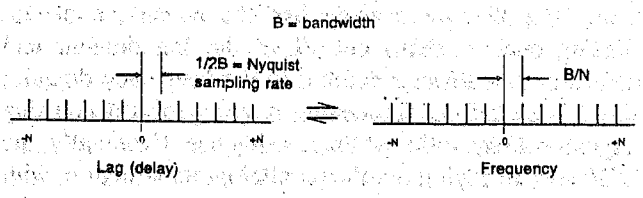

Figure 2 The two Fourier domains - lag and frequency - for digital correlator.

* Australia Telescope National Facility, CSIRO, PO Box 76, Epping NSW 2121, Australia.
** Australia Telescope National Facility, CSIRO, PO Box 94, Narrabri NSW 2390, Australia.
*** Canon Australia, PO Box 313, North Ryde NSW 2113, Australia.
Submitted to The Institution of Radio and Electronics Engineers Australia in June 1992.

technique of parallel processing, whereby a reduction in the speed required of the processing elements is achieved by replacing each one by a number of slower processors, operating in parallel. The lower speed requirement presented the opportunity to apply very large scale integration (VLSI) techniques which also made practical the increased number of processing elements.

2 ARCHITECTURE

The basic architecture of the ATCA correlator was determined largely by the requirements at maximum bandwidth where the specification called for 16 independent frequency channels across the full bandwidth. We will begin by considering the case of 1-bit correlation at the maximum bandwidth of 256 MHz. Here the 32 bits of each output from the delay system are in fact 32 samples, contiguous in time (see [5]). Taking two of these outputs, which have been delayed such that corresponding bits in the two outputs are aligned in time, and correlating each bit of one output with all bits from the second output, i.e. forming all possible combinations, results in the lag characteristic shown in Fig. 3(a). This is the simplest form of 'parallel' structure and is realised by a 32 x 32 square array of correlators, i.e. a total of 1024 correlators, each with an input data rate of 16 Mbits/s and operating at 16 million multiplications per second. As an illustration of the layout, an 8 x 8 square array of correlators is shown in Fig. 4. This structure has the disadvantage of not making use of all the data, in that not all samples in the original data streams are involved in all lag measurements. In fact, the full number of 32 measurements is only made at lag zero. This is because only 32 samples from each input are available to the correlators at any one time, so that correlations between groups of 32 samples are not performed.

An alternative layout has additional memory elements (delays) which are provided so that the previous group of 32 samples on each input are also made available to the correlators. Now 1024 correlators can be arranged in a 'parallelogram' structure in such a way that the lag characteristic is much flatter but does not extend far beyond lag ± 16 as shown in Fig. 5. As an illustration, a similar structure for the case of 8-bit input data words is shown in Fig. 6.

Both these structures satisfy the basic requirement for 16 independent frequency channels at maximum bandwidth. The 32 x 32 square array has the advantage of not having such a sharp cut-off in the lag domain and therefore has lower sidelobes in the frequency domain; but it also has the interesting property of a decreasing signal-to-noise ratio with increasing lag. Eventually, the difficulty of laying out the parallelogram structure, with its memory elements and inherent asymmetry, led to its being rejected in favour of the simple 32 x 32 square array structure.

Although the basic architecture of the AT correlator was very much driven by the requirements at maximum bandwidth, it was also required to provide efficient operation at lower bandwidths. Consider now the case of 1-bit operation at half the maximum bandwidth, i.e. 128 MHz. The input data rate required to satisfy the Nyquist criterion is 256 Mbits/s which is half that of the maximum bandwidth. If the delay unit output word rate is maintained at 16 Mwords/s, the data rate can be accommodated by using only 16 of the 32 bits in each output of the delay system. That is, on each 32-bit input to the 32 x 32 correlator array, only every second bit is active. Hence only 256 of the available 1024 correlator channels are in use, providing a lag characteristic similar to Fig. 3(a), but with a maximum of 16 measurements at lag zero and extending out to lag ± 16. The remaining channels are now available to make measurements at other lags and can be used to extend the total lag coverage. This is achieved by feeding the 16 unused input lines to the correlator array from the 16 active input lines through suitable delay elements, a process known as reconfiguration. The resulting lag characteristic is shown in Fig. 3(b), and can be seen to be composed of four of the ±16 lag triangular distributions placed side by side. Figure 7 shows the reconfiguration of a simple 4 x 4 correlator array. This reconfiguration procedure can be carried further as the bandwidth is decreased. As is shown in Fig. 3, each step of halving the bandwidth produces a lag characteristic which is a combination of four 'half-scale' versions of the one above. At the smallest bandwidth of 8 MHz, the 1-bit sample rate of 16 Msamples/s matches the correlator clock rate, and there is only one of the 32 input lines which is active. Now each correlator in the array measures a different lag.

In 2-bit correlation mode, the maximum bandwidth is 128 MHz. In this case, the correlator array is fed with 32 magnitude bits, representing the magnitudes of 32 contiguous samples, followed by the 32 sign bits of the same samples. The input data rate to each correlator channel is still 16 Mbits/s but they now operate at 8 million multiplications per second. The reconfiguration process can also be carried out in 2-bit mode, resulting in the same lag characteristics shown in Fig. 3, down to a minimum bandwidth of 4 MHz.

3 RECIRCULATION

At bandwidths below 4 MHz, the input data rate is less than the rate at which individual correlators operate (16 Mbits/s). In this case, a technique known as recirculation is employed. The input data, instead of being fed directly to the correlator channels, is stored in one half of a large 'recirculation' memory. After a time T, the input is switched to the second half of the memory and the first half is unloaded into the correlator at the full operational rate of 16 Mbits/s. The correlation will be completed in a time T/N, where the input bandwidth is 4/N MHz (2-bit mode). Hence the data can be

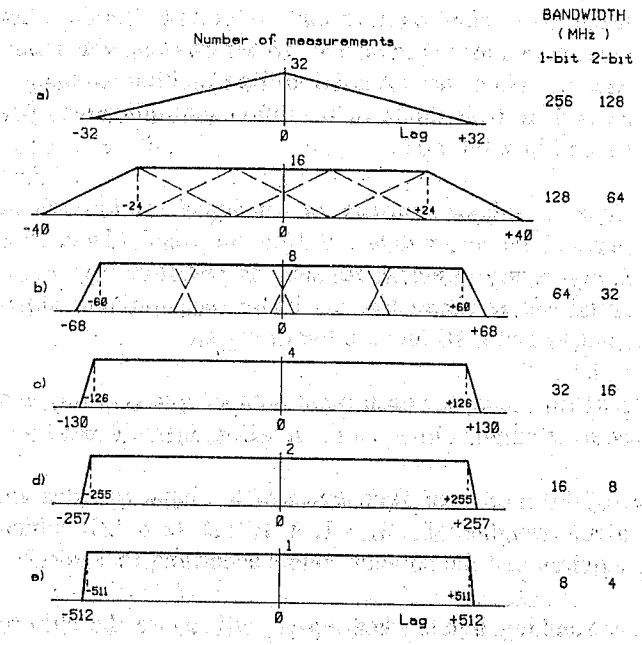

Figure 3 Showing the effect of reconfiguration on the lag characteristics of the AT correlator module at different bandwidths.

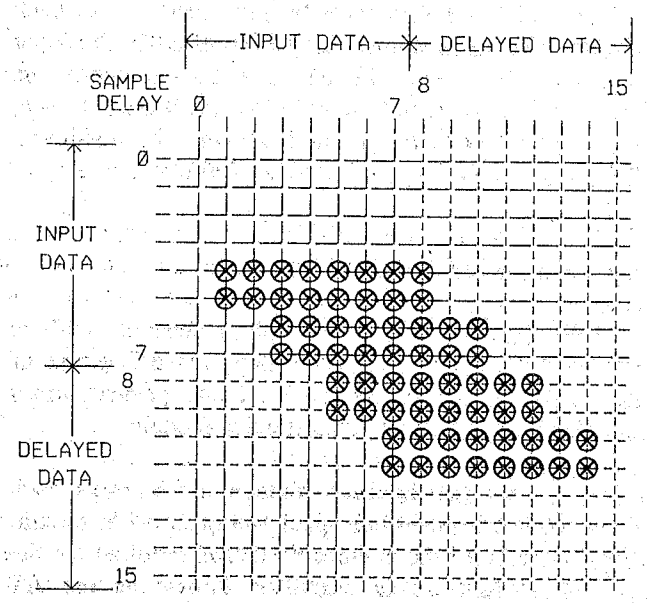

Figure 6 An 8-bit input 'parallelogram' structure.

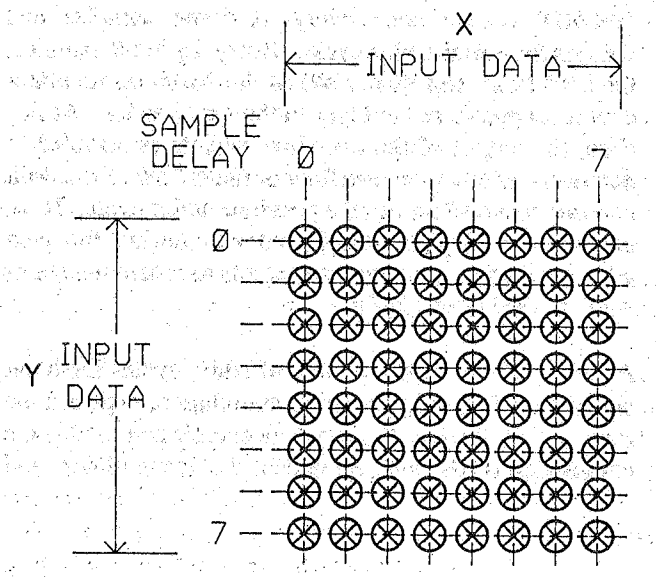

Figure 4 An 8-bit input square array of correlators.

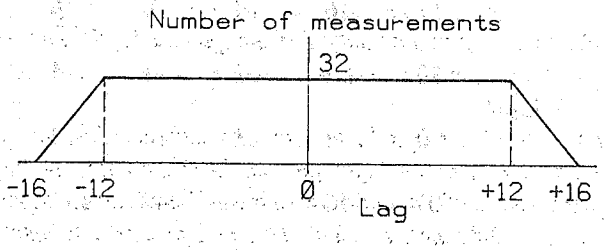

Figure 5 The lag characteristics of the 32-bit input 'parallelogram' structure.

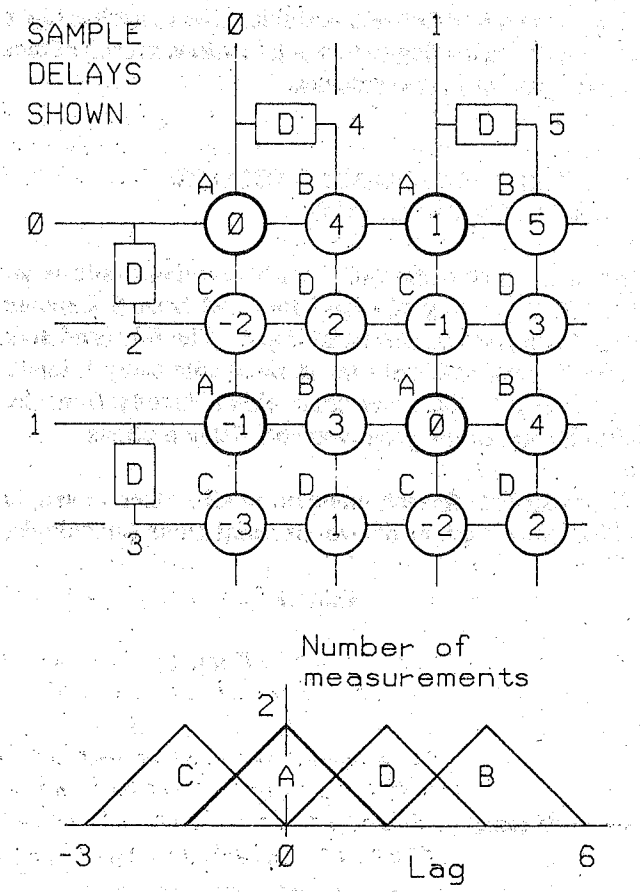

Figure 7 Reconfiguration of a simple 4 x 4 array of correlators. The numbers represent sample delays whilst the letters ABCD refer to the four groupings of 2 x 2 correlators.

recirculated through the correlator N times before the next set of input data must be processed. With each recirculation step, a new delay is inserted in the input data, leading to an N-fold increase in the number of lags covered in the overall correlation function. Hence, recirculation is a means of increasing the maximum frequency resolution at narrow bandwidths.

4 PHYSICAL LAYOUT

The 32 x 32 square array of correlator channels, with its programmable reconfiguration delays, is the basic unit of the correlator. It is contained on one printed-circuit board and is known as the correlator module.

The array is subdivided into sixteen, 8 x 8 arrays, each of which is contained in a special-purpose VLSI circuit, together with all the switchable delays required for the reconfiguration. This circuit is known as the AT correlator chip.

There are eight correlator modules required for each baseline (antenna pair) of the ATCA, allowing four polarization products to be formed at two simultaneous frequencies. These eight modules are contained in one card cage, which is known as the correlator block. One block is required for each baseline. The block has eight inputs, corresponding to two polarizations at each of two frequencies from two antennas.

5 THE AUSTRALIA TELESCOPE CORRELATOR CHIP

The basic architecture of the AT correlator chip is an 8 x 8 square array of correlators, fed from 8 X inputs and 8 Y inputs, as shown in Fig. 4. The 64 correlators form the correlation of each X input with every Y input. The inputs to the array come either directly from the chip inputs, or via programmable delay sections.

The input data format, common to all sixteen inputs, is either one-bit (sign) or two-bit serial mode (magnitude, sign). The circuit has two modes of operation to cover these two input data formats. In both modes, the maximum input data rate is 16 Mbits/s, at which rate each correlator performs 16 million multiplications per second in 1-bit mode or 8 million multiplications per second in 2-bit mode.

Each correlator consists of an input section which decodes the input data, an 8-bit pipelined Manchester Carry binary up/down counter, an overflow register, a serial adder/subtractor, a 16-bit accumulator shift-register and a 16-bit result shift-register.

In 1-bit mode, for each input data sample (i.e. bit), the counter counts either +n or -n according to Table 1.

In 2-bit mode, the four levels of the input samples are given weights of - 4, - 1, + 1, + 4 (see [2]) which requires that the counter counts according to Table 2.

A blanking input, when active, will cause the chip to cease operation and hold the present accumulated value.

The accumulated result can reach $\pm 2^{23}$ (24 bits) before overflow occurs. However, only the most significant 16 bits are available for readout.

There are two input signals which control the accumulation and readout of the circuit. The input 'WORD' occurs once every 16 input samples and defines the serial adder cycle. Every 16 input samples, the LSB (least significant bit) of the 16-bit accumulator contents appears at the input to the serial adder. At this time, the output of the overflow register is sampled to determine whether an overflow or underflow of the 8-bit counter occurred during the previous adder cycle. If so, the overflow register is cleared and during the next adder cycle the accumulator contents are incremented or decremented accordingly.

After a (usually large) number of adder cycles the input signal LOAD terminates the accumulation, captures the result, and begins the next accumulation. At the completion of the load sequence, the accumulator- and

Table 1

Y Input \ X Input	0	1
0	+n	-n
1	-n	+n

*n can be chosen to be 1, 4 or 16, determined by two control inputs. This option provides for a wide range of integration times in 1-bit mode.

Table 2

Y input \ X Input	11	10	00	01
11	+16	+4	-4	-16
10	+4	+1	-1	-4
00	-4	-1	+1	+4
01	-16	-4	+4	+16

Input data format: (sign, magnitude)

result-register contents have been exchanged, the first adder cycle of the new accumulation has been done (i.e. no loss of data during readout), and all 64 result registers within the chip are connected in series. The resulting 1024-bit shift register is shifted out on a serial output line during the following 1024-input sample periods, whilst being loaded from a serial input line. This provides a method of pre-setting the 16 most significant bits of the accumulators to particular values at the start of an accumulation. There is no provision for pre-setting the eight LSBs.

The programmable delay sections used in the reconfiguration process are tapped 2-bit dynamic shift registers. The programming is achieved through serially loaded static registers which control the data switching.

An on-chip clock generator provides either the two-phase (for 1-bit mode) or four-phase (for 2-bit mode) non-overlapping internal clock signals.

6 THE AUSTRALIA TELESCOPE DELAY CHIP

The AT delay chip is a special-purpose integrated circuit used on the correlator module to provide module concatenation delays (see below). It uses the same silicon die as the AT correlator chip, but with a different pin-out. In the delay chip, only the reconfiguration delay stages within the correlator chip are connected. The correlators are not used. The chip is configured as a 16-bit in, 16-bit out programmable delay circuit.

7 THE CORRELATOR BLOCK

The correlator block is made up of four key sections (Fig. 8):

(i) the block distributor
(ii) the correlator module(s)
(iii) the block switch
(iv) the block control computer.

A correlator block is assembled in a 9-U-high EURO sub-rack or bin. A power supply unit and a cooling fan unit, each designed to service an entire rack of correlator blocks, is provided by separate sub-rack units located within the respective rack. This configuration allows a maximum of three correlator blocks to be installed in a standard 'AT' 39-U rack.

Overall monitoring of power supply voltage and + 5V current to each block, as well as nominal cooling-air-exhaust temperature and air flow for each rack is performed by local environment monitors in each power-supply unit and each correlator block sub-rack connected to a standard AT dataset. The local environment monitor in the power-supply sub-rack is capable of shutting down the power supplies in the event of prolonged over-temperature, over-current (+ 5V), under-voltage or loss of air flow.

8 THE BLOCK DISTRIBUTOR

This unit distributes the input data streams via the correlator block backplane to the correlator modules. It also generates the clock signals for the correlator block which are locked to a 500-kHz reference signal sent from the delay units. This ensures that the correlator is always synchronized with the delay unit and makes the system less prone to clock/data phase errors caused by cable length between the delay unit and the correlator block. This reference signal is sent down two of the spare wires in the data cable from the delay units. An on-board oscillator is also available for stand-alone testing. Any of the four input data streams or the internal oscillator may be selected as the reference source.

The data are transmitted from the delay units to the correlator in 32-bit-wide balanced emitter-coupled logic (ECL). This is converted to transistor/transistor logic (TTL) for use within the correlator block. Optional terminators on the ECL input line allow each set of inputs to be at an intermediate point or an end point in the signal distribution network. There are four physical

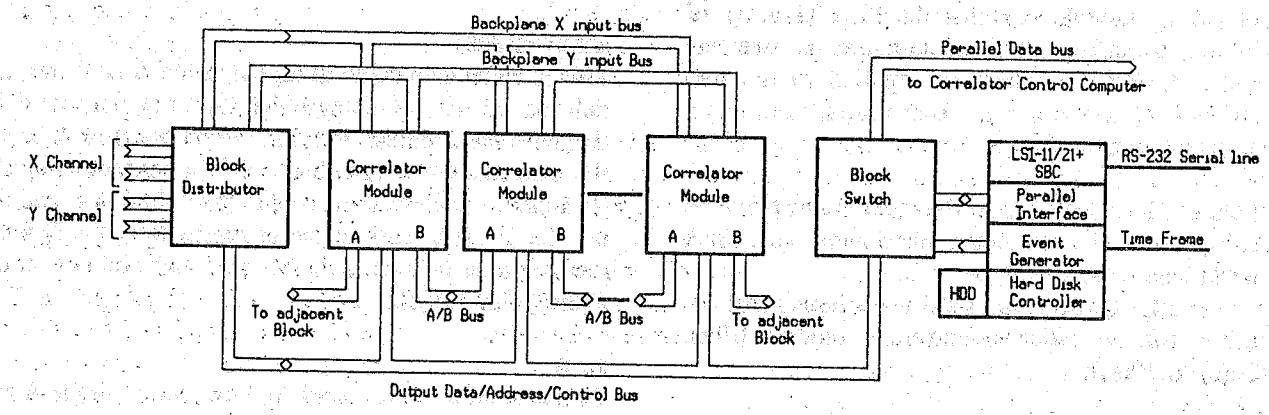

Figure 8 Correlator block schematic.

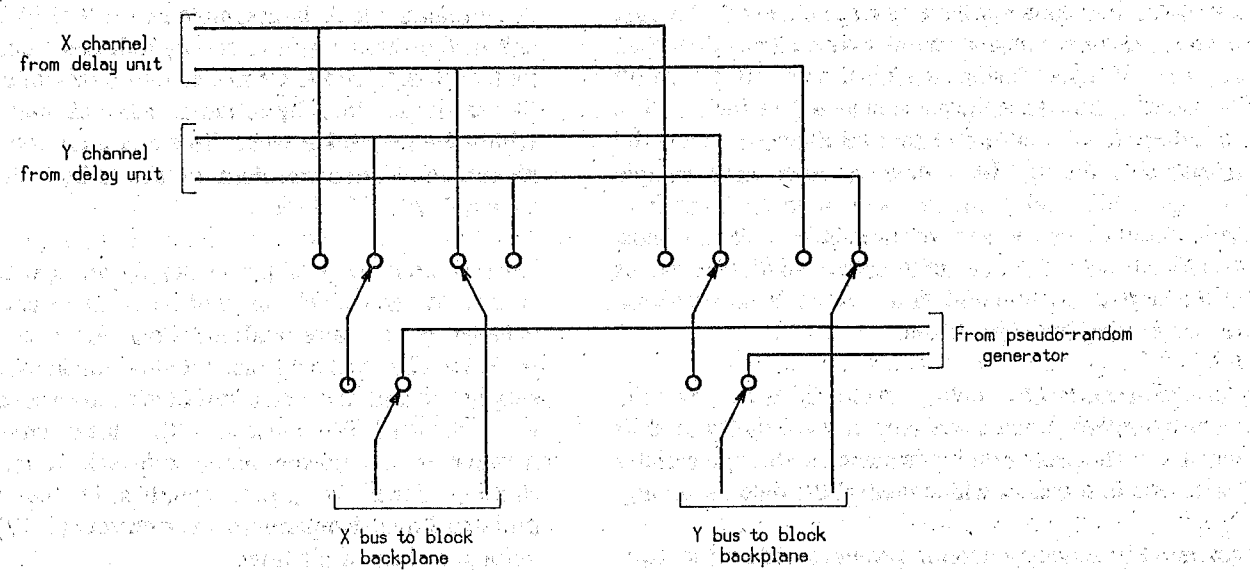

Figure 9 Input data streams switching matrix.

streams: two X and two Y, each made up of two time-division multiplexed, 32-bit wide, 16 Mbits/s signals. This gives eight sets of signals in total, four X signals corresponding to the four IF channels from the X antenna, and four Y signals from the Y antenna. As there may exist small phase errors between the selected clock reference and the other input data streams due to variations in propagation delays and cable lengths, all input data streams are re-synchronized to the selected clock.

A switching matrix (Fig. 9), controls the routing of the input signals to the backplane.

A pseudo-random data signal generator is also provided on the block distributor. By suitable configuring this may be switched through to one of the two X backplane buses and one of the two Y buses. The random data source is only 16 bits wide and so only every second bit of the 32-bit backplane bus is used.

9 THE CORRELATOR MODULE

The correlator module contains the 32 x 32 array of correlators. It performs the correlation of the two sets of input data streams which are applied to the two sides, X and Y, of the array. These inputs can come from one of two sources:

(i) both can be selected from the main inputs from the delay units via the block distributor and block backplane [Fig. 10(a)]; or
(ii) one can be selected from the main inputs and the other from an adjacent correlator module [Figs. 10(c) to 10(e)].

When one of the inputs comes from an adjacent module, the modules are said to be in concatenation mode.

An additional set of buffers on the input stage of each module allows a selected X or Y backplane signal to be connected to both the X and the Y sides of the correlator array, thus providing a means of performing auto-correlation [Fig. 10(b)].

When concatenating correlator modules, one input is selected from the main input while the other comes from the adjacent correlator module. This input is connected through the A/B bus (Fig. 8) and brought to the correlator array via AT delay chips which introduce delay in all active lines of that bus. Concatenation may occur in either the X or the Y input. In addition, this delayed input may be passed on to the next adjacent correlator module. There are three basic modes when concatenating: first, intermediate and last, indicating where each lies in the concatenation chain.

First
This is similar to no concatenation. Both inputs are taken from the main inputs, but the A and the B bus drivers are enabled. The data that come in on the X bus are sent out on the B bus and the data that come in on the Y bus are sent out on the A bus [Fig. 10(c)].

Intermediate
This is when data come in on either the A or B bus, are delayed by the AT delay chips, and not only used by that correlator module but sent out on the B or A bus to the next module in the chain. When concatenating the Y input, concatenated data come in on the B bus and out on the A bus, and when concatenating the X input concatenated data come in on the A bus and out on the B bus [Fig. 10(d)].

Last
This is similar to intermediate; however, both the A and B buses are disabled so that no data are passed on to the next module [Fig. 10(e)].

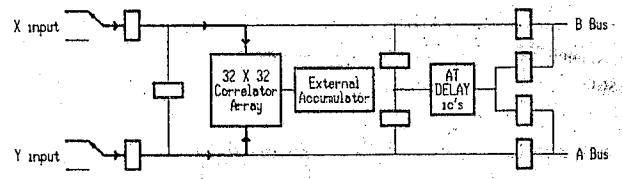

Figure 10(a) Correlation of main inputs.

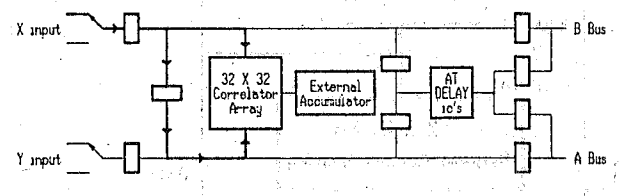

Figure 10(b) Autocorrelation of one main input.

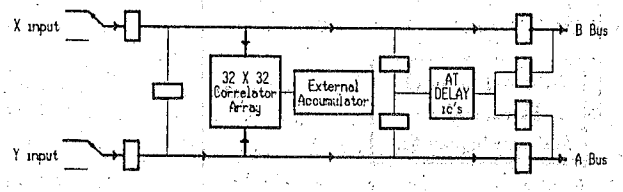

Figure 10(c) Correlation of main inputs with module in 'First' concatenation mode.

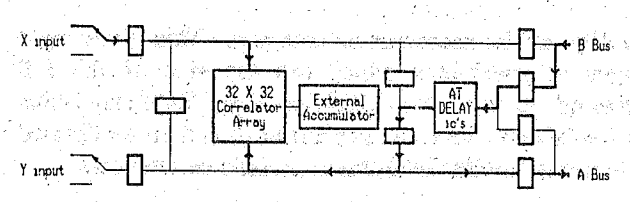

Figure 10(d) Correlation of one main input and one concatenated channel. Module in 'Intermediate' concatenation mode.

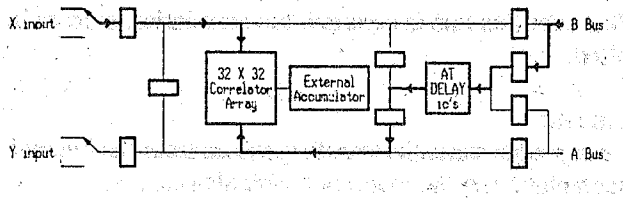

Figure 10(e) Correlation of one main input and one concatenated channel. Modules in 'Last' concatenation mode.

Correlator module concatenation allows an increase in the range of lags covered by the measured correlation function. This is because of the accumulating delays introduced as the data pass down the A or B bus. The direction of the lag range extension is determined by whether the X or the Y input is concatenated (Fig. 11).

Correlation occurs within the AT correlator chip. External hardware accumulators are provided on the module to allow integration periods of longer than typically 40 ms, this being the limit of the correlator chip's internal accumulator. On command from an external event generated by the 'event generator' in the block control computer, the contents of the internal accumulators are transferred to the external accumulators and added to the existing data stored there. The internal design of the correlator chip is such that the transfer operation has no effect on the integrating process.

The external accumulators (Fig. 12) consist of two identical sets of 24-bit-wide signed adder hardware and 8K x 24-bit memory arranged such that, as one set or bank is acting as the external accumulator, the memory in the other bank is free to have its data transferred to the correlator control computer. The external accumulation process, once initiated, runs automatically until all 1024 correlator elements making up the 32 x 32 correlator array have been processed.

The transfer and accumulation process is controlled by a 10-bit counter, a word-sequence controller and an address translation table (Fig. 13). The counter keeps a check on where the process is up to and provides the logical address of the data as they come from the correlator array; the word-sequence controller handles the 'read', 'addition' and 'write' operation of each word and the address translation table controls both where to put the result and how to process it. The address translation table is a random access memory (RAM) which is loaded when each correlator module is initialised, with the logical-to-physical address translation. It controls the accumulation process by either inhibiting data storage (i.e. throw data away) or by placing the data into the accumulator without adding the present contents in that position, on a location-by-location basis. This latter operation negates the need to do a specific 'accumulator clear' operation, usually needed at the start of each integration period. The address translation table also provides the means of mapping particular correlators in the 32 x 32 array into specific accumulator memory locations.

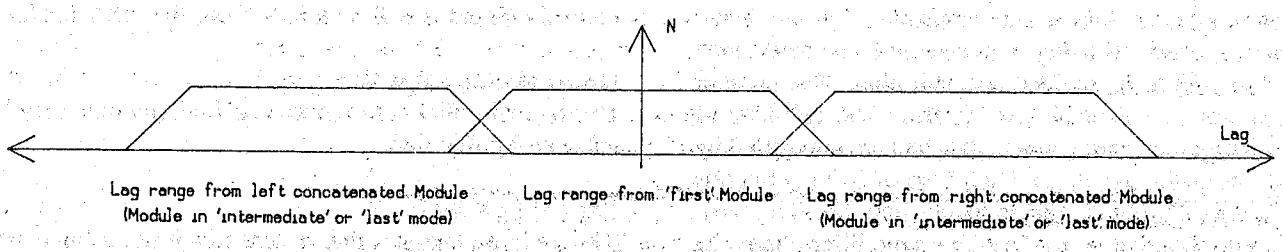

Figure 11 Extending the lag range from concatenation of 3 modules.

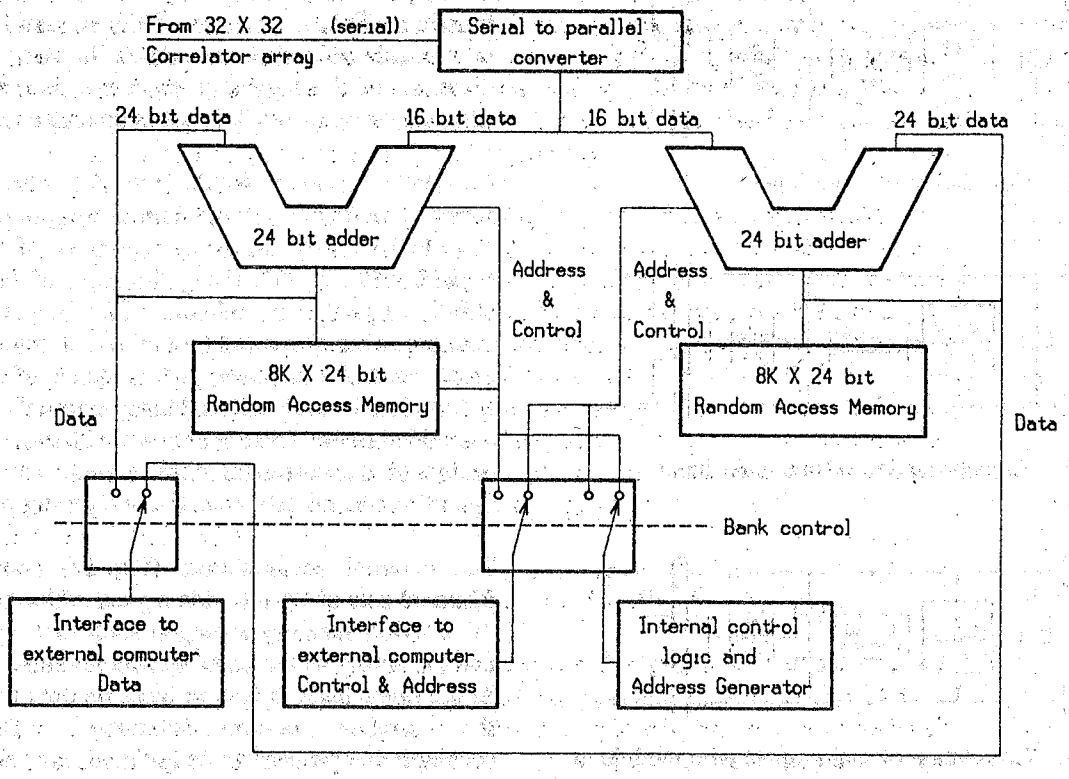

Figure 12 Correlator module external accumulator.

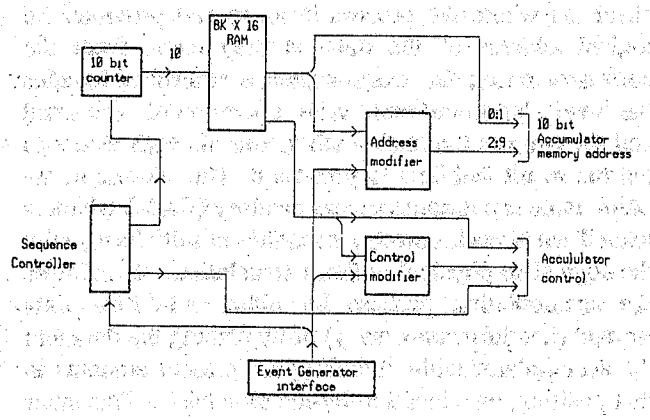

Figure 13 Correlator module accumulator control.

The address translation table output is further processed by an event-generator-driven address modifier. This address modifier allows 8 bits of the 10-bit accumulator memory address bus to be controlled by the event generator, thus allowing the accumulator work area (1024 words) to be divided into sub-bins. The number of sub-bins and their size range from 256 sub-bins of four contiguous words, when all 8 bits are controlled by the event generator, up to 2 sub-bins of 512 contiguous words when only 1 bit is controlled by the event generator. In addition to the address modifier, three bits of the event generator also control a 'page-select' facility on the accumulator memory. This gives eight pages or super-bins which are the size of the full accumulator work area (1024 words). Both super-bins and sub-bins allow an integration period to be divided into many smaller integration periods or windows.

The event generator within the block control computer controls the real-time sequencing of the correlator. The following signals are provided directly from the event generator:

Correlator Blank
Whenever this line is asserted, the correlation process is halted.

Transfer
A rising edge starts the transfer process from the internal accumulators to the external accumulators.

Bank
This sets which bank the accumulation process will occur in. By default this means that the correlator control computer will read data from the other bank.

Recirculation Control
During recirculation the source of the input data may be selected by this line.

Super-bin Select
Three event-generator lines select which super-bin to use as the accumulator work area.

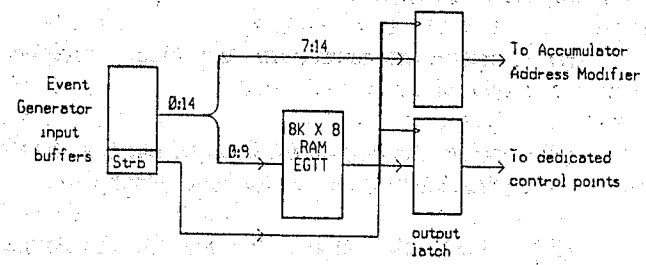

Figure 14 Correlator module event generator interface.

Adder Disable
This tells the accumulator to ignore the present contents of the accumulator memory and place the data coming from the correlator integrated circuits straight into the memory.

Address Modifier Eight event-generator lines select which sub-bin to use as the accumulator.

The event generator input to the correlator module is 15 bits wide and is accompanied by an event strobe (Fig. 14). At the beginning of the microsecond of the scheduled time, the 15 bits are loaded with the event as programmed. These signals propagate through the event generator translation table (EGTT) random access memory and arrive at the input to the event capture latch on each correlator module. At 750 ns after the start of this microsecond the event strobe is issued, loading the capture latch. The output of this latch feeds the various points on the correlator module.

The EGTT allows the function of 15 event generator lines to be expanded. The EGTT is made from an 8K x 8 RAM whose address is driven by 10 bits of the event-generator word to produce an 8-bit output. Thus, the final output arrangement which feeds the event capture latch is 16 lines wide; the top eight lines of the raw event-generator bus go to the top eight lines of the capture latch (which feeds the accumulator address modifiers), and the bottom 10 lines go to the EGTT whose output goes to the bottom eight lines of the capture latch.

10 THE SWITCH BOARD

The Switch Board is the interface between the block control computer, the main data processing computer (correlator control computer), the event generator, and the correlator modules and block distributor. It communicates with the correlator modules and the block distributor via a 16-bit address bus, and a 24-bit data bus that runs down the backplane. Each slot on the backplane has its own select line, so that whenever an appropriate board is inserted in a given slot, its address will be set by that slot and will appear as a 64K-byte block of memory.

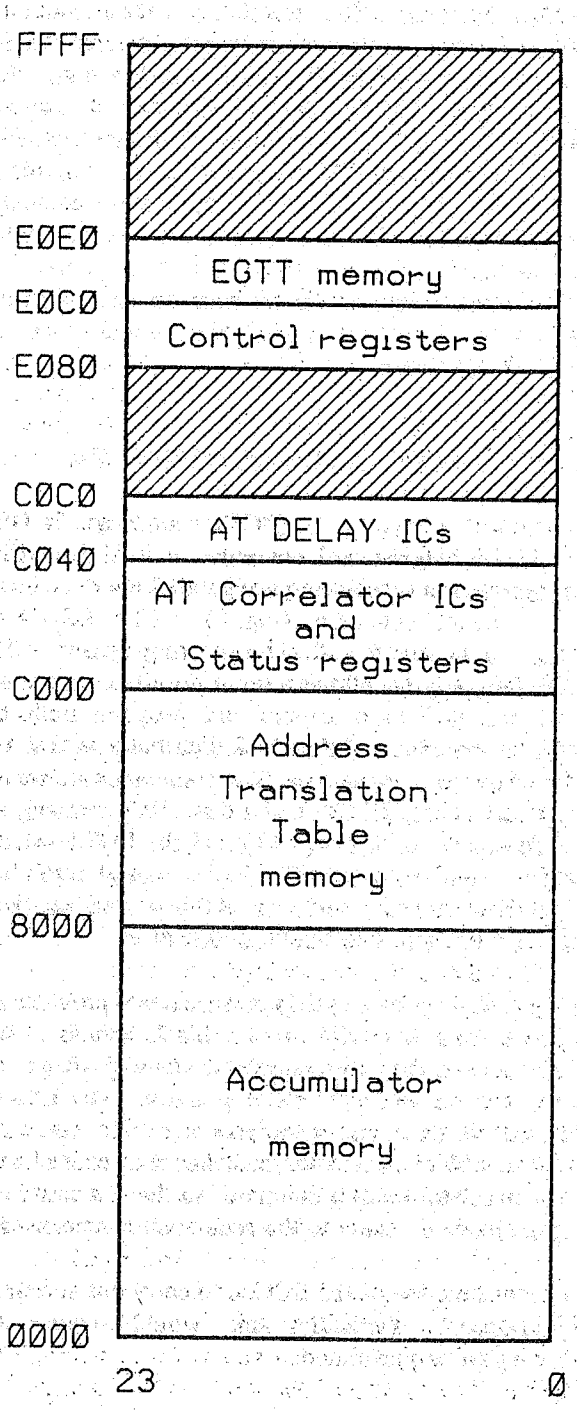

Figure 15 Correlator module memory map.

The address translation table, the non-active accumulator bank, and all programming and status registers, appear as full width and depth entities on the memory map (Fig. 15). The EGTT and the correlator and delay chips, however, appear as single registers. The address of the EGTT is set by the event generator, while the correlator chips and delay chips are sequentially loaded components. During programming, the block control computer takes control of the event-generator bus that is fed to the correlator modules so that the EGTT memory can be loaded.

Transferring data from each correlator module is controlled by both the correlator control computer and

the block switch. The correlator control computer initiates the transfer by first sending the start address for data and a 'Request' for data to the block switch. The block switch loads the start address into its address counters and then sends the first word of data back with an 'Acknowledge'. If more data are required, 'Acknowledge' signals the correlator control computer to send a 'Next' signal, whereupon the block switch increments the address counter and transfers the next word. This process continues until no more data are required and the correlator control computer de-asserts the 'Request' signal.

11 THE BLOCK CONTROL COMPUTER

The block control computer (BCC) is made up of a DEC LSI-11/21 + single-board computer, a hard-disk drive and controller, a special-purpose parallel interface board and an event generator (Fig. 8). The LSI-11 is configured to run the RT-11 operating system. The application program allows a set of primitive commands to be executed to configure and program both the correlator modules and the block distributor, and to run and load the event generator. The commands are sent to the LSI-11 via an RS-232 serial line. Programming the address translation table (ATT) and the EGTT usually requires large tables of files to be loaded into their respective memories, and to speed this process up, these tables can be stored on the hard-disk drive.

The special-purpose parallel interface board provides the interface from the BCC to the block switch. This interface maps the entire correlator memory image as a series of registers in the BCC memory. The LSI-11, whenever it does not need access to the correlator modules or block distributor, switches their control back to the correlator control computer so that the latter can gain unhindered access to the accumulator memories.

The main function of the BCC is to carry out correlator initialisation. Typically, this would require the following to be performed:

On the Correlator Module –

(i) program the correlator and delay chips for the reconfiguration and lag range function

(ii) load the ATT with appropriate translation data

(iii) load the EGTT with appropriate translation data

(iv) set up the control registers to select input data paths, correlator mode and reconfiguration, enable concatenation and recirculation if required, select both ATT and EGTT pages, enable accumulator address modifiers, and disable test bits.

On the Block Distributor –

(i) select the source of the clock reference signal

(ii) select the source for each of the four buses that feed the correlator block backplane

(iii) check the status to see if the block distributor clock generator has locked to the reference signal.

During operation, the BCC controls the event generator and monitors various status points within the block. Status data are passed to the correlator control computer only on request. Some time before the start of an observing period, one or more sets of event timing descriptions (ETD) are passed to the BCC. These ETDs describe when and what events are to occur over a planned period. By issuing a start command, along with a start time and an ETD identifier, the events described in the selected ETD list will occur relative to the start time.

12 CORRELATOR CONTROL COMPUTER

The correlator control computer (CCC) manages all aspects of the correlator operation, collects the data from the correlator modules and completes the on-line data processing. It receives its instructions from the array control computer (see [6]) via the local Ethernet network. The central processing unit is a DEC uVAXII running the VMS operating system.

The layout of the CCC and its connections to the correlator blocks and delay system are shown in Fig. 16. All programming and event timing information is transferred to the correlator blocks and delay system via RS232 serial lines. A special-purpose parallel direct-memory-access interface transfers data from the correlator module memories directly into CCC memory. This memory is shared between the CCC and an 18MFlop array processor which handles the bulk of the post-correlation data processing. When processing is complete, the data are converted into RPFITS format (see [6]) and written to a hard-disk file.

There are seven processes (Fig. 17) running concurrently within the CCC. These, and their functions, are :

(i) **COR_BOSS**, the main process, starts all other processes, controls the operator console and, on the operator console, maintains error logging and display, and provides status display.

(ii) **COR_CONFIG** controls the serial interfaces to the correlator blocks and delay system; receives commands and passes status information from/to COR_SYNCH, COR_BOSS and COR_DAT; provides menu-based operator interface for preparing

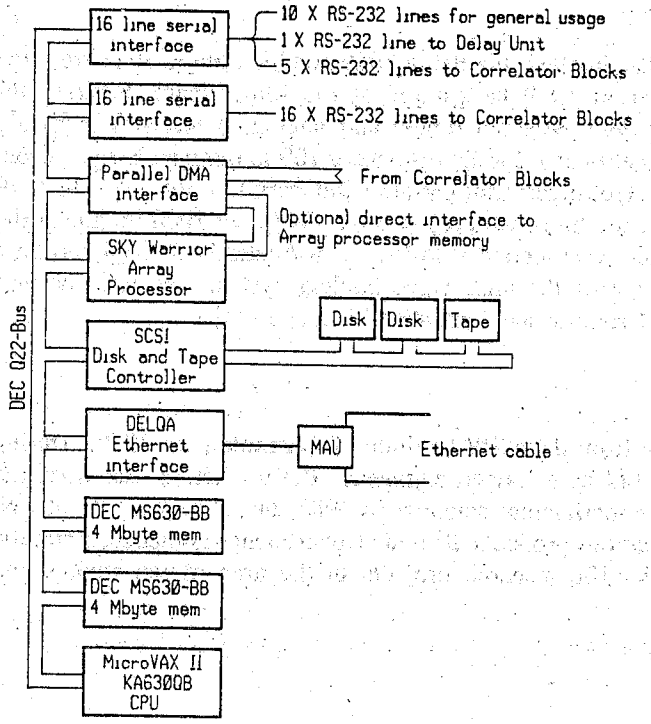

Figure 16 Main elements of the correlator control computer.

'configuration' files which define the programming and event timing of the correlator.

(iii) **COR_SYNCH** communicates with the array control computer, receiving commands and sending status.

(iv) **COR_CQT** controls the direct-memory-access transfer of data form the correlator blocks to CCC/AP memory.

(v) **COR_DAT** controls the array processor and processes data.

(vi) **COR_FITS** converts data to RPFITS format, assembles header information, writes data to disk.

(vii) **COR_DISP** provides on-line display of data via graphics terminals, either as time variables (also passed to the array control computer) or spectra (lag and frequency domains).

The processing carried out by the array processor within COR_DAT includes:

(i) Normalisation — i.e. it converts raw correlation outputs to correlation coefficients.

(ii) Correction from digital to analog correlation coefficients (see [2])

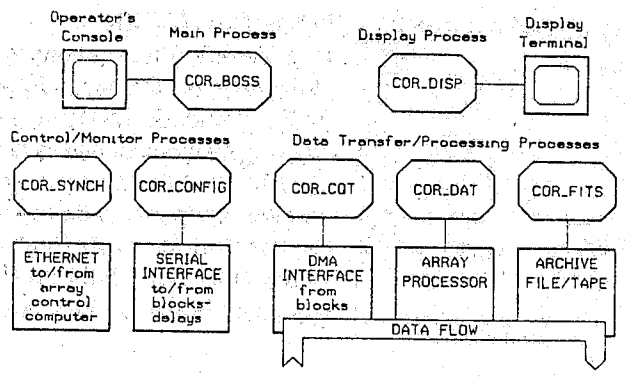

Figure 17 Software processes controlling the correlator.

(iii) Scaling by measured system temperatures to obtain correlation function.

(iv) Application of phase gradient across the lag domain to implement frequency shifting for on-line Doppler tracking (optional).

(v) Fourier transformation to obtain cross-power spectra.

(vi) Conversion of measured polarization products to Stokes parameters (optional).

13 ACKNOWLEDGMENTS

Jon Ables developed the original concept of the parallel processing correlator array. Andrew Hunt developed some early designs for the correlator chip, upon which the final designs were based.

14 REFERENCES

1. Nelson, G.J., "System Description," JEEEA, 1992, this issue.

2. Wilson, W.E. and Willing, M.W., "The Sampling and Data Synchronization Systems", JEEEA, 1992, this issue.

3. Weinreb, S., M.I.T Research Laboratory of Electronics, Rep. No. 412, 1963.

4. Workshop on the Australia Telescope Correlator System, Parkes, 21-22 November 1983, Doc. No. AT/10.4/003.

5. Wilson, W.E. and Carter, C.N. "The delay system", JEEEA, 1992, this issue.

6. Kesteven, M.J., McConnell, D. and Deane, J.F. "On-line Computing for the AT Compact Array," JEEEA, 1992, this issue.

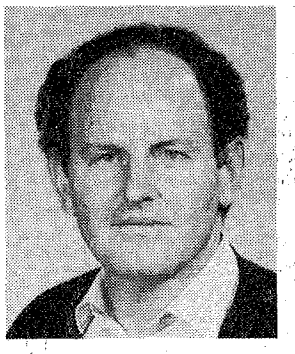

DR W.E. WILSON

Dr Warwick Wilson obtained his BSc in 1967, his BE in 1969 and his PhD in 1975 from the University of Sydney. From 1971 to 1979 he worked at the Max Planck Institute für Radioastronomie in Bonn, initially as a research fellow and later as a research engineer, working on receiver and systems development for the Effelsberg 100-m radio telescope. From 1977 to 1979 he was leader of the electronics group at the Effelsberg Observatory. In 1979 he returned to Australia to work on the Interscan project with AWA. In 1980 he joined the CSIRO Division of Radiophysics and was seconded to Interscan Australia Pty Ltd, working in the USA until 1983 on the design of the microwave landing system. In 1983 he was appointed leader of the Correlator Group in the Australia Telescope project.

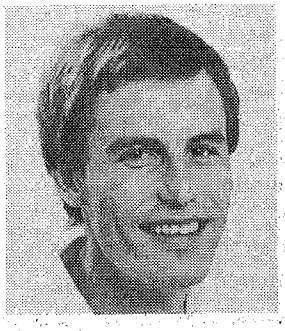

MR E.R. DAVIS

Evan Davis received his BE degree from the NSW Institute of Technology in 1979. During his studies he worked at EMAIL Ltd as a trainee engineer. Before joining the Australia Telescope Correlator group as an experimental scientist in 1985, he worked firstly at J.N. Almgren Pty Ltd on data communications products, then the Department of Science, Antarctic Division, on several Antarctic scientific research projects in the area of ice studies and glaciology.

MR D.G. LOONE

David Loone received the BSc degree in Computing Technology from the University of Tasmania in 1985. He joined the CSIRO Division of Radiophysics in 1986 where he worked in the Correlator Group of the Australia Telescope project doing software and hardware design for computer control of the Australia Telescope correlator. Since 1990 he has been working at the CSIRO Australia Telescope National Facility's Paul Wild Observatory, Narrabri in charge of digital design projects in the correlator, primary monitoring, and other areas of the observatory's development.

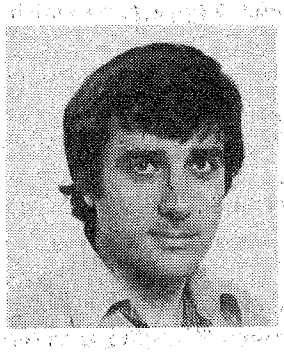

MR D.R. BROWN

David Brown obtained a BE in 1973 and MEngSc in 1978 from the University of New South Wales. In early 1982 he joined the Division of Radiophysics. During 1983 he was seconded to the Correlator Group to work on the correlator chip for the Australia Telescope project. In 1985 he transferred to the Division's Signal Processing Group where he became involved in the development of a VLSI chip to perform fast Fourier transforms. He resigned from CSIRO in May 1992 after accepting a position with Canon Australia Pty Ltd.

On-Line Computing for the Compact Array

M.J. Kesteven*, D. McConnell* and J.F. Deane**

SUMMARY The Australia Telescope Compact Array is made up of six 22-m antennas at Narrabri, NSW. The control system of the Compact Array has to deal with antennas and hardware distributed over 6 km. It needs to maintain synchronization of the sampling of astronomical data to a precision of better than 1 ns, coordinate the activities at the central site (data collecting, processing and archiving), and provide extensive monitoring of the data quality and the hardware status. These goals are achieved through a combination of distributed computing and special-purpose hardware.

1 INTRODUCTION

The Compact Array posed several novel problems for the on-line computing:

(i) the hardware is dispersed over 6 km;

(ii) four different groups were involved in developing the software;

(iii) synchronizing the data streams from the antennas has to be accurately maintained to within 1 ns. (For the most part the timing requirements are quite modest — almost all activities have margins of several seconds.)

The first two requirements pointed to a distributed architecture. This meant that each development group could operate largely in isolation, requiring only that the protocol of the communications be well defined. The last requirement is effectively beyond conventional computing machinery; our solution makes use of a special-purpose device to gate the data streams.

2 THE TIMING PROBLEM

During an observation we require all elements of the array to 'point' at the target. In effect, this means that we should tip the east-west rail track until it is at right angles to the direction to the target; this would ensure that a given wavefront from the target would reach all the antennas at the same instant. Since tipping the track is unrealistic we need to achieve this synchronization by other means — by delaying the signals from all but a reference antenna. In principle this is straightforward, since we can compute the geometrical relationship between the array configuration and the direction to the target.

The idea is therefore to place a common timing mark (at 12 noon, for example) in the data stream from each antenna and to use this mark as the reference point for the delay operations. The precision of the timing mark is set by our sampling rate — we must be accurate to one sample, that is, several nanoseconds, since the IF data is sampled at the antenna at a rate of 256 MHz.

Inserting the timing mark into the data stream is effected with a device known as the Integration Clock. Each antenna contains an Integration Clock [1] which uses the 256-MHz sampling clock as its timebase and produces a signal at the start of each observation cycle.

The observation cycle is one of two basic timing cycles used in the operation of the array. The other is the integration period which is the time for which data are accumulated in the correlator before being transformed to the spectral domain.[1] In all observing modes currently used, the integration period and observation cycle length are identical. In this case, the observation cycle time is set by astronomical requirements and is typically 10 s. The usable range of observation cycle lengths is approximately 1 to 30 s. Cycles much longer than this result in inadequate sampling of the astronomical visibilities in the spatial frequency domain (u - v plane) and a corresponding degradation of the synthesised image. The lower limit is set by the time required for configuring hardware in each antenna. Just

* Australia Telescope National Facility, CSIRO, PO Box 94, Narrabri NSW 2390, Australia.
** Australia Telescope National Facility, CSIRO, PO Box 76, Epping NSW 2121, Australia.
Submitted to The Institution of Radio and Electronics Engineers Australia in June 1992.

1 Note that the correlator has the capability of using integration times down to 2 ms [2].

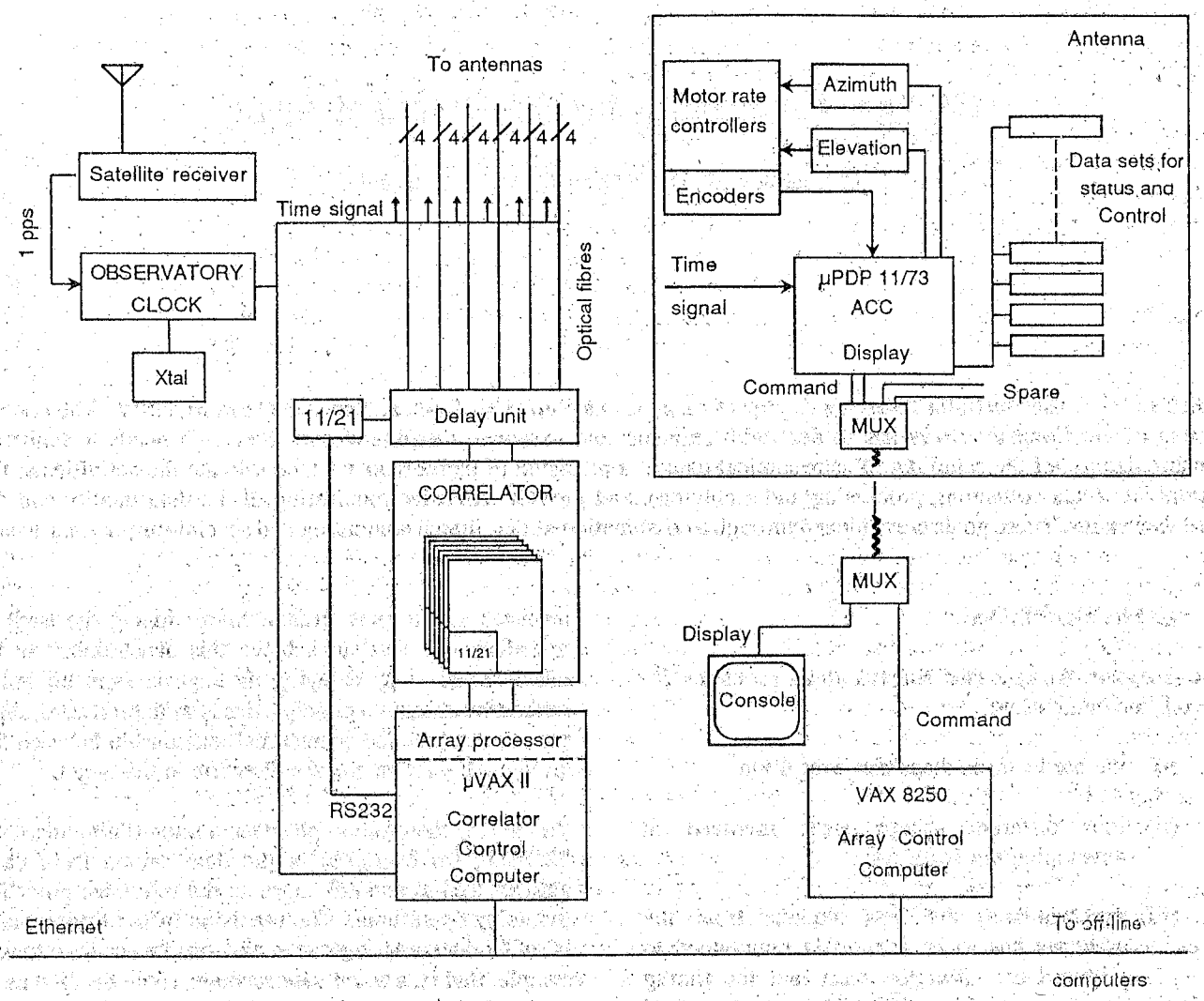

Figure 1 Compact Array on-line computers.

before the start of an observation cycle, the array control computer computes the system settings (such as the geometric delays), and dispatches them to the antennas and correlator for implementation. At the conclusion of a cycle, correlated data are dispatched from the correlator to the correlator computer for processing, calibrating and archiving.

3 MONITORING MATTERS

The array control computer provides two categories of monitoring:

Hardware
The engineers have established a comprehensive set of monitor points throughout the hardware. These points are examined every observation cycle and their values are returned to the central site. This allows the array control computer to maintain a watching brief on the health of the system. Warnings are issued whenever monitor points fall outside their operational range. This same body of monitor information greatly assists in diagnosing and preventing problems.

Data quality
The correlator computer also provides a compressed summary of the data collected in each cycle. The observer can access this summary to gain valuable indicators of the array's astronomical performance.

4 SYSTEM ARCHITECTURE

Figure 1 shows the architecture in place in 1992. The main functional groups are:

Antenna Control Computer (ACC)
Each antenna has a Micro–PDP11/73 control computer responsible for controlling and monitoring antenna motion and the antenna-based timing, receiving and sampling hardware.

Correlator Control Computer
This is a Micro–VAXII with a heavy burden. Astronomical data from each antenna are correlated by special-purpose hardware, the correlator [2]. The correlator control computer supervises the correlator and an array processor which calibrates and transforms the time-domain correlations into the spectral domain. It also disposes of the data, dispatching them to short-term storage (disk). The correlator control programs constitute a major part of the Compact Array on-line software and are described in a separate paper [2].

Array Control Computer
This is a VAX 8250[2], responsible for the overall coordination of the array activities. It commands the antenna and correlator control computers and provides the interface between Compact Array and astronomer.

4.1 Antenna control computer

The ACC has the following functions:

(i) to monitor and control the antenna position through a position encoder and hardware rate controller for each axis;

(ii) to control the synchronizing hardware which produces precisely timed events in the receiver and sampling systems;

(iii) to control the sampler decision levels so as to maintain the ideal distribution of sampled data values;

(iv) to provide general control and monitoring functions for the receiver;

(v) to maintain a communications channel to the array control computer for remote antenna control and monitoring;

(vi) to provide local control and monitoring of antenna motion from the console keyboard and display.

THE ACC PROGRAM AS A REAL-TIME SYSTEM

The prime responsibility of the ACC is antenna safety. It must avoid structural damage by ensuring that the antenna always operates within position, speed and acceleration limits. To satisfy this requirement it must perform the antenna servo task (i.e. read the antenna position, compute and set the new rate) at time intervals less than the dynamical response time of the antenna. Thus, the control program must be implemented as a true 'real-time' system. A real-time program is one in which the start and completion times of tasks are predictable, and guaranteed to meet the time requirements of the system.

2 PDP and VAX are trademarks of the Digital Equipment Corporation.

IMPLEMENTATION

Like many real-time systems, the ACC program includes a purpose-built operating system which is more closely coupled to the application software than in general purpose time-sharing systems. Indeed, the ACC program can be considered as a special-purpose operating system, with most modules designed to suit the machine's hardware architecture. The software is written in Digital's MACRO–11 assembly language for the PDP–11 computer family.

STRUCTURE

The ACC software is structured as two sets of periodic tasks and a number of asynchronous tasks. The servo task executes at the highest software priority and is invoked every 100 ms and runs for about 40 ms. Two observing tasks are invoked at different phases of the observation cycle. Typically, this cycle has a 10-s period and is synchronized with the observation cycles in the array control and correlator control computers. The first of these tasks arms various devices in the receiver for the next observation cycle. The second task initiates the reading of all monitor points and computes the new decision levels for the samplers. Asynchronous tasks include maintaining the ACC displays and processing commands received from the keyboard or the array control computer.

TIMING

A time signal generated in the observatory clock is distributed to each antenna. Each ACC has access to this signal through two interfaces: a Frame Grabber and an Event Generator. The Frame Grabber decodes the time from the signal, transfers it into ACC memory by DMA and delivers a hardware interrupt every 100 ms. This is the source of the timing for executing the servo task. The Event Generator drives a 16-bit output word whose state can be programmed to change at moments in the future timed to a precision of 1 μs. Two bits in this word are used to generate hardware interrupts which are used to synchronize the ACC program to the observation cycle.

COMMUNICATIONS

The ACC maintains serial communication links with data sets and the array control computer. Data sets are devices providing a standard interface with the antenna rate controllers and the receivers. Each rate controller has a dedicated data set on its own serial line. All other

control and monitor functions are performed through about 10 data sets which communicate on a single line at 38.4 kbaud. At present, about 400 hardware monitor points are interrogated and the data returned to the array control computer every 10 s. Communications with the array control computer use a simple synchronous protocol in which the array control computer initiates any dialogue. Each reply from the ACC is prefixed with a word indicating the state of vital antenna systems.

ANTENNA MOTION

The ACC reads the antenna position from an encoder on each axis. Each encoder position is read as a 23-bit word through a parallel interface and has a precision of $720°/2^{23}$ or about 0.31 arcsec. The antenna rate controllers are commanded through a 12-bit D/A converter whose least significant bit gives a rate of about 2 arcsec s^{-1}. The ACC servo task executes with a repetition rate of 10 Hz and uses a position control algorithm which allows for two states: slewing and tracking. While slewing, the antenna is moved to the demanded position as quickly as possible within the speed and acceleration limits. While tracking, the new rate x_i for each axis is computed from the current requested rate X_i, position error Δx_i and integral of the position error using the expression

$$x_i = X_i + G\left(\Delta x_i + C_I \sum_{j=0}^{i} \Delta x_j\right)$$

where G and C_I are constants. Here i indexes successive 100-ms time intervals and $i = 0$ labels the first execution of the servo task after a transition from slewing to tracking. The rate expression is computed independently for each axis. In the normalised units used by the ACC software where the time unit is 100 ms, the servo constants have values of $G = 0.1$ and $C_I = 0.04$.

4.2 Array control computer

The array control computer has three broad areas of responsibility:

(i) to perform the ephemeris calculations necessary for the array synchronization once every observation cycle, and dispatch these to the antennas and the correlator;

(ii) to supervise the hardware monitor system;

(iii) to provide the data quality monitoring.

The software is divided into a number of tasks which run as separate processes under the VMS operating system:

CAOBS is the main observing program. It provides the user interface through the console keyboard and through the astronomers' observing schedule files. From the ephemeris and the current array configuration (antenna locations) it computes delays and phases and phase rates for local oscillators and samplers. These calculations are performed once every observation cycle and transmitted to the correlator and antenna control computers.

ARRAY provides the communications link to the antenna control computers. It forwards commands from CAOBS to the antennas and receives and returns the ACCs' replies. It is also responsible for maintaining the list of monitor data available from each antenna. Each observation cycle, it requests these data and stores them in an area of memory which is shared with other processes.

CHECKER processes the monitor data received by ARRAY. It checks for data out of range, issuing warnings or alarms when fault conditions are detected. (Conditions which risk the safety of the array are monitored by a separate hardware system described elsewhere [3].) It also archives monitor data on disk for later analysis.

CAVIS provides a display of the complex visibilities. Every observation cycle, the correlator software computes a single complex visibility for each correlated product (this is a vector average over a selectable range of frequency channels) and transmits them to the array control computer. CAVIS uses a colour monitor to display the visibilities in a number of ways, providing the astronomer with a good indication of data quality.

5 LESSONS

The present system represents our thinking and policies dating from the mid-eighties when we started serious planning and development. Our needs and approach have evolved as has (much more dramatically) the computing scene. We are therefore now in the process of change. In the original development, each of the functional groups described in the architecture section above had a distinct software group. We found it a significant convenience that each group had a 'stand-alone' machine.

In spite of the convenience of separate development groups, the first years of operation have highlighted several shortcomings in the original system design.

5.1 Antenna control

The original design included two computers in each antenna. They were called the Position Control Computer (PCC) and Antenna Control Computer (ACC). The PCC was responsible for controlling the antenna rates so as to maintain the position demanded by the ACC. A number of difficulties arose from the ACC/PCC system.

PCC

(i) The PCC hardware was cumbersome in its design. It was fragile, and the microprocessor and some interface cards are no longer supported by their manufacturer.

(ii) The software was written in Pascal and was cumbersome to modify and maintain.

ACC

The ACC software was written in Pascal and ran under the Micropower/Pascal operating system. Communication between ACCs and the array control computer used the DECNET[3] protocol.

(i) The Micropower operating system was expensive in computing time. It was suspected of containing errors. Of particular concern was the lack of guaranteed future support for the Micropower DECNET interface.

(ii) The communications process on the array control computer which used DECNET as the link to the antennas was unable to survive loss of communications from an ACC.

In spite of these shortcomings, the Compact Array operated for two years with only mild inconvenience to astronomers. However, as the PCCs became increasingly difficult to maintain, and increased demands were placed on the ACC computing power from new modes of operation, it was decided to redesign the antenna control system. The crucial changes in design which have led to the present system were to:

(i) abandon the PCC, transferring its responsibilities to the ACC;

(ii) rewrite the ACC software as a true real-time system, thus avoiding the difficulties with the Micropower/Pascal operating system;

(iii) replace the DECNET protocol with a simpler one using only low-level calls to the VMS terminal driver on the array control computer and the new purpose written communications package in the ACC.

5.2 Array and correlator control

Many of the remaining operational difficulties arise from the communications between the array and correlator computers and from the relatively low processing power of the Micro-VAX. Now that the bulk of the development problems have been resolved we believe that combining the functions of both computers in a single more powerful machine would improve the Compact Array performance.

3 Micropower/Pascal and DECNET are a trademark of the Digital Equipment Corporation.

6 CONCLUSION

It is rather remarkable that the system works at all: the original architects are no longer with the project; the present team took over after the major decisions were effectively cast in concrete, but before any components were available for testing. The work of three of the groups has been deprecated. (Indeed, in two cases, discarded). Yet the software has always been in place, and working, before the hardware became available.

7 REFERENCES

1. Wilson, W.E. and Willing, M.W., "The Sampling and Data Synchronization Systems", JEEEA, 1992, this issue.

2. Wilson,W.E, Davis, E.R., Loone, D.G. and Brown, D.R., "The Correlator", JEEEA, 1992, this issue.

3. Hall, P.J., Kesteven, M.J., Beresford, R.J., Ferris, R.H., and Loone, D.G., "Monitoring and Protection Strategies for the Compact Array", JEEEA, 1992, this issue

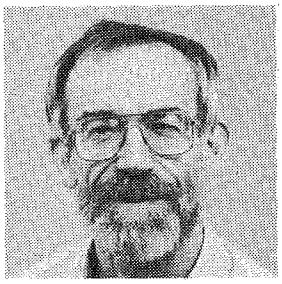

DR M.J. KESTEVEN

Dr Michael Kesteven was educated at Lycée Chateaubriand from which he graduated with Brevet d'Etudes du premier cycle du second degré, department de l'Isère. He is a graduate (in physics) of the University of Sydney (1963), and received his PhD in radio astronomy from the same university in 1968. He joined the Australia Telescope project in 1983. His professional interests include supernova remnants, radio source variability, interferometry and the problems of antenna metrology. In 1986 he was appointed head of the Computer Group at the Division of Radiophysics at Epping. He moved to the Australia Telescope's Paul Wild Observatory, Narrabri in April 1988.

DR D. McCONNELL

Dr David McConnell graduated from the University of Tasmania with a BSc in 1978 and a PhD (Physics) in 1981. He worked as a Research Fellow at the University of Maryland, USA, from 1981 - 1983, and at the University of Tasmania from 1986 - 1990. He spent three years with the CSIRO Division of Radiophysics at Parkes and at present is a member of the Software and Operations group of the Australia Telescope National Facility at its Paul Wild Observatory, Narrabri. His specialties are software for radio-telescope control and pulsar radio astronomy.

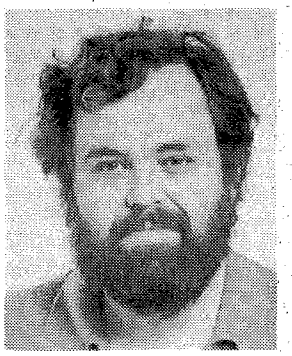

MR J.F. DEANE

John Deane received a BA in mathematics at Macquarie University in 1970. He worked for Tooth & Co. from 1972 to 1974 as a commercial programmer. He joined the Division of Radiophysics in 1974 as a programmer/operator for the Digital Equipment PDP-15. He has worked on projects for the Narrabri radioheliograph, the Epping 4-m telescope, the two-element synthesis telescope (TEST), and the Parkes 64-m telescope. He has co-written two computing books for Dick Smith Electronics. He joined the Australia Telescope project in 1985 and participated in the design, purchase and programming of the first version of the antenna control computers. He joined the Wireless LAN project in 1991.

Data Reduction and Image Processing

R.P. Norris*, M.J. Kesteven** and M.R. Calabretta*

SUMMARY We describe the systems used to process and calibrate the data from the Australia Telescope, starting with the data transfer from the Telescope and ending with the imaging and visualisation software. We also describe the continuing development of a specialised visualisation system, which allows astronomers to view cubes of data as three-dimensional objects.

1 INTRODUCTION

There is a very literal sense in which the six antennas which make up the Australia Telescope (AT) Compact Array at Narrabri corresponds to the objective lens of an optical telescope. In this analogy, the eyepiece of the telescope corresponds to the computers which use sophisticated algorithms to produce images from the recorded data. The principles behind this operation will not be discussed here since they are widely available elsewhere (e.g. see [1]).

Instead we describe the computing system which is used to produce images from the raw visibility data recorded from the correlator. We start with the format of raw data from the on-line system, and follow the computing process through to the production of images. Finally, we describe our plans for future developments.

2 DATA TRANSFER

The AT can produce a maximum of 65 kbyte/s, amounting to 6 Gbyte/day. At this data rate, archiving and storing the data becomes a major task. We have adopted 2.2-Gbyte Exabyte tapes as our standard data transport and archive medium, although 9-track tapes are also available. DAT (Digital Audio Tape) tapes were rejected as being neither standardised nor readily available in Australia at the time of starting AT operations.

An international format for the interchange of astronomical data (FITS, for Flexible Image Transport System) has long since been adopted by the astronomical community [2]. However, it is unsuitable for real-time use because of a number of factors:

(i) FITS is fragile to tape errors, because there is no built-in redundancy or error-checking;

(ii) the FITS standard requires the quantity of data to be specified in advance, which is inappropriate for a real-time system where an observation may be terminated prematurely for a number of reasons;

(iii) the FITS standard cannot cope easily with the AT's flexible observing modes, such as recording different numbers of spectral channels on different IFs.

For these reasons, we have adopted a data format, which we call RPFITS, which resembles FITS but has been modified to overcome these disadvantages.

An RPFITS data file, shown schematically in Fig. 1, consists of a number of headers, each of which is written by the on-line software at the start of each scan[1], interspersed by blocks of data. After each integration the on-line software writes out a visibility record for each baseline and each IF observed. These visibility records are logical, rather than physical, and of variable length.

* Australia Telescope National Facility, CSIRO, PO Box 76, Epping NSW 2121, Australia.
** Australia Telescope National Facility, CSIRO, PO box 94, Narrabri NSW 2390, Australia.
Submitted to The Institution of Radio and Electronics Engineers Australia in June 1992.

1 A scan normally consists of an observation of one source, or group of sources, over a period of, typically, tens of minutes. Each scan then consists of a number of integrations, each lasting for 5 to 15 seconds.

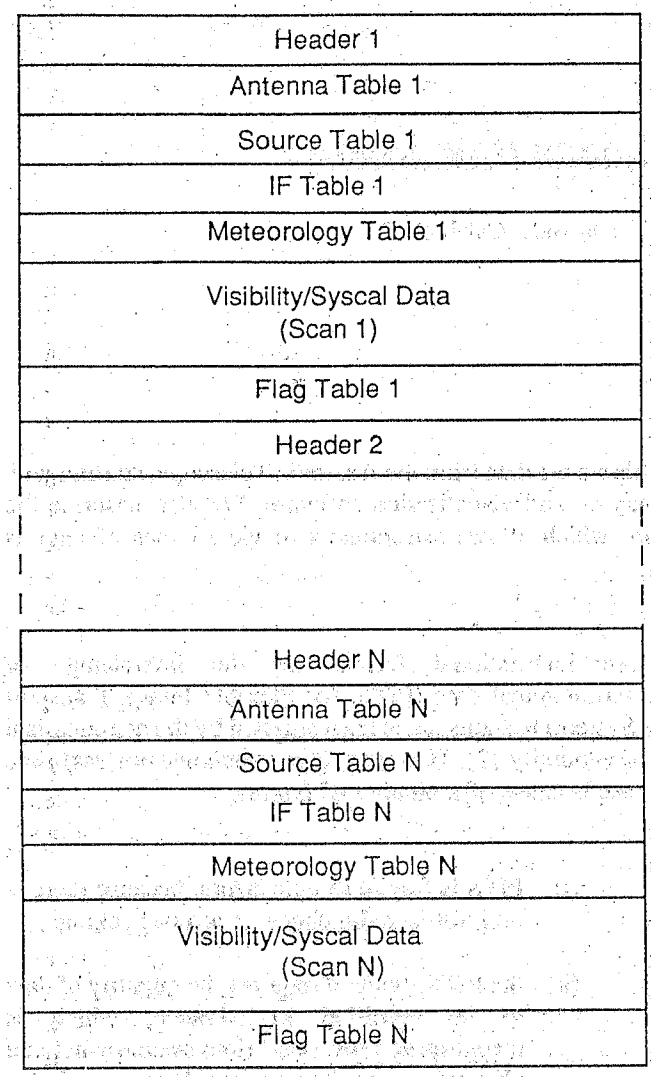

Figure 1 Structure of a typical RPFITS file. Each scan lasts typically 10-30 minutes and contains a number of visibility records and system calibration records.

The structure of a visibility record consists of a small number of header parameters, including one which gives the record length, followed by the visibility data on that baseline. A typical visibility record is shown in Fig. 2. Interspersed between these visibility records are special records which contain system calibration data such as system temperature and measured X-Y complex gain. These records have a similar structure to visibility records, and are also of variable length.

As well as headers and data records, the file can also contain a number of tables. These are used to carry additional data which change infrequently, such as antenna locations, meteorological data, or flagging information to indicate blocks of bad data. Each table can occur either immediately before or immediately after a header.

The file obtains its robustness from the redundancy inherent in the fact that header and table information are repeated on each scan. Thus bad physical media will generally result in the loss of only one scan, since the software used to read the data can recover easily after a data error by searching for the next header. In many cases, recovery can be effected even within a scan by searching for the start of a new record.

The RPFITS code and libraries, along with other VMS-based code, are maintained using the DEC Code Management System (CMS), which allows a rigorous check-in and check-out facility. Such a system is important when several programmers are working on a piece of code simultaneously. We maintain the code across the three sites (Narrabri, Parkes and Marsfield) by having the CMS library at only one site, and insisting that maintenance at other sites be done by checking the code across the DECNET links from the master site. We have found such a code management system to be a valuable tool, although the particular system we have adopted is by no means ideal.

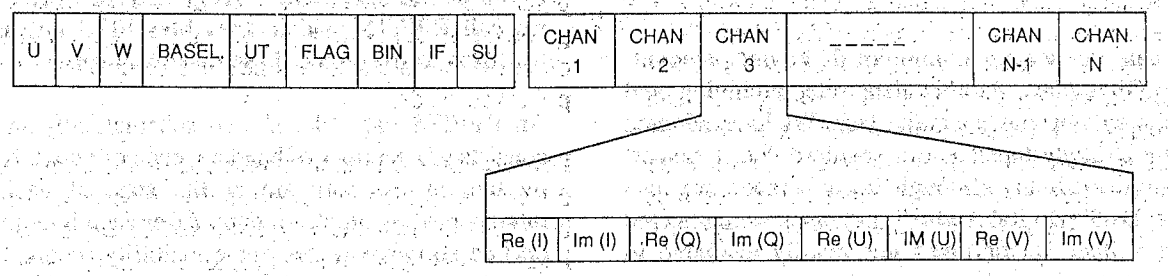

Figure 2 Structure of a typical RPFITS record. The first nine parameters identify the visibility group. One, the IF parameter, points to an entry in the IF table giving the number of Stokes parameters, spectral channels, etc. and thus defines the length of the record. The rest of the record contains the channels, each of which contains up to four complex visibilities, one for each polarization product. Other parameters give the baseline coordinates (u,v,w) in metres; a baseline number, a UT in seconds, a flag to indicate bad data, a bin number (for pulsar observations), an IF number, and a source number. Special system calibration records have a similar structure.

3 IMAGING

Early in the construction of the AT, human resource constraints forbade the construction of a new imaging package. After several packages had been reviewed we decided to use the AIPS (Astronomical Image Processing System) package, written and distributed by the NRAO (National Radio Astronomy Observatory, US) [3]. The package was written primarily for the VLA (Very Large Array), but only a small amount of additional software needed to be written to make it suitable for the AT.

Since then, Australia Telescope National Facility (ATNF) staff have added to and developed AIPS for AT use, and many ATNF enhancements have been added to the standard worldwide AIPS distribution from NRAO. Also, the way the ATNF manages AIPS differs from standard NRAO practice in several respects [4] as follows:

(i) AIPS is run from users' own accounts rather than from communal AIPS accounts;

(ii) various enhancements have been made to allow flexible access to network resources such as image display devices, bookable data disks, and tapes;

(iii) a locally developed code management system allows us to develop our implementation of AIPS while allowing efficient integration into new AIPS releases;

(iv) the AIPS system was restructured to adapt it to an environment consisting of many hosts of several architectures, without duplicating the source code.

To load AT data into AIPS, we use a task called ATLOD. As well as reading the RPFITS file and loading the data into AIPS, this task also contains a number of other AT-specific functions, such as using the on-line X-Y phase measurement to correct or flag data. Such functions have to be done in ATLOD because AIPS has no facilities for storing such parameters along with data files. Similarly, AT observations which have different numbers of spectral channels on different IFs must be converted to different AIPS files, since AIPS assumes that all IFs in a file have the same number of spectral channels.

4 AT OBSERVING MODES

In contrast to some earlier instruments such as the VLA, all observations on the AT are made in a 'spectral-line mode', in which several frequency channels are recorded rather than one continuum channel. This is a consequence of the AT design specification for wide-field imaging with high bandwidth, since using a single continuum channel would result in heavy radial (bandwidth) smearing. The number of channels may range from 32 for a continuum observation, to several thousand for spectral-line observations. Thus AT software must reflect the greater emphasis on multi-channel operation.

However, using several frequency channels also has benefits for even small fields, since the simultaneous measurement over a range of frequencies (up to 256-MHz instantaneous bandwidth) allows simultaneous sampling of a range of spatial frequencies – a technique known as multi-frequency synthesis (MFS; see e.g. [5]). Furthermore, the AT's ability to switch rapidly in frequency over a wide tuning range allows even greater ranges of spatial frequencies to be sampled, provided that spectral index variations of the target source are also modelled. An additional advantage is that narrow-band interference can be removed in subsequent processing.

So far, the use of MFS has been largely restricted to relatively narrow frequency ranges and we have assumed that the spectral index is uniform over the image. However, we plan to implement more sophisticated algorithms which will model spectral-index variations across the image.

Another technique we plan to use on the AT is mosaicing, where structures larger than the antenna primary beam are imaged by measuring visibilities at several different positions on the sky. In this way we can recover lower spatial frequencies than are otherwise available to the interferometer. Extra information at low spatial frequencies will be provided by adding single-dish data.

5 POLARIZATION CALIBRATION

All observations made with the AT are generally made in a mode which allows full recovery of the four Stokes parameters. However, the way the AT calibrates these polarization data differs significantly from that of most other synthesis telescopes because of the AT's linearly polarized feeds.

Polarization calibration makes use of the complex gain difference which is continually measured on line between the two linearly polarized feeds, to calibrate instrumental polarization. Further calibration is provided by observing a calibrator source with known polarization characteristics.

Software for performing this calibration is complex because of the inter-dependencies of the polarization error terms, and requires an iterative approach. Software to do this (written in another imaging package, MIRIAD) is currently in a testing phase, and may be ported to AIPS when complete.

6 HARDWARE

The main off-line computing system for the AT is located at the Marsfield laboratory, although three Sparcstations at Narrabri, and one at Parkes, are also available. Here we will concentrate on the facilities available at Marsfield.

The main computer purchased for AT data reduction is a 50-Mflop Convex C210 supercomputer, which has been upgraded to a 100-Mflop C220 and is now shared with the CSIRO Division of Radiophysics. As well as the Convex C220, the current Marsfield network carries about 40 RISC workstations (mainly Sun Sparcstations), 60 Macintoshes, 80 IBM-compatible PCs, and a number of other machines such as a VAX3400 which is retained for compatibility with the VMS-oriented sites. Seven of the Sparcstations (plus one X-terminal) are available for communal AIPS use, and a further seven are used primarily for AT software development and AIPS processing.

In addition, the network at Marsfield provides facilities such as networked laser printers and a colour printer. The network is organised to provide transparent mail access and flexible file-sharing between architectures, using primarily TCP/IP protocols and NFS services. Multinet is used to connect the VAX to these protocols, Gatorboxes provide connectivity to the Macintosh network, and PC-NFS provide PC connectivity.

In addition to the on-site network, Marsfield also maintains 9600-kbit/s leased line links (currently DECNET, but a change to TCP/IP is being considered) to Parkes and Narrabri, and a dedicated 48-kbit/s line to AARNET and Internet for connections to the outside world.

Experience with data processing so far has shown that the major bottleneck has been disk space rather than processing power. Thus, as well as upgrading the Convex to a total disk space of 11 Gbytes (five of which are available for AIPS data), we have provided a further 6 Gbytes for AIPS data on the Sparcstations, and a number of Exabyte drives to aid rapid data archiving and de-archiving.

The AIPS computing power at Marsfield is roughly equally divided between the central processing of the Convex and the distributed computing available in the workstations. Users are encouraged to do the first, user-intensive, stages of processing (data editing and calibration) on the workstations, and then transfer their data to the Convex for the computer-intensive operations. However, many continuum users find it convenient to do all their processing on the workstations, leaving the Convex available for the heavy spectral-line users.

7 VISUALISATION

Synthesis radio telescopes have, until recently, produced largely two-dimensional images, or a small number of such images stacked together in a 'data cube'. However, the AT will produce data cubes of unprecedented size (up to 2000 x 2000 x 2000 pixels). The astrophysical interpretation of this data requires the user (an astrophysicist) to get an intuitive 'feel' for the data. The present two-dimensional imaging systems, therefore, present a major conceptual barrier, separating user from data. For this reason, we have invested a significant amount of resources (largely funded separately by our Institute of Information, Science & Engineering [IISE]) into a project to explore the application of imaging and visualisation techniques to radio astronomy and other related branches of astrophysics.

Most of this work has been done on a Sun 4/370 equipped with a TAAC visualisation engine, but this has been recently upgraded to a 5-processor 320-Mflop MVX engine.

The project's most dramatic result so far is the display of three-dimensional data cubes. In such cubes, each voxel (the three-dimensional analog of a pixel) is assigned not only a brightness and colour, as in ordinary imaging, but also an opacity. A cube containing AT data on the neutral hydrogen in a galaxy, for example, will then appear as an object sitting in the centre of a transparent cube. By rotating the cube, the resulting visual cues convey to the astronomer far more information than could be conveyed by sequences of two-dimensional planes. An important step in this work was the development of a simple radiative transfer algorithm, which gives a much more 'realistic' impression than the surface-oriented algorithms supplied with standard libraries.

Other developments have explored facilities such as combining two images, using hue and intensity, or superimposing images in different colours.

A small number of spectral-line users have already started using our advanced visualisation facilities. Reactions so far have been very favourable. Some astronomers find that they obtain much more information from their data when viewed as a three-dimensional cube rather than as a movie of two-dimensional planes. It appears that these visualisation techniques allow full use to be made of the pattern recognition capabilities of the human brain, so that structures not seen in two-dimensional movies are immediately apparent in three-dimensional cubes.

Typical of the results is a well-studied, VLA synthesis observation of HI in a galaxy. These data have been used in the past to demonstrate the AIPS function TVMOVIE, which shows the sequence of planes in the data cube as a movie of two-dimensional images. When portrayed as a cube on the visualisation workstation it was immediately apparent that the disc of the galaxy was warped, a fact that had not previously been noticed.

To assist in disseminating these results, equipment is also provided for users to record their results on video tapes.

8 aips++

The AIPS package was developed about 1980. Since then, not only has computer technology changed enormously, but also modern synthesis telescopes such as the AT operate in modes which were unthought of at that time. For this reason, a successor to AIPS needs to be written, and an international collaboration has been formed to do this. The participants include the NRAO, the ATNF, and other participants from the US, the Netherlands, Britain, Canada and India.

The ATNF is contributing a significant amount of resources to this project in the hope that the resulting package, to be available in 1993, will be much better geared to the needs of the AT than AIPS is.

As its name implies, aips++ will be written in the object-oriented language C++, which should allow for easier maintenance, development, and upgrade paths. As well as taking advantage of newer technology, such as graphical user interfaces, massively parallel processors, and open systems standards, the new package will address the AT's need to have, for example, different numbers of channels on different IFs, and to calibrate linearly polarized feeds.

9 CONCLUSION

Off-line computing for the AT has departed a long way from the cluster of VAXes originally envisaged in the early stages of planning the AT, and continues to develop a path designed to take advantage of developing technology. In some cases (e.g. AIPS) we have been able to rely heavily on the work and experience of our predecessors, whilst in others (e.g. visualisation) we find ourselves following untrodden paths and developing new techniques. We aim to retain this flexible approach and to take advantage of technological development. At the same time, we aim to cater for the demands of new techniques that may be pioneered on the AT.

10 ACKNOWLEDGMENTS

We are grateful to Dr. R.H. Wand, under whose leadership the early stages of the design of this system were conceived, and to the late Paul Rayner, who played a major part in those early stages. We are also grateful to Dr. N.E.B. Killeen, Dr. R.J. Sault and Ms. H. May, who are responsible for several of the recent enhancements to the imaging system, and to other members of the computer group without whom the computer system would quickly crumble into chaos.

11 REFERENCES

1. Thompson, A.R., Moran, J.M., and Swenson, G.W., "Interferometry and Synthesis in Radio Astronomy", Wiley, New York, 1986.

2. Grosbol, P., Harten, R.H., Greisen, E.W., and Wells, D.C., "Generalized Extensions and Blocking Factors for FITS", Astron.Astrophys.Suppl.Ser., 73, 359-364, 1988.

3. Greisen, E.G., "The Astronomical Image Processing System", AIPS Memo 61, NRAO, Charlottesville; also in *Acquisition and Analysis of Two-Dimensional Images* ed. Lingo, G., and Schmack., G. (Observatorio di Capodimonte, PG, Napoli, Italy), 1988.

4. Calabretta, M.R., AIPS memo 74, NRAO, Charlottesville, US, 1991.

5. Conway, J.E., Cornwell, T.J., and Wilkinson, P.N., "Multi-Frequency Synthesis: A New Technique in Radio Interferometric Imaging", Mon.Not.R. Astron.Soc., 246, 490-509, 1990.

DR R.P. NORRIS

Dr Ray Norris received the degree of MA from the University of Cambridge in 1975 and a PhD from the University of Manchester (Jodrell Bank) in 1978. He moved to Australia in 1983 to work on the Australia Telescope project and is currently head of computing for the Australia Telescope National Facility and the Division of Radiophysics, CSIRO. He is also active in several programs of astrophysical research. His astrophysical research interests include the development of unified theories of active galaxies and quasars, and the study of interstellar masers and their implications for star formation. His technical research interests include Very Long Baseline Interferometry (VLBI) and the use of advanced visualisation techniques for interpreting astrophysical data.

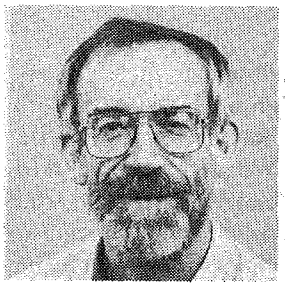

DR M.J. KESTEVEN

Dr Michael Kesteven was educated at Lycée Chateaubriand from which he graduated with Brevet d'Etudes du premier cycle du second degré, department de l'Isère. He is a graduate (in physics) of the University of Sydney (1963), and received his PhD in radio astronomy from the same university in 1968. He joined the Australia Telescope project in 1983. His professional interests include supernova remnants, radio source variability, interferometry and the problems of antenna metrology. In 1986 he was appointed head of the Computer Group at the Division of Radiophysics at Epping. He moved to the Australia Telescope's Paul Wild Observatory, Narrabri in April 1988.

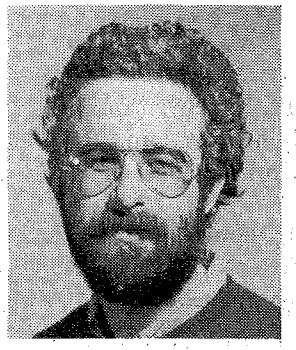

DR M.R. CALABRETTA

Dr Mark Calabretta received the degrees of BSc, PhD from the University of Sydney in 1978 and 1985 respectively. He joined the CSIRO Division of Radiophysics in 1985 to work on AT off-line software as programmer and manager of the Astronomical Image Processing System (AIPS). His contributions to AIPS include specialised software. He designed and implemented a software system for calibrating the single-dish pointing of the Australia Telescope antennas. He began work in mid-1991 on the design of AIPS++, the successor to AIPS, particularly in the area of system management and source code distribution. He spent the first half of 1992 working on the fundamental design with an international group of programmers gathered at the National Radio Astronomy Observatory, Charlottesville, USA.

Journal of Electrical and Electronics Engineering, Australia
Special Issue

THE AUSTRALIA TELESCOPE

Chapter 4

Operations

Monitoring and Protection Strategies for the Compact Array

P.J. Hall*, M.J. Kesteven*, R.J. Beresford*, R.H. Ferris** and D.G. Loone*

SUMMARY The Australia Telescope Compact Array consists of six 22-m antennas located on a 6-km East-West baseline. The geographical diversity of the array, the complexity of the antenna systems, and the vulnerability of the Observatory to damage from storms for example, makes effective monitoring and protection essential. We have implemented two monitoring, alarm and control systems which overlap in function. A hardware-based system examines a relatively small number of very important Telescope and environmental status inputs. A second system based on a minicomputer network acquires, checks and archives data from a much larger number of sensors. Our approach has enabled us to implement a relatively low-cost computer network and to proceed with complex software engineering tasks, including the current development of expert-system fault-diagnosis software, while being satisfied that the Telescope remains well protected. This paper describes the Telescope monitoring and protection schemes and discusses briefly the expected capabilities of the new expert system.

1 INTRODUCTION

In terms of engineering complexity the Australia Telescope (AT) Compact Array (CA) is comparable to many contemporary medium-scale industrial facilities. Unlike most such facilities however, the Telescope has only a few individuals allocated specifically to its operation and maintenance. Virtually all professional personnel have scientific research or engineering development roles in addition to their Telescope support responsibilities. The maintenance burden is increased by the physically distributed nature of the array, making an extensive computer monitoring capability essential if support for the instrument is to be feasible with the resources available. Furthermore, there are important additional requirements relating to the safe operation of the Telescope to be considered. It has proved convenient to address both the monitoring and protection strategies simultaneously.

We identify three main reasons for developing comprehensive monitoring and protection schemes. First, instrument safety is of major concern. There is a clear need to ensure the safety of the antennas and major sub-systems (e.g. cryogenics). The safety demands are high since the Australia Telescope National Facility's (ATNF) operational goal is unattended astronomical observing. Engineering-maintenance concerns provide a second strong motivation to implement an extensive monitoring system. The aim is to detect actual or incipient faults in the Telescope using both passive (alarm) and active (probing) modes. The intention is to allow non-specialist technicians to diagnose problems and maintain the instrument. Finally, the extensive Telescope monitoring allows a broad, real-time, quality assessment of astronomical data to be made. On the whole, a synthesis telescope such as the Compact Array has many graceful (partial) failure modes; we aim to correct or flag sub-standard data resulting from system problems.

Our approach has been to incorporate simple self-protection schemes into as many Telescope sub-systems as possible, with the intention of avoiding actual damage due to gross failures. We have also implemented two array-wide, partially redundant, monitoring, checking and alarm systems. One system is based on hardware while the other uses distributed minicomputers. In most other radio telescopes monitoring and protection have been added as something of an afterthought. Typically, computer or closed-circuit television surveillance of a fairly small number of points is used, together with a basic hardware protection scheme incorporating devices such as high wind and smoke detectors. In some instruments computer-initiated antenna stowing (parking) is also performed under some conditions (e.g. high wind) [1]. Before describing the two CA systems, we first review the areas of the Telescope which are most prone to damage, and discuss briefly the first-level protection strategies adopted.

* Australia Telescope National Facility, CSIRO, PO Box 94, Narrabri NSW 2390, Australia.
** Australia Telescope National Facility, CSIRO, PO Box 76, Epping NSW 2121, Australia.
Submitted to The Institution of Radio and Electronics Engineers Australia in June 1992.

2 FIRST-LEVEL PROTECTION

We identify four particularly vulnerable areas of the Compact Array:

(i) structures

(ii) power systems

(iii) signal distribution and data communications network

(iv) cryogenic refrigerators.

Damage or malfunction in any of these areas has the potential to be especially expensive and disruptive to Telescope operation. At the top level of protection, all physically separate parts of the instrument (including the individual antennas) have self-contained fire-alarm and protection controllers fitted. As well as reporting to the hardware monitoring system described in Section 4, the controllers respond to smoke and over-temperature alarms in a given area by removing power from that zone.

The most important Compact Array structures - the six 22-m antennas - are designed to withstand winds of up to 170 km hr^{-1} when in the upright (or stowed) position. Normal observations cease with winds greater than 40 km hr^{-1} and, in practice, the systems described in the next section ensure that the antennas are stowed under these conditions. In an attempt to anticipate the destructive high winds associated with thunderstorm cells, a thunderstorm early-warning device has been incorporated into the hardware monitoring system. These cells pose a real risk. Storms in recent years have resulted in wind speeds of more than 160 km hr^{-1}. To minimise the possibility of lightning damage the antenna structures are maintained at ground potential and have lightning arrestors fitted.

Apart from weather-related damage, the antennas are vulnerable to damage from collisions, either between a reflector and its support structure, or between individual antennas on the 3-km rail track during a 'long-travel' (re-positioning) operation. A series of software and hardware interlocks and limit switches, including a hardware 'watchdog' activated by failure of the servo-control computer, prevents the first type of accident. Soon, proximity sensors designed to stop antenna-antenna collisions during array re-configurations will be installed. At present, guaranteeing the driver an excellent forward view and using a long-travel drive system requiring a continuous 'drive' command reduces the risks to an acceptable level.

The Telescope signal distribution and data communications network is implemented using a combination of optical fibre, coaxial cable and multi-pair cables. The network is largely underground, emerging at antenna station posts, the control building and, in some cases, other Observatory buildings. The optical fibres carry astronomy data and computer communications and are of course largely immune to electrical transient damage. The fibres are separated from other cabling to prevent damage due to heating from catastrophically impaired copper conductors. Site coaxial cables are bonded to safety grounds at many points and according to Boyce [2], lightning-induced transients in such lines rarely exceed 250V, a value which can be dealt with using commercial coaxial transient suppressors.

We consider the shielded multi-pair cables to be at the greatest risk since, although grounding is still thorough, the network extends widely over the Observatory site and there are substantial unshielded sections around buildings. These cables carry signals such as telephone, digital intercom, fire-alarm and hardware monitoring. In our protection scheme each pair is protected using a succession of gas arrestors (600V flash point), metal oxide varistors (50V) and appropriately rated solid-state transient suppressors (Transorbs). The protection devices have been placed at all vulnerable points, and the distance between the protection stages chosen to make best use of cable impedance in the surge-limiting process.

Power distribution to the CA site is underground and conventional, with a 22-kV primary feed and several 415V distribution networks. Gas arrestors at each end of the 22-kV underground cables protect the 22-kV transformers from catastrophic damage while individual Observatory switchboards (including those at the six antennas) are fitted with high-energy metal-oxide varistors rated at 275V rms per phase. Critical systems (including computers) in both the Control Building and the antennas are powered from uninterruptible power supplies (UPSs), minimising observing time and monitoring down-time due to mains outages and other disturbances. As well as its 10-kVA UPS, each antenna is equipped with a 105-kVA diesel generator, allowing complete independence from the council mains for up to 24 hours. Power cycling between mains, UPS and genset is entirely automatic.

The control building UPS is a 100-kVA type manufactured by Thycon Systems (Australia). The unit is monitored comprehensively using a VAX-based software package (developed by the ATNF) in conjunction with the supplied user interface. In the future an 800-kVA genset will be added to extend the existing 20-min backup offered by the UPS. In the interim, a few very important Observatory systems — including the hardware monitoring described in the next section — have dedicated battery supplies, giving an endurance extension of several hours in the event of complete power failure.

The Compact Array is unique in Australia in having a number of closed-cycle cryogenic refrigerators operating continuously. At present, there are 12 refrigerators cooling the Telescope's low-noise receivers to

temperatures below 20 K. The main components of the units are supplied by Cryogenic Technology Inc. and the overall investment is of the order of $1m. The two major items in the refrigerators are the helium gas compressor and the cryodyne. The compressors in the Compact Array are well protected using standard over-temperature trip sensors, but considerable development was needed to give the cryodynes adequate protection. The most common cryodyne failure mechanism is initiated by inadequate lubrication due to failure of the fluid (helium) flow, perhaps as the result of compressor failure. To prevent such damage, electronic protection modules have been developed which shut down the cryodyne when in-line sensors detect low helium pressure. With approximately 15,000 hours of operation, two of these modules have tripped and we anticipate achieving or exceeding the maximum specified lifetime (80,000 hours before major overhaul) for all cryodynes.

3 THE TWO MONITORING SYSTEMS

Each of the Compact Array antennas is equipped with a PDP11/73 antenna control computer (ACC). The ACCs are networked, using a specially developed protocol, to a central VAX array control computer. Each ACC addresses about 500 monitor and control points spread over many antenna electronic, electrical and mechanical systems. Time-tagged antenna monitor data are placed in a common memory area in the central VAX, allowing convenient data sharing between several software tasks (e.g. display and checking programs). The extensive computer-based monitoring allows convenient and, indeed, partially automatic, engineering assessment of incipient and actual Telescope problems. Furthermore, continuous checks of major instrument parameters, such as receiver equivalent noise temperatures, are made and the results logged as part of the astronomical data records.

Notwithstanding the advantages of the computer monitoring system, experience has shown that distributed computing systems are disrupted occasionally for a variety of reasons. The Compact Array network is vulnerable in at least three areas, all of which result from compromises made on economic grounds. First, it has not been possible to dedicate one central computer to collect and check monitor data. In a research environment, fairly frequent software and hardware upgrades to the central computer system are not uncommon; sometimes these changes disrupt the network. Second, the network nodes are vulnerable to power disruption, perhaps due to electrical storms. Although the various UPS/diesel genset combinations in the array minimise such disruption, the fact remains that the computer network could be disrupted at the very times monitoring and control are needed most. Finally, the trade-offs made between network cost, network protocol and information transfer rate mean that very occasional dropouts can be expected.

In an attempt to minimise the possibility of Telescope damage during computer network outages, we have adopted the strategy of implementing a parallel, yet independent, monitoring and control system. This 'primary' monitoring is hardware-based and examines and controls a much smaller range of sub-systems than the computer or 'secondary' monitoring. It is, however, designed to be more robust in the face of power and other disruptions.

In practice, the primary and secondary monitoring systems are linked during normal Telescope operation (Fig. 1), effectively expanding the capability of the computer-based system and allowing it to dictate alarm response strategies. If the computer network is disrupted or if the antennas fail to respond to computer requests, the primary monitoring and control system continues to function and is, if necessary, able to drive the Compact Array antennas to the elevation stow position. In our implementation this control function is invoked as a last resort. However, the alarm distribution function of the primary monitoring system is always active and serves to alert operational and engineering staff and, outside normal working hours, on-call personnel, to serious system problems. Less serious anomalies are reported as terminal broadcasts from the computer-based monitoring system.

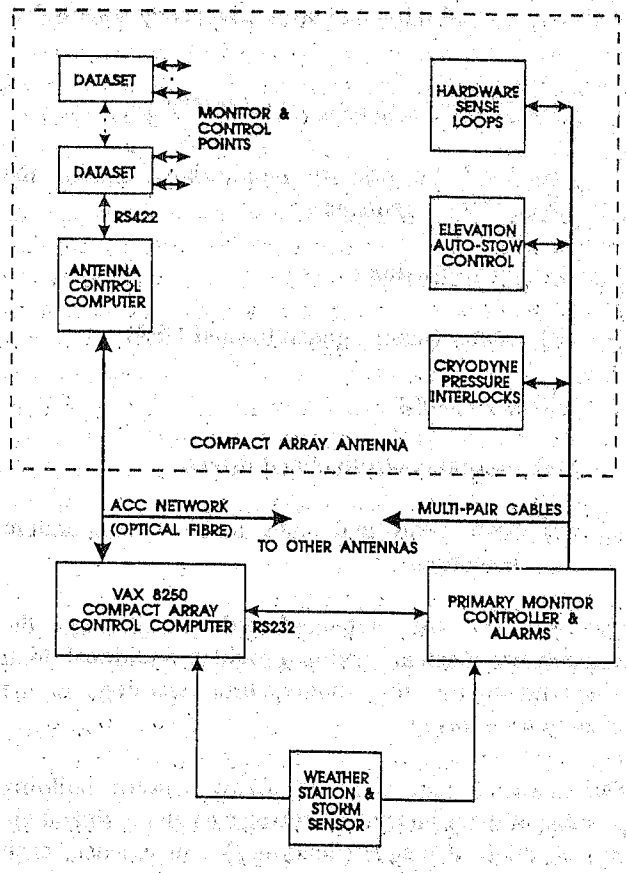

Figure 1 Block diagram showing the main elements of the Compact Array primary and secondary monitoring and the interaction between the two system.

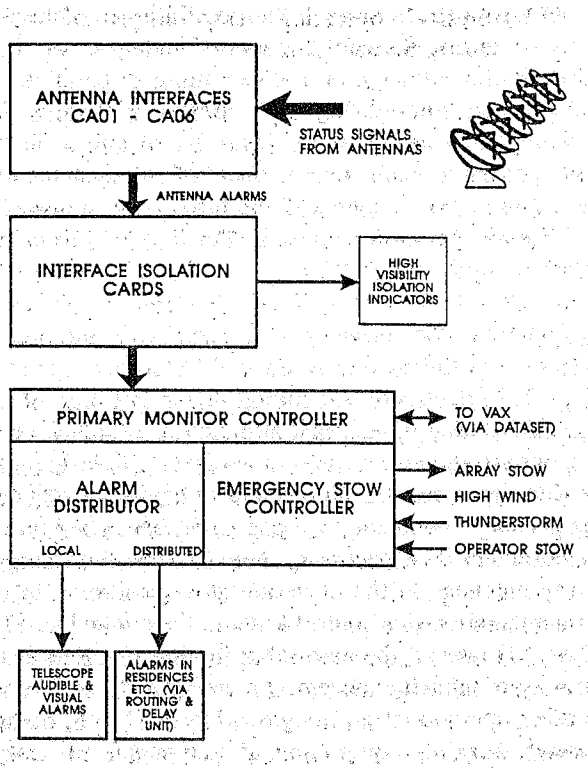

Figure 2 Block diagram of the primary monitoring system. The controller is the heart of the system and handles overall alarm generation, alarm distribution, computer communication and array emergency stow tasks.

4 PRIMARY MONITORING SYSTEM

The scope of the primary monitoring includes the following antenna systems:

(i) fire detection

(ii) power (mains, generator and UPS)

(iii) cryogenics

(iv) motion controllers and drives

(v) high wind and high ambient temperature detection.

As well as the antenna-based monitoring, the Observatory weather station provides additional high wind and approaching thunderstorm warnings to the primary monitoring.

The antennas and Compact Array control building portions of the primary monitoring system are linked via buried, shielded cables (Section 2). In essence, each primary monitor sense loop is a simple, normally closed, circuit completed by the sensors at the antennas. The monitoring system is modular and it is possible to isolate an antenna during, for example, antenna re-positioning (when the sense loops are opened intentionally).

Figure 2 gives an overview of the primary monitoring system. The four main functional modules are:

(i) the interface to the antenna sensors

(ii) the interface isolation cards

(iii) the primary monitoring controller

(iv) the antenna autostow controllers.

The first three modules are located in the control building and there is one autostow controller associated with the elevation-axis motion controller in each of the six antennas.

The antenna interfaces receive and display, on an LED matrix, information from sensors located in the antennas. The interfaces also generate alarm signals based on abnormal antenna status conditions. These alarms are passed, via the alarm isolation modules, to the primary monitoring controller. The controller has three functions:

(i) to generate a sequence of audible and visible alarms based on alarm signals from the antenna interfaces, the weather station and the storm warning system.

(ii) to provide two-way communication with the Observatory VAX array control computer;

(iii) to request the VAX and antenna control computers to stow the CA in the event of high winds or nearby thunderstorms and, in the event of computer failure, to command the autostow controllers at the antennas to initiate a hardware stow of the array.

By the time practical considerations such as sequencing delays and multiple-path decision making are accounted for, the resulting primary monitoring and autostow controllers are rather complex if implemented using conventional hardware. However, we consider that formal hardware design methodology has reliability advantages over alternative software-based realisations.

Using a modern digital systems approach, it has been possible to retain both reliability and flexibility in the controllers. Synchronous, state-machine design formalism has been used, and the resulting 'one-hot' controllers [3] implemented with programmable logic technologies rather than microprocessors. This method of implementation provides excellent matching of the circuit topology to the control algorithm, high flexibility, and predictable operation. While conventional CMOS PROMs form the basis of the autostow controllers, the primary monitoring controller is realised using the new Xilinx range of application-specific integrated circuits (ASICs). These devices are configured at power-up from a conventional PROM, allowing easy firmware revision.

The Observatory weather station is interfaced to both the primary and secondary monitoring systems. Much of the weather station is as described by Hall [4]. The most novel aspect is the incorporation of a 3-M WX120 Stormscope to predict and plot the paths of approaching thunderstorm cells. This instrument uses a very low frequency (50 kHz) receiver followed by digital signal processing stages to provide displays and warnings. After experimenting with sophisicated personal computer-based data-acquisition methods, we have settled on a simple Stormscope alarm, derived on the basis of a pre-set discharge rate within a 45-km guard radius, as the most appropriate input to the primary monitoring system.

Special care has been taken to provide back-up power for the primary monitoring system and weather station, with the main supplies being derived from standby batteries float-charged across a UPS-derived source. As well, continuous operational self-checking is a feature of the primary monitoring controller. In anticipation of potential power transients around the Observatory, the whole system is designed to provide multiple auto-reset and re-close operations in an attempt to allow the maximum possible opportunity for successful emergency stowing.

5 SECONDARY (VAX) MONITORING

The computer-based secondary monitoring system provides astronomers and engineers with a comprehensive Telescope performance and diagnostic facility. Importantly, it also supports data archiving, allowing long-term trends to be analysed and perhaps used in identifying signatures of actual or incipient faults. To date, most of the monitor points examined have been those provided in the original design of AT antenna-based systems. However, the secondary monitoring has proved so useful that it is being expanded to encompass areas such as antenna and control-building air-conditioning plants and switchboards.

The 500 or so monitor points per antenna currently yield quantities such as:

(i) antenna azimuth and elevation together with critical servo-loop performance parameters such as drive motor currents and position errors;

(ii) operating temperatures and bias currents of the cryogenically cooled low-noise amplifiers;

(iii) supply and return gas pressures in the cryogenic refrigerators;

(iv) voltages or status flags at critical monitor points within local oscillator, conversion chain and signal transmission modules;

(v) physical operating temperatures of many electronic modules;

(vi) important Telescope parameters such as receiver equivalent noise temperatures.

As well as these antenna-based inputs, the secondary monitoring system also accepts data from the Observatory weather station, the primary monitoring system and the main Compact Array observing software package, CAOBS.

The AT 'Data-sets' [5] are central to the operation of the computer monitoring. These devices allow each antenna control computer to address and control various points in the antenna via a few medium-speed (38.4 kb s^{-1}) RS422 serial busses. Monitor points may be either digital or analog (12-bit resolution) with general-purpose points being examined with a typical time resolution of 30 s; more critical points are measured once per telescope integration cycle (currently 10 s). Time-tagged monitor data from the individual ACCs are transferred to the central VAX array control computer (running the VMS operating system) via a 9.6 kb s^{-1} serial network which uses an efficient protocol developed by the ATNF. After some pre-processing, data are placed in a large common area of VAX memory, allowing several display and checking programs to have simultaneous access to data. This central data pool, therefore, permits astronomers and engineers to make use of the data for various purposes.

Details of the data analysis and display options have been described by Gough and Kesteven [6]. Figure 3, extracted from that paper, shows the interaction of the various software processes. The CHECKINI and CHECKER packages allow limits to be specified for each monitor point and incoming data to be tested for acceptability. The CHECKER program also writes data to disk storage from where it is archived periodically to Exabyte video cassette media. The XARCHIVE and CASUM programs allow current disk data (or restored archive data) to be examined and plotted, or the array faults to be summarised.

The CAMON package is the one by which most astronomers and engineers routinely access the monitoring database. It displays data on VT220-compatible terminals in page format, with individual users able to define custom pages if they wish. Readings and status flags for monitor points in error are highlighted in reverse video, and terminal audio warnings generated. For convenience, CAMON also has an 'error' page where all array monitor points generating abnormal readings are summarised. Although using terminals rather than, say, workstations, places some limits on display sophistication, we have found that this is compensated for by the flexibility of the simpler display. For example, Observatory staff are able to provide dial-up support from home using only modems and terminals or personal computers. Nonetheless, we recognise the potential of more sophisticated analysis

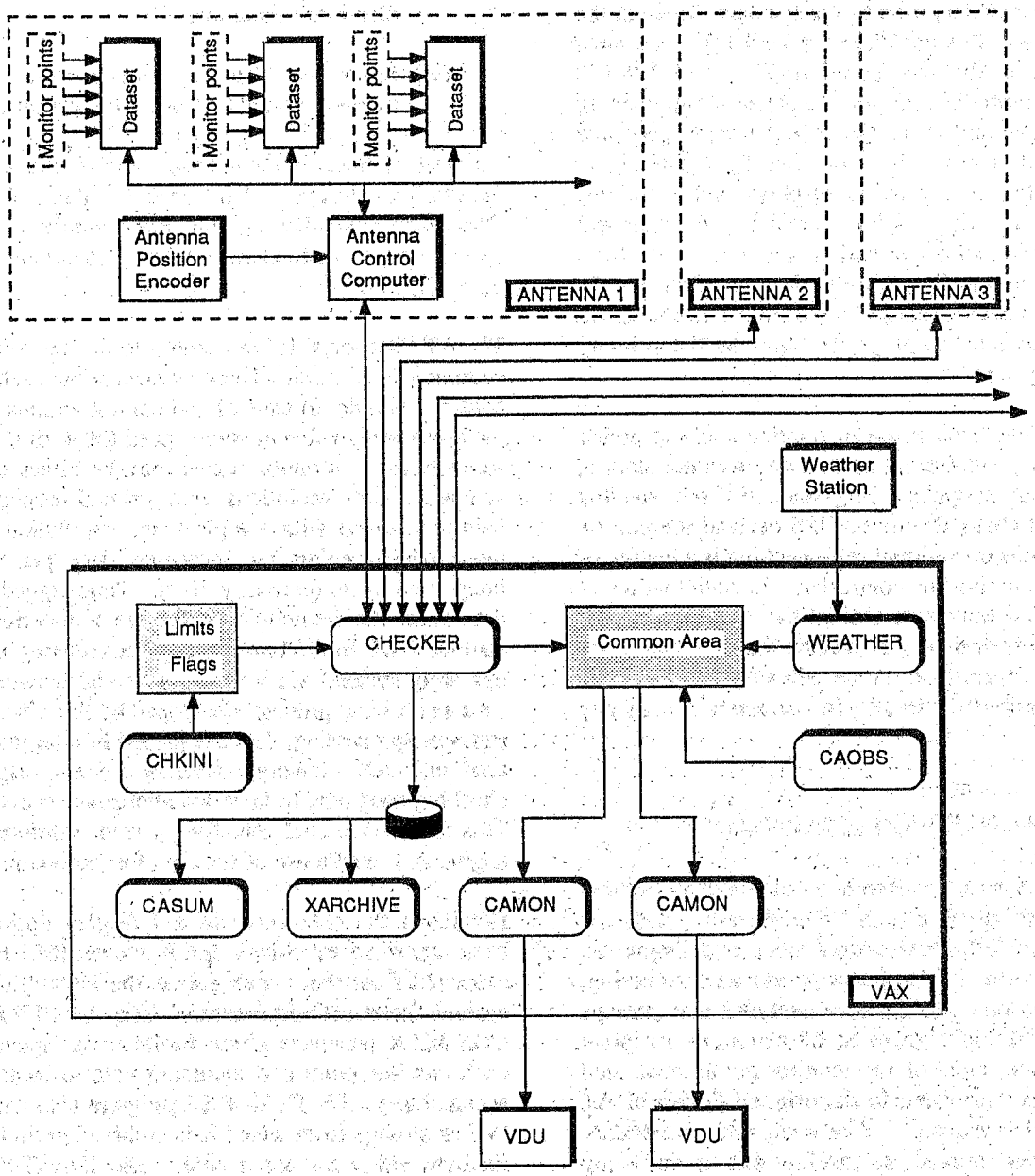

Figure 3 Diagram showing the operation of the secondary or computer monitoring system. The main user interface program, CAMON, can be executed simultaneously by a number of users.

and display software and, with the support of the CSIRO Institute of Information Science and Engineering (of which the ATNF is a part), a trial expert-system software package is currently being developed.

6 EXPERT SYSTEM

Our development in this area has two main objectives:

(i) to provide non-specialist astronomers, engineers and technicians with the means to assess Telescope performance and repair instrument faults;

(ii) to demonstrate the potential of modern expert system techniques in a medium-scale scientific or industrial complex.

The Compact Array monitor database provides an ideal foundation for an expert system. However, we recognise that there are many practical difficulties involved in developing a useful product, not the least of which involves convincing the human experts in the many diverse sub-systems to produce documentation to the level of diagnostic decision algorithms.

Work on the expert system began in mid-1991 and it is expected that an experimental version will be operational by the end of 1992 [R. Landau, private communication].

This should provide at least engineering-level assistance in major areas such as receivers and drives. A hierarchical pictorial (mimic) display of the Telescope is also planned, allowing users to select, from the top down, the level of complexity in displaying the monitor data. The expert system will reside on a DEC VAX7600 workstation with multiple-user access.

7 CONCLUSION

We have outlined the strategies adopted to monitor and protect a major national astronomical facility. Remote or unattended observing is currently being tested and indications are that the monitor systems allow safe operation in these modes. Furthermore, both monitoring systems are already proving invaluable in the timely diagnosis of instrument problems, with telescope down-time due to hardware failure reduced to about 2% of scheduled observing time.

We are adapting the hardware and software developed for the Compact Array to the monitoring and protection of the Australia Telescope 22-m antenna located at Mopra, near Coonabarabran. During normal operation, a low-speed data link between computers at Narrabri and Mopra will allow the two instruments to be monitored and controlled simultaneously. At this stage it is likely that a simple telephone link will be used but satellite and radio links are also being considered. Regardless of the link type however, our plan is to provide local primary and secondary monitoring systems at Mopra, giving the maximum possible safety margin.

8 ACKNOWLEDGMENTS

We thank the many AT staff who have contributed to the implementation of the monitoring systems. In particular John Deane, David McConnell, Russell Gough and members of the Narrabri Operations Group have made valuable contributions to the development of the secondary monitoring. Grahame Herbert, John Grenenger and members of the Narrabri Electronics Group undertook the task of implementing the primary monitoring and related telescope protection systems. George Chmiel was responsible for the early development of the AT data-sets which are so important to computer-based monitoring and control.

9 REFERENCES

1. Napier, P.J., Thompson, A.R. and Ekers, R.D., "The Very Large Array: Design and Performance of a Modern Synthesis Radio Telescope", Proc.IEEE, 71, 1295-1320, 1983.

2. Boyce, C.F., "The Protection of Telecommunication Systems" in Lightning, ed. R.H. Golde (Academic Press), 1977.

3. Prosser, F.P. and Winkel, D.E., "The Art of Digital Design", Prentice-Hall, 1987.

4. Hall, P.J., "The Australia Telescope Weather Station and Storm Warning System", IREE Monitor, June/July , 11-13, 1990.

5. Ferris, R.H., "Introducing the AT Data-sets", Australia Telescope National Facility Internal Report, February 1991.

6. Gough, R.G. and Kesteven, M.J., "The Monitoring System for the Australia Telescope", IREECON '91 International Proceedings, 385-388, 1991.

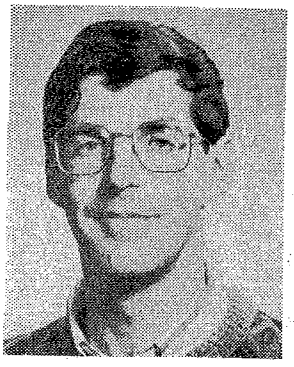

DR P.J. HALL

Dr Peter Hall received the degrees of BEng and BSc in 1980 and 1981 respectively. He completed his PhD in radiophysics at the University of Tasmania in 1985. After completing a postdoctoral fellowship with the CSIRO Division of Radiophysics, he joined the University of Sydney as a lecturer in Electrical Engineering. In July 1989 he was appointed as head (electronics) at the Australia Telescope National Facility's Paul Wild Observatory, Narrabri. His main research interests currently involve applied signal processing and millimetre-wave astronomy. Dr Hall holds the IREE's Norman W.V. Hayes Memorial Medal for meritorious original research.

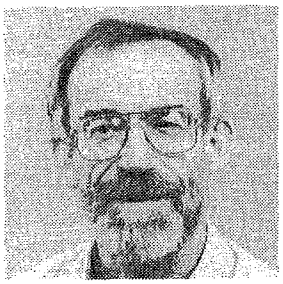

DR M.J. KESTEVEN

Dr Michael Kesteven was educated at Lycée Chateaubriand from which he graduated with Brevet d'Etudes du premier cycle du second degré, department de l'Isère. He is a graduate (in physics) of the University of Sydney (1963), and received his PhD in radio astronomy from the same university in 1968. He joined the Australia Telescope project in 1983. His professional interests include supernova remnants, radio source variability, interferometry and the problems of antenna metrology. In 1986 he was appointed head of the Computer Group at the Division of Radiophysics at Epping. He moved to the Australia Telescope's Paul Wild Observatory, Narrabri in April 1988.

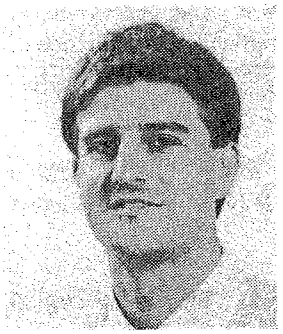

MR R.J. BERESFORD

Ron Beresford graduated from the University of Technology, Sydney in 1987 with a degree in Electrical Engineering. As an undergraduate he attained the Electronics Trade Certificate in 1984 and worked for two years with AWA Satellite Systems division. He joined the CSIRO Division of Radiophysics, Sydney, in 1986, working on the Australia Telescope project, and then was relocated to the telescope facility at the Paul Wild Observatory, Narrabri in 1988. He is currently the deputy leader of the electronics group of the CSIRO Australia Telescope National Facility at Narrabri. His interests include antenna control/monitor electronics, antenna drive and servo systems, antenna power systems and computer-aided design.

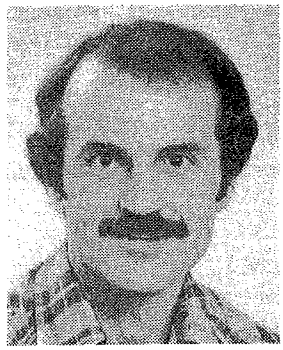

MR R.H. FERRIS

Dick Ferris graduated with the degree of BSc from the University of Tasmania in 1973. He joined CSIRO Division of Mineral Physics in 1981 and developed instrumentation for mineral exploration and remote sensing. He transferred to the Division of Radiophysics in 1985 to work on control systems for the Australia Telescope project. He is a member of the Australia Telescope National Facility's Correlator Group.

MR D.G. LOONE

David Loone received the BSc (Hons) degree in Computing Technology from the University of Tasmania in 1985. He joined the CSIRO Division of Radiophysics in 1986 where he worked in the Correlator Group of the Australia Telescope project doing software and hardware design for computer control of the Australia Telescope correlator. Since 1990 he has been working at the CSIRO Australia Telescope National Facility's Paul Wild Observatory, Narrabri in charge of digital design projects in the correlator, primary monitoring, and other areas of the observatory's development.

Operations Begin

G.J. Nelson* and J.B. Whiteoak**

SUMMARY The transition from construction to operation for the Australia Telescope involved appointing a Director, formally incorporating the Parkes telescope, and transforming the Australia Telescope Support Group from a group within the Division of Radiophysics to an independent unit within CSIRO – the Australia Telescope National Facility. Operation as a National Facility began in April 1990. To provide effective operation, several committees were established: an AT Advisory Committee, an AT Time Assignment Committee, an AT Users Committee, and several user-support groups. Of the six antennas which comprise the Compact Array at Narrabri, only five were outfitted for the first formal observations, at frequencies of 5.0 and 8.6 GHz, and only three of these were outfitted with 1.5- and 2.3-GHz systems, with limited spectral-line capability. Since then, outfitting at these frequencies has been completed, and services appropriate to a national facility have been set up at the sites to support visiting astronomers.

1 THE TRANSITION FROM CONSTRUCTION TO OPERATION

1.1 Management issues

On July 1 1987, the Parkes Observatory was formally incorporated into the Australia Telescope (AT) project.

At the end of 1987, Dr R.D. Ekers, then Director of the US Very Large Array, accepted the appointment as Foundation Director of the Australia Telescope. He arrived in Sydney to take up the position during the following February.

In July 1988, the Astrophysics Group of the CSIRO Division of Radiophysics was transferred to the Australia Telescope support group.

On January 1 1989, the AT support group was given independent CSIRO Divisional status as the Australia Telescope National Facility (ATNF). A management structure was set up, geared to operate a national facility. Despite this change, the ATNF still shares with Radiophysics some resources at the Radiophysics Laboratory – the computing network, engineering services, the library, some administration, and editorial services. Mr J.W. Brooks was appointed Engineering Manager to oversee the completion of the AT after the start of operation.

1.2 Final testing and outfitting

SYSTEM TESTING

During 1986, as part of the testing procedure of the new AT receiving systems, monitor systems and associated electronics, a single receiver system containing prototype units operating at the four AT frequencies was installed on the Parkes telescope for real-time testing. The system proved very reliable, and even today remains the front-line system at Parkes for observing at these frequencies. At the same time, the Parkes-Tidbinbilla Interferometer (PTI) was set up using the Parkes telescope, NASA's 70-m antenna at its Tidbinbilla Tracking Station, and a connecting Telecom microwave link. The main purpose was to test techniques (including computer software) intended for use with the AT. In addition to fulfilling this aim, the PTI has produced some important radio-astronomical results at frequencies between 1.6 and 12.2 GHz [1,2].

In November 1987, testing overall systems before installation at Narrabri was instituted at Radiophysics. A dedicated test room was set up, complete with compressors, helium piping for receiver cryogenics, fibre-optics links for clock and signal transfers, and computer links. The tested components included receivers, correlators, local-oscillator chains, fibre-optics transmission, and computer control.

* Australia Telescope National Facility, CSIRO, PO BOX 94, Narrabri NSW 2390, Australia.
** Australia Telescope National Facility, CSIRO, PO Box 76, Epping NSW 2121, Australia.
Submitted to The Institution of Radio and Electronics Engineers Australia in June 1992.

Outfitting the Compact Array antennas with receiver systems and associated electronics began in 1988. In August, the first interferometer tests, using two antennas, were successfully accomplished.

Four months later, and 30 years after using the Dover Heights Cliff Interferometer to discover that the 'radio stars' were supernova remnants and galaxies, Dr O.B. Slee made the first astronomical observations. He used two antennas of the Compact Array to detect radio emission from flare stars. At about the same time, one of the antennas was successfully used in conjunction with other antennas around Australia for very long baseline interferometry (VLBI) observations.

In April 1990, the Compact Array, with only five antennas, one polarization, and one pair of frequencies (5.0-GHz/8.6-GHz) available, began operating as a national facility, available for use by astronomers at large. As a result of periodic outfitting, slotted between periods of observation, the major outfitting was completed during 1991; by March the six Compact Array antennas were fully operational at four frequencies, and the capability for simultaneous observations with two different frequency bands followed a few months later. By the end of 1991, the Mopra antenna at Coonabarabran was also outfitted, and antenna performance tests were under way; on November 24, it was successfully used for VLBI observations. In November 1991, the AT Steering Committee formally declared the AT construction complete.

2 THE FIRST YEARS OF OPERATION

2.1 Establishing support groups

As part of the effective operation of the Australia Telescope National Facility, several support and feedback groups were established:

ATNF STEERING COMMITTEE

Shortly after the official opening of the Australia Telescope in September 1988, in accordance with recommendations of the Australian Science and Technology Council (ASTEC) [3], the Minister for Science, Customs and Small Business appointed an Australia Telescope National Facility Steering Committee; Professor L.E. Cram of the University of Sydney chaired the inaugural meeting in May 1989. The main roles of this committee are to determine the broad directions for the scientific and technical activities of the ATNF, including the future development of the Australia Telescope, to oversee time-assignment policy, and to advise CSIRO on policy and other issues affecting the operation of the ATNF. The Committee contains representatives from the Australian and overseas astronomical communities, and from CSIRO. In recognition of the value of mutual interaction between the ATNF and Australian industry, leading industrialists have been invited to serve on the Committee. The Committee is responsible for the production of an annual report on the activities of ATNF.

AT TIME ASSIGNMENT COMMITTEE

At its first meeting, the Steering Committee established a Time Assignment Committee, whose role was to assess observing proposals and allocate time on AT instruments. Membership includes the ATNF Director and four astronomers representative of the Australian astronomical community. Initially, the Committee met at three-monthly intervals; this was later extended to four.

In preparation for the formal start of operation (of course, the Parkes telescope had been in operation for many years, but not on a formal national facility basis), the first proposals for observing time on the Compact Array were solicited by the Committee at the end of 1989, and reviewed in February 1990.

AT USERS COMMITTEE

In 1989 the Steering Committee also set up a group to represent the Australian users of the AT. Its role is to provide information to the ATNF on the operation of the AT, and to advise on future developments. It has a membership of about twenty representatives from the Australian user community. It meets at six-monthly intervals in conjunction with a general users meeting at which the current status and planned development of AT facilities are discussed. The program includes a small symposium on scientific results obtained with the AT.

AT USER ASSISTANCE

In 1990, a small User Support group was set up at the Sydney headquarters to assist AT users, particularly visitors to the ATNF. It assists with travel and accommodation needs, arranges for experienced ATNF staff to help prepare telescope observing schedules and the subsequent processing of observations, and arranges support for observing. Also, the group prepares and distributes observing schedules and site information, assists with a student vacation employment program, and prepares and distributes documentation such as AT preprints, AT newsletters, and user manuals. A communications manager is responsible for preparing media releases, displays, other publicity activities, and annual reports.

Observers inexperienced with ATNF telescopes are helped by local staff or scheduled 'duty astronomers' provided mostly from the ATNF's Astrophysics Group.

As part of user support, the ATNF, during 1990, provided visitor accommodation on its Sydney site. The demand for this was so high that the accommodation was enlarged twelve months later.

2.2 Operations begin

COMPACT ARRAY

At the beginning of formal operations in 1990, the Compact Array had all five of the antennas on the 3-km track equipped for single-polarization observations in frequency bands centred at 5.0 and 8.6 GHz. Three of the antennas were also equipped to operate at 1.5 and 2.3 GHz. All 35 observing stations on the 3-km railtrack were available. The correlator system was set up to process two outputs for ten pairs of antennas. This yielded 32 channels spread over a 128-MHz band for continuum observations. Spectral-line observers were limited to a combination of 128 channels covering 64 MHz, or 256 channels over 8 MHz. For the latter, prominent interference 'spikes' were found at intervals of 0.5 MHz in the initial spectra, and use of the combination had to be postponed until the interference could be eliminated.

The initial operational plan included using a minimum-redundancy set of four antenna configurations (taken from the original study for the 6-km array [4]) each quarter. A three-week cycle was adopted: the first twelve days following a configuration change were used for equipment installation, and equipment and array testing, and the remaining nine days were programmed for radio astronomy observations. As time progressed, the quarterly allocation period was extended to four months; new configuration sets were derived, including a set of lower resolution arrays (down to 220 m); and with a more uniform distribution of antenna spacings; and the installation/observation cycle was changed to enable longer observing periods.

PUBLICITY

To provide publicity about radio astronomy, the ATNF and CSIRO, a new visitors centre was constructed at Narrabri, and opened to the public early in 1990. The Parkes Observatory has had such a centre since 1969, but for 20 years it was operated by CSIRO Headquarters in Canberra. The ATNF took over the Centre in 1990, making it part of the overall management of Parkes Observatory. A total of about 45,000 people visited the Centre that year.

2.3 Observing statistics

From the very beginning, there has been considerable international interest in using the AT. For Compact Array operation during the nine months of 1990, 64 programs involving 92 scientists from 34 different institutions were allocated observing time. Of these, 25 different programs involved 32 overseas observers from 20 different institutions. For the Parkes radio telescope (operating throughout 1990), observing time was allocated to 43 different programs involving 88 scientists from 32 institutions and, of these, 24 programs involved 33 overseas observers from 24 different institutions.

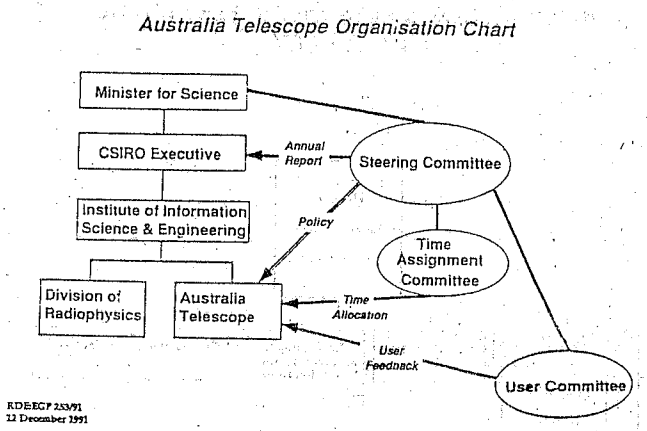

Figure 1 ATNF and external groups influencing its operation.

3 OPERATIONS TODAY

This section summarises the current organisation of the ATNF and the operation of its observatories. Figure 1 shows the external organisational structure; the three committees have been already discussed in Section 2. The ATNF is part of CSIRO's Institute of Information Science and Engineering and, as such, is answerable to both the Executive of CSIRO and the Minister for Science. As explained in Section 1, ATNF staff and facilities were part of the CSIRO Division of Radiophysics until after the construction of the new AT antennas. The two organisations maintain close links. They share a site in Sydney and, in many service areas, staff are jointly employed. Continuing formal and informal collaboration benefits both groups.

The ATNF's management structure is shown in Figure 2. At the top is the Director (Dr R.D. Ekers), with the same status as a Chief of a CSIRO Division, Deputy Director (Dr J.B. Whiteoak), and Assistant Director (Mr J.W. Brooks, who is also Assistant Chief of the Division of Radiophysics). The computing group is shared with Radiophysics. The ATNF's resources are balanced between operating the observatories, engineering development, and astrophysical research.

Coordinating activities at ATNF sites is an important task. Frequent operational, management and research meetings form the basis of this coordination. Regular meetings are held in Sydney to review and coordinate issues involving outfitting and operating the AT antennas. Site management meetings are held in turn at each of the three major sites. Other *ad hoc* meetings are held by 'teleconferencing'; more modern collaboration technologies such as video conferencing and electronic whiteboards will be used in the future.

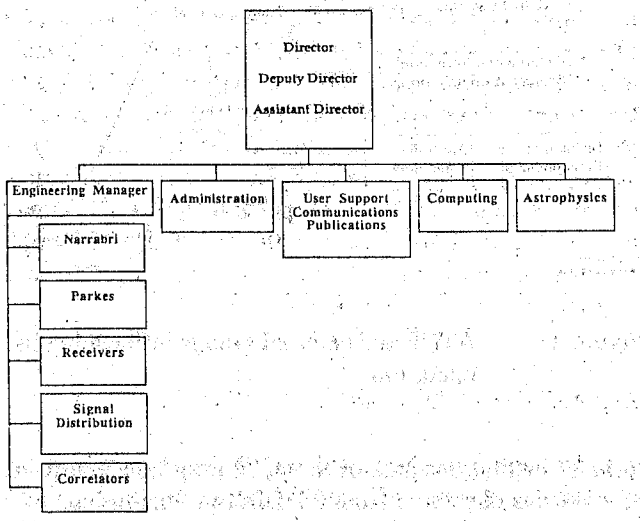

Figure 2 Management structure of ATNF.

3.1 Operations at the Paul Wild Observatory

At Narrabri, a staff of 35 is responsible for operating, and participating in, the development of the AT antennas on site (i.e. both the Compact Array and elements of the Long Baseline Array), and the Mopra antenna. During a four-month scheduling period for the Narrabri antennas, typically one month is devoted to installing, testing and maintaining new equipment, one week to system testing, one week to observing as part of the Long Baseline Array, and the balance to Compact Array observing. Observations are scheduled on a 24-hour, 7-day week basis, with any short gaps used for emergency maintenance, system testing or 'target of opportunity' observing. Despite its short operating life, the Compact Array has performed with few unscheduled interruptions. The unplanned 'down-time' has averaged at about 4% during 1990 and 1991, which is at about the same level as for the Parkes radio telescope.

A typical Earth-rotation synthesis observation takes about 14 hours. During this time, the system has to be set up and calibrated, and the target source observed from horizon to horizon, with periodic short interruptions to observe nearby phase-calibration sources. In other observations where the targets are sufficiently intense and their structure not too complex, observations of several sources can be interleaved, with each source observed for short periods at typically six different hour angles. Where complex regions are being imaged, the UV coverage may be increased by observing simultaneously at two frequencies, or sequentially at a larger number of frequencies. Where this is not possible or adequate, regions may be reobserved with the array in additional configurations.

Of the 14 standard configurations presently in use, about eight can be made available in a four-month scheduling period. Reconfiguring and calibrating the array currently takes about two days. Some routine maintenance and testing is done while the antennas are being moved. On completion, the system is made operational, and astronomical observations are carried out to determine the 'pointing' parameters of the antennas on their new stations, the baseline lengths between antennas, and the time delay for transmitting data from each antenna to the correlator. Any remaining time is used for system testing and emergency maintenance. It is anticipated that reconfigurations will eventually require less than a day, when systems are in place to measure directly the 'tilt' of the azimuth axis of each antenna and its 'rotation' in azimuth on its station. Measurement of, and correcting for, changes in the 'round-trip' phase of the local-oscillator signal for each antenna will also speed up the accurate measurement of baselines.

At the Observatory, astronomers are provided with motel-style accommodation, and transport to and from airport and bus terminals. While they are operating the telescope, they are provided with three levels of support. A duty astronomer or local staff member assists them in setting up and carrying out their observations, an Observatory staff member is on-call at all times to resolve equipment problems, and an Observatory resident is on automatic call to respond to serious emergencies such as fire, high wind and loss of power. The staff on call can monitor the operation of the telescope from their homes via telephone modems; in many cases they can resolve problems without going to the Observatory. The ultimate aim is for the Compact Array to be able to operate safely unattended, with appropriate people called out automatically when problems with data quality or equipment are detected.

3.2 Operations at the Parkes Observatory

The Parkes telescope has gradually changed from being an 'in-house' instrument to being a national facility with many non-CSIRO users.

It is operated and maintained by a staff of 20. Observations are scheduled for the same four-monthly periods as for the Compact Array, but are grouped according to the receiving system requested. (In contrast, Compact Array observations are grouped by array configuration.) If necessary, long integrations can be spread out over several days. Maintenance, installation and testing are carried out during previously scheduled periods, or during the mornings of week days. Normally, observations are scheduled for at least 16 hours each weekday and 24 hours during weekends. Observing programs are typically allocated between 2 and 5 days, sometimes longer. Increasingly, the Parkes telescope is being used to measure the 'zero spacing' component, or large-scale structure, to complement the finer scale structure measured with the Compact Array.

Similar services to those at Narrabri are provided to support visiting astronomers at Parkes. Assistance is available for astronomers who are unfamiliar with the telescope's operation; a formal training scheme is currently being organised. Staff are on call at all times to solve system problems. Unattended operation will not be possible at Parkes, but plans are in hand to reduce the number of people required for safe operation from two to one. On-site motel-style accommodation is provided; additional self-contained lodging is available for visiting families.

3.3 Long Baseline Array operations

The AT Long Baseline Array incorporating the Mopra antenna was used for the first time in November 1991, but without wideband tape recorders and accurate phasing via satellite. Since then, it has also operated as part of a larger, very long baseline interferometry (VLBI) network containing a number of non-ATNF telescopes. The scheduling of this type of array cannot be done entirely within the ATNF; at present, the Time Assignment Committee rates proposals, which are then scheduled in detail by the wider community of VLBI astronomers. In each four-month interval, a week is set aside when the Parkes, Mopra and Narrabri antennas are made available for use in VLBI experiments. On other occasions, the Parkes radio telescope alone is made available for PTI observations, or for VLBI observations in conjunction with other Australian and overseas antennas.

It is anticipated that, with the installation of wideband tape recorders and a correlator, the amount of observing with the Long Baseline Array will increase. In addition, when the Mopra antenna is fitted out with a millimetre-wave receiver, its use as a stand-alone instrument will increase significantly. At present, it is envisaged that this antenna will be maintained and operated from Narrabri. However, a small number of support staff may be located at Coonabarabran if the demand for observing time becomes high.

4 CONCLUSION

The transition from construction to operation of the AT has been a gradual process spanning several years, and in many ways the process still continues. To date the proposed usage of the various instruments has been between 150 and 300% of the available time. All Australian astronomical institutions have been awarded time, and up to 40% of Compact Array time has been awarded to overseas users. This percentage is seen as a good indication of the standing of the instrument in the international community and also helps to maintain the access of Australian scientists to overseas facilities.

The operation of the ATNF is changing to suit the changing needs of the users, and the new capabilities and requirements of the instruments. In the future, the possibility of unattended operation of the Compact Array, the requirements of some programs for interference-free observing, and the demands for a dry and stable atmosphere during millimeter-wave observing, may see a move to more dynamic scheduling. The development of Long Baseline Array capabilities and millimetre-wave instrumentation may see the Mopra antenna becoming an observatory in its own right. Commitments to Space VLBI, and to the support of programs by NASA and other agencies, will play a major role in the future operation of the Parkes telescope, and possibly the Mopra and Narrabri antennas as well. It is important that the Australia Telescope National Facility be alert to the need for changes, and flexible enough to make them.

5 REFERENCES

1. Norris, R.P., McCutcheon, W.H., Caswell, J.L., Wellington, K.J., Reynolds, J.E., Peng, R.S. and Kesteven M.J., "Milliarcsecond Maps of 12-GHz Methanol Masers", Nature, 335, 149, 1988.

2. Bailes, M., Manchester, R.N., Kesteven, M.J., Norris, R.P. and Reynolds, J.E., "The Parallax and Proper Motion of PSR 1451-68", Nature, 343, 240-241, 1990.

3. Australian Science and Technology Council, (1984), "Guidelines for the Operation of National Facilities", Canberra, AGPS, 1984.

4. Frater, R.H., Whiteoak, J.B. and Brooks, J.W. "The Australia Telescope: Overview", JEEEA, 1992, this issue.

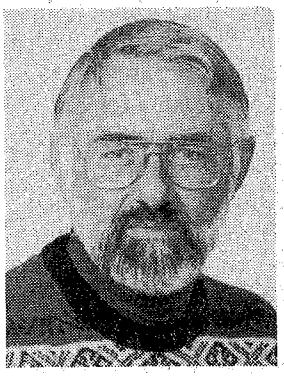

DR G.J. NELSON

Dr Graham Nelson is a graduate of the University of Sydney. He was awarded the degrees of BSc in 1962, BE in 1964, and PhD in 1968. During 1965 he worked as an electrical engineer in the NSW Electricity Commission. In 1968 he was a Nuffield Foundation Fellow working on the development of the Fleurs Synthesis Radiotelescope. During 1969 and 1970 he worked at the Arecibo Observatory in Puerto Rico. In 1971 he joined the CSIRO Division of Radiophysics' then solar observatory at Narrabri, NSW, using optical techniques to study magnetic fields and flares on the Sun, and later using the metre-wave radioheliograph and radiospectrograph to study the dynamics of the solar corona. During this time he was also the resident radio engineer for these instruments. In 1985, with the closing of the radioheliograph he moved to the Division's Epping Laboratory to work on the overall system design of the Australia Telescope and to do research into the coronae of active stars. In 1988 he returned to Narrabri as Officer-in-Charge of the Paul Wild Observatory and maintains his interest in the physics of the atmospheres of the Earth, Sun and stars and in the development of radio-telescope systems.

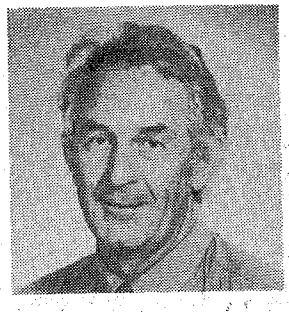

DR J.B. WHITEOAK

Dr John Whiteoak has a BSc degree from the University of Melbourne and a PhD in astronomy from the Australian National University (1962). He joined the CSIRO Division of Radiophysics in 1965, after a two-year Carnegie Fellowship at Mt Wilson and Palomar Observatories and a year at the California Institute of Technology. In 1971-1973 he spent two years on leave at the Max-Planck-Institut für Radioastronomie, Bonn. Dr Whiteoak was involved in the construction of the Australia Telescope as Project Secretary. Since 1989 he has been Deputy Director of the CSIRO Australia Telescope National Facility. His main research interest lies in the study of molecular clouds in our Galaxy and other galaxies.

Journal of Electrical and Electronics Engineering, Australia
Special Issue

THE AUSTRALIA TELESCOPE

Chapter 5

Radio Astronomy

The First Radio Astronomy: Results and Future Developments

R.D. Ekers* and J.B. Whiteoak*

SUMMARY Since the Compact Array began operating as a National Facility in April 1991, new exciting results have been provided by observations of southern galaxies (normal galaxies, radio galaxies, megamaser galaxies), supernova remnants in the Magellanic Clouds, and objects within our Galaxy (a Galactic Centre transient source, maser regions in molecular clouds, pulsar identifications and stellar radio emission).

Major future development of the Australia Telescope includes the 'tieing' of the six 22-m antennas of the Compact Array at Narrabri, providing better short-baseline configurations, extending observing frequencies on both the Compact Array and the Mopra (near Coonabarabran) antennas to 115 GHz, and completing the correlator, recording system and satellite for the Long Baseline Array (which includes the Mopra antenna and the Parkes 64-m antenna). Further downstream will see the development of focal-plane arrays, and baseline additions to the Compact Array.

1 THE FIRST RADIO ASTRONOMY RESULTS

Observations with the Compact Array are now producing exciting results; some have already won international acclaim. A selection of results follows.

1.1 Radio galaxies

The extended radio-emitting lobes ejected from some galaxies to distances of millions of light years continue to be of intense interest to radio astronomers. The southern skies also contain good examples of such objects, but little was known about their structure until the Compact Array began operation.

The first image with the Array

In June 1989, observations of a prominent southern radio galaxy, listed in the Parkes Catalogue of Radio Sources as PKS 2152-69, provided the first Compact Array image of a radio galaxy [1]. Figure 1 shows the most recent image.

PKS 2356-64

An extensive Compact Array study of PKS 2356-64, one of the brightest southern high-luminosity radio galaxies, has been carried out by a group from Mount Stromlo and Siding Spring Observatories, the Netherlands Foundation for Radio Astronomy, and the Australia Telescope National Facility (ATNF). Figure 2 shows the final radio image, obtained at 5-GHz frequency using observations with four different antenna configurations. It shows an elongated distribution with two prominent hot spots protruding well outside the two inner diffuse regions of emission. At a distance of 550 million light years, the separation between the outer hotspots is one million light years. The optical counterpart, from which the radio emission originated, is a 16th-magnitude elliptical galaxy, about 30 arcsec in diameter. It is of special interest because it contains regions of intense narrow-line optical emission, extended over distances of up to 65,000 light years. The nucleus of this galaxy contains a small-diameter radio source, which is located in the centre of the radio image.

1.2 Another 'Einstein Ring'?

The detection of close pairs of quasars with identical spectral characteristics and redshifts supports the existence of cosmic gravitational lenses [2]. With the gravitational bending of light in accordance with Einstein's general theory of relativity, a massive object such as a galaxy can, when viewed along the line of sight to a quasar, act as a gravitational lens and produce multiple images of that quasar. Moreover, if the quasar and the intervening gravitational lens are exactly aligned, the image has the form of an 'Einstein Ring'.

* Australia Telescope National Facility, CSIRO, PO Box 76, Epping NSW 2121, Australia.
Submitted to The Institution of Radio and Electronics Engineers Australia in June 1992.

Until recently, only two candidate rings were known. Now, a third has been identified [3], one hundred times stronger than the others at radio wavelengths. Images of the radio-source PKS 1830-211, obtained using several radio astronomy arrays, including an international very long baseline interferometry (VLBI) network incorporating Australia Telescope (AT) antennas, show a complete faint elliptical 'ring' with two strong compact components at each end of the major axis. This morphology, together with other features such as the high brightness of the components, suggests that the radio source has been produced by gravitational lensing. Further study should provide a better understanding of gravitational lenses.

1.3 Supernova SN 1987A.

February 1987 provided one of the most exciting events of modern astronomy, with the sudden appearance of a bright supernova (SN 1987A) in the Large Magellanic Cloud (LMC). It provided astronomers in the Southern Hemisphere with an unprecedented opportunity to follow the evolution of a supernova from its very beginning. At radio wavelengths, an initial outburst of radio emission [4] was followed by three and a half years during which the emission was undetectable. However, it reappeared in July 1990 [5,6], and since then has been monitored at several frequencies with the Compact Array. The first images, obtained with 3-km configurations, showed a radio source near the optical image. The radio position was not accurate enough to show whether the radio emission was associated with the stellar object, or with the front side of a surrounding ring of ionized matter which an image obtained with the Hubble Space telescope revealed. If the latter, emission from other regions of the ring should have been detectable within a further six months. To enable this prediction to be tested, outfitting the 6-km array was accelerated to provide the required resolution. In March 1991, 9-GHz observations with the 6-km configuration (resulting in an 0.85-arcsec beam) resolved the radio image. The radio emission appeared to be from a region with a deconvolved size of 1 arcsec (1 light year), probably inside the ionized ring (Fig. 3).

1.4 Supernova remnants in the Magellanic Clouds

The study of supernova remnants in our Galaxy is severely limited by the obscuring nature of the interstellar dust, uncertain estimates of distance, and variations in the radio-emission background. Our nearest neighbouring galaxies, the Large and Small Magellanic Clouds, have low dust and background radio emission levels, allowing clear views of the remnants in these galaxies. Moreover, the remnants have similar distances, making comparison easier, and angular structure well matched to the resolving power of the Compact Array. The high potential of research involving Magellanic Cloud objects is shown by several projects now in progress; the results are already providing evidence of a number of different physical processes occurring in the remnants.

Several Compact Array studies of supernova remnants indicate that synchrotron emission and hot shocked gas have different locations in the remnants. The LMC object SNR 0540-693 [6] is especially interesting because it contains a radio pulsar, emitting a burst of radio waves every 50 ms, near its centre. The first well-resolved image shows a central radio core, about four light years across; it is associated with optical and X-ray radiation. This core is surrounded by a shell-like nebula about 50 light years in diameter, which presumably marks the edge of the debris ejected from the supernova.

Another LMC remnant, designated N132D (Fig. 4), shows a shell-like image similar to X-ray and optical [OIII] images [7]. However, an extra radio feature, in the form of a faint outer arc to the southeast, suggests a difference between the distribution of the magnetic fields and relativistic particles responsible for the synchrotron emission, and the distribution of the hot shocked gas associated with the X-ray emission.

1.5 Binary radio pulsar with a Be star companion

Pulsar PSR 1259-63 was discovered during a large-scale high-frequency search using the Parkes radio telescope. The observations indicated that the object is in a highly eccentric orbit around a massive companion. Using Compact Array observations to obtained accurate positions, a group of scientists from the ATNF, Jodrell Bank, Princeton University, Peking University, and the Universita di Palermo identified the companion as a 10th-magnitude Be star [8]. The system forms a link between Be X-ray binary systems and recycled pulsars.

1.6 Stellar radio emission

Radio emission emitted by stars (other than the Sun) is usually very weak. The Compact Array is ideal for observing this emission, particularly that from young pre-main-sequence objects, older active-chromosphere main-sequence stars and evolved giants. It is being used to study both stellar flares and the quiescent emission from stellar coronas. Monitoring the radio emission associated with the star AB Doradus led to the first conclusive evidence for rotational modulation of stellar radio emission [9].

1.7 Spectral-line studies with the Compact Array

Abundant molecules in the dense molecular clouds give rise to many narrowband spectral lines in the radio spectrum, particularly at frequencies above 50 GHz. The lines can appear in emission, or in absorption if the

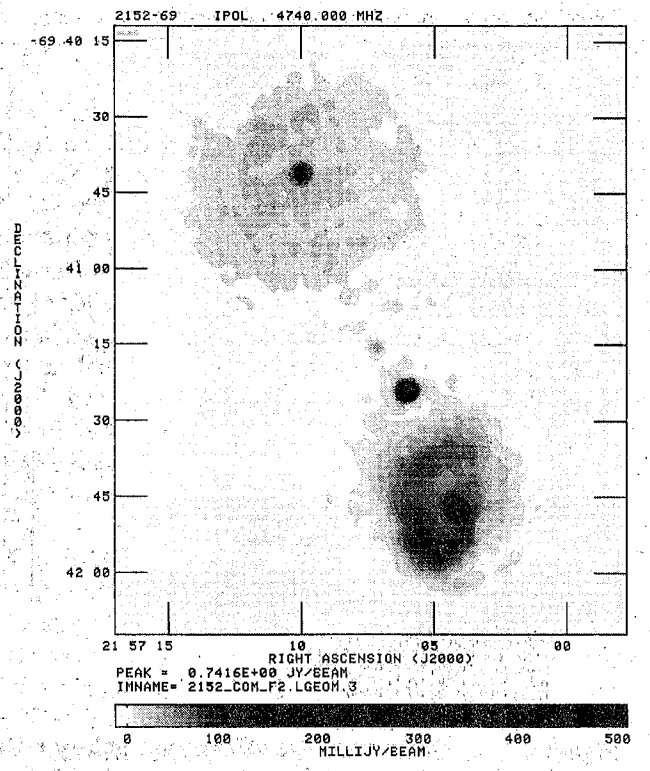

Figure 1 PKS 2152-69.

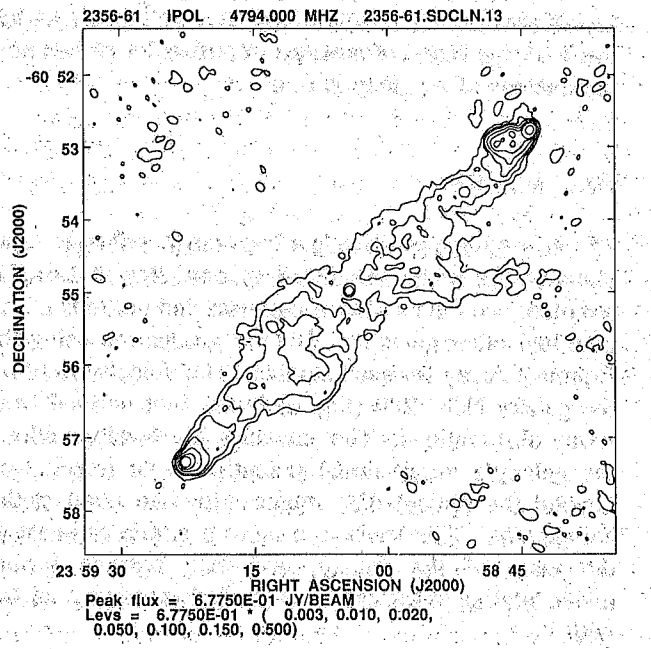

Figure 2 PKS 2356-64.

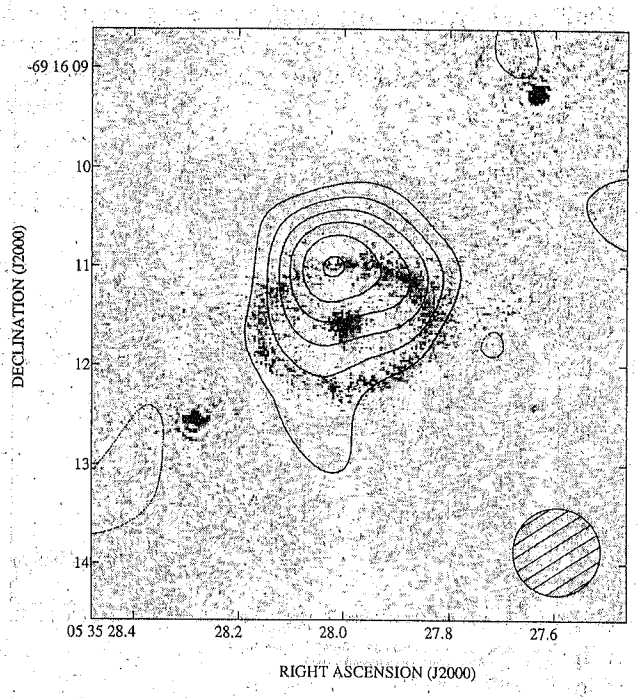

Figure 3 LSS helf-tone showing the radio contours of SN 1987A superimposed on the Hubble Space Telescope image at the [0III] wavelength.

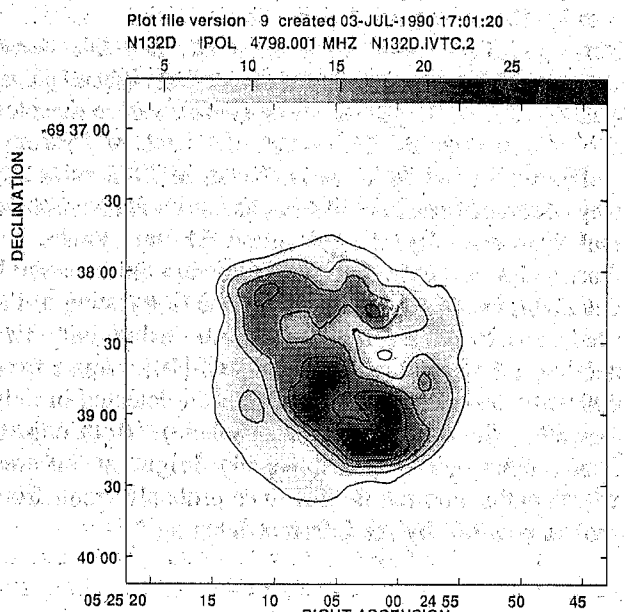

Figure 4 5-GHz image of LMC supernova remnant N132D.

clouds overlie a bright radio source. Each molecule produces a set of lines with a specific signature of frequencies which, however, can be Doppler shifted (redshifted) by the line-of-sight motion of the molecule. Consequently, spectral lines are important because they provide information not only about the chemical composition and physical conditions in molecular clouds, but also about the motions of the clouds, and the galaxies in which the clouds are situated. The Compact Array was planned to make important contributions to spectral-line studies, by virtue of a wide frequency coverage and high-capacity correlator.

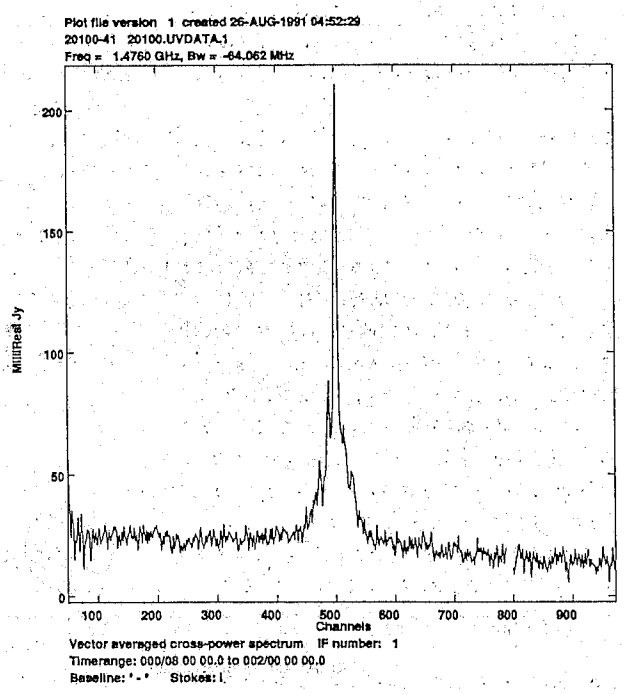

Figure 5 1.6-GHz OH spectral-line profile for megamaser galaxy IRAS 20100-4156.

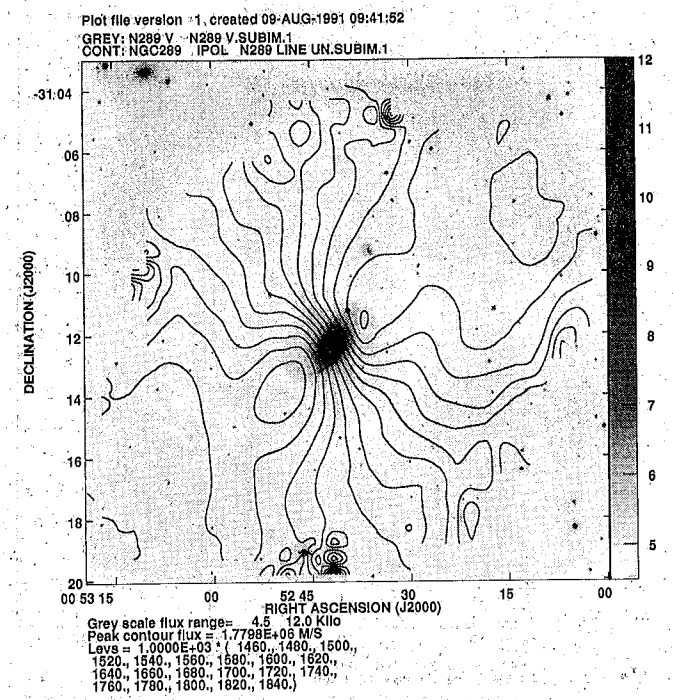

Figure 6 Contours of HI velocity for galaxy NGC 289, superimposed on the optical image.

The cloudy galaxy NGC 4945

This spiral galaxy is seen edge on, and has dense molecular clouds surrounding its radio-bright nucleus. Several molecular spectral lines have now been detected from these clouds. Low-excitation lines of hydroxyl (OH) at 1.6 GHz were first detected in 1973 using the Parkes radio telescope. Ideally, several lines are needed to define the physical conditions in the clouds, but subsequent searches at Parkes were unsuccessful. However, in January 1989, during the first testing of the Compact Array spectral-line system using only two antennas, 6-GHz lines were detected [10]. Apart from our own Galaxy, such lines have been detected in only one other (in the Northern Hemisphere). Both objects have nuclei which are unusually bright at infrared wavelengths, and the 6-GHz lines probably result from OH 'excitation' by the infrared radiation.

'Megamaser' emission in IRAS 20100-4156

In our Galaxy, intense OH and H_2O 'maser' emission, some with features only a few kHz wide, are often associated with dense molecular clouds in which stars are forming. However, for a few other galaxies, even more luminous ('megamaser') emission is associated with the nucleus. This emission is wideband, and still puzzles radio astronomers because they don't understand how it is produced. At Parkes several years ago, redshifted 1.6-GHz megamaser emission was detected towards the infrared bright galaxy IRAS 20100-4156. It was suspected that the emission covered an unusually large velocity range, but instrumental baseline effects in spectra rendered the results uncertain. However, a sideband spectrum of the emission, obtained with the Compact Array (Fig. 5), has a flat baseline, and shows an OH profile with a width of 1300 km s^{-1} (i.e. 7 MHz). Such a large range of motions in molecular clouds near the nucleus of a galaxy is rare.

HI in galaxies

HI is extremely abundant in most galaxies, and observations of its associated spectral line at 1.4 GHz are often used in studies of the mass and motions of our own and other galaxies. Several groups are using the Compact Array for such studies. The velocity field for the galaxy NGC 289 (Fig. 6) is the first derived from Array observations. The extensive HI envelope allows the galaxy's gravitational potential to be traced well beyond the optical disc representing the main stellar component. This leads to a more accurate estimate of the mass of the galaxy, and may provide further understanding of the nature of the dark matter associated with it.

Transient radio source near the Galactic Centre

In March 1991, a team of US and Australian radio astronomers using the US Very Large Array detected a bright, transient radio source in a direction towards the centre of our Galaxy. It was suspected, but not known for certain, that the source was located near the centre. At this time, plans to bring into operation the sixth antenna of the Compact Array, located at the 6-km site,

were accelerated. This enabled the first high-resolution observations with the 6-km configuration a few days later, while the transient source was still quite strong.

HI and OH spectra were observed towards both the transient source and the compact radio source [known as Sagittarius (Sgr A*)] at the nucleus of our Galaxy [11]. The spectra of the transient source contained an absorption feature from a well-known dense molecular cloud believed to be located near the Galactic Centre, indicating that this source was at least as distant as this cloud. At the same time, there were no absorption features to suggest that the source was beyond the molecular clouds located not far behind the nucleus. Therefore, the results indicated, for the first time, that the transient source was located in the vicinity of Sgr A*, the nucleus of our Galaxy. The source is probably transient radio emission from synchrotron-radiating plasma associated with an X-ray binary system.

New methanol masers in our galaxy

The methanol molecule (CH_3OH) has a large number of spectral lines with frequencies below 100 GHz. A few years ago, strong CH_3OH maser emission was detected at 12 GHz. Observations with Australian VLBI networks (some incorporating a Compact Array antenna) indicated that the positions of maser spots within individual clouds followed curved lines. This is consistent with maser production in outflows or discs of proto-planets.

During 1991, even stronger CH_3OH maser emission was detected elsewhere at 6.7 GHz. Although this frequency is beyond the specified band-edge of the 6-GHz receivers of the Compact Array, test observations early in 1992 showed that the brightest masers could be easily imaged despite the reduced performance of the receiver systems. A series of observations in February resulted in the very first images of these masers. These enabled them to be located with sub-arcsecond accuracy relative to associated OH masers and ionized hydrogen gas regions [12]. In several cases, 6-GHz masers were found to be coincident (to within 0.020 arcsec) with 12-GHz masers at the same velocity (see example in Fig. 7). This provided new constraints on mechanisms proposed to explain the maser process.

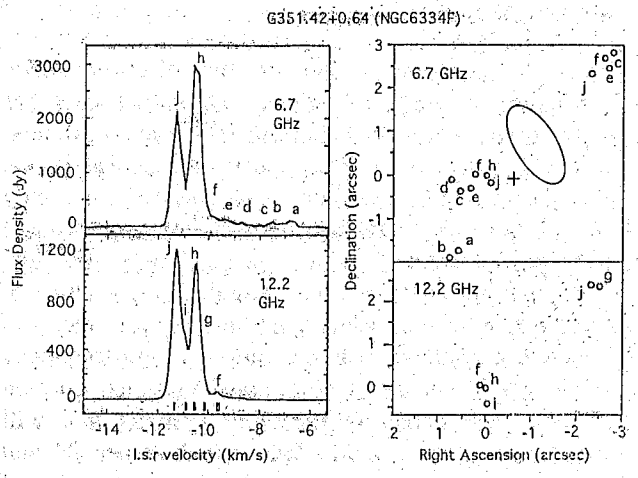

Figure 7 Map and spectra of the 6.7- and 12.2-GHz maser emission from G351.42+0.64. Letters on the maps correspond to the lettered features on the spectra, and the same letters are used in both transitions for corresponding maser features. Relative positional uncertainty is estimated at 0.02 arcsec. The cross represents the position of the continuum peak, and the ellipse the approximate position of the OH masers.

2 FUTURE DEVELOPMENT

2.1 Compact Array

The first stage of outfitting the Compact Array is virtually complete: dual-polarization, dual-frequency observations can be carried out in frequency bands centred at 1.5, 2.4, 5.3 and 8.6 GHz, using all six antennas. Projects involving the accurate measurement of linear polarization are now under way. Its highest frequency band is far below the planned limit of 116 GHz. In addition, higher spectral resolution is needed for studies of molecular masers. Filters of bandwidth 4 MHz will be installed soon at the antennas, and will provide a resolution of 2 kHz under full operational conditions. This will be still inadequate for some projects, and future 1- and 2-MHz filters will provide a resolution as high as 250 Hz.

Even with the present limited range of frequency and spectral resolution, the Compact Array is successfully fulfilling its national and international obligations as a National Research Facility. For example, for the first eleven months of 1991, of the eighty different programs that were allocated observing time, Australian scientists outside the ATNF were associated with 64% of the programs, and overseas scientists were associated with 40%. Scientists from 40 different institutions (28 overseas) and 37 PhD students are currently using these facilities for their research.

Plans for future development cover several areas. One is to extend operation to higher frequencies. Several spectral lines important for studies of molecular clouds have frequencies between 12 and 25 GHz, and receiver systems covering this spectral range are under construction. In future retrofits involving the 5.3-GHz/8.6-GHz systems, the 5.3-GHz receivers will be replaced by wide-band HEMTs covering the 6.7-GHz methanol maser line.

It is proposed to 'tie' together all the Compact Array antennas. This will provide a system with a collecting area equivalent to a 54-m diameter antenna, with an obvious increase in sensitivity over a single 22-m

antenna for VLBI, LBA and high time-resolution observations.

The high-frequency region of the electromagnetic spectrum is a unique window. Operating here are several important mechanisms which produce continuum radio emission. In addition, many molecules in the interstellar medium emit microwave spectral lines only at high frequencies. For the Compact Array operating at 100 GHz, a combination of high sensitivity and high angular resolution would provide a wealth of opportunities for new science, particularly for objects in the southern sky inaccessible to all other high-frequency instruments. Because of these considerations, we plan to design and construct receiving systems that will operate in the atmospheric 'window' between 84 and 116 GHz. The design, prototype development, and final production could be undertaken by the ATNF's receiver group, with construction carried out in the workshops of the CSIRO Radiophysics Laboratory.

A focal-plane feed array would greatly enhance the capability of a mm-wave array. At high frequencies, the field of view of a radio telescope large enough to provide good sensitivity becomes smaller than the typical objects to be imaged. In principle, the problem can be solved by combining the power of an array of antennas with a small focal-plane array for each antenna. Whereas some single-dish focal-plane arrays are now under construction, their use in conjunction with a synthesis array is new and untried. The most challenging problem is to construct a close-packed array, and the antenna group of the Division of Radiophysics is a world leader in this area of feed design. We will concentrate initially on the production of an eight-element prototype unit.

Further enhancement would be provided by a 1-km north-south spur track, equipped with four observing stations and turn-table linked to the existing east-west track. This would enable better imaging of objects near the equatorial zone of the sky. Moreover, operation at high frequency is much more dependent on weather conditions than at low frequency, and images must be made rapidly to minimise the effects of changing weather conditions, rather than waiting for the movement of the Earth to rotate the baseline.

The addition of a low-precision track between the 6-km site and east-west track would enable the 6-km antenna to be moved into the small-scale configurations used for high-frequency observations. This would not only increase the collecting area, but also the number of instantaneous spacings from 10 to 15.

The Array lacks the antenna stations to provide adequate sets of small configurations. Such sets are useful for low-frequency spectral-line studies of ionized-hydrogen regions of our Galaxy, and are mandatory for high-frequency operation. Discussions are under way to provide means of setting the antennas closer together.

2.2 Mopra antenna

A mm-wavelength capability will be available on the 22-m Mopra antenna near Coonabarabran by mid-1993. This will enable the antenna to be used in stand-alone mode for observations of molecular-line transitions with frequencies between 85 and 115 GHz. The design of a sensitive SiS receiving system is being completed in a collaborative venture between the ATNF and the US National Radio Astronomy Observatory. A correlator system based on the design used for the Compact Array will provide spectral bandwidths of up to 1000 MHz. This correlator may be supported by a wideband acousto-optical spectrograph provided by the Max-Planck Institut für Radioastronomie, Bonn.

In addition to these developments, the antenna will be outfitted for its role as an element in the AT Long Baseline Array by having suitable data-recording facilities and frequency-reference hardware provided.

2.3 Long Baseline Array

One problem associated with completing the Long Baseline Array has been the lack of a suitable tape-recording system. Although individual antennas have been incorporated into VLBI networks, old mkII narrowband recording equipment was used, and the correlation of the recorded observations had to be carried out using imported playback facilities. A wideband S2 Canadian recording system has now been developed, and several will be purchased for the LBA sites. For signals correlation, a large correlator is under construction which will be capable of processing recorded observations simultaneously from as many as six stations. For continuum observations, four products 16 MHz wide can be handled per baseline. For spectral-line operation and 2-bit sampling, the highest resolution will be provided by a combination of 2048 channels extending over 1 MHz (4096 channels for 1-bit sampling); other combinations of channels and bandwidth will be also available up to a bandwidth of 16 MHz.

The final step is to complete the reference-frequency transfer system, using the communications satellite OPTUS B1. With this in place, the Long Baseline Array will be ready for operation, either alone, or as part of the giant VLBI networks planned for the next decade. When this milestone is reached, the total concept of the Australia Telescope will then be a reality.

3 REFERENCES

1. Norris, R.P., Kesteven, M.J., Sramek, R.A., Wilson, W.E., Brooks, J.W., Calabretta, M.R., Ekers, R.D., Sinclair, M.W. and Young, A.C., "2152-69: The First Image from the Australia Telescope". Proc.Astron.Soc.Aust., 8, 252-253, 1990.

2. Jauncey, D.L., Reynolds, J.E., Tzioumis, A.K., "An Unusually Strong Einstein Ring in the Radio Source PKS 1830-211". Nature, 352, 132-134, 1991.

3. Turtle, A.J., Campbell-Wilson, D., Bunton, J.D., Jauncey, D.L., Kesteven, M.J., Manchester, R.N., Norris, R.P., Storey, M.C. and Reynolds, J.E., "A Prompt Radio Burst from Supernova 1987A in the Large Magellanic Cloud". Nature, 327, 38-40, 1987.

4. Turtle, A.J., Campbell-Wilson, D., Manchester, R.N., Staveley-Smith, L. and Kesteven, M.J., "Supernova 1987A in the Large Magellanic Cloud". IAU Circ., No. 5086, 1992.

5. Staveley-Smith, L., Manchester, R.N., Kesteven, M.J., Campbell-Wilson, D., Crawford, D.F., Turtle, A.J., Reynolds, J.E., Tzioumis, A.K., Killeen, N.E.B. and Jauncey, D.L., "The Birth of a Radio Supernova Remnant in Supernova 1987A". Nature, 355, 147-149, 1992.

6. Kesteven, M.J., Manchester, R.N. and Staveley-Smith, L., "First AT Observations of SNR 0540-693". IAU Symp., 148, The Magellanic Clouds and their Dynamical Interaction with the Milky Way, Kluwer (eds Haynes, R. F. and Milne, D.K.), 323-324, 1991.

7. Dickel, J.R. and Milne, D.K., "Radio Imaging of the Supernova Remnant N132D in the Large Magellanic Cloud", IAU Symp., 148, The Magellanic Clouds and their Dynamical Interaction with the Milky Way, Kluwer (eds Haynes, R.F. and Milne, D.K.), 349-352, 1991.

8. Johnston, S., Manchester, R.N., Lyne, A.G. Bailes, M., Kaspi, V.M., Guojun, Q. and D'Amico, N. "PSR 1259-63: a Binary Radio Pulsar with a Be Star Companion", Astrophys.J., 387, L37-L41, 1992.

9. Lim, J., Nelson, G.J., Castro, C., Kilkenny, D. and van Wyk, F., "First Conclusive Evidence for Rotational Modulation of Stellar Radio Emission". Astrophys.J., 388, L27-L30, 1992.

10. Whiteoak, J.B. and Wilson, W.E., "Australia Telescope Observations of Excited-state OH Transitions in NGC 4945". Mon.Not.R.Astron. Soc., 245, 665-669, 1990.

11. Zhao, J.-H., Roberts, D.A., Goss, W.M., Frail, D.A., Lo, K.Y., Subrahmanyan, R., Kesteven, M.J., Ekers, R.D., Allen, D.A., Burton, M.G. and Spyromilio, J., "A Transient Radio Source Near the Centre of the Milky Way Galaxy". Science, 255, 1538-1543, 1992.

12. Norris, R.P., Whiteoak, J.B., Caswell, J.L. and Wieringa, M., (1992), "Synthesis Images of 6.7-MHz Methanol Masers". Proc. Conf. on Astrophys. Masers, Washington, DC, March 1992, in press.

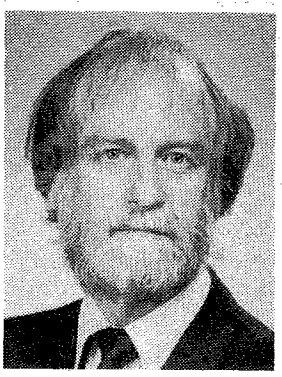

DR R.D. EKERS

Dr Ron Ekers is a graduate of the University of Adelaide (1963) and gained his PhD at the Australian National University (1967). He went on to work at the California Institute of Technology, the Institute of Theoretical Astronomy in Cambridge, the Kapteyn Laboratory in Groningen, and the US National Radio Astronomy Observatory. He has been involved with most of the world's major synthesis telescopes. From 1980 until his appointment as Director of the Australia Telescope he was responsible for running the Very Large Array at Socorro, New Mexico. Dr Ekers was a member of the Australia Telescope Advisory Committee from 1983 until 1988. His interests lie in extragalactic astronomy, especially galactic nuclei and cosmology, and in the problems of indirect image formation. He was appointed Director of the Australia Telescope (now the Australia Telescope National Facility) in 1988.

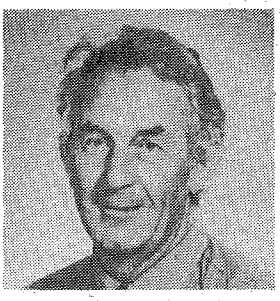

DR J.B. WHITEOAK

Dr John Whiteoak has a BSc degree from the University of Melbourne and a PhD in astronomy from the Australian National University (1962). He joined the CSIRO Division of Radiophysics in 1965, after a two-year Carnegie Fellowship at Mt Wilson and Palomar Observatories and a year at the California Institute of Technology. In 1971-1973 he spent two years on leave at the Max-Planck-Institut für Radioastronomie, Bonn. Dr Whiteoak was involved in the construction of the Australia Telescope as Project Secretary. Since 1989 he has been Deputy Director of the CSIRO Australia Telescope National Facility. His main research interest lies in the study of molecular clouds in our Galaxy and other galaxies.

THE AUSTRALIA TELESCOPE — OVERVIEW

KEY WORDS : Australia Telescope National Facility, radio astronomy, synthesis telescope.

ABSTRACT : On the second day of September, 1988, at a windy ceremony held at CSIRO's Paul Wild Observatory near Narrabri, some 600 kilometres north-west of Sydney, Australia's then Prime Minister, the Hon. R.J.L. Hawke, declared the Australia Telescope officially open. This heralded a new exciting era in Australian scientific research, because the Australia Telescope is an advanced radio telescope network which will keep Australia at the forefront of radio astronomy for many years to come. Designed and built in Australia, and containing a high Australian content, this 50-million dollar national facility is a substantial monument to Australian manufacturing expertise and high-technology capability.

REFERENCE : Frater, R.H., Brooks, J.W. and Whiteoak, J.B., "Overview", Journal of Electrical and Electronics Engineering, Australia, Special Issue on Australia Telescope, June 1992, Vol. 12, No. 2, pp. 103-112.

THE AUSTRALIA TELESCOPE — SYSTEM DESCRIPTION

KEY WORDS : Australia Telescope National Facility, radio astronomy, astronomy instrumentation, long-baseline arrays.

ABSTRACT The Australia Telescope Compact Array comprises six 22-m moveable antennas with a maximum east-west baseline of 6 km. Provision is made for operation in the frequency range 0.3 to 116 GHz. Flexible array configurations, wide, instantaneous bandwidths and tuning ranges, high polarization purity, aberration-free wide-field imaging, simultaneous operation at two frequencies, powerful spectral-line capabilities and high time-resolution operation are important features of the system.

REFERENCE : Nelson, G.J., "The Australia Telescope - System Description", Journal of Electrical and Electronics Engineering, Australia, Special Issue on Australia Telescope, June 1992, Vol. 12, No. 2, pp. 113-120.

THE ANTENNAS

KEY WORDS : Australia Telescope National Facility, radio astronomy, antennas, radio astronomy arrays.

ABSTRACT As part of the Australia Telescope construction project CSIRO, in conjunction with Macdonald Wagner & Priddle (now Connell Wagner), produced two new designs for 22-m diameter antennas (one mounted on bogies, the other fixed), to operate at frequencies up to 116 GHZ. In the evolution from currently operating antennas, special attention was given to transportability, azimuth transfer, control systems, thermal performance, wind loading, and surface panel manufacture. Seven antennas were constructed, six movable instruments in an array near Narrabri, and a single, fixed ('wheel-on-track') antenna near Coonabarabran.

REFERENCE : Cooper, D.N., James, G.L., Parsons, B.F. and Yabsley, D.E., "The Antennas", Journal of Electrical and Electronics Engineering, Australia, Special Issue on Australia Telescope, June 1992, Vol. 12, No. 2, pp. 121-136.

THE FEED SYSTEM

KEY WORDS : Australia Telescope National Facility, radio astronomy, antennas: feed systems, orthomode transducers.

ABSTRACT This paper describes the wideband feed system of the elemental Cassegrain antenna used to form the Australia Telescope array. The development of the feed horn and orthomode transducer is put in an historical perspective and how the system evolved is discussed. Results are given showing the performance of the various components as well as the overall behaviour of the antenna.

REFERENCE : James, G.L., "The Feed System", Journal of Electrical and Electronics Engineering, Australia, Special Issue on Australia Telescope, June 1992, Vol. 12, No. 2, pp. 137-146.

THE RECEIVER SYSTEM

KEY WORDS : Australia Telescope National Facility, radio astronomy, microwave radiometers, cryogenics, IF and conversion systems.

ABSTRACT The seven 22-metre antennas of the Australia Telescope (six at Narrabri and one at Coonabarabran, NSW) have been equipped with a range of low-noise microwave receivers. The system requirements, design concepts and construction techniques of the overall receiver system are discussed and some early performance date indicated.

REFERENCE : Sinclair, M.W., Graves, G.R., Gough, R.G. and Moorey, G.G., "The Receiver System", Journal of Electrical and Electronics Engineering, Australia, Special Issue on Australia Telescope, June 1992, Vol. 12, No. 2, pp. 147-160.

THE LOCAL OSCILLATOR SYSTEM

KEY WORDS : Australia Telescope National Facility, radio astronomy, phase-stable local oscillators.

ABSTRACT The Australia Telescope receivers require a complex, highly stable local oscillator system for signal tuning and for conversion to lower frequencies. All twelve oscillators within each antenna must be precisely phaselocked to a central frequency reference oscillator up to 5 km away. One oscillator in each antenna must also be phase rotated at many thousands of degrees per second whilst maintaining a phase accuracy of 1°. This paper outlines the combination of techniques used to meet these requirements.

REFERENCE : Young, A, McCulloch, M.G., Ables, S.T., Anderson, M.J. and Percival, T.M., "The Local Oscillator System", Journal of Electrical and Electronics Engineering, Australia, Special Issue on Australia Telescope, June 1992, Vol. 12, No. 2, pp. 161-173.

THE SAMPLING AND DATA SYNCHRONIZATION SYSTEMS

KEY WORDS : Australia Telescope National Facility, radio astronomy, high-speed samplers.

ABSTRACT The sampler, digitiser and data synchronization systems of the six antennas which make up the Australia Telescope Compact Array are described. The sampler/digitiser units, which are located at the antennas, convert the analog outputs of the receivers to digital form and encode the resulting data streams into a form suitable for transmission via fibre-optic links to the central control building. The method by which the various data streams are synchronized is explained.

REFERENCE : Wilson, W.E. and Willing, M.W., "The Sampling and Data Synchronization Systems", Journal of Electrical and Electronics Engineering, Australia, Special Issue on Australia Telescope, June 1992, Vol. 12, No. 2, pp. 173-182.

THE OPTICAL FIBRE SYSTEM

KEY WORDS : Australia Telescope National Facility, radio astronomy, optical fibre.

ABSTRACT The Australia Telescope has made extensive use of optical fibres for the return of high-speed signals from the receivers. This unusual application of fibres required many short links operating at 1-Gigabit speeds in combination with the need for easy disconnection in a dusty or wet environment. The system also uses fibres to carry a local-oscillator reference over a 5-km distance and to carry communication links to all antennas. This paper outlines the techniques used to meet these requirements.

REFERENCE : Young, A.C., Anderson, M.J., Hayes, M.J.W. and Ticehurst, R.C., "The Optical Fibre System", Journal of Electrical and Electronics Engineering, Australia, Special Issue on Australia Telescope, June 1992, Vol. 12, No. 2, pp. 177-182.

THE DELAY SYSTEM

KEY WORDS : Australia Telescope National Facility, radio astronomy, digital delay systems.

ABSTRACT We describe the delay system for the six antennas which make up the Australia Telescope Compact Array. The digital data from the antennas arriving at the central site first pass through the delay system. The amount by which each data stream is delayed differs from antenna to antenna, and changes over the course of an observation. The delay system performs this function and converts the data into a format suitable for subsequent processing.

REFERENCE : Wilson, W.E. and Carter, C.N., "The Delay System", Journal of Electrical and Electronics Engineering, Australia, Special Issue on Australia Telescope, June 1992, Vol. 12, No. 2, pp. 183-186.

THE CORRELATOR

KEY WORDS : Australia Telescope National Facility, radio astronomy, digital correlators.

ABSTRACT This paper describes the correlator system of the Australia Telescope Compact Array. The Compact Array is located at Narrabri, NSW and comprises six of the Australia Telescope's eight antennas. The correlator is a special-purpose real-time digital processor which performs the first stage of data reduction for the Compact Array (CA). It operates at the maximum data rate of 12 Gbits/s at the input, reducing this by a factor of order 5000 at the output.

REFERENCE : Wilson, W.E., Davis, E.R., Loone, D.G. and Brown, D.R., "The Correlator", Journal of Electrical and Electronics Engineering, Australia, Special Issue on Australia Telescope, June 1992, Vol. 12, No. 2, pp. 187–198.

ON-LINE COMPUTING FOR THE COMPACT ARRAY

KEY WORDS : Australia Telescope National Facility, radio astronomy, radio astronomy: on-line computing.

ABSTRACT The Australia Telescope Compact Array is made up of six 22-m antennas at Narrabri, NSW. The control system of the Compact Array has to deal with antennas and hardware distributed over 6 km. It needs to maintain synchronization of the sampling of astronomical data to a precision of better than 1 ns, coordinate the activities at the central site (data collecting, processing and archiving), and provide extensive monitoring of the data quality and the hardware status. These goals are achieved through a combination of distributed computing and special-purpose hardware.

REFERENCE : Kesteven, M.J., McConnell, D. and Deane, J.F., "On-Line Computing for the Compact Array", Journal of Electrical and Electronics Engineering, Australia, Special Issue on Australia Telescope, June 1992, Vol. 12, No. 2, pp. 199-204.

DATA REDUCTION AND IMAGE PROCESSING

KEY WORDS : Australia Telescope National Facility, radio astronomy, data reduction, image processing.

ABSTRACT We describe the systems used to process and calibrate the data from the Australia Telescope, starting with the data transfer from the Telescope and ending with the imaging and visualisation software. We also describe the continuing development of a specialised visualisation system, which allows astronomers to view cubes of data as three-dimensional objects.

REFERENCE : Norris, R.P., Kesteven, M.J. and Calabretta, M.R., "Data Reduction and Image Processing", Journal of Electrical and Electronics Engineering, Australia, Special Issue on Australia Telescope, June 1992, Vol. 12, No. 2, pp. 205-210.

MONITORING AND PROTECTION STRATEGIES FOR THE COMPACT ARRAY

KEY WORDS : Australia Telescope National Facility, radio astronomy, radio telescope: monitoring, radio telescope: protection.

ABSTRACT The Australia Telescope Compact Array consists of six 22-m antennas located on a 6-km East-West baseline. The geographical diversity of the array, the complexity of the antenna systems, and the vulnerability of the Observatory to damage from storms for example, makes effective monitoring and protection essential. We have implemented two monitoring, alarm and control systems which overlap in function. A hardware-based system examines a relatively small number of very important Telescope and environmental status inputs. A second system based on a minicomputer network acquires, checks and archives data from a much larger number of sensors. Our approach has enabled us to implement a relatively low-cost computer network and to proceed with complex software engineering tasks, including the current development of expert-system fault-diagnosis software, while being satisfied that the Telescope remains well protected. This paper describes the Telescope monitoring and protection schemes and discusses briefly the expected capabilities of the new expert system.

REFERENCE : Hall, P.J., Kesteven, M.J., Beresford, R.J., Ferris, R.H. and Loone, D.G., "Monitoring and Protection Strategies for the Compact Array", Journal of Electrical and Electronics Engineering, Australia, Special Issue on Australia Telescope, June 1992, Vol. 12, No. 2, pp. 113-120.

OPERATIONS BEGIN

KEY WORDS : Australia Telescope National Facility, radio astronomy, radio telescope: operating.

ABSTRACT The transition from construction to operation for the Australia Telescope involved appointing a Director, formally incorporating the Parkes telescope, and transforming the Australia Telescope Support Group from a group within the Division of Radiophysics to an independent unit within CSIRO — the Australia Telescope National Facility. Operation as a National Facility began in April 1990. To provide effective operation, several committees were established: an AT Advisory Committee, an AT Time Assignment Committee, an AT Users Committee, and several user-support groups. Of the six antennas which comprise the Compact Array at Narrabri, only five were outfitted for the first formal observations, at frequencies of 5.0 and 8.6 GHz, and only three of these were outfitted with 1.5- and 2.3-GHz systems, with limited spectral-line capability. Since then, outfitting at these frequencies has been completed, and services appropriate to a national facility have been set up at the sites to support visiting astronomers.

REFERENCE : Nelson, G.J. and Whiteoak, J.B., "Operations Begin", Journal of Electrical and Electronics Engineering, Australia, Special Issue on Australia Telescope, June 1992, Vol. 12, No. 2, pp. 219-224.

THE FIRST RADIO ASTRONOMY: RESULTS AND FUTURE DEVELOPMENTS

KEY WORDS : Australia Telescope National Facility, radio astronomy, radio astronomy: future.

ABSTRACT Since the Compact Array began operating as a National Facility in April 1991, new exciting results have been provided by observations of southern galaxies (normal galaxies, radio galaxies, megamaser galaxies), supernova remnants in the Magellanic Clouds, and objects within our Galaxy (a Galactic Centre transient source, maser regions in molecular clouds, pulsar identifications and stellar radio emission).

Major future development of the Australia Telescope includes the 'tieing' of the six 22-m antennas of the Compact Array at Narrabri, providing better short-baseline configurations, extending observing frequencies on both the Compact Array and the Mopra (near Coonabarabran) antennas to 115 GHz, and completing the correlator, recording system and satellite for the Long Baseline Array (which includes the Mopra antenna and the Parkes 64-m antenna). Further downstream will see the development of focal-plane arrays, and baseline additions to the Compact Array.

REFERENCE : Ekers, R.D. and Whitoak, J.B., "The First Radio Astronomy: Results and Future Developments", Journal of Electrical and Electronics Engineering, Australia, Special Issue on Australia Telescope, June 1992, Vol. 12, No. 2, pp. 225-232.